SINTEF

TR A7307- Unrestricted

Report

Deep Sea Offshore Wind R&D Conference 24 – 25 January 2013

Royal Garden Hotel, Trondheim

Author:
John Olav Tande (editor)

SINTEF Energy Research
Electric Power Systems
2013-06-28

SINTEF Energi AS
SINTEF Energy Research

Address:
Postboks 4761 Sluppen
NO-7465 Trondheim
NORWAY

Telephone:+47 73597200
Telefax:+47 73598354

energy.research@sintef.no
www.sintef.no/energi
Enterprise /VAT No:
NO 939 350 675 MVA

KEYWORDS:
Keywords

Report

Deep Sea Offshore Wind R&D Conference 24 – 25 January 2013

Royal Garden Hotel, Trondheim

VERSION
1.0

DATE
2013-06-28

AUTHOR(S)
John Olav Tande

CLIENT(S)

CLIENT'S REF.

PROJECT NO.
12X650

NUMBER OF PAGES/APPENDICES:
272

ABSTRACT
This report includes the presentations from the 10th Deep Sea Offshore Wind R&D Conference, DeepWind'2013, 24 – 25 January 2013 in Trondheim, Norway. This anniversary of the conference attracted a good selection of high quality presentations and posters. Presentations include plenary sessions with broad appeal and parallel sessions on specific technical themes:

a) New turbine technology
b) Power system integration and Grid connection
c) Met-ocean conditions
d) Operations & maintenance
e) Installation & sub-structures
f) Wind farm modelling

Plenary presentations include frontiers of science and technologies and strategic outlook. The presentations and further conference details are also available at the conference web page http://www.sintef.no/Projectweb/Deepwind_2013/

Full papers of selected presentations will be published online in Energy Procedia (Elsevier).

PREPARED BY
John Olav Tande

SIGNATURE

CHECKED BY
Quality Assuror

SIGNATURE

APPROVED BY
Knut Samdal

SIGNATURE

REPORT NO.	ISBN	CLASSIFICATION	CLASSIFICATION THIS PAGE
TR A7307	978-82-594-3555-2	Unrestricted	Unrestricted

SINTEF

Document history

VERSION	DATE	VERSION DESCRIPTION
1.0	2013-06-28	

SINTEF

Table of contents

C1 Met-ocean conditions

C2 Met-ocean conditions

Posters presentations.

D Operation & maintenance

DeepWind 2013 - 10th Deep Sea Offshore Wind R&D Conference

24 - 25 January 2013, Royal Garden Hotel, Kjøpmannsgata 73, Trondheim, NORWAY

	Thursday 24 January		
09.00	Registration & coffee		
	Opening session – Frontiers of Science and Technology Chairs: John Olav Tande, SINTEF/NOWITECH and Trond Kvamsdal, NTNU/NOWITECH		
09.30	Opening and welcome by chair		
09.40	*Innovations in offshore wind technology*, John Olav Tande, SINTEF/NOWITECH		
10.05	*Key research topics in offshore wind energy,* Kristin Guldbrandsen Frøysa, CMR/NORCOWE		
10.30	*Research at Alpha Ventus deep offshore wind farm,* Stefan Faulstich, Fh IWES		
11.00	*WindFloat deep offshore wind operational experience*, Pedro Valverde, EdP		
11.30	*HyWind deep offshore wind operational experience*, Finn Gunnar Nielsen, Statoil		
11.55	Closing by chair		
12.00	Lunch		
	Parallel sessions		
	A1) New turbine technology Chairs: Michael Muskulus, NTNU Prof Gerard van Bussel, TU Delft	**B1) Power system integration** Chairs: Prof Kjetil Uhlen, NTNU Prof Olimpo Anaya-Lara, Strathclyde Uni	**C1) Met-ocean conditions** Chairs: Prof J Reuder, Uni of Bergen Erik Berge, Kjeller Vindteknikk
13.00	Introduction by Chair	Introduction by Chair	Introduction by Chair
13.10	*Design Optimization of a 5 MW Floating Offshore Vertical Axis Wind Turbine*, Uwe Schmidt Paulsen, Technical Uni of Denmark, DTU	*Wind Turbine Electrical Design for an Offshore HVDC Connection*, Olimpo Anaya-Lara, Strathclyde Univ.	*Wave-induce characteristics of atmospheric turbulence flux measurements*, Mostafa Bakhoday Paskyabi, UiB
13.40	*Operational Control of a Floating Vertical Axis Wind Turbine*, Harald Svendsen, SINTEF Energi AS	*Frequency Quality in the Nordic system: Offshore Wind variability, Hydro Power Pump Storage and usage of HVDC Links*, Atsede Endegnanew, SINTEF Energi AS	*Experimental characterization of the marine atmospheric boundary layer in the Havsul area, Norway*, Constantinos Christakos, UiB
14.00	*Control for Avoiding Negative Damping on Floating Offshore Wind Turbine,* Prof Yuta Tamagawa, Uni. of Tokyo	*Coordinated control for wind turbine and VSC-HVDC transmission to enhance FRT capability*, A. Luque, Uni. Strathclyde	*Buoy based turbulence measurements for offshore wind energy applications*, M. Flügge, UiB
14.20	*Towards the fully-coupled numerical modelling of floating wind turbines*, Axelle Viré, Imperial College, London	*North Sea Offshore Modeling Schemes with VSC-HVDC Technology: Control and Dynamic Performance Assessment*, K. Nieradzinska, University of Strathclyde	*Effect of wave motion on wind lidar measurements - Comparison testing with controlled motion applied*, Joachim Reuder, Univ of Bergen
14.40	*Geometric scaling effects of bend-twist coupling in rotor blades*, Kevin Cox, PhD stud, NTNU	*Upon the improvement of the winding design of wind turbine transformers for safer performance within resonance overvoltages*, Amir H Soloot, PhD, NTNU	*Turbulence analysis of LIDAR wind measurements at a wind park in Lower Austria*, Valerie-Marie Kumer, UiB
15.00	Refreshments		
	A2) New turbine technology Chairs: Michael Muskulus Prof Gerard van Bussel, TU Delft	**B2) Grid connection** Chairs: Prof Kjetil Uhlen, NTNU Prof Olimpo Anaya-Lara, Strathclyde Uni	**C2) Met-ocean conditions** Chairs: J Reuder, Uni of Bergen Erik Berge, Kjeller Vindteknikk
15.30	Introduction by Chair	Introduction by Chair	Introduction by Chair
15.35	*High Power Generator for Wind Power Industry: A Review,* Zhaoqiang Zhang, PhD stud, NTNU	*Planning Tool for Clustering and Optimised Grid Connection of Offshore Wind Farms,* Harald G. Svendsen, SINTEF	*Wave driven wind simulations with CFD*, Siri Kalvig, University of Stavanger / StormGeo
15.55	*Superconducting Generator Technology for Large Offshore Wind Turbines,* Niklas Magnusson, SINTEF Energi AS	*The role of the North Sea power transmission in realising the 2020 renewable energy targets - Planning and permitting challenges*, Jens Jacob Kielland Haug, SINTEF Energi AS	*New two-way coupled atmosphere-wave model system for improved wind speed and wave height forecasts*, Olav Krogsæter, StormGeo / University of Bergen
16.15	*Laboratory Verification of the Modular Converter for a 100 kV DC Transformer-less Offshore Wind Turbine Solution*, Sverre Gjerde, PhD stud, NTNU	*Technology Qualification of Offshore HVDC Technologies*, Tore Langeland, DNV KEMA	*Measurement of wind profile with a buoy mounted lidar*, Jan-Petter Mathisen, Fugro OCEANOR
16.35	*Multi-objective Optimization of a Modular Power Converter Based on Medium Frequency AC-Link for Offshore DC Wind Park*, Rene A. Barrera, NTNU	*Evaluating North Sea grid alternatives under EU's RES-E targets for 2020*, Ove Wolfgang, SINTEF Energi AS	*Numerical Simulation of Stationary Microburst Phenomena with Impinging Jet Model*, Tze Siang Sim, Nanyang Technological University
16.55	Closing by Chair	Closing by Chair	Closing by Chair
17.00	**Poster session with refreshments**		
19.00	Dinner		

	Thursday 24 January
17.00	**Poster Session with refreshments** 1. *Aeroelastc analysis software as a teaching and learning tool for young and old students of wind turbines, Paul E. Thomassen, NTNU* 2. *Magnetically Induced Vibration Forces in a Low-Speed Permanent Magnet Wind Generator with Concentrated Windings,* Mostafa Valavi, PhD stud, NTNU 3. *Coupled 3D Modelling of Large-Diameter Ironless PM Generator*, Zhaoqiang Zhang, PhD stud, NTNU 4. *Stability in offshore wind farm with HVDC connection to mainland grid,* Jorun I Marvik, SINTEF Energi AS 5. *Perturbation in the acoustic field from a large offshore wind farm in the presence of surface gravity waves,* Mostafa Bakhoday Paskyabi, UiB 6. *Autonomous Turbulence Measurements from a Subsurface Moored Platform,* Mostafa Bakhoday Paskyabi, UiB 7. *A Markov Weather Model for O&M Simulation of Offshore Wind Parks,* Brede Hagen, stud, NTNU 8. *Turbulence Analysis of LIDAR Wind Measurements at a Wind Park in Lower Austria,* Valerie-Marie Kumer, UiB 9. *Investigation of droplet erosion for offshore wind turbine blade,* Magnus Tyrhaug, SINTEF 10. *A Fuzzy FMEA Risk Assessment Approach for Offshore Wind Turbines, Fateme Dinmohammadi, Islamic Azad University* 11. *NOWIcob – A tool for reducing the maintenance costs of offshore wind farms,* Iver Bakken Sperstad, SINTEF Energi AS 12. *Long-term analysis of gear loads in fixed offshore wind turbines considering ultimate operational loadings,* Amir Rasekhi Nejad, PhD, NTNU 13. *Methodology to design an economic and strategic offshore wind energy Roadmap in Portugal,* Laura Castro-Santos, Laboratório Nacional de Energia (LNEG) 14. *Methodology to study the life cycle cost of floating offshore wind farms,* Laura Castros Santos,Laboratório Nacional de Energia (LNEG) 15. *Two-dimensional fluid-structure interaction of airfoil*, Knut Nordanger, PhD stud, NTNU 16. *Experimental Investigation of Wind Turbine Wakes in the Wind Tunnel*, Heiner Schümann, NTNU 17. *Numerical Study on the Motions of the VertiWind Floating Offshore Wind Turbine,* Raffaello Antonutti, EDF R&D 18. *Coatings for protection of boat landings against corrosion and wear*, Astrid Bjørgum, SINTEF Materials and Chemistry 19. *Analysis of spar buoy designs for offshore wind turbines, C. Romanò,* DIMEAS, Politecnico di Torino 20. *Numerical model for Real-Time Hybrid Testing of a Floating Wind Turbine,* Valentin CHABAUD, PhD stud, NTNU 21. *Advanced representation of tubular joints in jacket models for offshore wind turbine simulation,* Jan Dubois, ForWind – Leibniz University Hannover 22. *Comparison of coupled and uncoupled load simulations on the fatigue loads of a jacket support structure,* Philipp Haselbach, DTU Wind Energy 23. *Design Standard for Floating Wind Turbine Structures*, Anne Lene H. Haukanes, DNV 24. *Nonlinear irregular wave forcing on offshore wind turbines. Effects of soil damping and wave radiation damping in misaligned wind and waves,* Signe Schløer, DTU
19.00	Dinner

DeepWind 2013 - 10th Deep Sea Offshore Wind R&D Seminar 24-25 January 2013, Royal Garden Hotel, Kjøpmannsgata 73, Trondheim, NORWAY			
	Friday 25 January		
	Parallel sessions		
	D) Operations & maintenance Chairs: Matthias Hofmann, SINTEF Stefan Faulstich, Fh IWES	**E) Installation & sub-structures** Chairs: Hans-Gerd Busmann, Fh IWES Jørgen Krogstad, Statkraft	**F) Wind farm modelling** Chairs: Prof Trond Kvamsdal, NTNU Thomas Buhl, DTU Wind Energy
08.30	Introduction by Chair	Introduction by Chair	Introduction by Chair
08.35	*Development of a Combined Operational and Strategic Decision Support Model for Offshore Wind,* Iain Dinwoodie, PhD Stud, Univ Strathclyde	*Structures of offshore converter platforms - Concepts and innovative developments*, Joscha Brörmann, Technologiekontor Bremerhaven GmbH	*Wind farm optimization*, Prof Gunner Larsen, DTU Wind Energy
09.05	*Vessel fleet size and mix analysis for maintenance operations at offshore wind farms*, Elin E. Halvorsen-Weare, SINTEF ICT/MARINTEK	*Dynamic analysis of floating wind turbines during pitch actuator fault, grid loss, and shutdown*, Erin E. Bachynski, PhD stud, NTNU	*Blind test 2 - Wind and Wake Modelling*, Prof Lars Sætran, NTNU
09.25	*NOWIcob – A tool for reducing the maintenance costs of offshore wind farms,* Iver Bakken Sperstad, SINTEF	*Use of a wave energy converter as a motion suppression device for floating wind turbines*, Michael Borg, Cranfield University	*A practical approach in the CFD simulations of off-shore wind farms through the actuator disc technique*, Giorgio Crasto, WindSim AS
09:45	*WINDSENSE – a joint development project for add-on instrumentation of Wind Turbines*, Oddbjørn Malmo, Kongsberg Maritime AS	*Loads and response from steep and breaking waves. An overview of the 'Wave loads' project,* Henrik Bredmose, Associate Professor, DTU Wind Energy	*3D hot-wire measurements of a wind turbine wake*, Pål Egil Eriksen, PhD stud, NTNU
10:05	*Long-term analysis of gear loads in fixed offshore wind turbines considering ultimate operational loadings,* Amir Rasekhi Nejad, PhD stud, NTNU	*Effect of second-order hydrodynamics on floating offshore wind turbines*, Line Roald, ETH Zürich	*Near and far wake validation study for two turbines in line*, Marwan Khalil, GexCon AS
10.35	Closing by Chair	Closing by Chair	Closing by Chair
10.40	Refreshments		
	Closing session – Strategic Outlook Chairs: John Olav Tande, SINTEF/NOWITECH and Michael Muskulus, NTNU/NOWITECH		
11.00	Introduction by Chair		
11.05	*Deep offshore and new foundation concepts*, Arapogianni Athanasia, European Wind Energy Association		
11.35	*Optimal offshore grid development in the North Sea towards 2030,* Daniel Huertas Hernando, SINTEF Energi AS		
12.05	*New turbine technology*, Svein Kjetil Haugset, Blaaster		
12.35	Poster award and closing		
13.00	Lunch		

List of participants

Name	Institution
Anaya-Lara, Olimpo	Strathclyde University
Antonutti, Raffaello	EDF R&D LNHE
Arapogianni, Athanasia	European Wind Energy Association
Bachynski, Erin	CeSOS/NTNU
Bardal, Lars Morten	NTNU
Barrera-Cardenas, Rene Alexander	NTNU
Berge, Erik	Kjeller Vindteknikk
Bergh, Øivind	Institute of Marine Research
Bjørgum, Astrid	SINTEF Materials and Chemistry
Bolleman, Nico	Blue H Engineering BV
Borg, Michael	Cranfield University
Bredmose, Henrik	DTU Wind Energy
Brörmann, Joscha	Teknologiekontor Bremerhaven
Buhl, Thomas	DTU Wind Energy
Busmann, Hans-Gerd	Fraunhofer IWES
Castro Santos, Laura	University of A Coruña
Chabaud, Valentin	NTNU
Christakos, Konstantinos	University of Bergen
Cox, Kevin	NTNU
Crasto, Giorgio	WindSim AS
De Laleu, Vincent	EDF R&D
de Vaal, Jabus	NTNU
Delhaye, Virgile	SINTEF M&C
Deng, Han	NTNU
Dinwoodie, Iain	University of Strathclyde
Dubois, Jan	Leibniz Universitaet Hannover Stahlbau
Dufourd, Frederic	EDF
Eecen, Peter	ECN
Egeland, Håkon	Statkraft Energi AS
Endegnanew, Atsede	SINTEF Energi AS
Eriksen, Pål Egil	NTNU
Eriksson, Kjell	Det Norske Veritas
Faulstich, Stefan	Fh IWES
Flügge, Martin	University of Bergen

Fredriksen, Tommy	HiT
Frøyd, Lars	4Subsea AS
Frøysa, Kristin Gulbrandsen	NORCOWE / CMR
Gao, Zhen	CeSOS/NTNU
Gjerde, Sverre Skalleberg	NTNU
Grønsleth, Martin	Kjeller Vindteknikk AS
Haarr, Geirr	Statoil Hywind
Hagen, Brede	NTNU
Halvorsen-Weare, Elin Espeland	SINTEF IKT
Haselbach, Philipp Ulrich	DTU Wind Energy
Haugset, Svein Kjetil	Chapdrive
Hofmann, Matthias	SINTEF Energi
Hopstad, Anne Lene	DNV
Huertas Hernando, Daniel	SINTEF Energi
Iversen, Viggo	Proneo
Jakobsen, Tommy	Kongsberg Maritime
Johnsen, Trond	MARINTEK AS
Kalvig, Siri	Storm Geo
Kamio, Takeshi	The University of Tokyo
Karlsson, Sara	Hexicon AB
Kastmann, Pål Arne	Innovation Norway / Norwegian Embassy in Beijing
Khalil, Marwan	GexCon AS
Kielland Haug, Jens Jakob	SINTEF Energi
Kjerstad, Einar	Fiskerstrand BLRT
Kocewiak, Lukasz	DONG Energy Wind Power
Korpås, Magnus	SINTEF Energi
Krogsæter, Olav	Storm Geo
Krokstad, Jørgen	Statkraft
Kumer, Valerie-Marie	University of Bergen
Kvamme, Cecilie	Institute of Marine Research
Kvamsdal, Trond	NTNU
Kvittem, Marit Irene	CeSOS/NTNU
Langeland, Tore	DNV
Larsen, Gunner	DTU Wind Energy
Lauritzen, Tore Lennart	Access Mid-Norway
Ljøkelsøy, Kjell	SINTEF Energi
Lund, Berit Floor	Kongsberg Maritime
Lund,Per Christer	Norwegian Embassy in Tokyo
Lunde, Knut-Ola	NTNU
Luque, Antonio	University of Strathclyde
Lynum, Susanne	NTNU

Magnusson, Niklas	SINTEF Energi
Malmo, Oddbjørn	Kongsberg Maritime
Manger, Eirik	Acona Flow Technology
Martinussen, Mads	Blaaster
Marvik, Jorun	SINTEF Energi
Mathisen, Jan-Petter	Fugro OCEANOR
Midtsund, Tarjei	Statnett SF
Muskulus, Michael	NTNU
Natarajan, Anand	DTU Wind Energy
Nejad, Amir R.	NTNU
Niedzwecki, John	Texas A/M University
Nieradzinska, Kamila	Strathclyde University
Nilsen, Finn Gunnar	Statoil ASA
Nodeland, Anne Mette	NTNU
Nordanger, Knut	NTNU
Nysveen, Arne	NTNU/Elkraftteknikk
Oggiano, Luca	IFE
Oma, Per Norman	Kongsberg Maritime AS
Ong, Muk Chen	MARINTEK
Paskyabi, Mostafa Bakhoday	Geophysical Institute/NORCOWE
Paulsen, Uwe Schmidt	DTU Wind Energy
Rebours, Yann	EDF R&D
Reuder, Joachim	UiB
Roald, Line	ETH Zürich
Schaumann, Peter	Leibniz Universitaet Hannover Stahlbau
Schløer, Signe	DTU Wind Energy
Schramm, Rainer	Subhydro AS
Schümann, Heiner	NTNU
Seterlund, Anne Marie	Statkraft Development
Sim, Tze Siang	Nanyang Technological University
Singstad, Ivar	Innovation Norway
Skaare, Bjørn	Statoil ASA
Soloot, Amir Hayati	NTNU
Sperstad, Iver Bakken	SINTEF Energi
Stenbro, Roy	IFE
Svendgård, Ole	VIVA - Testsenter for vindturbiner
Svendsen, Harald	SINTEF Energi
Sæter, Camilla	NTNU
Sætran, Lars	NTNU
Sørheim, Hans Roar	CMR
Tamagawa, Yuta	Tokyo University

Tande, John Olav	SINTEF Energi
Thomassen, Paul	NTNU
Tveiten, Bård Wathne	SINTEF
Tyrhaug, Magnus	NTNU
Uhlen, Kjetil	NTNU
Undeland, Tore	NTNU
Valverde, Pedro	EDP Inovação, S.A.
van Bussel, Gerard	TU Delft
Van Der Pal, Aart	ECN
Vire, Axelle	Imperial College London
Wolfgang, Ove	SINTEF Energi
Zhang, Zhaoqiang	NTNU
Østbø, Niels Peter	SINTEF ICT
Öfverström, Anders	Hexicon AB
Øyslebø, Eirik	Norges vassdrags- og energidirektorat

SINTEF

3 Scientific Committee and Conference Chairs

An international Scientific Committee was established with participants from leading research institutes and universities for reviewing submissions and preparing the conference programme. The members of the Scientific Committee of DeepWind'2013 are listed below.

Anaya-Lara, Olimpo, Strathclyde University
Berge, Erik, Kjeller Vindteknikk
Buhl, Thomas, DTU
Busmann, Hans-Gerd, Fraunhofer IWES
Bussel, Gerard J.W. van, TU Delft
Faulstich, Stefan, Fraunhofer IWES
Krokstad, Jørgen, Statkraft
Kvamsdal, Trond, NTNU
Langen, Ivar, UiS
Leithead, William, Strathclyde University
Madsen, Peter Hauge, DTU
Moan, Torgeir, NTNU
Molinas, Marta, NTNU
Muskulus, Michael, NTNU
Nielsen, Finn Gunnar, Statoil
Nygaard, Tor Anders, IFE
Reuder, Jochen, UiB
Sirnivas, Senu, NREL
Tande, John Olav, SINTEF
Uhlen, Kjetil, NTNU
Undeland, Tore, NTNU

The conference chairs were

- John Olav Giæver Tande, Director NOWITECH, senior scientist SINTEF Energy Research
- Trond Kvamsdal, Chair NOWITECH Scientific Committee, Associate Professor NTNU
- Michael Muskulus, Vice Chair NOWITECH Scientific Committee, Professor NTNU

Opening session - Frontiers of Science and technology

Innovations in offshore wind technology,
John Olav Tande, SINTEF/NOWITECH

Key research topics in offshore wind energy,
Kristin Guldbrandsen Frøysa, CMR/NORCOWE

Research at Alpha Ventus deep offshore wind farm ,
Stafan Faulstich, Fh IWES

WindFloat deep offshore wind operational experience,
Pedro Valverde, EdP

HyWind deep offshore wind operational experience,
Finn Gunnar Nielsen, Statoil

Innovations in Offshore Wind Technology through R&D

www.nowitech.no

John Olav Giæver Tande
Director NOWITECH
Senior Scientist
SINTEF Energy Research
John.tande@sintef.no

NOWITECH in brief

- **a joint pre-competitive research effort**
- **focus on deep offshore wind technology (+30 m)**
- **budget (2009-2017) EUR 40 millions**
- **co-financed by the Research Council of Norway, industry and research partners**
- **25 PhD/post doc grants**
- **Vision:**
  - **large scale deployment**
  - **internationally leading**

Research partners:
- SINTEF (host)
- IFE
- NTNU

Industry partners:
- Det Norske Veritas
- DONG Energy Power
- EDF R&D
- Fedem Technology AS
- NTE Holding AS
- SmartMotor AS
- Statkraft
- Statnett SF
- Statoil Petroleum AS

Associated research partners:
- DTU Wind Energy
- MIT
- NREL
- Fraunhofer IWES
- Uni. Strathclyde
- TU Delft
- Nanyang TU

Associated industry partners:
- Access Mid-Norway
- Devold AMT AS
- Energy Norway
- Enova
- Innovation Norway
- NCEI
- NORWEA
- NVE
- Wind Cluster Mid-Norway

Multidisciplinary Research Challenges

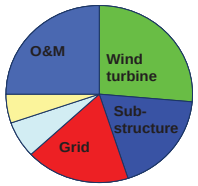

LPC distribution of offshore wind farm (example)

Key issue: Innovations reducing cost of energy from offshore wind

A large growing global market

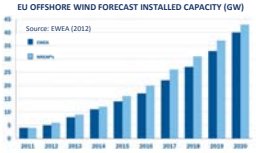

OFFSHORE WIND KEY INDICATORS

Key indicators	2010	2016
Capex (NOK)	26.6 bn NOK	92bn NOK
Capex (USD)	4.7 bn USD	16 bn USD
Added capacity	1 GW	3.6 GW
Turbines	370	975
Foundations	639	1,435
Cables	518 km	1,972 km
Installation vessels	21	45
PTVs	86	277

Source: Douglas-Westwood (2012)

- Firm European commitment to develop offshore wind
- EU offshore wind forecast 2020:
  - Total installed capacity 40 GW
  - Total investments EUR 65.9 billions
- EU offshore wind forecast 2030:
  - Total installed capacity 150 GW
  - Total investments EUR 145.2 billions
- Significant developments also in China, Japan, Korea and USA
- The near-term large commercial market is mainly for bottom-fixed wind farms at shallow to intermediate water depths (50 m)
- Significant interest in developing floating concepts expecting large volume after 2020
- Threat: International financial crisis / economic recession

Main drivers

- Battle climate change
- Security of supply
- Industry value creation

Stern Review (2006): ..strong, early action on climate change far outweigh the costs of not acting.

Figure 1.10 Fuel mix in electricity generation, by scenario

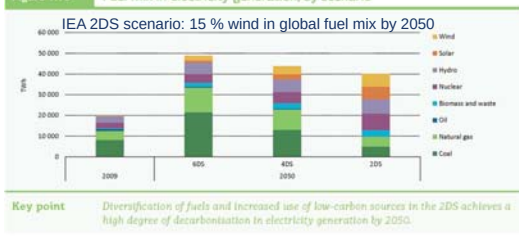

Copy from IEA Energy Technology Perspectives 2012

A possible Norwegian market, but uncertain

- NVE has identified 15 areas for development of offshore wind farms (total ~10 GW); five are suggested prioritized (public inquiry due 4/4-13)
- Applying the petroleum taxation regime to offshore wind farms for supply to oil and gas installations may create a immediate Norwegian market (total ~100-1000 MW)
- A significant Norwegian market for onshore turbines are expected through green certificates, e.g. 6 TWh by 2020 (total market for green certificates in Norway and Sweden is 26 TWh).

Exciting floating concepts

NOWITECH 10 MW reference turbine

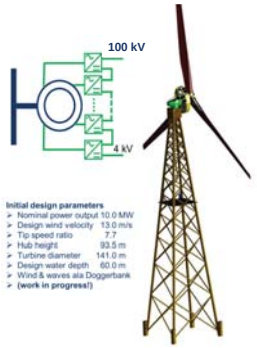

The NOWITECH 10 MW reference turbine introduces a new generator and support structure concept

- New generator concept allows for direct HVDC connection to shore and avoiding costly offshore sub-station
- New support structure avoid costly transition piece between tubular tower and jacket

Innovative DC grid solutions for offshore wind farms avoiding need for large sub-station

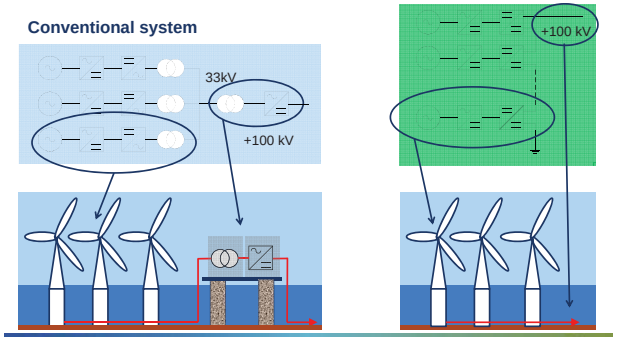

Superconducting generators reduce weight

- 100 times the current density compared to copper
- More than doubles the achievable magnetic field
- Eliminates rotor losses
- Operating at 20-50 K

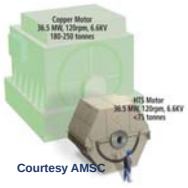

- New materials give new electromagnetic designs
- Possible step-changing technology
- Activity in new FP7 project: InnWind

Optimization of the offshore grid

- **Inside and between wind farms**
- **New market solutions are required**
- **New technology (HVDC VSC, multi-terminal, hybrid HVDC/HVAC, ..)**
- **Protection, Fault handling, Operation, Control, Cost, Security of Supply**

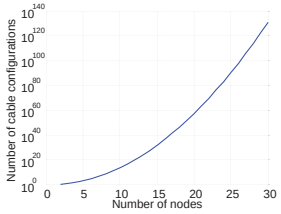

Remote presence reduce O&M costs

- It is costly and sometimes impossible to have maintenance staff visiting offshore turbines
- Remote presence:
  - Remote inspection through a small robot on a track in the nacelle equipped with camera / heat sensitive, various probes, microphone etc.
  - Remote maintenance through robotized maintenance actions

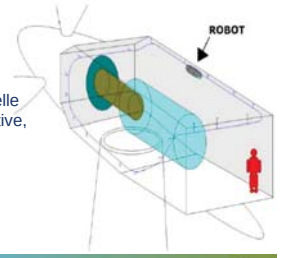

Integrating structural dynamics, control and electric model

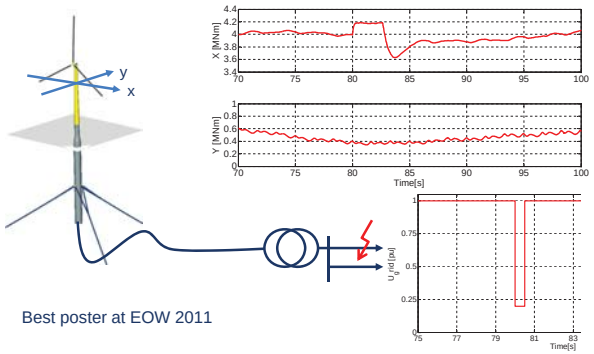

Best poster at EOW 2011

Reducing uncertainties by better models

- Integrated models simulate the behavior of the complete turbine with substructure in the marine environment: SIMO-RIFLEX (MARINTEK) and 3DFloat (IFE)
- Model capability includes bottom fixed and floating concepts
- Code to code comparison in IEA Wind OC3 and OC4
- Model to measurements comparison in progress

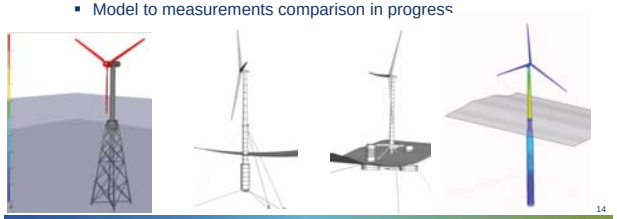

SEAWATCH Wind Lidar Buoy

- Cost efficient and flexible compared to offshore met mast
- Measure wind profiles (300 m), wave height and direction, ocean current profiles, met-ocean parameters
- Result of NOWITECH "spin-off" joint industry project by Fugro OCEANOR with Norwegian universities, research institutes and Statoil.

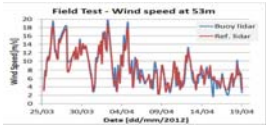

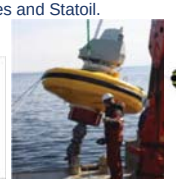

Strong research infrastructure in development

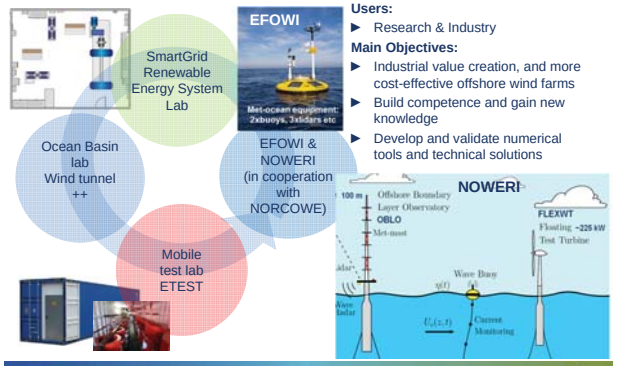

Users:
- Research & Industry

Main Objectives:
- Industrial value creation, and more cost-effective offshore wind farms
- Build competence and gain new knowledge
- Develop and validate numerical tools and technical solutions

From Idea to Commercial Deployment

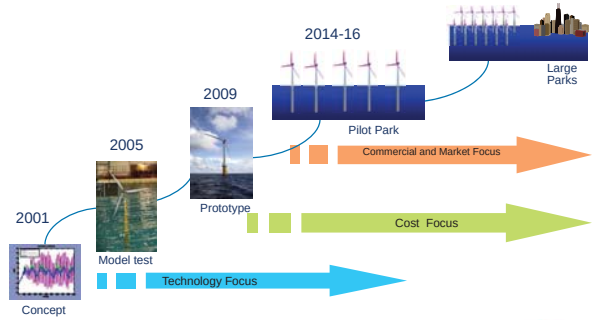

Graphic is copy from Statoil presentation on HyWind at Wind Power R&D seminar, 20-21 January 2011, Trondheim, Norway

NOWITECH achievements

- **NOWITECH is about education, competence building and innovations reducing cost of energy from offshore wind**

- Significant budget and duration: EUR 40 millions (2009-2017)
- Strong consortium with leading research and industry parties
- Excellent master and PhD programme: 25 PhD & post doc grants
- Strong scientific results: ~100 peer-reviewed publications
- R&D results give value creation and cost reductions
- Innovation process is enhanced through TRL
- Two new business developments (Remote Presence + SiC coatings)
- Strong infrastructure in development: NOWERI
- A high number of spin-off projects: total volume EUR 125 millions (EU (11), KPN etc. (10), IPN (7) and research infrastructure (3))

- **Vision: large scale deployment & internationally leading**

Rounding up

- Remarkable results are already achieved by industry and R&D institutes on deep offshore wind technology
- Technology still in an early phase – Big potential provided technical development and bringing cost down
- Research plays a significant role in providing new knowledge as basis for industrial development and cost-effective offshore wind farms at deep sea
- Cooperation between research and industry is essential for ensuring relevance, quality and value creation
- Test and demonstration, also in large scale, is vital to bring research results into the market place

- Offshore wind is a multidisciplinary challenge – international collaboration is the answer!
- Outlook is demanding, but prosperous with a growing global market

NOWITECH Norwegian Research Centre for Offshore Wind Technology

NOWITECH is a joint 40M€ research effort on offshore wind technology.

- **Integrated numerical design tools**
- **New materials for blades and generators.**
- **Novel substructures (bottom-fixed and floaters)**
- **Grid connection and system integration**
- **Operation and maintenance**
- **Assessment of novel concepts**

www.NOWITECH.no

NOWITECH Norwegian Research Centre for Offshore Wind Technology

Key research topics in offshore wind energy
DeepWind 2013

Kristin Guldbrandsen Frøysa
Director NORCOWE
kristin@cmr.no

Outline

- Motion compensation
- Measurements and database
- Wind farm layout
- Wind farm power control and prediction

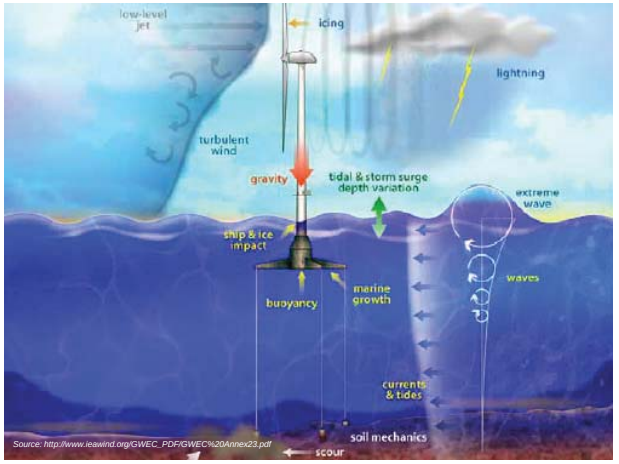

Description of wind shear

- Empirical power law description of the vertical wind shear:

$$\overline{u(z)} = u_{ref}\left(\frac{z}{z_{ref}}\right)^{\alpha}$$

- The logarithmic wind profile

$$\overline{u(z)} = \frac{u_*}{k}\ln\frac{z}{z_0}$$

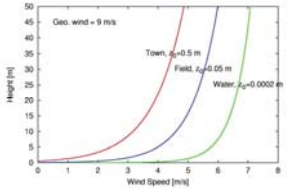

Wind profiles and stability

- Measurements at high towers show, that these wind profiles based on surface-layer theory and Monin-Obukhov scaling are only valid up to ca. 50-80 m

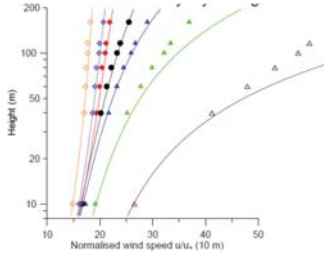

Only few offshore measurements

Measurements up to 100 m
Shallow waters (~ 20 m)

Deep water measurements possible
Measurements only up to ~ 20 m

J. Reuder, Geophysical Institute, University of Bergen

Satellite data (SAR, QuickScat)

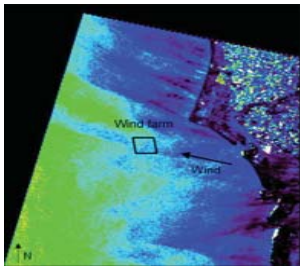

Ocean wind speed map from ERS SAR from Horns Rev in the North Sea, Denmark observed 6 October 2004. The Horns Rev offshore wind farm is located in the trapezoid.

Shortcomings:

- limited temporal resolution
- uncertainty in determination of relevant wind speed over the rotor disk

- *Source: http://galathea3.emu.dk/satelliteeye/projekter/wind/back_uk.html*

Lidar going offshore

- Why?
  - Poor information on the offshore wind field in the relevant height interval (30..200 m)
  - Corresponding mast structures are expansive and rather inflexible
- Challenges
  - Motion avoidance or motion correction
  - Adaptation to harsh marine environment
  - Energy for long term deployments

Lidar going offshore

SeaZephIR (Natural Power)

ZephIR lidar on spare or tension leg buoy

Flidar (3E)

Windcube on industrial buy; mechanical stabilization

WindSentinel (Axys)

Vindicator on a boat structure

Wavescan ZephIR (Fugro Oceanor)

ZephIR on Wavescan buoy

Lidar movement testing

Stewart platform

- Application of 55 different motion patterns on a 6-DOF motion platform, 3 hours each

Offshore comparison

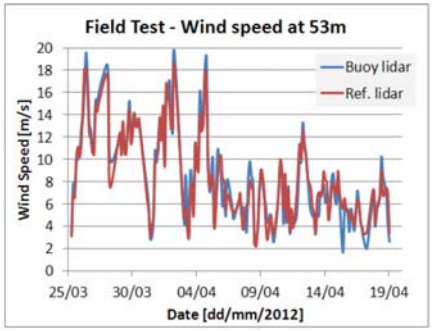

source: Final Report of the project "Measurements of Wind Profile from a Buoy using Lidar" in cooperation between Fugro OCEANOR, Statoil, University of Bergen, Uni Research, Christian Michelsen Research (CMR) and Marintek

Experimental Work

- Motion laboratory at University of Agder (UiA)
- Calibration of simulation model
- Use of Stewart platforms to perform an offshore payload transfer experiment.

Source: Magnus B Kjelland, UiA

HMF 2200-K4 Loader Crane

- 2012:
  - Foundation
  - Instrumentation
  - Modeling & Simulation
  - (Real Time Simulation)
- Future work (2013):
  - Control System
  - Experimentation

Source: Magnus B Kjelland, UiA

Real Time Simulation

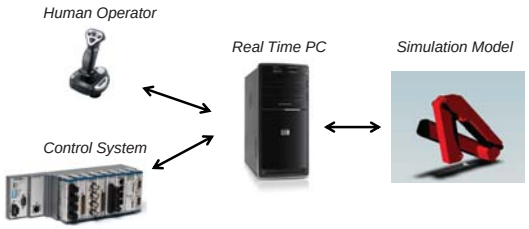

Source: Magnus B Kjelland, UiA

Strengths of model reduction technics

- **Physical**
  - The method solves the non-linear flow equations in a reduced space.
- **Fast**
  - The method provides CFD quality results within seconds of computational time (single CPU).
- **Power production**
  - Individual turbine production calculated.
- **Turbulence**
  - 3D flow fields for both velocity and turbulent kinetic energy are computed.
- **Transfer**
  - The model reduction technique can take advantage of improvements in the CFD tool, such as improved turbine and turbulence models.

Illustration of interface

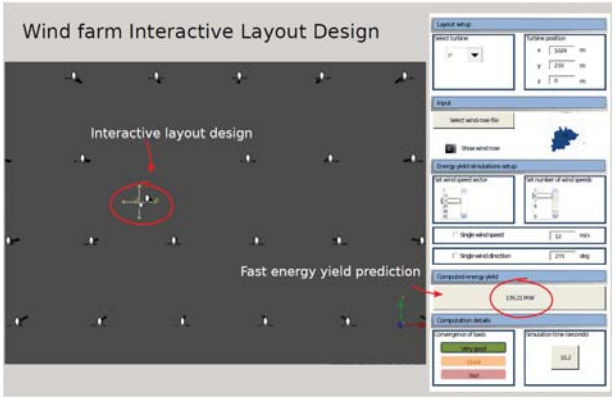

Regular grid

- Regular layout: what is the sensitivity of the estimated power production on changing turbine distance (± .5 D)?

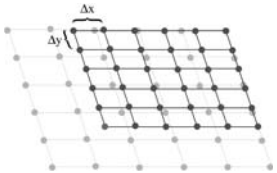

Irregular grid

- Non-regular layout: investigate selected non-regular layouts. What is the energy yield compared to a regular layout setup?

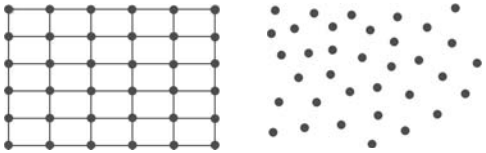

Power production sensitivity

- Regular / non-regular layout: What is the sensitivity of the power production on variations of the wind rose?

- This could highlight how changes in the inflow conditions due to nearby wind farms potentially would affect the power production of the downstream wind farm.

Where we are today

- A prototype model reduction tool has been developed in NORCOWE
  - The technique has been verified by comparison to CFD results for simple cases of a few turbine rows.
  - Flow cases with more than 20 turbines have been computed within seconds on a single CPU.

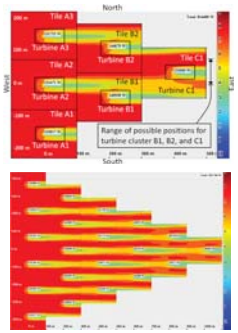

The results so far are documented in a paper:
Heggelund Y., Skaar I.-M., and Jarvis C. *Interactive design of wind farm layout using CFD and model reduction of the steady state RANS equations*, 11th World Wind Energy Conference, Bonn, Germany. 3-5 July (2012)

Wind farm power control and prediction

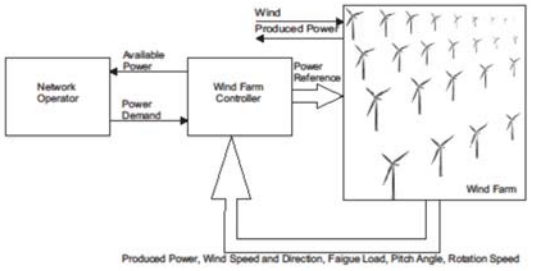

Source: Torben Knudsen, AAU

Can a dynamic controlled power set point control of all turbines improve total production further?

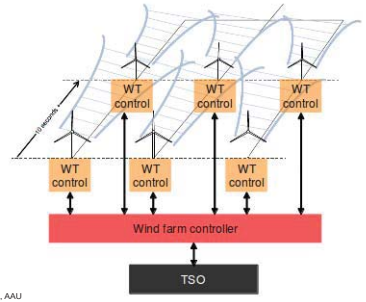

Source: Torben Knudsen, AAU

Can "total" fatigue be reduced with control of power set points on farm level?

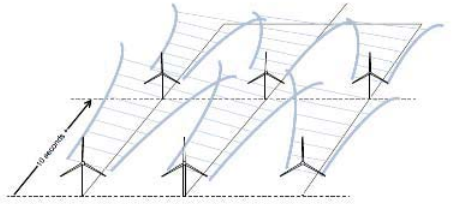

- Fatigue for farm turbines are highly dependent on wakes and increased turbulence from neighbor turbines.

Source: Torben Knudsen, AAU


Thank you for
your attention!
www.norcowe.no

Content

Alpha ventus,…
- milestones
- layout

…RAVE…
- Objectives
- Measurements
- Exemplary results

…and beyond
- Continuation of RAVE
- Technology monitoring

The Fraunhofer Institute for Wind Energy and Energy System Technology IWES


Wind energy


Photovoltaics


Bioenergy

Applications-oriented research in wind energy & energy systems technology for renewable energies

- One of 80 Fraunhofer Institutes
- Budget ~ 22 million €
- Staff ~ 300
- Funding by Federal Ministries, Länder and the EU; Industry


Electricity grids

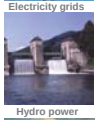
Hydro power


Marine energies

The Fraunhofer IWES – experimental facilities Exemplary Highlights

Competence Center Rotor Blade

Climate chamber

200 meter measuring mast

www.fraunhofer.iwes.de

alpha ventus and RAVE

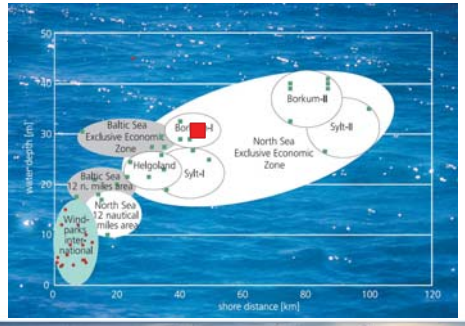

Alpha ventus: milestones

- 2001 Approval
- 2003 FINO 1 operating
- 2008 Substation install
  Export cable install
- 2009 All WT installed
  Infield cable installed
  All WT operational
- 2010 Official inauguration

Alpha ventus: project details

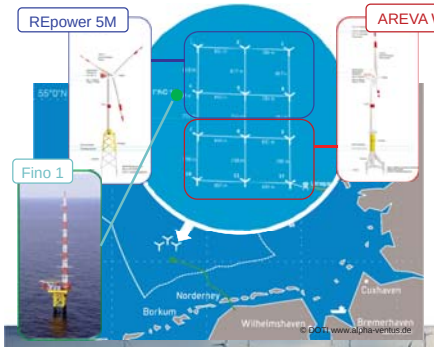

- North Sea
- 45 km north of Borkum
- Water depth: 30 m
- 12 turbines
- 5 MW class -AREVA Wind M5000 -Repower 5M

Alpha ventus / results 2011

- Production (2011): 267 GWh
  4,450 full load hours

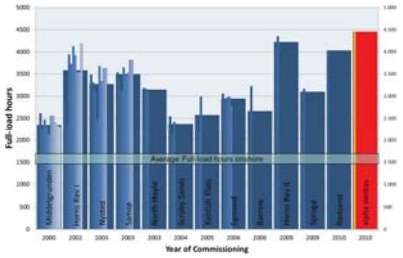

RAVE – Research at alpha ventus

- Funded by the German Federal Ministry for the Environment, Nature Conservation and Nuclear Safety (BMU)
- Accompanying research at the alpha ventus test site
- 33 R&D projects
- 51 mill. €
- 50+ project partners ~200 Scientists

- RAVE – Steering Committee :

Main objectives of RAVE

Demonstration | Development | Investigation of OWP issues

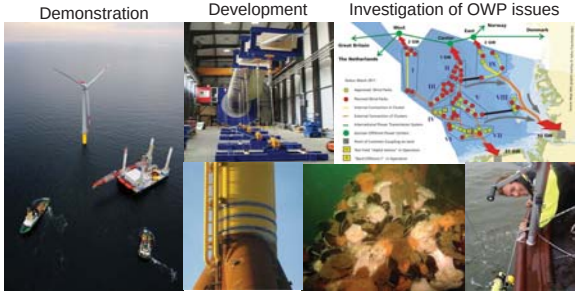

Expand research, experience & expertise

RAVE – R&D contents

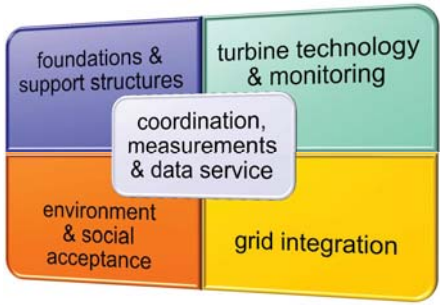

RAVE – measurements

coordination, measurements & data service

Environmental investigations | Turbine-specific measurements

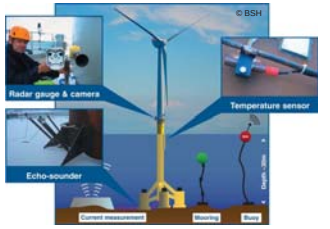

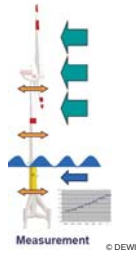

RAVE – measurements

coordination, measurements & data service

- Detailed Load and turbine data from four wind turbines
- LiDAR (upwind and downwind)
- SCADA data of all turbines
- Geological, oceanographic and environmental data
- Electrical data from substations
- Meteorological data from FINO1

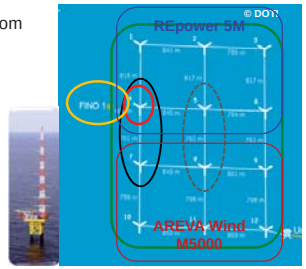

RAVE – measurements

coordination, measurements & data service

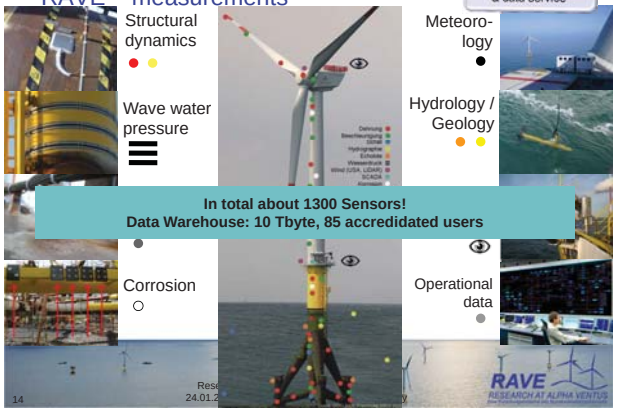

RAVE 2012: exemplary research results

foundations & support structures

- Development and test of non invasive methods to monitor imperfections
- Development of a monitoring device/tool for grouted joints
- Wave load models: real/measured loads from breaking waves will be included in future design

RAVE 2012: exemplary research results

turbine technology & monitoring

- Lidar based control can improve the energetic output of a turbine by 1-2 %
- Progress in turbulence and wake simulation and in understanding turbulence interaction between offshore wind farms
- An operation and failure statistics data base is of high relevance – progress is underway

RAVE 2012: exemplary research results

environment & social acceptance

- Bubble curtains reduce pile driving noise emission effectively
- Operational sound is of lower ecological relevance
- Social acceptance increased 2011 compared to 2009;

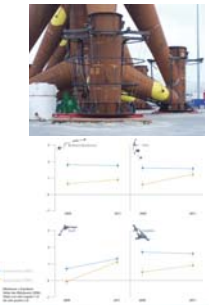

RAVE 2012: exemplary research results

grid integration

- Offshore-specific wind power forecasts and power fluctuation forecasts
- Control of offshore wind farm clusters

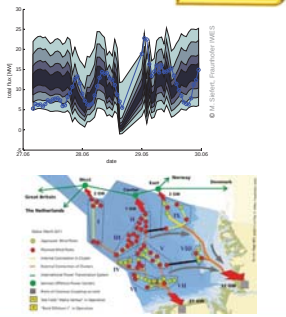

RAVE

RAVE has achieved its goals:

- Proven the offshore-capability of the 5 MW turbine class
- Facilitated further development of offshore wind technology in many areas
- Improved the knowledge about offshore wind utilisation
- Produced an invaluable and unique data set of measurements

RAVE will continue, but the focus will move:

- from design and erection to operation and maintenance
- from demonstration to research

What is RAVE today?

- A research lab in the middle of the North Sea
- A huge unique set of measurement data
- A research community dedicated to OWP
- An interdisciplinary knowledge base for OWP topics

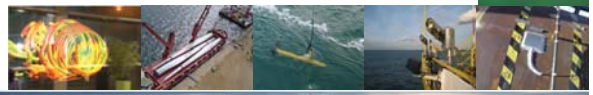

Technology Monitoring

Scientific **M**easurement and **E**valuation **P**rogram („250 MW Wind“ (1989-2006))

193.000 monthly operation reports
and 64.000 Incident reports
from 1.500 wind turbines

Technology development

Learning curves

Reliability

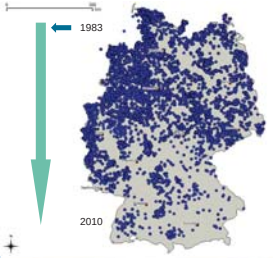

Technology Monitoring

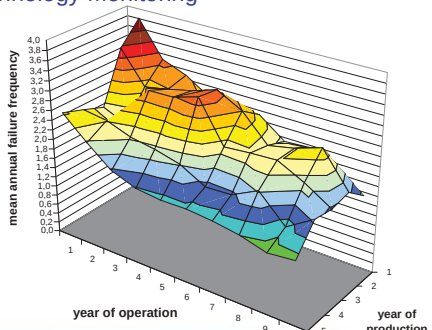

Technology Monitoring

To answer fundamental questions on development of wind power offshore

➔General monitoring

To optimize operation and maintenance

➔Systematic collection and evaluation of operational experiences

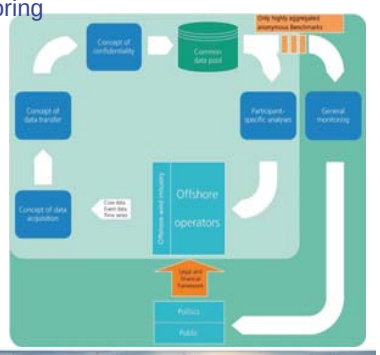

Thank you for your attention!

WWW.RAVE-OFFSHORE.DE

- with info about the individual research projects

WWW.RAVE2012.DE

- presentation slides of the International Conference RAVE 2012

RAVE SCIENCE DOCUMENTARY
“Challenge Offshore”

- www.youtube.com/user/RAVEoffshore/videos

The WindFloat Project

WindFloat 2 MW Floating Offshore Wind

Trondheim, 24th of January, 2013

Why Floating Offshore Wind?

Why Offshore Wind?

- Higher wind resource and less turbulence
- Large ocean areas available
- Best onshore wind locations are becoming scarce
- Offshore wind, including deep offshore, has the capacity to deliver large amount of energy

Why Floating Offshore Wind?

- Limited locations with shallow waters (mostly in the North Sea)
- Most of the offshore wind resource is in deep waters
- Unlimited installation sites available
- Less restrictions for offshore deployments and reduced visual impacts
- Enormous potential around the world: PT, Spain, UK, France, Norway, Italy, the Americas, Asia …

The WindFloat Technology

The main characteristics of the WindFloat leads to High Stability even in rough seas

Turbine Agnostic

- Conventional turbine (3-blade, upwind)
- Changes required in control system of the turbine

High Stability Performance

- Static Stability - Water Ballast
- Dynamic Stability - Heave Plates and active ballast system
  - Move platform natural response above the wave excitation (entrained water)
  - Viscous damping reduces platform motions
- Efficiency – Closed-loop Active Ballast System

Depth Flexibility (>40m)

Assembly & Installation

- Port assembly – Reduced risk and cost
- No specialized vessels required, conventional tugs
- Industry standard mooring equipment

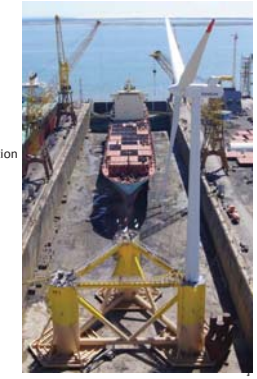

The WindFloat Technology

Due to the features of the WindFloat, the risk and cost of offshore works is significantly reduced

The WindFloat…

… requires **NO PILLING**

…is structurally **decoupled from seadbed**

…is **independent from depth**

…is **assembled and commissioned quayside**

…does **NOT require high lift capacity vessels**

Reduced Risk and Cost

The WindFloat Technology

WindFloat technology development – derived from an O&G concept and is now being tested full scale at sea

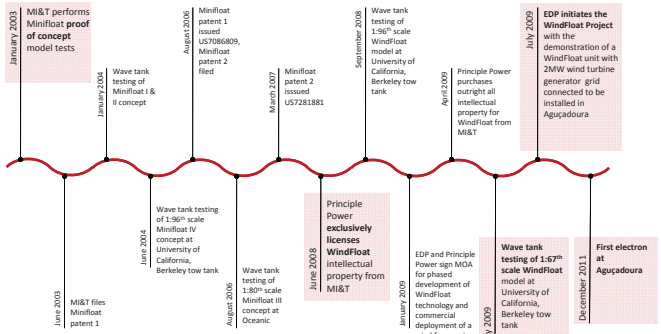

The WindFloat Project

The WindFloat project is structured to follow a phased / risk mitigation approach

Phase 1 – Demonstration

Capacity: 2MW WindFloat prototype
Location: Aguçadoura, grid connected
~6 km of coast, 40 - 50 m water depth
Turbine: 2MW offshore wind turbine
Test period: 24+ months

Phase 2 - Pre-commercial

Capacity: ~27MW (~5 WindFloat units)
Location: Portuguese Pilot Zone
Turbine: Likely Vestas and other, Multi MW

Phase 3 - Commercial

Capacity: 150MW, gradual build-out
Location: TBD
Turbine: TBD

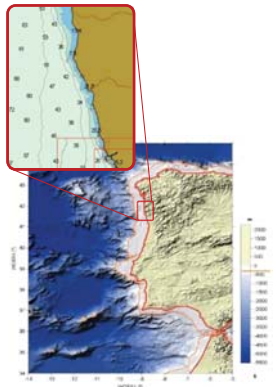

The WindFloat Project

The WindFloat project was structured as a Joint Venture, WindPlus

The Project is promoted by…

…in a joint venture…

WindPlus

…and counts with the support of…

The WindFloat Project

The development of the WindFloat project carried enormous challenges due to the lack of know-how in Portugal

The project followed a risk mitigation approach but…

…the challenges were enormous…

- …project being done for the first time
- …Lack of offshore know-how in Portugal
- …different cultures involved(US, Denmark, Portugal, France)
- …Collaboration between two different industries that have never worked together (Oil & Gas and Wind Industry)
- … Standards & Rules for design exist but need to adapted

The WindFloat Project

The project followed the typical stages of an engineering project

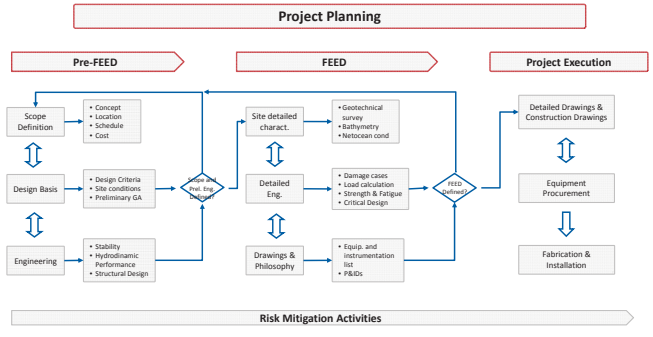

The WindFloat Project

Effective Risk Management must be embed into the project since the very early beginning

Risk Management methodologies implemented through out the project were key for the success of the project

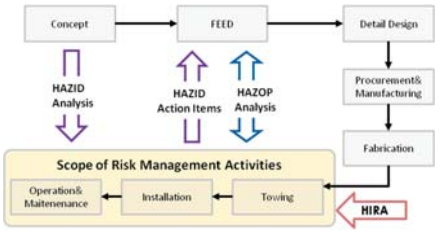

- **HAZID** – Hazard Identification Study
  - Conducted at an early stage of the project
  - Focus in the Project Execution stage
  - Provided inputs to the FEED stage
- **HAZOP** – Hazard and Operability Study
  - Several workshops conducted during FEED
  - Participants were the teams involved in the activities and engineering team
  - Provides input to the FEED stage
- **HIRA** – Hazard Identification and Risk Assessment
  - Workshop conducted prior to execution of the activities
  - Plan and procedures of each activities already defined
  - Outcome provides inputs to reduce the risk while executing the activities

The WindFloat Project

The project was implemented under a tight scheduled

Project was completed in less than 2,5 years
Fabrication completed in less than 9 months

Task	Timeline
Project Start	Sep, 09
Pre-FEED	Jan, 10
PDR	
FEED	Sep, 10
Turbine Selection	
Final Investment Decision	
Project Execution	Sep, 11
Detail Design	Sep, 11 – May, 11
Fabrication	Sep, 11
Offshore Installation	Nov, 11
Offshore Commisioning	Dez, 11
Testing and Monitoring	Ago, 13

Significant space to improve project implementation schedule!

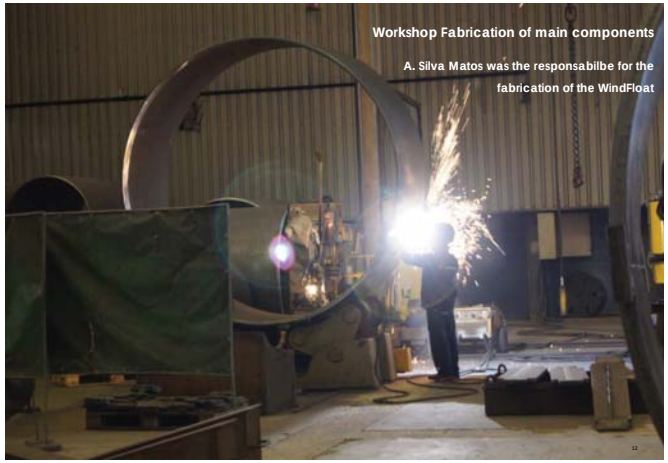

Pre-assembly of the columns outside the Dry-dock in Setúbal

Columns moved to Dry-dock

Dry-dock assembly

Mooring Pre-Lay in parallel with the fabrication

Turbine Installation in the Dry Dock using the shipyard's gantry crane

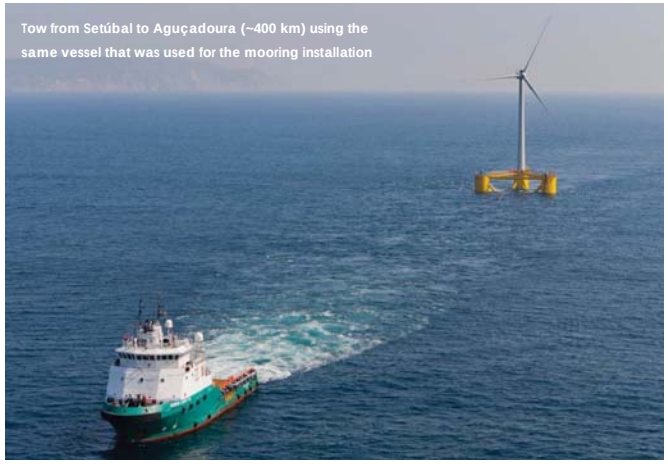

Tow from Setúbal to Aguçadoura (~400 km) using the same vessel that was used for the mooring installation

Preliminary performance analysis

The WindFloat is monitored 24 hours a day remotely

Preliminary performance analysis

Survivability and performance proved in normal and extreme conditions

22 Oct 2011
Installation complete

01 Nov 2011
15 meters wave

20 Dec 2011
First Electron produced

03 Jan 2012
Operation in Hs=6m and Hmax=12,6m

Conclusions

- The fabrication and installation were successfully complete despite all the challenges faced
- The technical results of the first 6 months of operation of the WindFloat are very promising
- The testing and monitoring of the WindFloat will continue during the next years
- WindPlus will start to prepare the Pre-Commercial phase
- One step towards the development of deep offshore wind

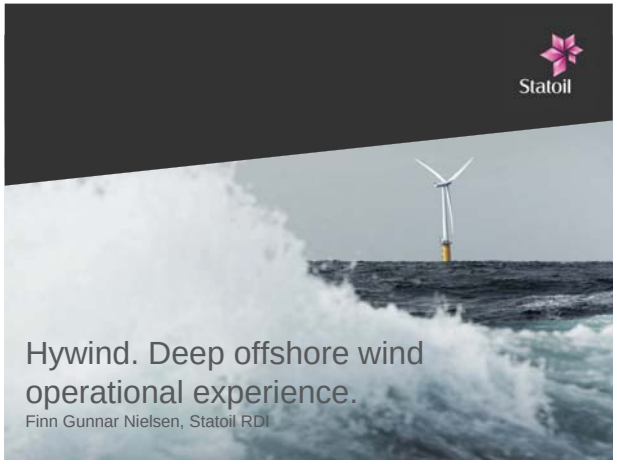

Hywind. Deep offshore wind operational experience.

Finn Gunnar Nielsen, Statoil RDI

The starting point -2001

- Inspired by floating sailing marks.
  - "Seawind" matured during 2002

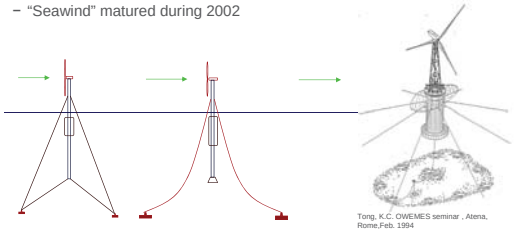

Tong, K.C. OWEMES seminar , Atena, Rome,Feb. 1994

The Hywind concept

Key features

Combines known technologies
Designed for harsh environment
"Standard" offshore turbine
Water depth >100 m
Assembled in sheltered waters, towed to field

Relies upon experience from :

Floating platforms
Electrical power production
Onshore wind turbines

From idea to commercial concept

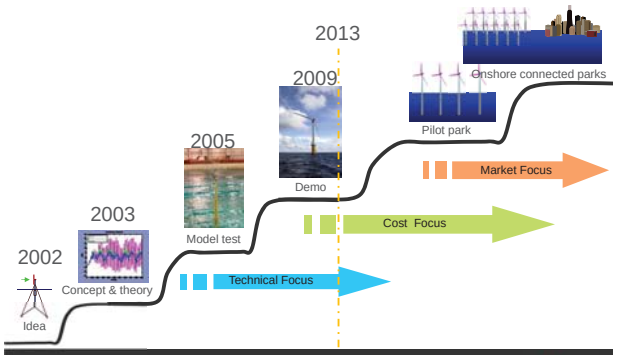

What does it take?

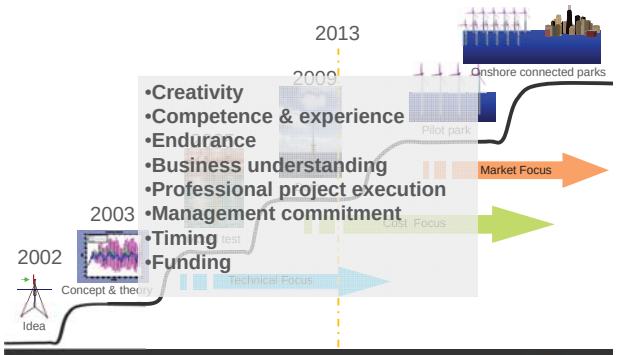

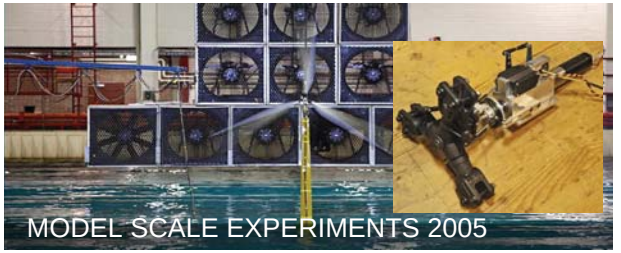

MODEL SCALE EXPERIMENTS 2005

- Demonstration of system behaviour
- Validation of numerical tools
- Model scale 1:47
- Irregular waves, turbulent wind, and various control strategies

Assembly and installation of Hywind Demo Summer 2009

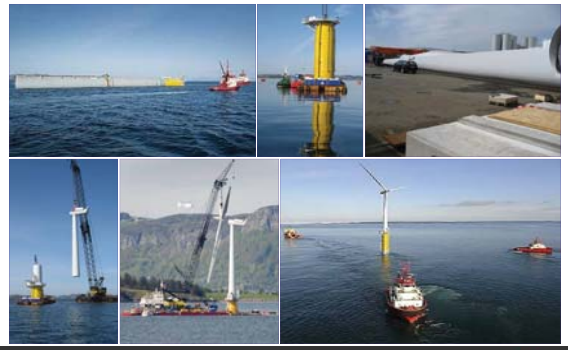

Operation in harsh environment

- Max wind velocity: 40 m/sec
- Max sign wave height: 10.5 m

Full scale measurements

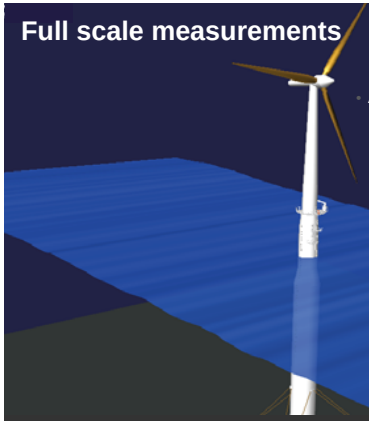

- A total of more than 200 sensors:
  - Waves wind and current (magnitude and direction)
  - Motion (6 DOF) and position of floater
  - Mooring line tension
  - Strain gauges at tower and hull (4 levels – bending moments and axial force)
  - Rotor speed, blade pitch and generator power
  - Flap- and edgeways rotor bending moments
  - Motion (tower pitch) / blade pitch controllers

Hywind Operation and monitoring

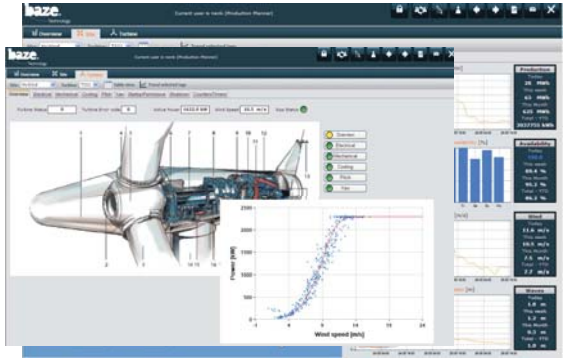

Integrated Operations – implementing O&G experience

- Integration of people process and technology
- Use of data, collaborative technology and multidisciplinary work

A base for testing vessels and access systems

- Fob Trim, Stril Merkur (MSDC12), Buddy, Fob Swath1, Bayard 3
- Undertun prototype access system, MaXccess access system

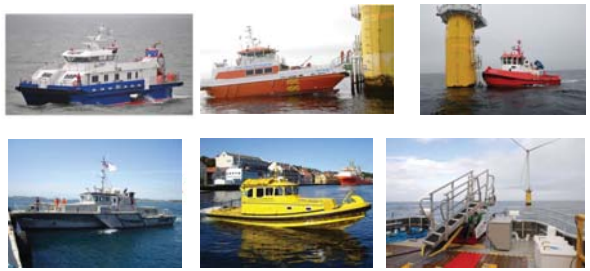

Hywind performance in 2012

- 2 stops in Q1 due to external grid faults, total 57 days. Production loss of ~1,5 GWh
- Production 2012 is 7,4 GWh (8,9 GWh without grid error)
- 11% lower than normal wind speed
- Capacity factor 2012: 37% (would be 44% without grid error)
- September production 1,1 GWh, Capacity factor 54%.
- Focus on improvements, lower O&M cost

Grid faults

Production during a storm condition

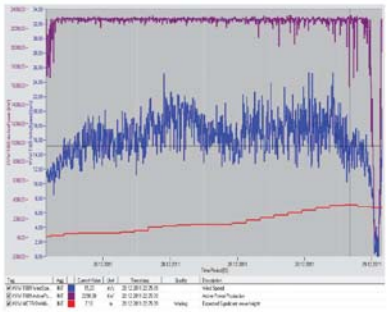

- 24 hour period during storm "Dagmar", Dec 2011
- Avg. wind speed 16 m/sec
- Max wind speed 24 m/sec
- Max significant wave height 7.1m
- Power production 96.7% of rated

Metocean data. Measured versus design basis

Wind statistics

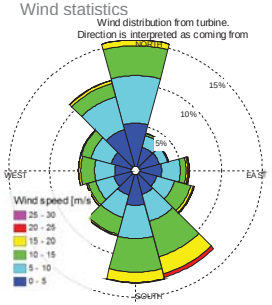

Nacelle wind distribution

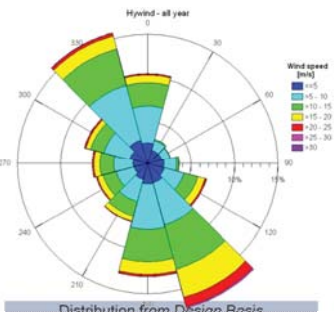

Distribution from Design Basis

Data interpretation and validation

- Spectrogram of mooring line force
- 1 month of data shown
- Used for:
  - Error detection
  - Identification of natural frequencies.

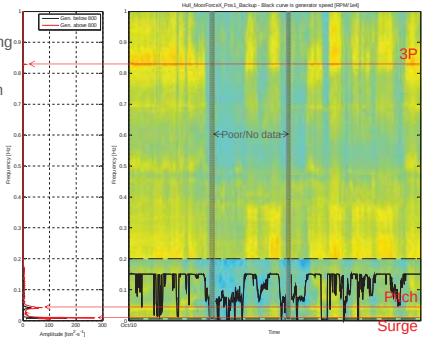

Full scale versus computations

- Wind speed 17.5 m/sec, Significant wave height 4.0m, Current 0.4 m/sec
- Estimated wave time history.
- Computed motion response
- Wind forces included from measured wind spectrum
- Visualization

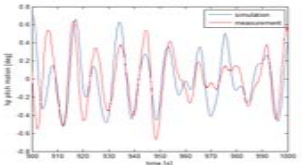

Tower pitch motion

Bending moment in tower.

- Mean wind: 13.2 m/s Hs: 3.2 m Tp: 9.0 s
- East – West and North – South axis

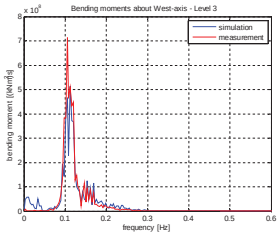

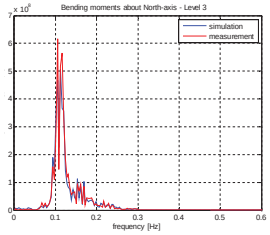

Importance of motion controller

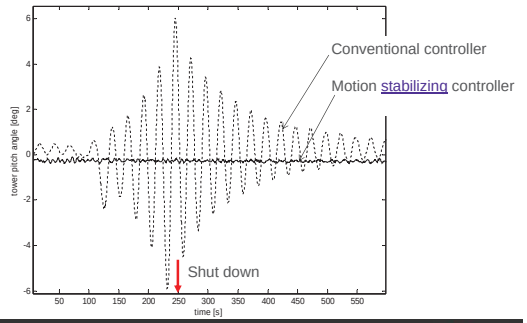

19

Hywind evolution

Use of experience - Improved design

Hywind Demo Hywind II

- Bigger turbine
- Smaller hull
- Lower costs
- Site specific

20

Floating wind will compete with conventional bottom fixed solutions in a mature market

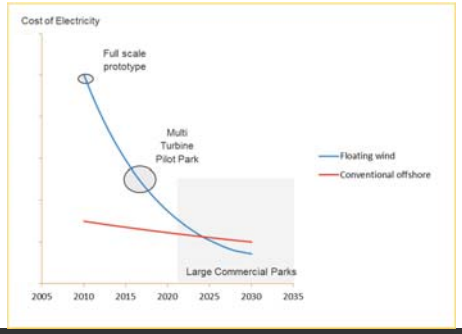

21

The next step

22

23

A1 New turbine technology

Design Optimization of a 5 MW Floating Offshore Vertical Axis Wind Turbine, Uwe Schmidt Paulsen, Technical Univ. of Denmark, DTU

Operational Control of a Floating Vertical Axis Wind Turbine,
Harald Svendsen, SINTEF Energi AS

Control for Avoiding Negative Damping on Floating Offshore Wind Turbine,
Prof Yuta Tamagawa, Uni. of Tokyo

Towards the fully-coupled numerical modelling of floating wind turbines,
Axelle Viré, Imperial College, London

Geometric scaling effects of bend-twist coupling in rotor blades,
Kevin Cox, PhD stud, NTNU

Design Optimization of a 5MW Floating Vertical-Axis Wind Turbine

DeepWind'2013-10th Deep Sea Offshore Wind R&D Conference
24-25 January 2013 Trondheim, No

Uwe Schmidt Paulsen[a]
uwpa@dtu.dk

[b]Helge Aagård Madsen, Per Hørlyck Nielsen
[c]Jesper Henri Hattel, Ismet Baran

[a,b] DTU Department of Wind Energy, Frederiksborgvej 399 Dk-4000 Roskilde Denmark
[c] DTU Department of Mechanical Engineering, Produktionstorvet Building 425 Dk-2800 Lyngby Denmark

DTU Wind Energy
Department of Wind Energy

DeepWind
Contents

DeepWind
Contents

DeepWind
The Concept

- No pitch, no yaw system

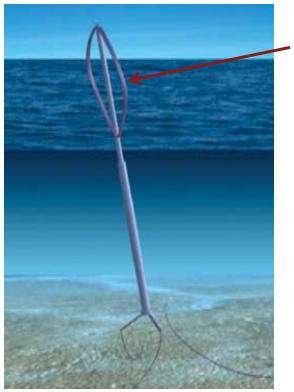

- Light weight rotor with pultruded blades

DeepWind
The Concept

- No pitch, no yaw system
- Floating and rotating tube as a spar buoy

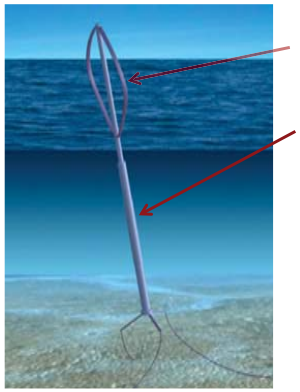

- Light weight rotor with pultruded blades
- Long slender and rotating underwater tube with little friction

DeepWind
The Concept

- No pitch, no yaw system
- Floating and rotating tube as a spar buoy
- C.O.G. very low – counter weight at bottom of tube

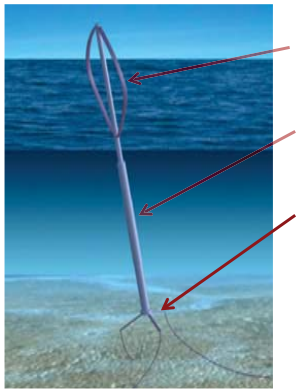

- Light weight rotor with pultruded blades
- Long slender and rotating underwater tube with little friction
- Torque absorption system

DeepWind
The Concept

- No pitch, no yaw system
- Floating and rotating tube as a spar buoy
- C.O.G. very low – counter weight at bottom of tube
- Safety system

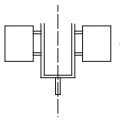

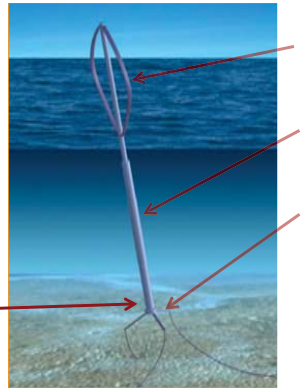

- Light weight rotor with pultruded blades
- Long slender and rotating underwater tube with little friction with little friction
- Torque absorption system

DeepWind
The Concept

- No pitch, no yaw system
- Floating and rotating tube as a spar buoy
- C.O.G. very low – counter weight at bottom of tube
- Safety system

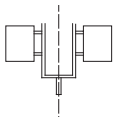

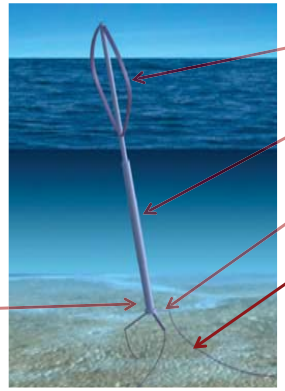

- Light weight rotor with pultruded blades
- Long slender and rotating underwater tube with little friction
- Torque absorption system
- Mooring system

DeepWind
The Concept- Blades technology

- The blade geometry is constant along the blade length

DeepWind
The Concept- Blades technology

- The blade geometry is constant along the blade length
- The blades can be produces in GRP

DeepWind
The Concept -Blades technology

- The blade geometry is constant along the blade length
- The blades can be produces in GRP
- Pultrusion technology:

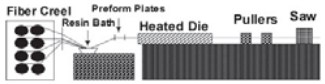

outlook- 11 m chord, several 100 m long blade length

DeepWind
The Concept- Blades technology

- The blade geometry is constant along the blade length
- The blades can be produces in GRP
- Pultrusion technology:

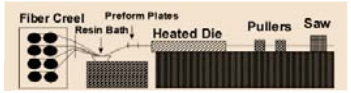

outlook- 11 m chord, several 100 m long blade length

- Pultrusion technology could be performed on a ship at site

DeepWind

The Concept- Blades technology

- The blade geometry is constant along the blade length
- The blades can be produces in GRP
- Pultrusion technology:

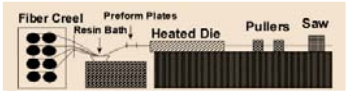

outlook- 11 m chord, several 100 m long blade length

- Pultrusion technology could be performed on a ship at site
- Blades can be produced in modules

DeepWind

Concept- Generator configurations

- The Generator is at the bottom end of the tube; several configuration are possible to convert the energy

DeepWind

Concept- Generator configurations

- The Generator is at the bottom end of the tube; several configuration are possible to convert the energy
- Three selected to be investigated first:

DeepWind

Concept- Generator configurations

- The Generator is at the bottom end of the tube; several configuration are possible to convert the energy
- Three selected to be investigated first:
  1. Generator fixed on the torque arms, shaft rotating with the tower

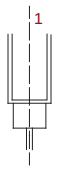

DeepWind

Concept- Generator configurations

- The Generator is at the bottom end of the tube; several configuration are possible to convert the energy
- Three selected to be investigated first:
  1. Generator fixed on the torque arms, shaft rotating with the tower
  2. Generator inside the structure and rotating with the tower. Shaft fixed to the torque arms

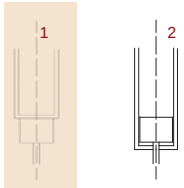

DeepWind

Concept- Generator configurations

- The Generator is at the bottom end of the tube; several configuration are possible to convert the energy
- Three selected to be investigated first:
  1. Generator fixed on the torque arms, shaft rotating with the tower
  2. Generator inside the structure and rotating with the tower. Shaft fixed to the torque arms
  3. Generator fixed on the sea bed and tower. The tower is fixed on the bottom (not floating).

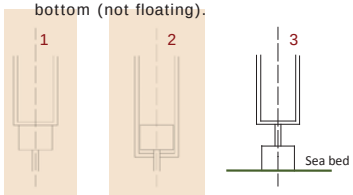

DeepWind

Concept- Installation, Operation and Maintenance

- INSTALLATION
  - ✓Using a two bladed rotor, the turbine and the rotor can be towed to the site by a ship. The structure, without counterweight, can float horizontally in the water. Ballast can be gradually added to tilt up the turbine.
- O&M
  - ✓Moving the counterweight in the bottom of the foundation is possible to tilt up the submerged part for service.
  - ✓It is possible to place a lift inside the tubular structure.

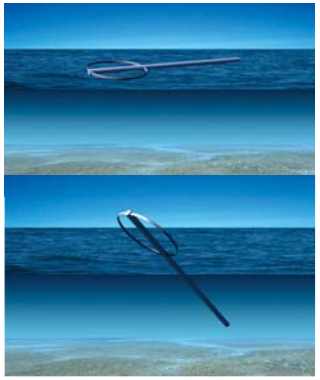

Rotor and Blades Design

1 st BaseLine 5 MW Design Performance

Performance		
Rated power	[kW]	5000
Rated rotational speed	[rpm]	5.26
Rated wind speed	[m/s]	14
Cut in wind speed	[m/s]	5
Cut out wind speed	[m/s]	25

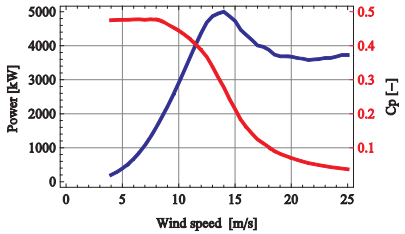

DeepWind

1 st BaseLine 5 MW Design Floater

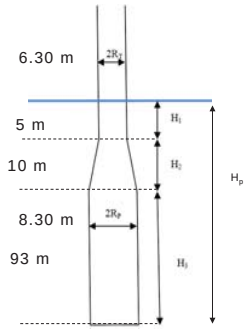

Geometry		
Total length ($H_p=H_1+H_2+H_3$)	[m]	108
Depth of the slender part (H_1)	[m]	5
Radius of the slender part (R_T)	[m]	3.15
Thickness of the slender part	[m]	0.02
Length of the tapered part (H_2)	[m]	10
Length of the bottom part (H_3)	[m]	93
Maximum radius of the platform (R_P)	[m]	4.15
Thickness of the bottom part	[m]	0.05

DeepWind

1 st BaseLine 5 MW Design Blades

- blade weight 154 Ton
- blade length 187 m
- Blade chord 7.45 m constant over length
- All GRP
- NACA 0018 profile

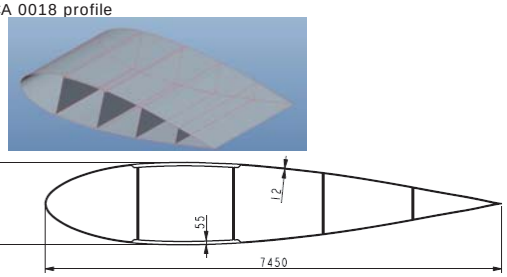

DeepWind

Contents

DeepWind

Optimization process

- Sensitivity analysis: rotor mass does not affect floater design significantly
- Determine the Rotor Power and Thrust curve, then

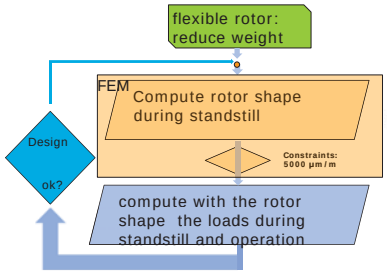

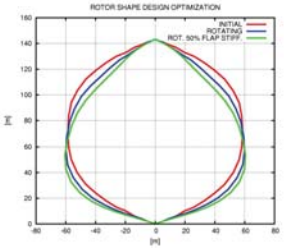

DeepWind

2 nd iteration 5 MW Design Rotor

Geometry

Rotor radius (R_0)	[m]	58.5
$H/(2R_0)$	[-]	1.222
Solidity ($\sigma = Nc/R_0$)	[-]	0.15
Swept Area (S_{ref})	[m²]	12318

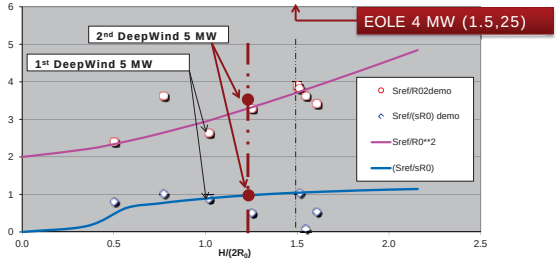

DeepWind

2 nd iteration 5 MW Design Rotor

Geometry

Rotor radius (R_0)	[m]	58.5 (-8%)
$H/(2R_0)$	[-]	1.222
Solidity ($\sigma = Nc/R_0$)	[-]	0.15 (-33%)
Swept Area (S_{ref})	[m²]	12318(+15%)

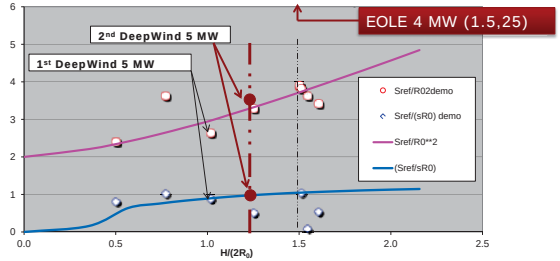

DeepWind

C_P vs thickness / profile

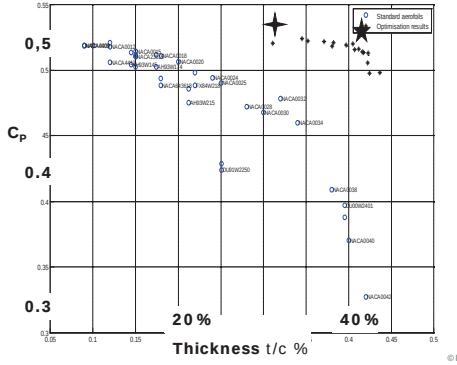

DeepWind

C_P vs dimensionless flapwise Inertia

(bending stiffness)

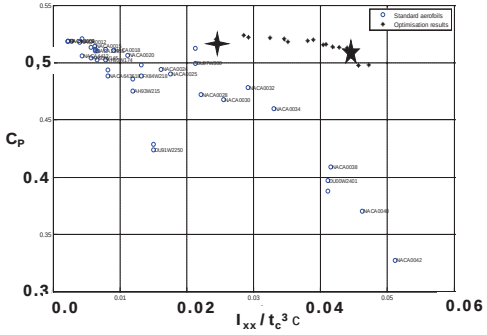

DeepWind

2 nd iteration 5 MW Design Rotor

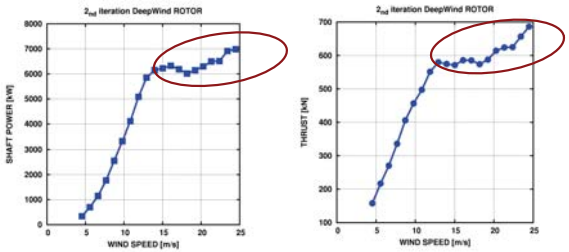

- uniform blade profiles NACA00xx, constant chord
- piecewise uniform profilesNACA0025,18,21, constant chord, Case-1,Case-2

DeepWind

Contents

DeepWind

Results uniform profiles Case-1

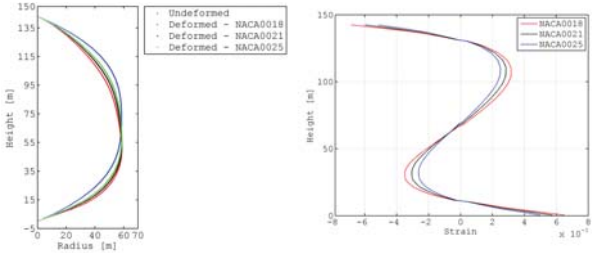

- Highest stiffness in NACA0025 profile leading the smallest displacement field and linear elastic strain level
- NACA0015 has the highest weight
- The tips of the rotor are fully constrained in all directions. Therefore, the maximum elastic strain occurs close to the tips.
- Apart from in the area of the tips, smaller strains, i.e. smaller than 5000 μm/m strain are obtained.

DeepWind

Results-Constant blade chord with different profile thickness Case-2

- Similar strain distribution for Case-2 as compared to the one obtained for the uniform rotor having the NACA0025 profile except at the middle section. are obtained.
- It should be noted that the total weight of the sectionized rotor in Case-2 is lower than the uniform rotor having the NACA0025 profile which has the highest stiffness.
- Using a thicker blade profile at the top (Case-2) decreases the strain values as compared to Case-1 in which a thicker profile is used at the middle

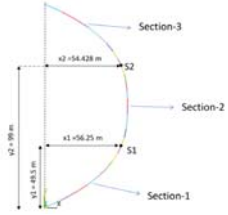

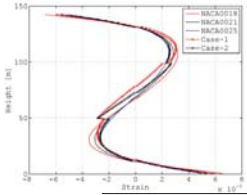

	Section-1 (Bottom)	Section-2 (Middle)	Section-3 (Top)
Case-1	NACA0025	NACA0021	NACA0018
Case-2	NACA0025	NACA0018	NACA0021

DeepWind

Results case-2

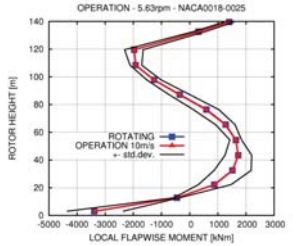

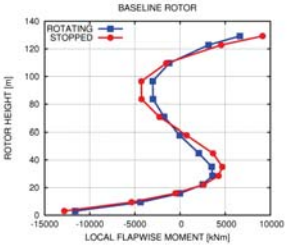

DeepWind

Results case-2

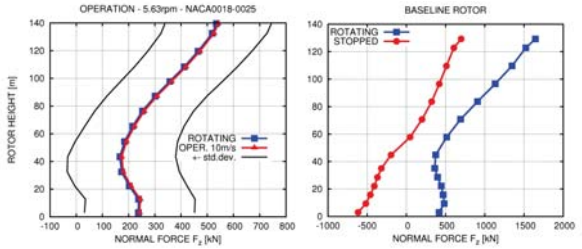

DeepWind

Results case-2+ 1iteration

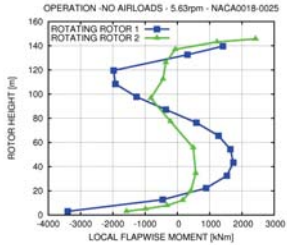

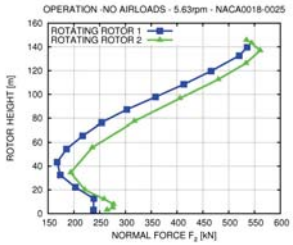

DeepWind

Contents

DeepWind

Conclusion

- Demonstration of a optimized rotor design
  - √Stall controlled wind turbine
  - √Pultruded sectionized GRF blades
  - √2 Blades with 2/3 less weight than 1st baseline 5MW design
  - √Less bending moments and tension during operation
  - √Potential for less costly pultruded blades
- Use of moderate thick airfoils of laminar flow family with smaller CD_0 and good C_P
- Exploration of potential for joints
- Investigation for edgewise vibrations due to deep stall behavior

DeepWind

Conclusion

10th Deep Sea Offshore Wind R&D conference
Trondheim, 24 – 25 Jan 2013

Operational Control of a Floating Vertical Axis Wind Turbine – *start-up and shut-down*

Harald G Svendsen
Karl O Merz

Overview

- Control system for the DeepWind turbine
- Start-up and shut-down scheme

The DeepWind concept

- Floating VAWT
- Rotating spar buoy
- Stall-regulated
- No pitch, no yaw, no gearbox
- Simple blade geometry, simple installation

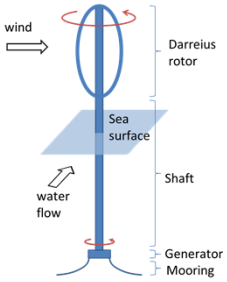

- EU FP7-project led by DTU ("DeepWind") – www.deepwind.eu

Control system

- Objectives
  - Maximise energy capture
  - 2p variations
  - Limit over-speed and over-torque
  - Start and stop
- How?
  - Via generator torque

Control architecture

- Basic structure:

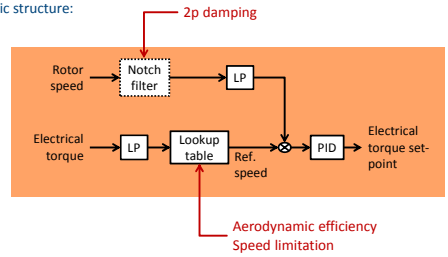

Simulation model

- **Aerodynamics:** Fourier approximation that includes 2p and 4p variations

$$T_{aero}(\psi, V, \Omega) = T_0 + T_2 \cos(2\psi + \psi_2) + T_4 \cos(4\psi + \psi_4)$$

  - ψ = turbine azimuth angle relative to the wind speed
  - $T_0, T_2, \psi_2, T_4, \psi_4$ given by look-up tables for wind = V and rotor speed = Ω, computed by a BEM model and includes dynamic stall effects (Merz)
- **Hydrodynamics and mooring system:** Bottom end assumed fixed except in yaw
  - Magnus lift force
  - torque absorption (one degree of freedom) spring–damper mooring system
- **Structural mechanics:** Spring–damper representations of tower twisting and tilting
- **Electrical system:** Generator torque = controller set-point

Turbine start-up and shut-down

- Achieved by adjusting the speed reference value
  - Start: 0 → target value
  - Stop: present value → 0
- Avoid conflict between normal/start/stop/parked operation by defining operational states

Operational states

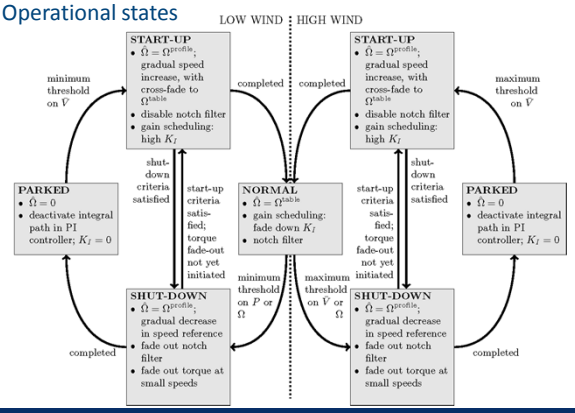

Normal operation

- Torque–speed map

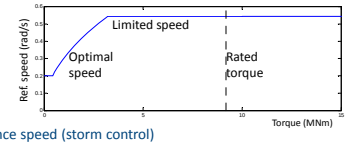

- High wind: Reduced reference speed (storm control)
  - Based on wind measurements
  - Limit torque
  - Capture more energy

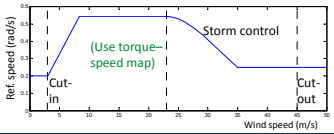

Start-up

- Speed ramp-up profile with end-point determined from slow-filtered wind measurement
- Cross-fade to speed reference given by torque–speed map (normal speed control)

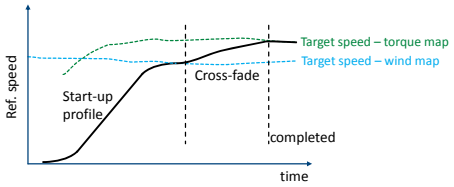

Start-up: Example (high wind)

- Smooth start
- Critical: Transition from ramp-up to steady speed
  - Increased integral gain for faster response during start

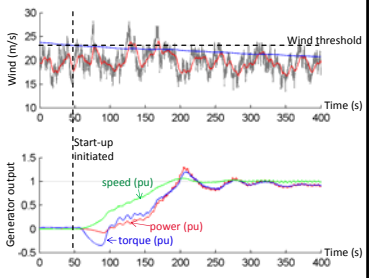

Shut-down

- Speed ramp-down to zero
- Extra torque needed to initiate shut-down
- Parked state: Reference speed = 0, integral path in PI control disabled

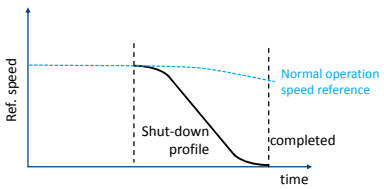

Shut-down: Example (high wind)

- Critical: Wind gust at the same time as braking is initiated
  → large torque

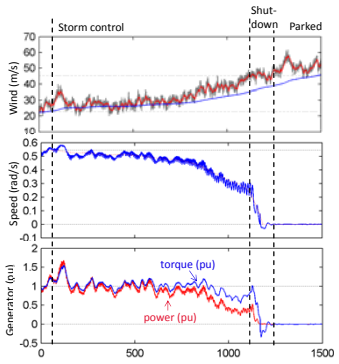

Conclusions

- Baseline control system for the Deepwind floating VAWT turbine has been completed
  - Damps 2p variations
  - Minimises stress on mooring system
  - Maximises energy capture
  - Safe start-up and shut-down procedures

SINTEF

Technology for a better society

Basic parameters – initial 5 MW design

Parameter	Value
Under-water length	108 m
Darrieus rotor height	130 m
Darrieus rotor radius	64 m
Rated wind speed	14 m/s
Rated rotational speed	0.52 rad/s (5 rpm)
Rated torque	$9 \cdot 10^6$ Nm

Control architecture

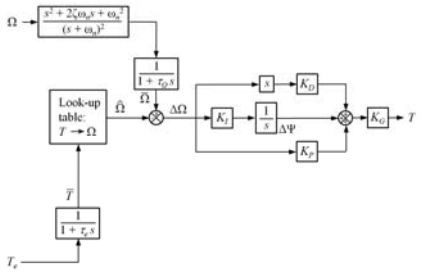

Control for Avoiding Negative Damping on Floating Offshore Wind Turbine

2013/1/24
Yuta Tamagawa, Tokyo univ.
Makoto Iida, Tokyo univ.
Chuichi Arakawa, Tokyo univ.
Toshiki Chujo, NMRI

Introduction

- Demand for renewable energy is increasing
  - Securing laying area for wind farm
  - Wind is consistent and strong over the sea
  - ⇨ Establish offshore wind turbine technology
  - – Floating Wind Turbine
    - Able to use on Deep Water
    - Unstable foundation

Verification test cases
・ Hywind (statoil, Norway)
・ Small test turbine (Nagasaki Japan)

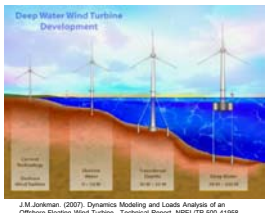

J.M.Jonkman. (2007). Dynamics Modeling and Loads Analysis of an Offshore Floating Wind Turbine. Technical Report. NREL/TP-500-41958. November 2007

Negative damping of Floating Wind Turbine

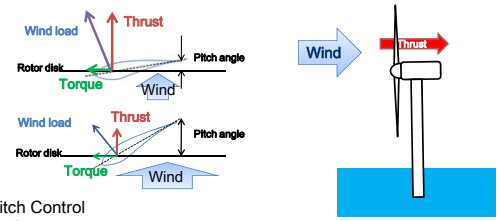

- Pitch Control
  Change blade pitch depend on the wind speed variation.
  – Torque : Constant ⇔ Thrust : Vary
- Relative wind speed vary dew to the motion of tower.
  – Lean to the front (back) ⇨ Relative wind speed increase (decrease) , Thrust decrease (increase)

⇨ *Negative damping*

Purpose of research

- Applying conventional pitch control

  ⇩

  Motion of float is negative damped

  ⇩

  Reducing rated power
  (Power decrease)
  Increasing fatigue load

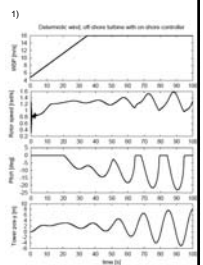

Larsen, T. J., & Hanson, T. D. (2007). A method to avoid negative damped low frequent tower vibrations for a floating, pitch controlled wind turbine. *Journal of Physics: Conference Series, 75*

- We needs to develop new pitch control corresponding to floating wind turbine

We propose a new control method for floating turbine to suppress the negative damping with power kept to rate.

Control method

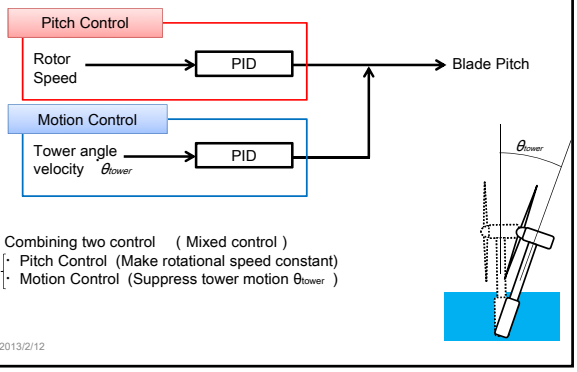

Combining two control (Mixed control)
・ Pitch Control (Make rotational speed constant)
・ Motion Control (Suppress tower motion θtower)

Experiment and Simulation

- Set floating wind turbine model on test tank with fan.
  (Cooperated with NMRI : National Maritime Research Institute)

Test tank and turbine model

- Software for numerical simulation : FAST
  ・ Developed by NREL (National Renewable Energy Laboratory)
  ・ Able to compute floating wind turbine (NREL 5MW)

J.M.Jonkman. (2007). Model Development and Analysis of an Offshore Wind Turbine on a Tension Leg Platform, with a Comparison to Other Floating Turbine Concepts. Subcontract Report. NREL/SR-500-45891. February 2010

Turbine and condition

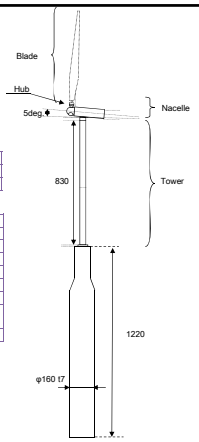

Wind speed [m/s]		3.9			
Wave (regular)	Height [cm]	4.22	6.3	8	8.7
	Period [s]	3.0	2.5	1.8	1.4

Wind turbine	Blade	Length	600mm
		Number	3
		Rotor diameter	1300mm
	Nacelle	Weight	1150g
	Tower	Hub height	900mm
Float	Float	Diameter	160mm
		Draft	1270mm
		Displaced volume of water	23kg
	Mooring line	Number	6

Validation of simulation

Blade load (Thrust)

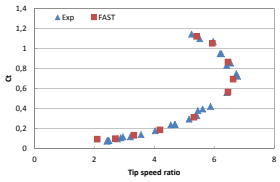

Thrust coefficient of test turbine in onshore.
(Change blade pitch on wind speed 3.9 m/s)

Float response to the wave

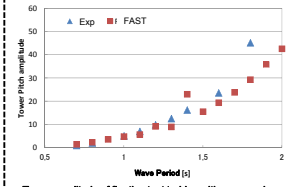

Tower amplitude of floating test turbine with wave and no wind.
(Tower amplitude is non-dimensionalized by wave height and wave number)

- Aero dynamic force of blade and float response to the wave are generally consistent

Negative damping on experiment

(Wind speed:3.9m/s, Wave period:2.5s, Wave height:6cm)

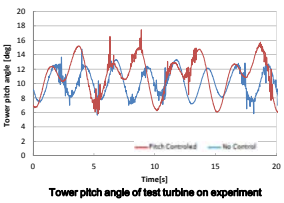

Tower pitch angle of test turbine on experiment

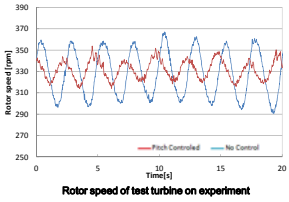

Rotor speed of test turbine on experiment

- Tower pitch amplitude : increase ⟺ rotor speed vibration : decrease
- Negative damping has occurred on experiment

Negative damping on simulation

(Wind speed:3.9m/s, Wave period:2.5s, Wave height:6cm)

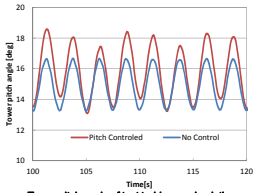

Tower pitch angle of test turbine on simulation

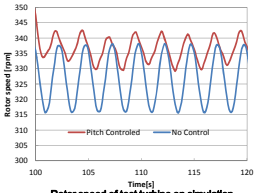

Rotor speed of test turbine on simulation

- Tower motion and rotor speed vibration are smaller than experiment.
- Trends of parameter are matched with experiment.

Mixed control on simulation

(Wind speed:3.9m/s, Wave period:2.5s, Wave height:6cm)

- K_p: Control parameter of motion controller on mixed control.
- Basis of rate on right side is parameter on conventional control. (when K_p=0)

Control parameter K_p	Θ_{tower} Amplitude (deg)	Rotor speed average (rpm)
0	5.51 (100%)	336 (100%)
0.0001	5.38 (97.6%)	336 (99.97%)
0.001	5.24 (95.1%)	335 (99.7%)
0.01	3.70 (67.2%)	326 (97.1%)
0.1	5.01 (91.0%)	239 (71.3%)
1	5.32 (96.6%)	74.7 (22.2%)

- As K_p=0.01, Tower motion is much suppressed though rotor speed is not so much changed.

➡ Mixed control can suppress the negative damping with little affect to the rotor speed.

Conclusion

- On simulation aero dynamic force of blade and float response to the wave are generally match to experiment.
- We confirmed that tower motion is amplified by onshore pitch control on experiment and simulation.
- We proposed the new control, mixed control, and shows that mixed control can reduce the tower motion with maintaining rotor speed.

Further study

- Improving simulation model, we will apply this control to practical turbine, verification test turbine or full scale turbine and investigate the applicability and effectiveness of this control in actual seas.

Imperial College London

1. Modelling fluid-solid interations

Coupling between two unstructured finite-element models

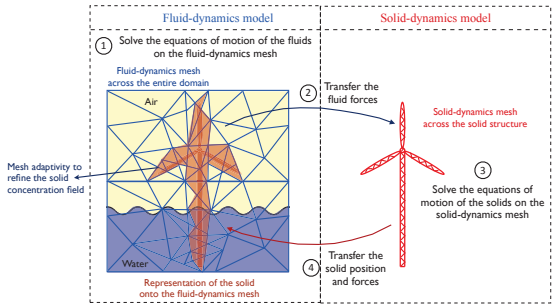

A.Viré, Reviews in Environmental Science and Bio/Technology (2012)

Imperial College London

Towards the fully-coupled numerical modelling of floating wind turbines

Axelle Viré, J Xiang, M Piggott, C Cotter, J Latham, C Pain

avire@imperial.ac.uk
Applied Modelling and Computation Group (AMCG)
Department of Earth Science and Engineering

10th Deep Sea Offshore Wind R&D Conference – 24 January 2013

Imperial College London

1. Modelling fluid-solid interations

Coupling between two unstructured finite-element models

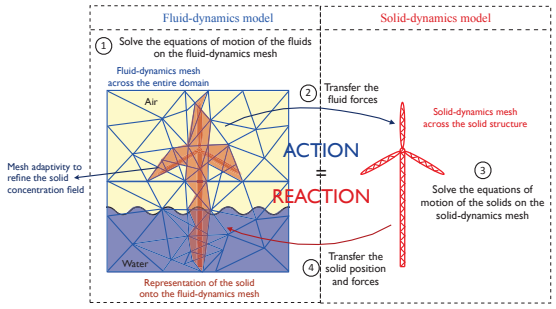

The fluid and solid models use different spatial and temporal discretisations

A.Viré, Reviews in Environmental Science and Bio/Technology (2012)

Imperial College London

Motivation

Scope of a 2-year Marie Curie Intra-European Fellowship

- Couple two finite-element models for modelling fluid-structure interactions
- Apply them to the various components of a floating wind turbine

Photo: Trude Refsahl/Statoil

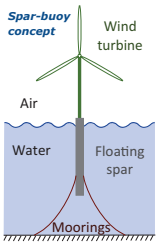

Imperial College London

1. Modelling fluid-solid interations

Fluid-dynamics model: Fluidity-ICOM

$$\bar{\nabla}\cdot\bar{u}=0 \qquad (\rho_f=\text{constant})$$

$$\rho_f\frac{\partial\bar{u}}{\partial t}+\rho_f\left(\bar{u}\cdot\bar{\nabla}\right)\bar{u}=-\bar{\nabla}p+\bar{\nabla}\cdot\bar{\bar{\tau}}+\bar{F}_f$$

- The equations are solved for a monolithic velocity: $\bar{u}=\alpha_f\bar{u}_f+\alpha_s\bar{u}_s$
- An additional force accounts for the presence of the solids:

$$\bar{F}_f=\beta\left(\alpha_s\bar{u}_s-\alpha_s\bar{u}\right)=\bar{F}_2-\bar{F}_1 \qquad \beta=\text{fct}\left(\frac{\rho_f}{\Delta t},\frac{\nu}{L^2}\right)$$

Solid-dynamics model: Y3D-Femdem

$$\frac{D}{Dt}(\rho_s\bar{u}_s)=\bar{\nabla}\cdot\bar{\bar{\tau}}_s+\bar{F}_s \qquad \bar{F}_s=\bar{F}_1-\bar{F}_2$$

Conservation

$$\boxed{\int_V F_f dV=-\int_{V_s}F_s dV_s}$$

Imperial College London

Outline

1. Modelling fluid-solid interations for floating solids
2. Parameterisation of wind turbines
   - Actuator-disk modelling
   - Results for a fixed turbine
3. Tracking of an interface between two fluids
   - Conservative advection method
   - Results for a floating pile
4. Future work

Imperial College London

1. Modelling fluid-solid interations

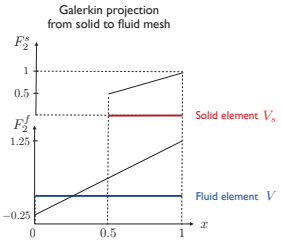

$$\int_{V_s} F_2^s dV_s = \int_V F_2^f dV$$

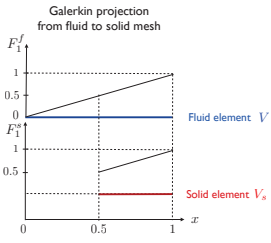

$$\int_{V \cap V_s} F_1^f dV_\cap = \int_{V_s} F_1^s dV_s$$

Imperial College London

1. Modelling fluid-solid interations

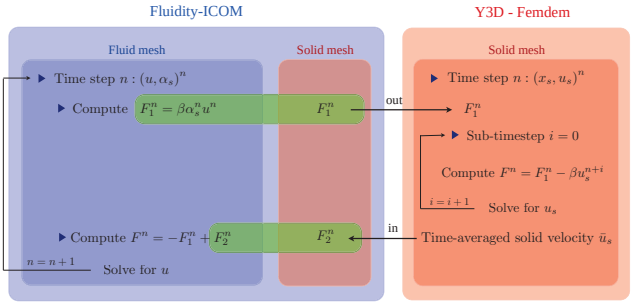

Viré *et al.*, Ocean Dynamics, Vol. 62 (2012)

Imperial College London

1. Modelling fluid-solid interations

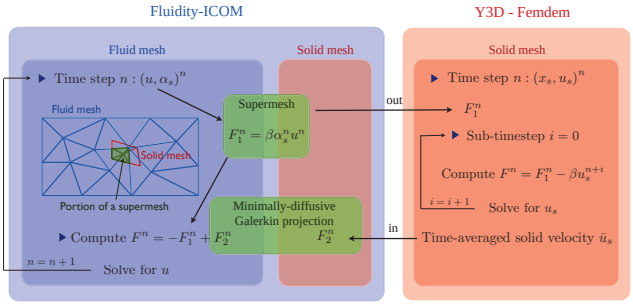

Viré *et al.*, Ocean Dynamics, Vol. 62 (2012)

Imperial College London

1. Modelling fluid-solid interations

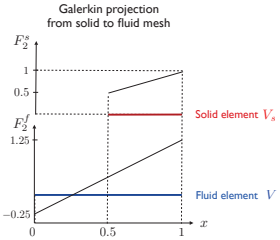

$$\int_{V_s} F_2^s dV_s = \int_V F_2^f dV$$

Imperial College London

2. Parameterisation of wind turbines

The turbine is parameterised through an actuator-disk model

(Conway, J Fluid Mech, 1995)

- The disk is meshed separately from the fluid domain
- The thrust force is spread uniformly across a thin disk

$$T = \frac{1}{2} \rho u_0^2 A_{hub} C_T$$

- The reference velocity u_0 is computed from C_T and u_{hub}

$$a = 1 - \frac{u_{hub}}{u_0} = \frac{1}{2} \left(1 - \sqrt{1 - C_T} \right)$$

- The fluid mesh is adapted dynamically in time

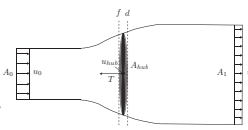

Imperial College London

1. Modelling fluid-solid interations

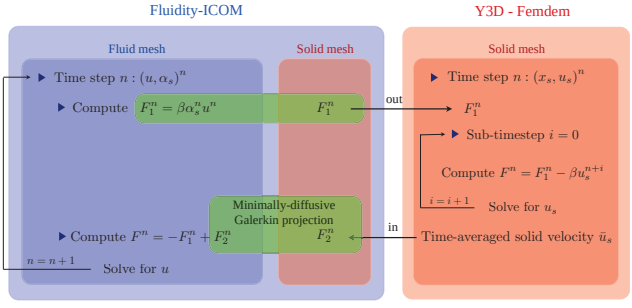

Viré *et al.*, Ocean Dynamics, Vol. 62 (2012)

Imperial College London

4. Next steps

- Detailed analysis of the results on the floating pile
- Assemble the turbine and the floating monopile
- Modelling of the mooring lines

Acknowledgements

European Commission: FP7 Intra-European Marie-Curie Fellowship

Applied Modelling and Computation Group: Prof Chris Pain, Dr Matt Piggott, Dr Jiansheng Xiang, Dr Patrick Farrell, Dr Colin Cotter, Dr Stephan Kramer, Dr Cian Wilson, Dr John-Paul Latham, Mr Frank Milthaler

Imperial College London

2. Parameterisation of wind turbines

Uniform flow past a 3D turbine of constant thrust coefficient and $Re_D = 1000$

- The size of the fluid domain is $25D \times 10D \times 10D$
- The disk thickness is 2% of the disk diameter D
- The fluid mesh adapts to the curvatures of the velocity and pressure fields
- Reference: Potential flow past an actuator disk with constant loading
  (J. Conway, J. Fluid Mech. 297, 327–355, 1995)

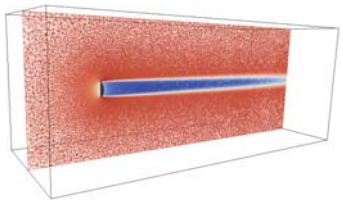

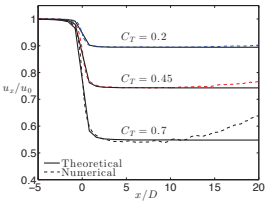

Imperial College London

3. Tracking of an interface between two fluids

Air-water flow with a half-submerged 3D pile

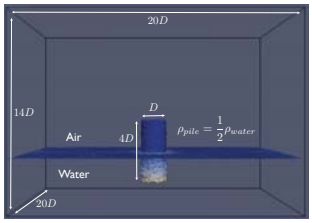

- The fluid phases are immiscible
- The fluid concentration field is α_f
- An advection-diffusion equation for α_f
- α_f is constant over the elements

Imperial College London

3. Tracking of an interface between two fluids

Air-water flow with a half-submerged 3D pile

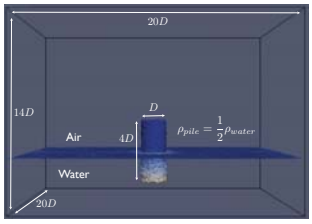

Geometric scaling effects of bend-twist coupling in rotor blades

Deep Sea Offshore Wind R&D Seminar
Royal Garden Hotel, Trondheim, Norway
24 January, 2013

Kevin Cox, PhD Candidate
kevin.cox@ntnu.no

Andreas Echtermeyer, Professor
andreas.echtermeyer@ntnu.no

Dept. of Engineering Design and Materials
NTNU, Norwegian University of Science and Technology

Outline

1. Motivation
2. Bend-twist coupling
3. Up-scaling relations
4. Design of baseline blades
5. Bend-twist (adaptive) blades
6. Load reduction
7. Control system
8. Mass reduction
9. Conclusions
10. Future work

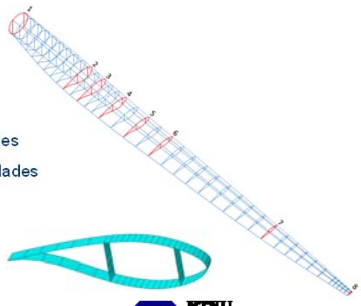

NTNU Norwegian University of Science and Technology

Motivation

- Mass and loads grow faster than power output
  f = scaled length/nominal length

$$m_s = f^3 m_n \qquad M_s^{aero} = f^3 M_n^{aero} \qquad M_s^{grav} = f^4 M_n^{grav} \qquad P_s = f^2 P_n$$

m = mass *M = bending moment* *P = Power*

- How can the loads and mass be reduced?
  - Materials → Mass
  - Control system → Loads
  - Adaptive blades → Mass and Loads

3

Bend-twist coupling

- Adaptive blade through passive technique
- Coupling from unbalanced composite layup
- Material design affects mass and loads

$$\varphi_{tip} = \frac{\alpha L^2 F}{2(1-\alpha^2)\sqrt{EIGJ}}$$

L = beam length
F = applied bending load
EI = beam bending stiffness
GJ = beam torsional stiffness
α = coupling coefficient

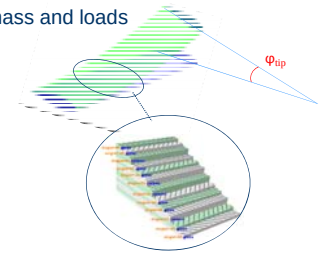

4

Up-scaling relations

- Does bend-twist coupling depend on blade geometry?
  - Nonlinear FE analysis
  - Linear scaling equations
- Flap load $F_n = \frac{1}{2}\rho A C_L V^2 \qquad F_s = f^2 F_n$
- Bending stiffness $GJ_s = f^4 GJ_n$
- Torsional stiffness $EI_s = f^4 EI_n$

$$\varphi_{tip} = \frac{\alpha L^2 F}{2(1-\alpha^2)\sqrt{EIGJ}} \qquad \varphi_s = \frac{f^2 f^2}{\sqrt{f^4 f^4}}\varphi_n = \varphi_n$$

5

Design of baseline blades

- 4 blades selected: 30-90m (1.6 – 13 MW)
- Carbon fiber used in spar flanges
- Biaxial glass fiber used in all regions
- 30, 50, 90m blades use only the NACA 64(3)-618 airfoil
- 70m blade is the 10MW NOWITECH blade
- Load applied: 70 m/s gust with 15° yaw error

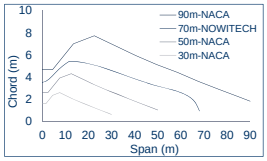

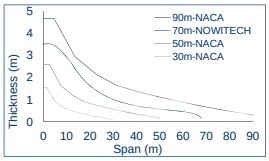

6

Results of baseline blades

Blade length	Carbon in flange (% mass)	Tip deflection (m)	1st flapwise freq. (Hz)
30m-NACA	19.52	4.08	1.443
50m-NACA	19.31	7.06	0.883
90m-NACA	19.27	13.22	0.489
70m-NOWITECH	35.37	4.78	0.698

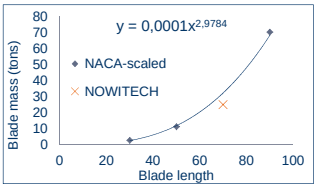

Bend-twist (adaptive) blades

- Carbon fibers rotated to 23º off axis in NACA blades
- Carbon fibers rotated to 20º off axis in NOWITECH blade
- Mass, geometry, composite layups, loads held constant

Blade	Tip Twist (deg)	Tip Def (m)	1st Flap Freq (Hz)	Carbon in flanges (% mass)
30m-NACA	6.96	147.30 %	80.80 %	19.52
50m-NACA	5.84	147.50 %	81.20 %	19.31
90m-NACA	6.16	146.30 %	81.45 %	19.27
70m-NOWITECH	6.56	170.20 %	76.47 %	35.37

- Tip twist ~ constant!

Bend twist coupling on load reduction

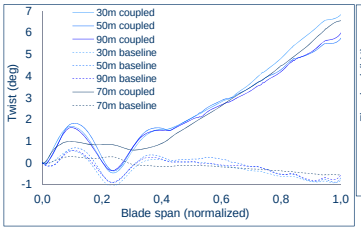

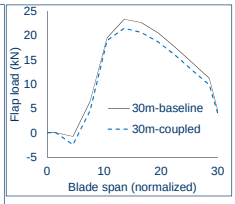

Blade	% Reduction in Flap Load	% Reduction in Bending Moment
30m-NACA	10.84	10.01
50m-NACA	10.83	9.25
90m-NACA	9.93	8.68
70m-NOWITECH	10.42	10.48

Bend-twist coupling on control system

- Further studies performed on 70m blade
  - Induced twist vs. wind speed (with and without control system)
  - Control system pitch angle vs. wind speed
    - Load reduction → C_p reduction
    - Constant C_p requires pitch back to stall → nullifies load reduction

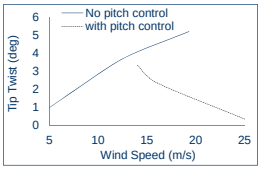

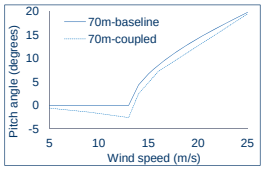

Bend twist coupling on blade mass

- Load reduction only effective for non-operating conditions
- Maximum load condition: 70 m/s gust
- 70m NOWITECH blade:

  10-11% reduction in flap load → 2.2% mass reduction

Conclusions

- 4 blades between 30 and 90m were designed
- Linear beam method: induced twist is independent of up-scaling
- Nonlinear FEA: agrees with linear beam
- However, velocity not actually constant
  - Increases with blade length (hub height) → higher loads
  - Higher loads → more induced twist on larger blades?
- Bend-twist coupling on flap load alleviation
  - Independent of blade size
  - 10-11% reduction with 6-7º tip twist (during 70 m/s gust)

Conclusions

- Bend-twist coupling on flap bending moment reduction
  - Independent of blade size (possibly more effective for smaller blades)
  - 9-10% reduction with 6-7º tip twist (during 70 m/s gust)
- Bend-twist coupling on control system
  - Induced pitch towards feather requires CS pitch towards stall
    - Nullifies load alleviation during operation
  - Load alleviation only effective during non-operational gusts
- Bend-twist coupling on blade mass
  - Reduction in maximum load allowed for lighter blade

13

NOWITECH Norwegian Research Centre for Offshore Wind Technology

Future studies

- All studies were performed as quasi-static analyses
  - How do the blades behave dynamically
    - Natural frequencies
    - Control system
    - Power collection
- Shear failure and damage evolution in the composite layup was not considered
- Additional blade designs to be studied to confirm results
- Consider other off-axis carbon angles: 10º and 15º
- Change % of carbon fibers in spar flanges

14

NOWITECH Norwegian Research Centre for Offshore Wind Technology

Thank you for your attention!

Kevin Cox, PhD candidate, NTNU
Dept. of Engineering Design and Materials
kevin.cox@ntnu.no

Andreas Echtermeyer, Professor, NTNU
Dept. of Engineering Design and Materials
andreas.echtermeyer@ntnu.no

NTNU
Norwegian University of Science and Technology

15

NOWITECH Norwegian Research Centre for Offshore Wind Technology

A2 New turbine technology

High Power Generator for Wind Power Industry: A Review,
Zhaoqiang Zhang, PhD stud, NTNU

Superconducting Generator Technology for Large Offshore Wind Turbines,
Niklas Magnusson, SINTEF Energi AS

Laboratory Verification of the Modular Converter for a 100 kV DC Transformer-less Offshore Wind Turbine Solution, Sverre Gjerde, PhD stud, NTNU

Multi-objective Optimization of a Modular Power Converter Based on Medium Frequency AC-Link for Offshore DC Wind Park, Rene A. Barrera, NTNU

High-power generators for offshore wind turbines

Presented by: Zhaoqiang Zhang (NTNU)

Authors: Zhaoqiang Zhang, Robert Nilssen, Arne Nysveen (NTNU)
Anyuan Chen, Alexey Matveev (SmartMotor)

Outline

- Introduction of this research
- Review of the generators in operational offshore wind farms
  - Average rating of turbine; Drive trains; Generators
- Generator mass
  - Problems description; Modeling approach; Optimization results
- Review of the solutions for high power generators
  - Direct-driven DFIG; Conventional radial-flux PM generators; Ironless PMSG; Super conducting generator; HVDC generator
- Conclusion

Introduction

- Objective:
  - Investigate the technological challengies related to the high-power generators for offshore wind turbines
  - High-power: >6MW

Generators in operational offshore wind farms (I)

- By the end of 2012, 1886 wind turbines installed in 57 offshore wind farms; total operational capacity of 5.45 GW.

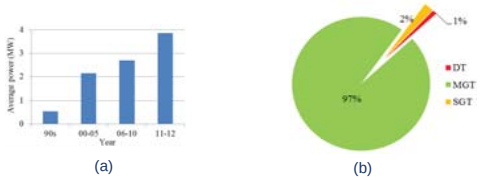

(a) (b)

Figure 1: (a) Development of average rating per turbine.
(b) Market share of drive trains.
DT: Direct drive Train; MGT: Multi-stage Geared drive Train; SGT: Single-stage Geared drive Train

Generators in operational offshore wind farms (II)

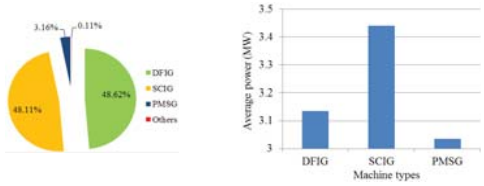

Figure 2: (a) Market share of different machine types
DFIG: Doubly-Fed Induction Generator; SCIG: Squirrel-Cage Induction Generator;
PMSG: Permanent Magnet Synchronous Generator
(b) Average power vs. machine types for 2008-2012.

Generator mass

- It is not clear how the structural mass evolves as the power grows.
- Estimation with scaling law gives much error.
- Structural design demands extensive knowledge on mechanical and structural analysis.
- In this paper
  - The total mass: estimated by statistically investigation of the commercial design and curve fitting;
  - Active mass: finite element analysis and optimization;
  - Supporting mass: Total mass-active mass

Modeling (I)

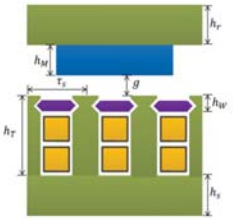

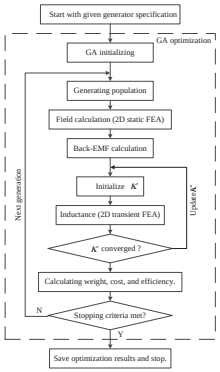

Modeling (II)

Table 1: Generator specification.

Quantity	Value				
Power (MW), P_N	6	7	8	9	10
Speed (rpm), n	14	13	12	11	10
Stator voltage (kV), U_N	3.3				
Phase number, m	3				
Air gap (mm), g	$0.001D_o$				
Fill factor, k_f	0.65				
1st AC resistance ratio, k_1,	1				
Staking factor, k_s	0.95				
PM B_r (T) at working temperature	1.2				
PM relative permeability	1.05				
Slot per pole per phase, q	1				
Number of parallel branch, a	1				
Slot wedge thickness (mm)	5				
Min. area of 1 turn coil (mm^2), S_T	5				
PM specific cost (€/kg)	80				
Copper specific cost (€/kg)	27				
Steel specific cost (€/kg)	16				

Table 2: Free variables.

Quantity	Range
Frequency (Hz), f	10-60
Outer diameter (m), D_o	6-10
PM thickness (mm), h_M	5-100
Thickness of rotor back iron (mm), h_r	5-100
Thickness of stator back iron (mm), h_s	5-100
Ratio of tooth height over tooth width, k_{sh}	4-10
Ratio of PM width over pole pitch, k_M	0.5-0.9
Ratio of tooth width over slot pitch, k_T	0.3-0.7
Current density (A/mm^2), J	2-5

Table 3: Constrains.

Quantity	Range
Slot pitch (mm), τ_s	>5
Flux density in yoke of stator and rotor (T)	<3
Electric load (kA/m), E_L	<50

Modeling (III)

- Total mass

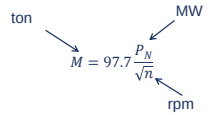

- Optimization objective
  - Cost function: cost of the active material
  - Constrain in efficiency: >95%

Optimization results (I)

- Mass and Cost

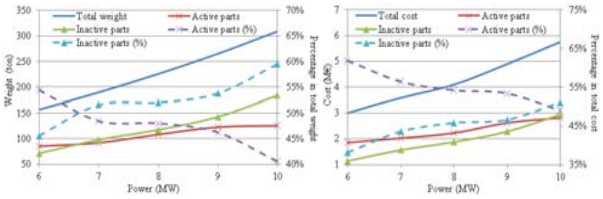

Optimization results (II)

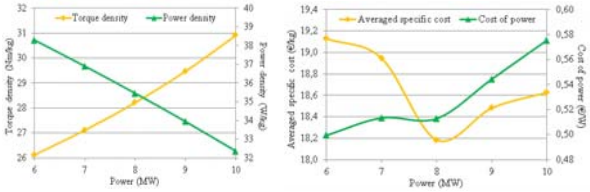

Solutions for high-power generators

- Industry and academic designs
- Less system components, less generator mass and higher efficiency are the concerns of these solutions.
  - Direct-driven DFIG
  - Conventional radial-flux PM generator
  - Ironless PM generator
  - Super conducting generator
  - HVDC generator

13

Direct-driven DFIG

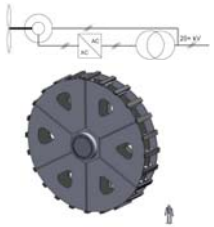

Quantity	Value
Power	10 MW
Speed	10 rpm
Stator voltage	23.5 kV
Rotor voltage	0.7 kV
Slip	0.2
Stator internal diameter	6 m
Pole number	600
Current density	2.5 A/mm^2
Magnetic load	0.6 T
Slot per pole per phase	1.5 (stator) and 2 (rotor)
Air gap	1 mm
Length	1.3 m
Efficiency	94%
Copper weight	30 ton
Laminations weight	36 ton
Construction weight	282 ton

14

Conventional radial-flux machine (I)

Quantity	Value
Power	10 MW
Speed	10 rpm
Stator diameter	10 m
Pole number	320
Slot per pole per phase	1
Air gap	10 mm
Pole number	600
Copper weight	12 ton
PM	6 ton
Lamination weight	47 ton
Construction weight	260 ton
Total	325 ton

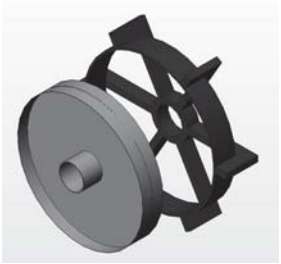

15

Conventional radial-flux machine (II)

Quantity	Value
Power	8 MW
Speed	11 rpm
Stator voltage	3.3 kV
Stator segments	12
Pole number	120
Slot number	144
Pole number	600
Air gap diameter	6.93 m
Length	1.1 m
Air gap	8.66 mm
Electric load	150 kA/m
Efficiency	92%
Copper weight	9.2 ton
Magnet weight	3.6 ton
Laminations weight	31 ton
Construction weight	NA

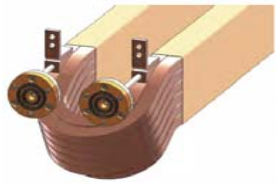

16

Ironless PM generator

6MW Generator Structure by BWP

6.5MW, 48 poles PM machine

17

Super conducting generator

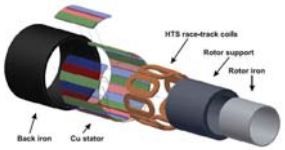

Rated power P_N (MW)	10
Poles	16
Diameter D_{gen} (m)	4.7
Length L_{gen} (m)	1.15
Rotation speed ω_{N_gen} (rpm)	10
Shaft torque τ_T (10^6 N m)	9.7
Mass superconductor m_{sc} (ton)	22
Mass Cu m_{Cu} (ton)	14
Mass Fe m_{Fe} (ton)	32
Mass glass fiber m_{GF} (ton)	20
Mass total (ton)	88
Length of SC (km)	1450
Current density J_e (A m^{-2})	6.3×10^7
Temperature T (K)	20
Maximum field B_{max} (T)	9.1

18

HVDC generator

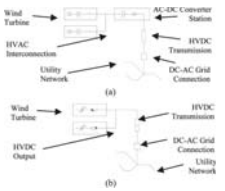

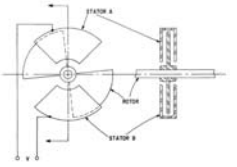

Compare with Vestas V90-3MW

Conventional system	Output voltage	Generator	Transformer	Total
	34.5kV$_{AC}$	8,500kg	8000kg	16,500kg
V-C system	Output voltage	Generator and auxiliaries	Additional gearbox	Total
	±50kV$_{DC}$	15,000kg	690kg	15,690kg

Conclusions (I)

- This presentation presents a thorough investigation of the global operational offshore wind farms from the perspective of generators, and gives the quantitative analysis.
- It is found that the dominant solution for offshore energy conversion system is the multi-stage geared drive train with the induction generators.

Conclusions (II)

- With the help of numrerical method and genetic algorithm, it is found that most of the cost and mass for high-power generators go to the supporting structure.
- It is therefore not economic to simply upscale the conventional technology of iron-cored PM generator.
- Furthermore, developing lightweight technology or other cost-effective solutions becomes necessary.

Conclusions (III)

- It reviews the generator solutions for high-power offshore wind turbines.

References

[1] Zhang Z, et al. State of the art in generator technology for offshore wind energy conversion system. Proc. IEMDC, 15-18 May 2011, p. 1131-1136.
[2] Colli VD, et al. 2-D mechanical and magnetic analysis of a 10 MW doubly fed induction generator for direct-drive wind turbines. Proc. IECON09, p. 3863-3867.
[3] Colli VD, et al. Feasibility of a 10 MW doubly fed induction generator for direct-drive wind turbines. Proc. IEEE PES/IAS, 28-30 Sept. 2009, p. 1-5.
[4] Polinder H, et al. 10MW wind turbine direct-drive generator design with pitch or active speed stall control. Proc. IEMDC, 3-5 May 2007, p. 1390-1395.
[5] Alexandrova Y, et al. Defining proper initial geometry of an 8 MW liquid-cooled direct-drive permanent magnet synchronous generator for wind turbine applications based on minimizing mass. Proc. ICEM2012, p. 1250-1255.
[6] Polikarpova M, et al. Thermal design and analysis of a direct-water Cooled direct drive permanent magnet synchronous generator for high-power wind turbine application. Proc. ICEM2012, p. 1488-1495.
[7] Report on next generation drivetrain development program. Boulder Wind Power.
[8] Spooner E, et al. Lightweight ironless-stator PM generators for direct-drive wind turbines. Proc. IEE. Elec. Power Appl., 2005, vol.152, no.1, p. 17-26.
[9] Kobayashi H, et al. Design of axial-flux permanent magnet coreless generator for the multi-megawatts wind turbines. EWEC2009.
[10] O'Donnell, et al. Design concepts for high-voltage variable-capacitance DC generators. IEEE Trans. Ind. Appl., Sep.-Oct. 2009, vol.45, no. 5, p. 1778-1784.
[11] Philp SF. The vacuum-insulated, varying-capacitance machine. IEEE Trans. Electri. Insul., April 1977, vol. EI-12, no. 2, p.130-136.
[12] Abrahamsen A. et al. 2010 Supercond. Sci. Technol. 23 034019 doi:10.1088/0953-2048/23/3/034019

Superconducting Generator Technology for Large Offshore Wind Turbines

Niklas Magnusson[1], Bogi Bech Jensen[2], Asger Bech Abrahamsen[2], Arne Nysveen[3]

[1]SINTEF Energy Research, Norway
[2]Technical University of Denmark, Denmark
[3]Norwegian University of Science and Technology, Norway

1. Motivation 2. Current trends 3. Superconductor generators in InnWind.EU

SINTEF DTU NTNU – Trondheim Norwegian University of Science and Technology

Motivation

- Weight and volume reductions
- Practically rare earth metal independent

In the end, it is all about costs

Superconductors

- Materials that carry large DC current densities lossfree at low temperatures
- Exhibit losses under AC operation
- Widely used in MRI diagnostics equipment at hospitals
- Under evaluation for several large scale power applications

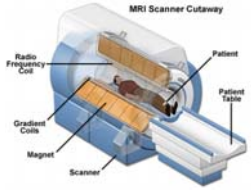

The concept

- Rotor field generated by superconducting coils at cryogenic temperatures
- Stator (armature) windings composed of copper conductors at room temperature

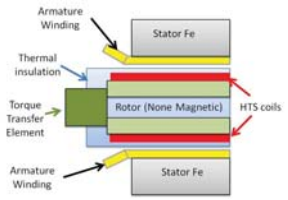

B.B. Jensen et al., 2nd International Conference E/E Systems for Wind Turbines, Bremen, 2012

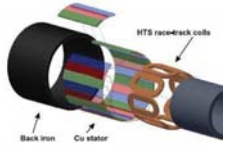

Abrahamsen et al., SUST23, 034019, 2010

Volume and weight is magnetic field dependent

- $P = \omega \tau$
  - ω is the angular frequency (given by maximum tip speed)
  - τ is the torque
- $\tau \propto B\, I\, V$
  - B is the air gap magnetic field
  - I is the stator current (given by stator constraints)
  - V is the generator volume

The only variables to play with are the magnetic field strength and the volume

Volume and weight: Superconductor versus permanent magnets

- Permanent magnet air gap flux density ~ 1 T
- Superconductor air gap flux density ~ 2.5 T

- Superconductor generator volume 40% less than corresponding permanent magnet generator

Additionally, the superconductor field windings are light weighted.

Rare earth metal dependency: Superconductor versus permanent magnets

10 MW generator:

- **Permanent magnet based:** **6 ton RE PM**
- **Superconductor based:** **10 kg RE in HTS**

A permanent magnet based off-shore generator technology would double the world market for such magnets

The superconductor possibility – Current trends in research

Choosing superconductor

- **Choice of operating temperature, magnetic field strength, cost and availability**
- **Superconducting wires are under development – increasing performance, reducing costs**

Several actors – several concepts

Conductors

Material type	Operating temperature	Magnetic field	Current density	Cost 2012	Cost 2020 (at large scale deployment)
NbTi	4.2 K	5 T	1000 A/mm^2	1 €/kAm	1 €/kAm
YBCO	40 K	3 T	200 A/mm^2	300 €/kAm	30 €/kAm
MgB_2	20 K	3 T	200 A/mm^2	10 €/kAm	3 €/kAm
Cu	50°C	< 1 T	4 A/mm^2	50 €/kAm	50 €/kAm

Generator activities

Material type	Transmission	Power rating	Industrial interest
NbTi	Direct drive	10 MW	General Electric
YBCO	Direct drive	10-15 MW	AMSC
MgB_2	Direct drive	10 MW	Advanced Magnet Lab European consortia – Suprapower, InnWind.EU

DTU

General Electric (GE) 10-15MW

- LTS – Superconducting field winding
- Extensive experience from the MRI sector
- Rotating armature

- Challenge
  - Complicated cooling system and higher cooling power
- Advantage
  - Proven technology from MRI
  - Cheaper superconductor

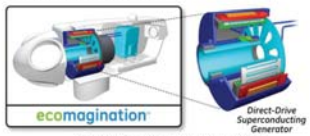

Reproduced with permission from GE

DTU

American Superconductor (AMSC) SeaTitan 10MW

- HTS – Superconducting field winding
- Copper armature winding
- Generator diameter: 4.5–5 meters
- Weight: 150-180 tonnes (55-66Nm/kg)
- Efficiency at rated load: 96%

Highest torque HTS machine intended for ship propulsion:
- 36.5MW @ 120rpm
- 2.9MNm @ 75 tons
- 39Nm/kg

- Challenge
  - HTS price and availability
- Advantage
  - Relatively simple cooling system with off-the-shelf solutions
  - Cooling power

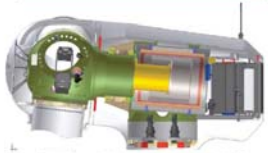

Reproduced with permission from AMSC

DTU

Advanced Magnet Lab (AML) 10MW fully superconducting

- MgB_2 – Fully superconducting generator
- Superconducting field winding
- Superconducting armature winding

- Challenge
  - Complicated cooling system and higher cooling power
  - Improvement in MgB_2 wire is needed
  - AC losses
- Advantage
  - Cheap superconductor
  - Fully superconducting
  - More torque dense

Reproduced with permission from AML

$P = \omega \times T$, $T \propto A \times B \times V$

INNWIND.EU

Aiming at integrated wind turbine concepts with:

- Light weight rotor
- Low-weight, direct drive generator
- Standard mass-produced tower and substructure

- Design of 10-20 MW concepts
- Hardware demonstrators of critical components

A joint European effort with more than 25 partners

INNWIND.EU
MgB_2 superconducting rotor coils

- MgB_2 superconductors from multiple producers

- Scaled race-track coils

H. Taxt et al., IEEE Trans. Appl. Supercond. 23, 8200204, 2013

A.B. Abrahamsen, et al., Physica C 471, 1464–1469, 2011

Evaluating key components

INNWIND.EU
MgB_2 superconducting rotor coils

- Testing at full-scale thermal and electromagnetic conditions
- 15-20 K, 3-4 T, 200 A/mm^2

Taking advantage of existing magnet technology

Summary

- Superconducting generators may reduce volume and weight
- Material development intensive
- Basic design concept under evaluation
- Reliability to be proven
- Cost is both the prime concern and the prime driver

Laboratory Verification of the Modular Converter for a 100 kV DC Transformerless Offshore Wind Turbine Solution

Sverre Gjerde[1], Kjell Ljøkelsøy[2], Tore Undeland[1]

[1]NTNU
[2]Sintef Energy Research

Deepwind 2013: Jan. 24 2013

Outline

- Why transformerless turbine?
- Proposed concept with control system
- Laboratory verifcation
- Conclusion

Why transformerless turbine? I

- 10 MW offshore wind turbine
- Weight of generator
- Low voltage – heavy cables
- Transformer in nacelle

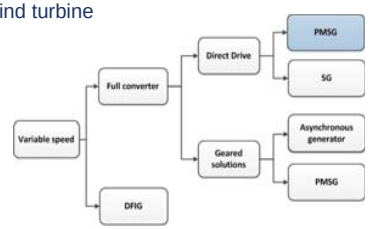

Why transformerless turbine? II

- Transformerless system:
  - Reduce nacelle weight
  - Modularity
  - DC-distribution directly from converter
- Challenges:
  - Insulation of generator
  - Modular converter system
    - Design,Operation,Control
- Unproven technologies

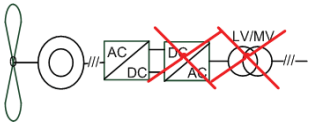

Proposed concept

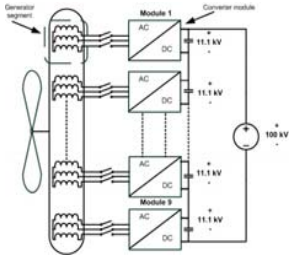

- Modular stator
  - Ironless
- Standard AC/DC-converter modules
- Seriesconnected DC-bus
- 100 kV DC output
  - Light weight

Converter control

- Modular control
- Standard 3-phase control system
- Independent/ asynchronous
- Voltage- and torque reference from master

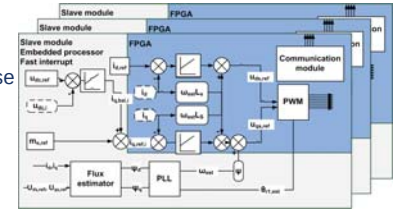

Laboratory set-up I

- 45 kW prototype
  - Modular, ironless
  - SmartMotor
- 3 stator segments and converters
- DC-grid:
  - Resistor load
  - Fixed DC-voltage

Laboratory set-up II

- Generator modelling
- Operation of series connected converters
- Modular control
- *Fault tolerance*

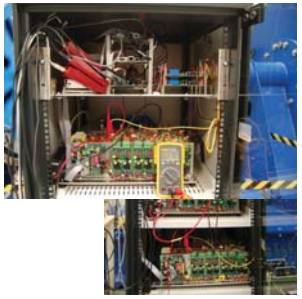

Experimental results I

Magnetic decoupling of stator segments

- Converter 3 disconnected
- Step change load resistor
- No coupling effect

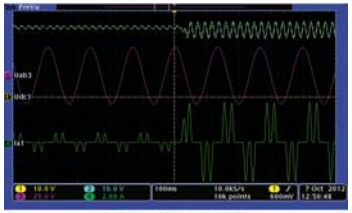

Experimental results II

Current control mode

- Constant torque
- Speed ramp
- Stable, unbalanced operation

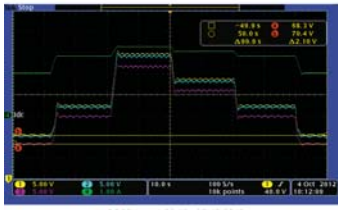

Experimental results III

Comparison with simulation

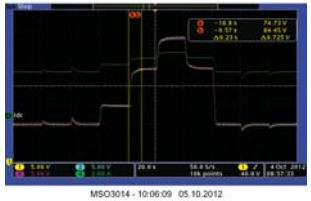

Experimental

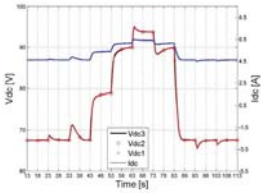

Simulation

Conclusions on converter control

- Series connected, modular converter for transformerless wind turbine
- Laboratory set-up presented
- Experimental verification
  - Generator behaviour
  - Series connected converter
  - DC-bus voltage control
- ***Further work***: Fault analysis, generator insulation verification

Thank you

Sverre Skalleberg Gjerde
sverre.gjerde@ntnu.no

Experimental results I

Comparison of 3-phase and segmented stator winding

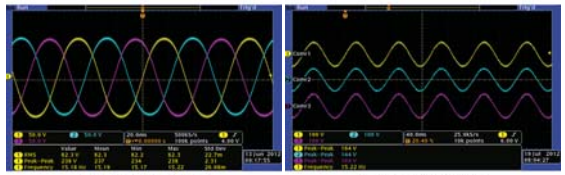

3-phase voltages

Three 3-phase voltages

Proposed system III

- Medium voltage level
- Inherent redundancy possibility

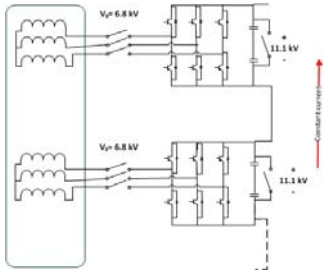

Proposed system II

- Axial Flux PMSG
  - IronLess Stator
- Modular design
  - SmartMotor
- Innovative insulation solution

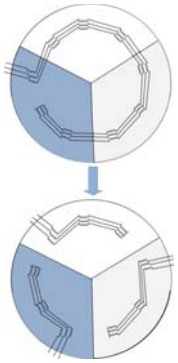

Converter control I

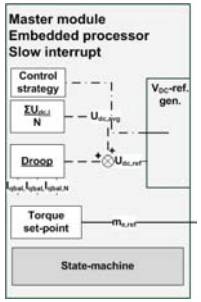

- Main control:
  - Power
  - speed control
  - Pitch
  - DC-voltage reference
- DC-voltage
  - Set-point
  - Droop regulated
  - Priority: Balanced bus-voltages

1

Multi-objective Optimization of a Modular Power Converter Based on Medium Frequency AC-Link for Offshore DC Wind Park

Rene Barrera-Cardenas
Marta Molinas
(rene.barrera, marta.molinas) @elkraft.ntnu.no
Department of Electric Power Engineering

10th Deep Sea Offshore Wind R&D Conference,
DeepWind'2013, Trondheim, Norway

NOWITECH
Norwegian Research Centre for Offshore Wind Technology

NTNU – Trondheim
Norwegian University of Science and Technology

NTNU – Trondheim
Norwegian University of Science and Technology

Outline:

1. **Introduction**
2. Power converter topologies
3. Models and Constraints
4. Results
5. Conclusions

3

Offshore Wind turbine challenges

Optimal design targeting three objectives

Maximize efficiency (η): Reduce power losses. Less conversion stages.
Maximize power density (ρ) and **Maximize Ratio power to mass (σ)** of conversion system: Minimize weight/Size for a given power. Increase the Frequency.

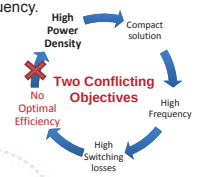

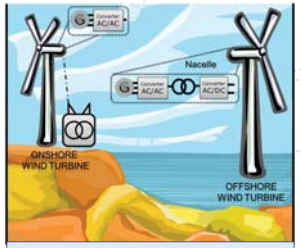

Assumption: DC Grid is more convenient for offshore wind farms [MEYER]
New WECS architectures for offshore applications. Design taken into account all stages of the system.

4

Study of operative frequency in Power converter

Power electronics:
- *IGBT Module, Topology, Modulation…*

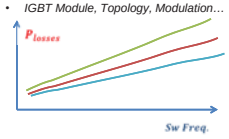

Magnetic components
- *Material, waveform, Rating…*

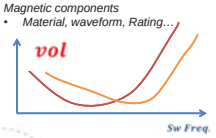

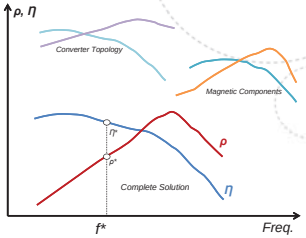

f : Optimal Operating Frequency*

Different stages ➔ Optimum
Take into account all stages in the Power converter

5

WECS Studied*

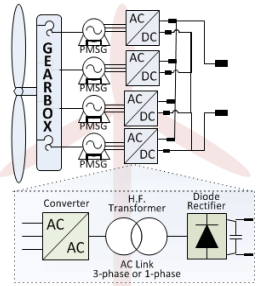

AC/DC Converter Module

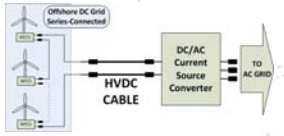

- Modularity ➔ Reliability.
- Transformer: Insulation, Ratio.
  - Flexibility for series or parallel connection.
- Constrains parameters:
  - Circuit breaker Technology
  - Generator Voltage and Power rating

*A. Mogstad, M. Molinas, "Power collection and integration on the electric grid from offshore wind parks," In proc. NORPIE 2008,

---

6

WECS Studied: Modular Power Converter

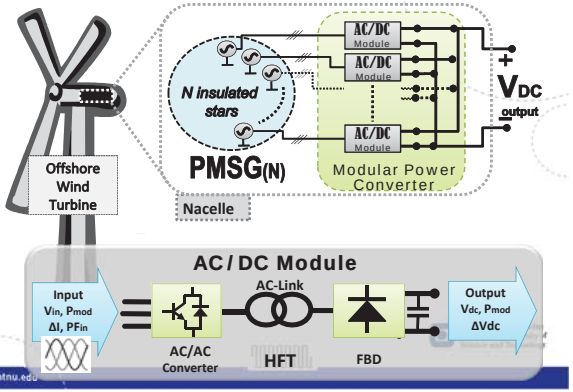

NTNU – Trondheim
Norwegian University of Science and Technology

Outline:

1. Introduction
2. **Power converter topologies**
3. Models and Constraints
4. Results
5. Conclusions

Case of Study

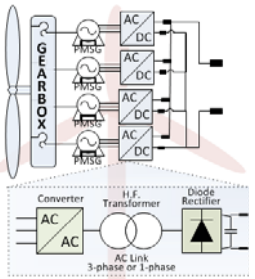

AC/DC Converter Module

AC-LINK	Converter Topology (AC/AC)		
3 phase Sinusoidal waveform	B2B Back-to-Back	IMC Indirect Matrix Converter [Holtsmark]	DMC Direct Matrix Converter [Holtsmark]
Squared waveform	B2B-3pSq B2B with 3-phase output	B2B-1p B2B with 1-phase output	RMC Reduced Matrix Converter [Garces]

Selection of the AC-Link frequency and the Power per module in order to obtain the best relation of the three objectives

*Holtsmark and Molinas, "Matrix converter efficiency in a high frequency link offshore WECS," in IECON 2011.
**A. Garces. "Design, Operation and control of series connected power converters for offshore wind parks". Thesis for the Degree of Doctor of Philosophy. NTNU 2012.

Module based on Back-to-Back Converter topology (B2B)

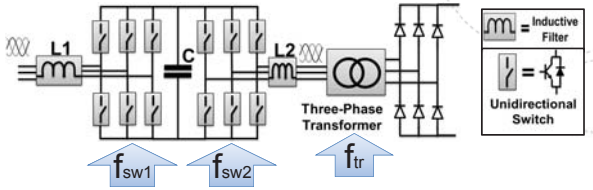

f_{tr} : AC-Link frequency. Operating transformer frequency.
f_{sw1} : Switching Freq. generator side. It can be lower than sw. freq. of transformer side. It is optimized in this study. Minimum value of 500[Hz] (10*50Hz).
f_{sw2} : Switching Freq. transformer side. It should be higher than transformer freq. It is equal to $6*f_{tr}$ in this study.

Module based on Back-to-Back Converter with three phase squared wave output.(B2B3p-Sq)

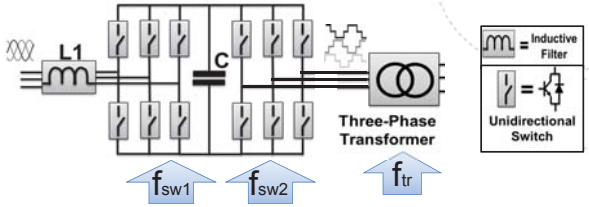

f_{tr} : AC-Link frequency. Operating transformer frequency.
f_{sw1} : Switching Freq. generator side. It can be lower than sw. freq. of transformer side. Optimal selection in the switching frequency. Minimum value of 500[Hz] (10*50Hz).
f_{sw2} : Switching Freq. transformer side. It is equal to the transformer freq.

Module based on Back-to-Back single-phase Converter topology (B2B-1p)

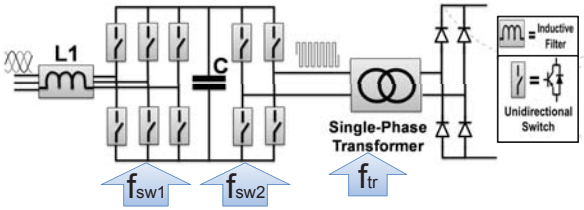

f_{tr} : AC-Link frequency. Operating transformer frequency.
f_{sw1} : Switching Freq. generator side. It can be lower than sw. freq. of transformer side. It is optimized in this study. Minimum value of 500[Hz] (10*50Hz).
f_{sw2} : Switching Freq. transformer side. It is equal to transformer freq.

Module based on Indirect Matrix Converter topology (IMC)

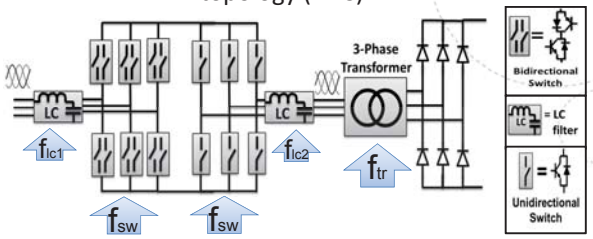

f_{tr} : AC-Link frequency. Operating transformer frequency.
f_{sw} : Switching Freq. It should be higher than transformer freq. It is equal to $6*f_{tr}$ in this study.
f_{lc} : Cut-off frequency of LC filter. Setting it to be 3 times lower than the switching frequency and limiting it to 20 times the supply frequency (20*50=1[KHz]).
*In this study the Clamp Circuit is not taken into account.

Module based on Direct Matrix Converter topology (DMC)

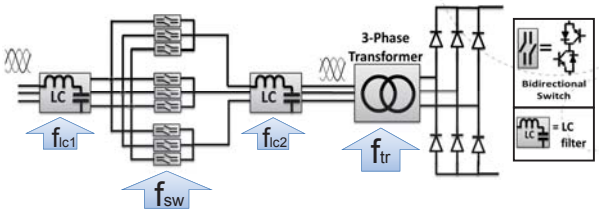

f_{tr} : AC-Link frequency. Operating transformer frequency.
f_{sw} : Switching Freq. It should be higher than transformer freq. It is equal to 6*f_{tr} in this study.
f_{lc} : Cut-off frequency of LC filter. Setting it to be 3 times lower than the switching frequency and limiting it to 20 times the supply frequency (20*50=1[KHz]).
*In this study the Clamp Circuit is not taken into account.

Module based on Reduced Matrix Converter topology (RMC)

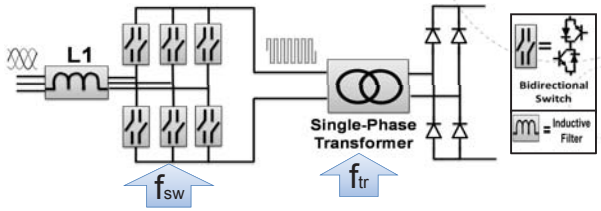

f_{tr} : AC-Link frequency. Operating transformer frequency.
f_{sw} : Switching Freq. It is equal to transformer freq. The minimum value is 800[Hz], this limit is considered controllability and harmonics distortion in generator side.
*In this study the Clamp Circuit is not taken into account.

NTNU – Trondheim
Norwegian University of Science and Technology

Outline:

1. Introduction
2. Power converter topologies
3. **Models and Constraints**
4. Results
5. Conclusions

Objectives Evaluation

Efficiency

$$\eta = \frac{P_{out}}{P_{in}} = \frac{P_{in} - P_{losses}}{P_{in}}$$

Power Density

$$\rho = \frac{P_{out}}{vol} = \frac{P_{in} - P_{losses}}{volume}$$

Ratio Power to mass

$$\sigma = \frac{P_{in} - P_{losses}}{mass}$$

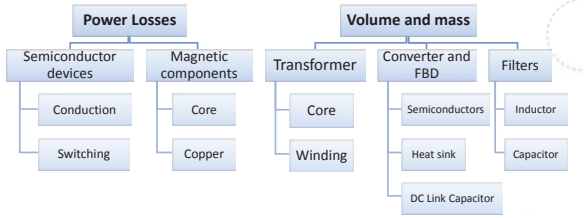

Barrera and Molinas. "A Simple procedure to evaluate the efficiency and power density of power conversion topologies for offshore wind turbines." In proc. DeepWind 2012. Elsevier Energy Procedia.

Semiconductor Losses

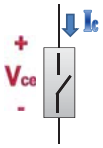

Conduction

$$P_{cond} = \frac{1}{T}\int_{t_0}^{t_0+T} V_{ce}(t) \cdot I_c(t) \cdot dt$$

$$V_{ce}(t) = K_{ce1} + K_{ce2} \cdot I_c(t)$$

Switching

$$P_{sw} = \frac{1}{T}\sum_{T} E_{on} + E_{off} + E_{rr}$$

$$E_{sw} = E_{test}\frac{V_{ce}(t) \cdot I_c(t)}{V_{test} \cdot I_{test}}$$

Evaluate at moment of each switching action. Switch On, Switch Off and Reverse Recovery

Number of switching actions are dependent of modulation scheme.

NTNU – Trondheim Norwegian University of Science and Technology

Converter volume

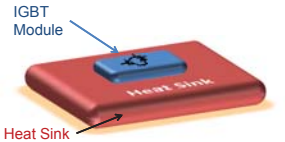

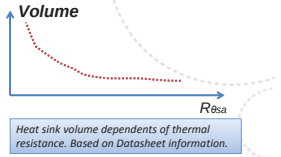

Heat sink volume dependents of thermal resistance. Based on Datasheet information.

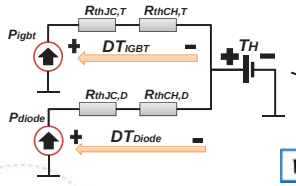

$$Vol_{HS} = \frac{K_{HS}}{R_{\theta sa}} = \frac{K_{HS}}{\Delta T_{Hmax}} P_{loss}$$

ΔT_{Hmax} based on worst case assumption in thermal design.

$$Vol_{conv.} = n_{sw} \cdot (vol_{device} + vol_{HS})$$

DC link Capacitor

Proportional model in order to estimate the capacitor volume from the reference capacitor.*

$$Vol_{cap} = \frac{C}{C_{ref}}\left(\frac{V_{DC}}{V_{ref}}\right)^2 \cdot Vol_{ref}$$

- The capacitance is designed in order to limit the DC voltage ripple*.

$$C \propto \frac{I_{rms}}{V_{DC} f_{sw}}$$

*M. Preindl and S. Bolognani, "Optimized design of two and three level full-scale voltage source converters for multi-MW wind power plants at different voltage levels," in IECON 2011.

Filters

The Inductance is designed in order to limit the current ripple*,**.

$$L_{B2B} \propto \frac{V_{DC}}{I_{rms} f_{sw}}$$

Proportional model in order to estimate the Inductor volume* and losses from the reference Inductor.

$$Vol_{induc.} = K_{ind} \cdot \left(L_{filter} \cdot I^2\right)^{3/4}$$

$$P_{loss\_L} = \left(P_{cuRef} + P_{coreRef} \cdot \left(\frac{f_{ref}}{f}\right)^{\frac{(7\alpha-2)}{(12\beta-\alpha)}}\right) \cdot \left(\frac{Vol_{ind.}}{Vol_{Ref}}\right)$$

*M. Preindl and S. Bolognani, "Optimized design of two and three level full-scale voltage source converters for multi-MW wind power plants at different voltage levels," in IECON 2011.
**M. hamouda, F. Fnaiech, and K. Al-Haddad, "Input filter design for SVM Dual-Bridge matrix converters," in 2006 IEEE International Symposium on Industrial Electronics, vol. 2. IEEE, Jul. 2006.

Magnetic components losses

- Core Losses → based on Steinmetz equation

$$P_{core} = K_{core} \cdot Vol_{core} \cdot f^{\alpha_c} \cdot B^{\beta_c}$$

highly dependent of magnetic material, volume and waveform voltage

- Copper Losses → losses of all windings

$$P_{cu} = \sum_{i=1}^{nw} K_{cu(i)} \frac{\rho_{cu} N_{(i)} MLT_{(i)}}{A_{w(i)}} I_i{}^2 (1 + THD^2)$$

K_δ as a function of frequency, winding design (layers, conductor)

NTNU – Trondheim Norwegian University of Science and Technology

Transformer volume and losses

Design process aims to minimize the volume of the transformer taking into account some assumptions.

- Type transformer structure
  - dry shell-type transformers
  - optimal set of relative dimensions***
- Temperature rise
  - α Power losses
  - α 1 / (surface area)
- Power rating
  - each winding carry the same current density

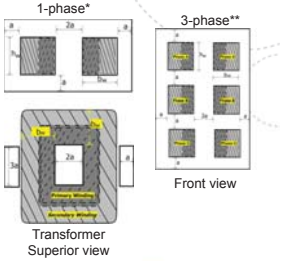

*S. Meier, et al. "Design Considerations for Medium-Frequency Power Transformers in Offshore Wind Farms." IEEE 2010.
** T. Mclyman. "Transformer and Inductor Design Handbook." CRC Press 2004.
***N. Mohan, T. M. Undeland, and W. P. Robbins, Power Electronics: Converters, Applications, and Design, 3rd ed. Wiley, Oct. 2002

Transformer volume and losses

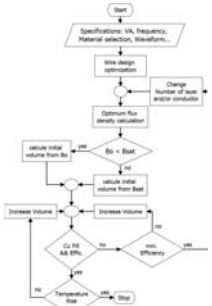

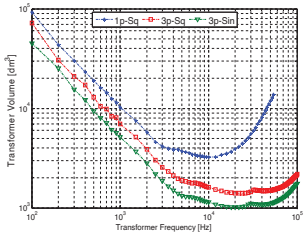

Example: Transformer volume evaluation
P= 625 [kW] Voutput = 33 [KV]

*Optimum flux density calculation based on W. G. Hurley, W. H. Wolfle, and J. G. Breslin, "Optimized transformer design: inclusive of high-frequency effects," IEEE Transactions on Power Electronics, vol. 13, no. 4, pp. 651–659, Jul. 1998.
**Wire design based on Litz wire structure: http://www.elektrisola.com/litz-wire/technical-data/formulas.html

NTNU – Trondheim
Norwegian University of Science and Technology

Outline:

1. Introduction
2. Power converter topologies
3. Models and Constraints
4. ***Results***
5. Conclusions

25

Parameters and Design Constraints

Parameter	Value
Total Power	10 [MW]
Input Voltage	690[V]
Output DC Voltage	33 [kV]
Generator Frequency	50[Hz]
DC-Link Voltage ripple	1%
Current Input ripple	20%
Current Output ripple	20%
Generator Power factor	0.9
Magnetic material	Metglas alloy 2605SA1
Max. DT Transformer	70 K
AC-Link Freq. [kHz]	[0.5, 10]
Power x module [MW]	[0.2, 10]

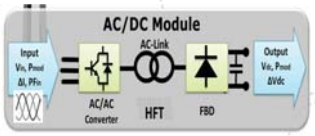

Device	Reference
Ref. Inductor (filters)	Siemens 4EU and 4ET
Ref. DC-link Capacitor	EPCOS MKP DC B256
Ref. AC-Capacitor	EPCOS MKP AC B2536
IGBT Module	Infineon IGBT4 FZXXR17HP4
DIODE Module	Infineon IGBT3 DDXXS33HE3
Heat Sink	Bonded Fin - DAU series BF
Axial FAN – Heat sink	Semikron SKF 3-230 series

26

Back-to-Back Topologies: Generator Side VSI and input filter

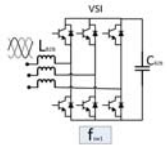

Optimal selection of switching frequency.

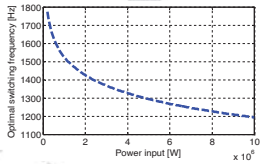

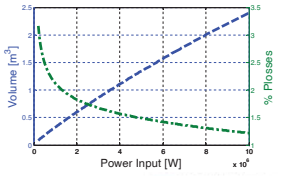

27

AC Link Frequency

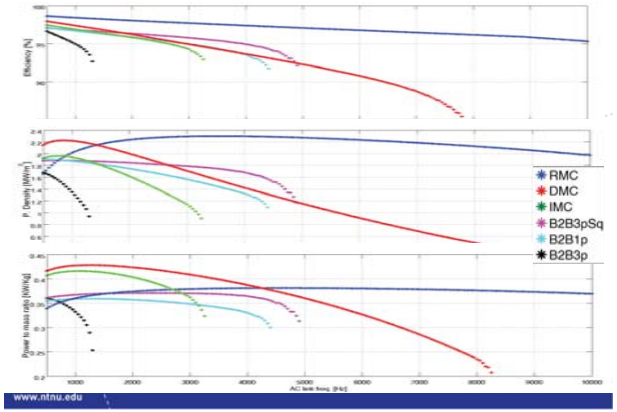

28

Power per module

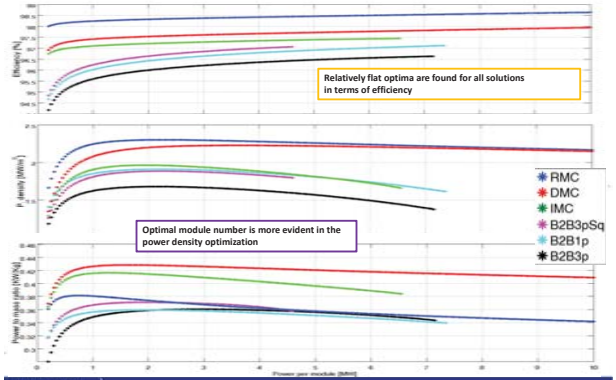

29

Pareto Front

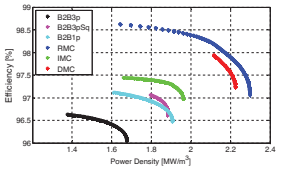

RMC the best tradeoff between efficiency and power density

DMC the best tradeoff between Efficiency and ratio power to mass

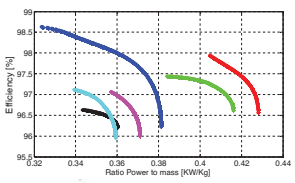

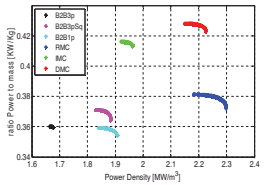

30

Conclusions

- Six different modular power converters solution based on medium frequency link have been compared and their convenience for offshore WECS is evaluated.
- It has been found that WECS based on RMC and square wave AC-Link will lead the best tradeoff between efficiency and power density in range of AC-Link frequencies from 500[Hz] to 10[KHz].

NTNU – Trondheim Norwegian University of Science and Technology

NOWITECH
Norwegian Research Centre for Offshore Wind Technology

Thanks for your attention

Multi-objective Optimization of a Modular Power Converter Based on Medium Frequency AC-Link for Offshore DC Wind Park

Rene Barrera-Cardenas and Marta Molinas
(rene.barrera, marta.molinas) @elkraft.ntnu.no
Department of Electric Power Engineering

NTNU – Trondheim
Norwegian University of Science and Technology

B1 Power system integration

Wind Turbine Electrical Design for an Offshore HVDC Connection,
Olimpo Anaya-Lara, Strathclyde Univ.

Frequency Quality in the Nordic system: Offshore Wind variability, Hydro Power Pump Storage and usage of HVDC Links, Atsede Endegnanew, SINTEF Energi AS

Coordinated control for wind turbine and VSC-HVDC transmission to enhance FRT capability, Antonio Luque, University of Strathclyde

North Sea Offshore Modeling Schemes with VSC-HVDC Technology: Control and Dynamic Performance Assessment, K. Nieradzinska, University of Strathclyde

Upon the improvement of the winding design of wind turbine transformers for safer performance within resonance overvoltages, Amir H Soloot, PhD, NTNU

Wind Turbine Electrical Design for an Offshore HVDC Connection,

Olimpo Anaya-Lara
Max Parker
Kerri Hart
Alasdair McDonald

Content

1. Offshore wind generation: sub-systems
2. Offshore transmission alternatives
3. Conventional wind turbine generator technology
4. Alternative WT generator topologies
5. Grid code compliance and fault management
6. More key questions to answer

Offshore wind generation: sub-systems

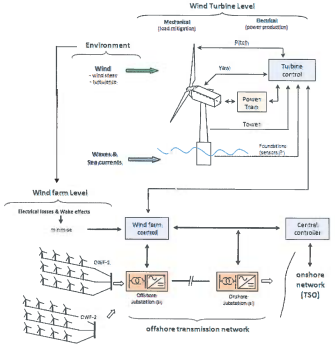

Complex mix of sub-systems and technology (and very possibly vendors)

Different control objectives

Offshore transmission alternatives

- Simple point-to-point:

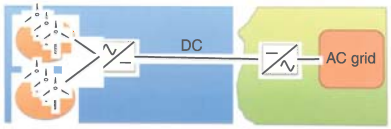

- Complex connections:

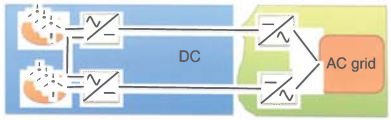

Courtesy of IBERDROLA

Offshore transmission alternatives

- DC Grid Configurations:

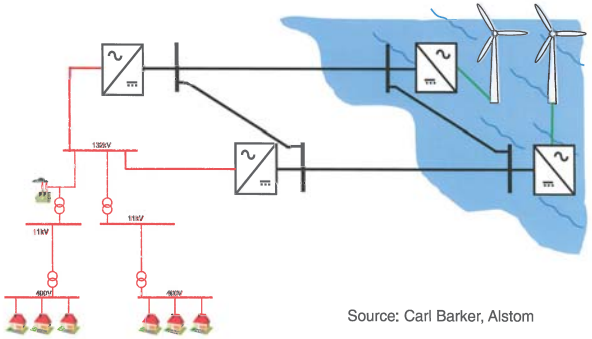

Source: Carl Barker, Alstom

Conventional wind turbine generator technology (on- and off-shore)

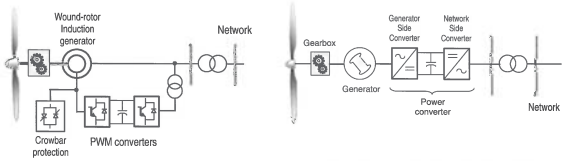

Doubly fed induction generator (DFIG)

Fully-rated converter wind turbine (FRC)

- Variable-speed wind turbines have more control flexibility and improve system efficiency and power quality.
- Exploit features provided by WT power electronics

Wind turbine generator technology

- Technical characteristics of wind turbine technologies are significantly different from conventional power plants
- And electrical networks were designed around conventional plant based on synchronous generators
- Should wind generators emulate synchronous machines and provide similar dynamic characteristics in terms of voltage/frequency control, system damping, etc.?

Accurate modelling and control of wind turbine systems for power system studies are still a challenge

8

Full Converter wind turbine

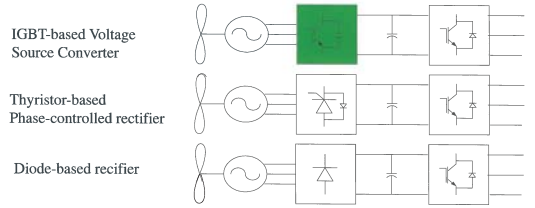

Generator-side converter configurations

9

Overview of connection methods

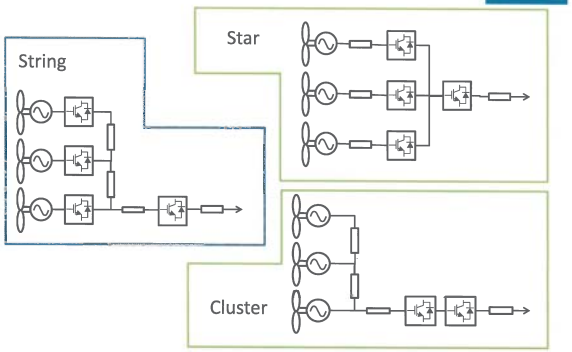

AC String

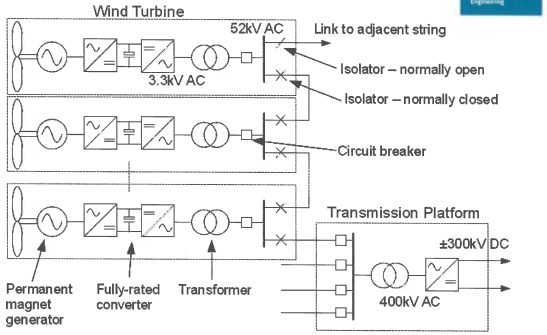

DC String

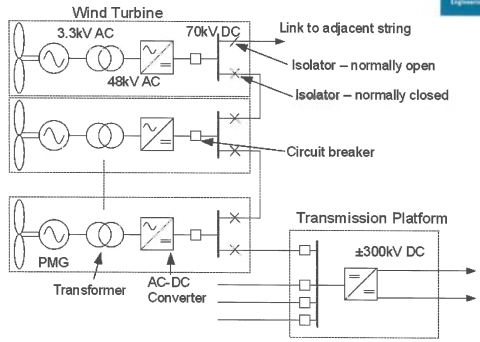

AC Cluster

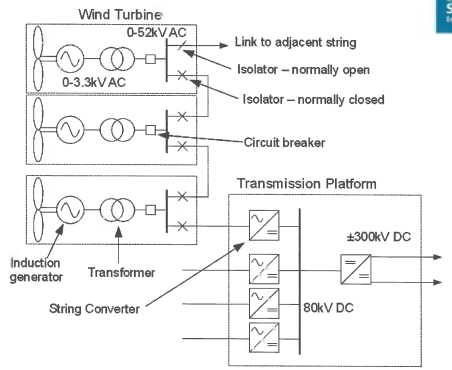

DC Cluster

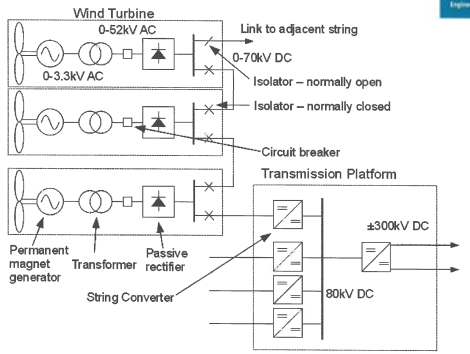

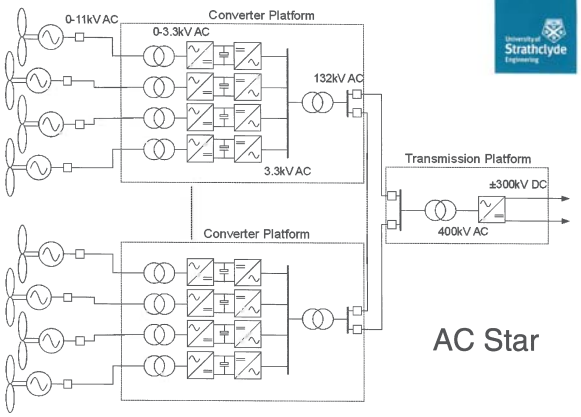

AC Star

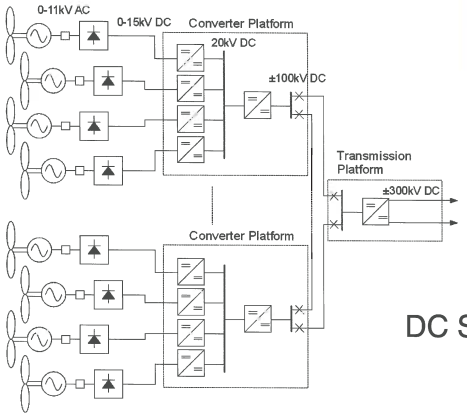

DC Star

Example Wind Farm Layout

- 1GW transmission platform rating.
- ±300kV HVDC link.
- Turbines: 10MW, Swept diameter 170m.
- Spacing: 7 diameters, 1190m.
- 10x10 square.

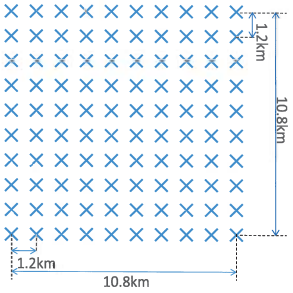

Windfarm Layout, Radial Strings

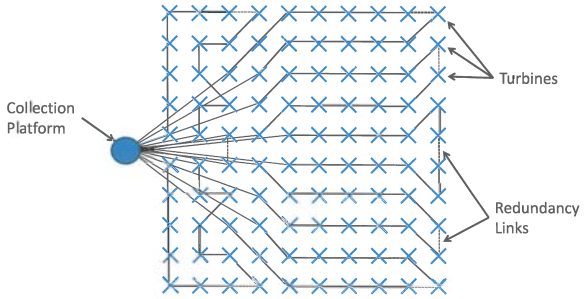

Windfarm Layout, Star Connection

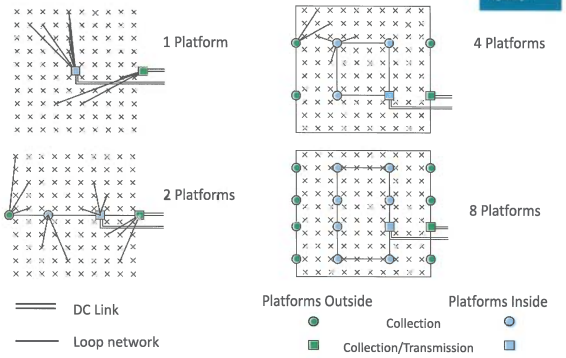

Breakdown of losses

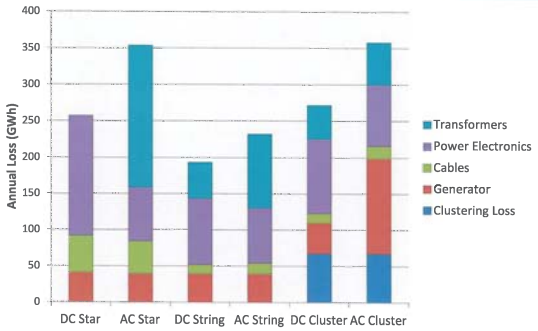

Breakdown of costs

Only cable, platform and loss costs considered at this stage

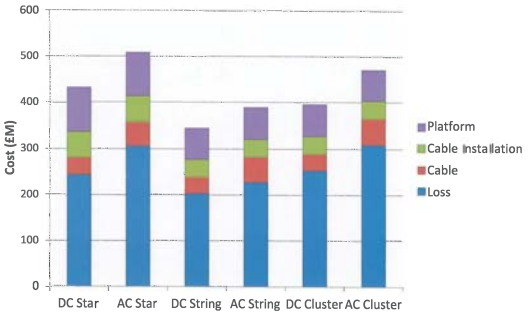

Grid Code Compliance:

Converter-connected generation and inertia issues

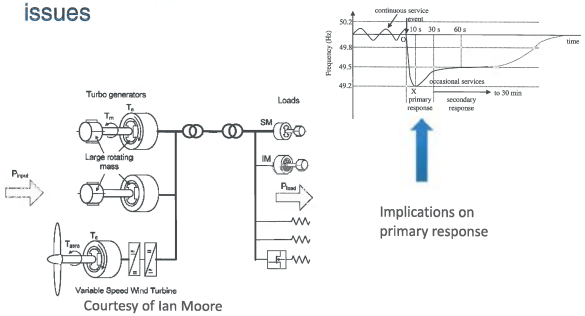

Courtesy of Ian Moore
Cardiff University

Implications on primary response

Grid Code Compliance – fault management

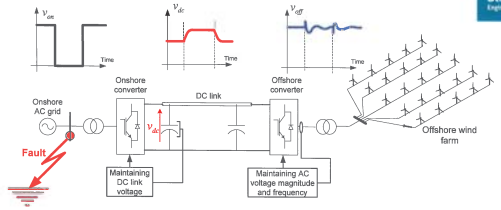

GB FRT requirement

- Enhanced control strategies to facilitate Fault Ride-Through
- Investigate the requirements for control of offshore wind farms to contribute to onshore network performance

TSO and point of Grid Code compliance

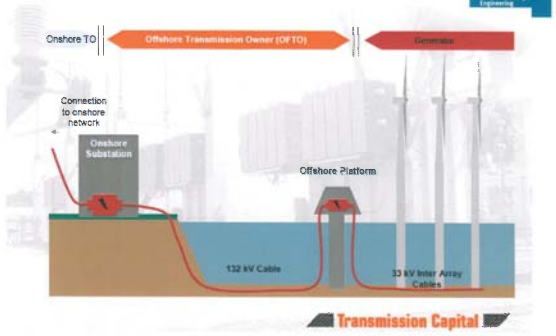

More key questions to answer

- What is the optimum wind turbine design for a HVDC-connected wind farm?
- What are the most appropriate grid connection and power quality requirements for a DC transmission system?
- What is the overall reduction in cost of the optimised wind turbine?
- What is the potential increase/decrease in O&M costs and overall benefit to the economics of a wind farm?

Source: Kerri Hart, Strathclyde (PhD research project with SSE renewables)

University of Strathclyde Glasgow

Evaluation of cable lengths

breakdown of costs

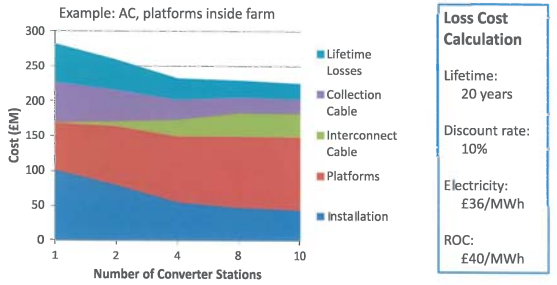

Evaluation of losses

Site and Turbine Parameters

- Average wind speed: 9.8m/s
- Cut-in wind speed: 3m/s
- Cut-out wind speed: 25m/s
- Rated wind speed: 12m/s

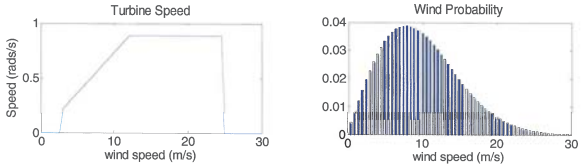

Evaluation of cable lengths

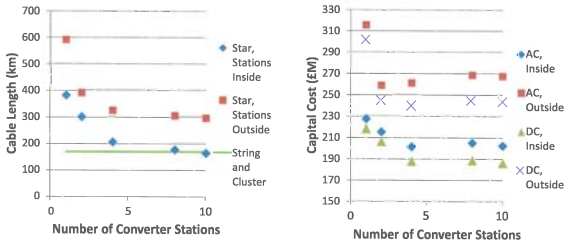

Alternative WT generator topologies

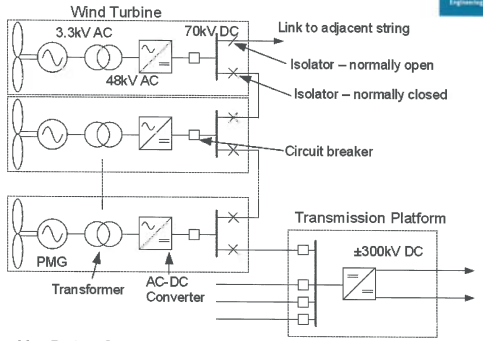

Source: Max Parker, Strathclyde

Frequency Quality in the Nordic system: Offshore Wind variability, Hydro Power Pump Storage and usage of HVDC Links

by
Atsede G. Endegnanew
Hossein Farahmand
Daniel Huertas-Hernando

SINTEF Energy Research

DeepWind'2013, 24-25 January 2013, Trondheim, Norway

Introduction

- Large development of offshore wind power in the North Sea (in 2020 : > 35 GW and 2030: 96 GW[1])
- Large potential for hydro power generation in Norway with pumped storage (11 GW[2])
- Price difference between system price and water value
- Pumped storage used during high wind production
- Investigate the effect of wind power variability (on North sea) and pumped storage on Nordic power system frequency

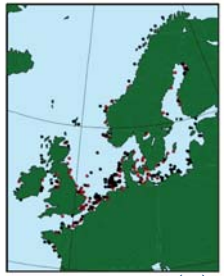

Offshore wind farms in 2020 (red) and 2030 (red+black)

[1] Offshore Wind Power Data, DTU Wind Energy, Twenties, 2012
[2] Increasing balance power capacity in Norwegian hydroelectric power stations, TR A7195, Sintef Energy, 2012

Pumping Vs. Offshore wind production

Tonstad & NorGer HVDC cable
& German offshore wind

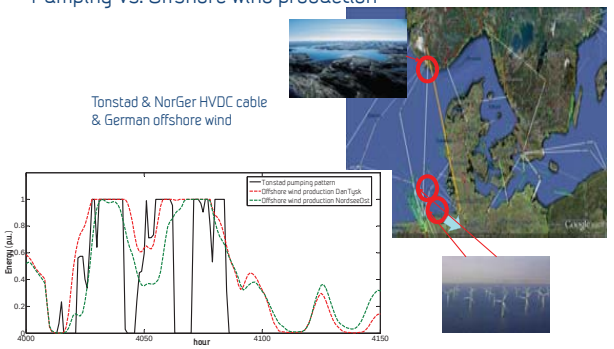

Model description

- Nordic synchronous power system
  - Norway, Sweden, Eastern Denmark, and Finland
- Continental European synchronous system
  - West Denmark and rest of UCTE
- Primary control: 6% droop and ±0.2 Hz
- Secondary control: LFC on generators and HVDC links
- Wind farms and NorGer power flow are modeled as a negative load
- Initial power flow data are taken from NordPool data from 11 November 2010
- NorGer flow and pumping data taken from market analysis

Wind variation

- Modelled as linear power production change of ΔP within time span of ΔT
- Average wind speeds above 25 m/s
- NorGer HVDC link flow changes were also modelled linearly

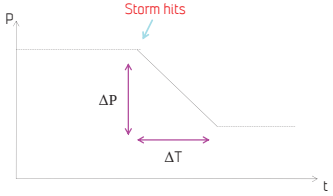

HVDC Controller

- Same basic control topology as the original structure
- Constant current control mode

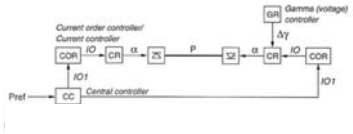

- The central controller has an additional input ΔP
  - compensate for a given power imbalance
  - ΔP signal comes from Ramp Following Controller (RFC)

Ramp Following Controller (RFC)

- Two inputs: frequency deviation and power flow deviation
- Gets signal from ACE between two interconnected areas, change in load, change in production or flow on HVDC
- HVDC cable track changes in wind power production

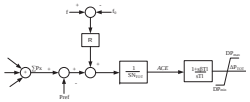

Load Frequency Controller (LFC)

- Area control error (ACE) shared among several generators
- Each generator contributes according to its rating

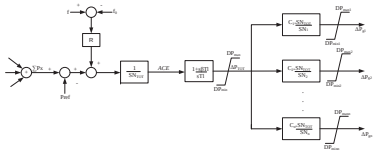

LFC controllers

- LFC in Danmark:
  - ± 90 MW capacity
  - Three largest thermal generators
  - Monitor the German-Danish border flows
- LFC in Norway
  - ± 375 MW capacity
  - 3 aggregated hydro power plants
  - Monitor the AC-transmission with Sweden and HVDC connections with Denmark

Simulation

- Loss of 2000 MW offshore wind power generation in western Denmark
- Power flow variation from Germany to Norway (NorGer): 970 MW → 530 MW
- Initial pumping load at Tonstad: 160 MW
- Two cases
  - **Case 1**: Reduction and stop of pumping (Slow)
  - **Case 2**: Stop of pumping (Fast) and change to generation
- **Studied result**
  - Nordic frequency

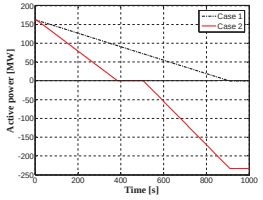

Results

- Western Danish power system loses ΔP≈2000 MW
- RFC on HVDC links between Nordic and western Danish systems follow the change
- Frequency deviation in Nordic power system due to LFC in Norway
- 443 MW variation in power flowing from Germany to Norway
- Different rate of change in pumping

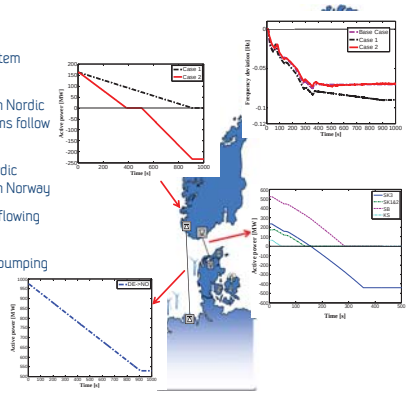

Conclusions

- Large offshore wind production variations in North Sea will correlate with variable power flows between Continental Europe and Nordic region.
- RFC control together with LFC in the Nordic region and West Denmark can contribute to power system balance restoration (in the event of large variations in offshore wind generation). RFC will have an impact on the Nordic frequency quality.
- In addition, the rate of change of pumped storage in hydropower stations will introduce an additional load, which also will affect the Nordic frequency. The relative rate of change in pumping stations with respect to the variations of wind power and flows between the Nordic and Continental Europe system / North Sea will also affect the frequency.
- Frequency deviations found in this study, assuming realistic wind power and power flows variations and pumping rates, although significant are still within the allowed limits in all the cases studied.
- Offshore wind variability, pumped storage loads and power flow on the HVDC links connected to the Nordic power system are likely to have significant influence on the Nordic frequency quality in the future.

Thank You for your attention!

Questions?

Simulation Results (2)

Case B => ΔP=2000 MW

- Excess power observed in the Western Danish power system
- Reversing the power flow on SK3 reduces the steady state imbalance at the German-Danish border
- Nordic frequency deviation remains within allowed limits

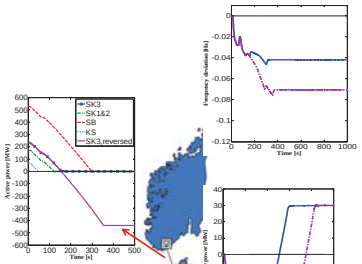

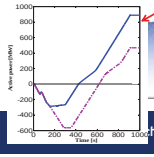

HVDC control + LFC in Denmark + LFC in Norway

HVDC control, SK3 reversed + LFC in Denmark + LFC in Norway

Coordinated control for wind turbine and VSC-HVDC transmission to enhance FRT capability

University of Strathclyde
Institute of Energy and Environment

PhD Antonio Luque
Dr Olimpo Anaya-Lara
Dr *Grain. P. Adam*

Outlines

Variable-speed Wind Turbines
- DFIG
- FRC

HVDC Systems
- Voltage Source Converter "VSC"

Case Studies - Control Strategies
- Case Study
- VSC Control Strategies

Simulation Results
- Wind Farms Output (V-I)
- Cluster Platform (V-I)
- HVDC Link

Variable Speed Wind Turbines

DFIG and FRC Wind Turbine

Higher control flexibility and improve system efficiency and power quality : Independent control of the P_{ref} and Q_{ref}

- Partially control of the WT: DFIG
- Full control of the wind turbine: FRC
- Fast control of the WT: Power electronic system
- Voltage-reactive support for large transients: without altering the wind turbine dynamics

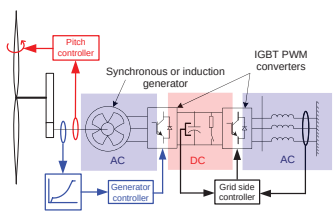

Fig. 1: FRC Wind Turbine

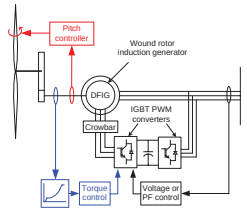

Fig. 2: DFIG Wind Turbine

Source: Nick Jenkins

HVDC Systems

- Technical advantage of HVDC

1. HVDC link can work between two ac system with different frequency
2. Capability to recover from power failures utilizing adjacent grids: "black start"
3. DC High transmission capacity: "No inductance or capacitance effects " ,"no skin effect"
4. Accurate and fast control of the active and reactive power

- Economic Considerations

1. For distance higher than ≈ 50 km HVAC higher investment
2. Long distance: less power losses

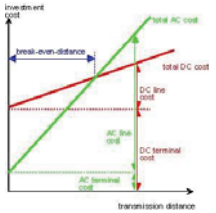

Fig. 3: Break curve HVAC-HVDC

Source: Siemens

HVCD System

Voltage Source converter "VSC"

- Technical advantage of VSC

1. Fast powers control: P_{ref} and Q_{ref}
2. Almost instantly communication between converters
3. DC link is totally decoupled: Different frequencies
4. Flexibility to reverse power: Better dynamic performance
5. Reliable performance in weak or passive grids
6. Absorb or provide reactive power during large transients

- Technical disadvantage of VSC

1. Mature Technology
2. Switching power losses
3. No specific power protection

- Economic Considerations

1. Less harmonics distortion: less filter "offshore"
2. Offshore structure smaller

Case Study – Control Strategies

Case Study

Electrical Array for large Offshore Wind Farm

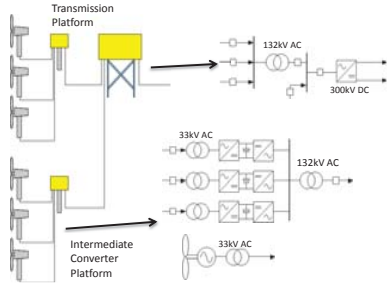

Fig. 8: AC Star Connection

Source: Max Parker

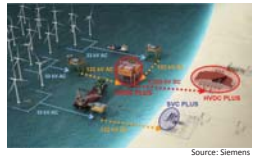

Source: Siemens

Control Strategies – Case Study

Basic VSC Control

Active and reactive power control

$$P = \frac{E_g V_t}{X_g} \sin X_g$$

$$Q = \frac{E_g^2 - E_g V_t \cos X_g}{X_g}$$

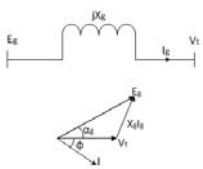

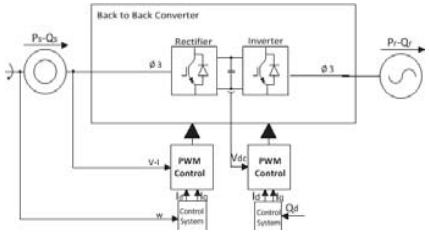

Fig. 4: Back to Back Converters

Control Strategies – Case Study

Control Strategies

Coordinated VSC Control: P/f – V_{dc}/f and Q Control

- P/f power controller:

Pt= P1+P2+P3

1. The dynamic responds of the P/f power controller has improved the implemented system
2. Faster response to load changes or transients, adaptive to damping support

- Reactive Power Controller:

1. Control of reactive power
   Qt = Q1+Q2+Q3

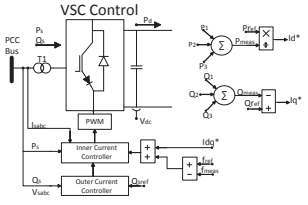

Fig. 5: Simple VSC scheme with P/f Controller

Control Strategies – Case Study

Control strategies:

- DC voltage Controller:

1. Combined with Frequency controller improve network dynamic performance
2. Control of the medium voltage of the inverter capacitors

- Third Harmonic Injection:

1. Prevent over-modulation and improving 15 % voltage output

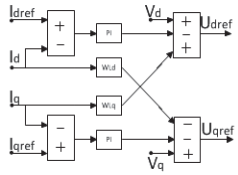

Fig. 6: Inner and Outer current controller

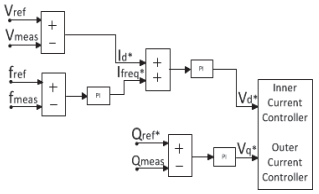

Fig. 7: Referential signals for the Inner and Outer current controller

Simulation Results

V-I First Transient

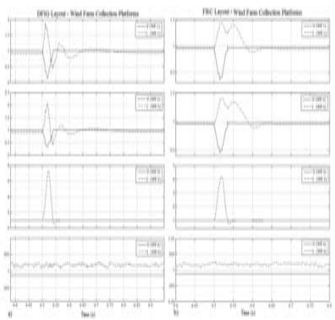

Fig. 9: Wind Farm Performances

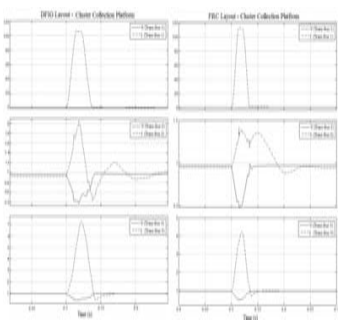

Fig. 10: Cluster Collection Platform

Simulation Results

V-I Second Transient

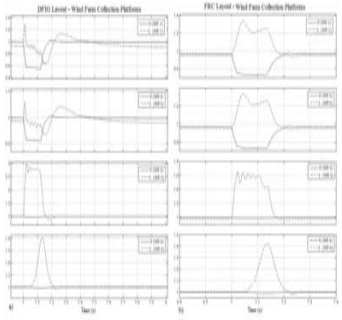

Fig. 11: Wind Farm Performances

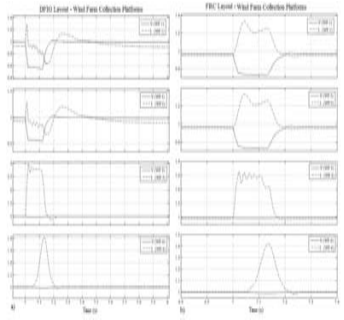

Fig. 12: Cluster Collection Platform

Simulation Results

Transmission Platform and Grid

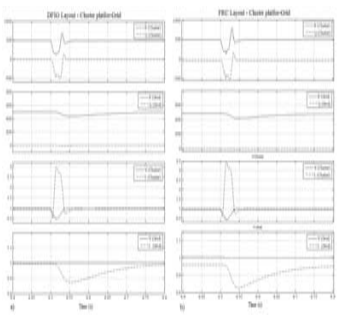

Fig. 13: First Transient

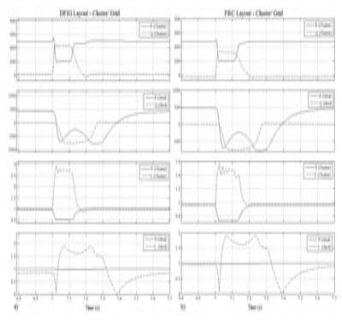

Fig. 14: Second Transient

Simulation Results

HVDC Link 1

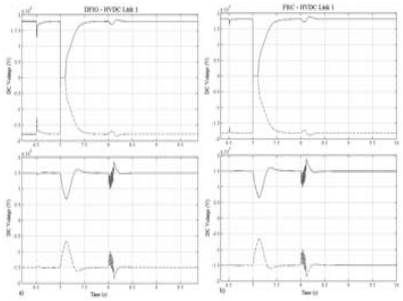

Fig. 15: DC voltage Performance

Conclusions

- The results further demonstrate flexibility of the proposed control system to integrate different offshore wind farms during large transients.
- It has been shown also high improvements in the fault ride-through capability of both systems. Thus, mentioned controllers have improved the recovery time from large transients in the ac and dc scheme.
- By using mentioned controllers, the results has shown great controllability and flexibility of the power transferred from both schemes.
- It is possible to conclude that an integration of both layouts into one scheme where DFIG and FRC wind farms are connected together; the mentioned control system should coordinate and transfer the active and reactive without causing major hazards to the control system

Thanks You

North Sea Offshore Modeling Schemes with VSC-HVDC Technology: Control and Dynamic Performance Assessment

K. Nieradzinska, J.C. Nambo, G. P Adam, G. Kalcon, R. Peña-Gallardo, O. Anaya-Lara, W. Leithead
University of Strathclyde

Outline of Presentation

- North Sea Connection
- VSC-HVDC
- Control strategy
- Tested systems configuration
- Results
- Conclusions

North Sea Connections

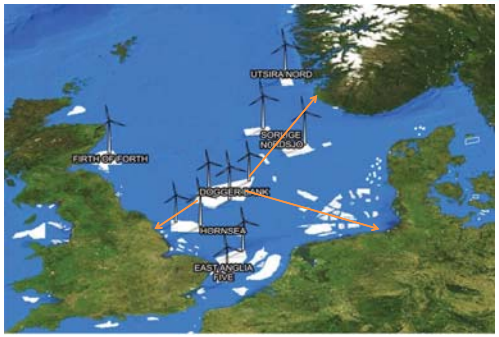

What is VSC

- VSC = Voltage Source(d) Converter
- Capacitor is normally used as energy storage
- VSC uses a self-commutated device such as GTO (Gate Turn Off Thyristor) or IGBT (Insulated Gate Bipolar Transistor)

Why VSC-HVDC…

- Power transfer over long distances
- Lower power losses compared to AC transmission
- Independent control over active and reactive power
- Voltage support
- Wind farm is decoupled from the onshore grid,
- Connected to the weak network
- Black start capability

Point-to-point Connection

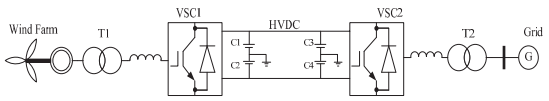

Different control strategies employed for offshore wind farm and onshore grid.

Vector Control

- Three-phase rotating voltage and current are transformed to the *dq* reference frame
- Comparative loops and PI controllers are used to generate the desired values of *M* and θ and fed their values to the VSC
- Phase-locked-loop (PLL) is used to synchronize the modulation index.

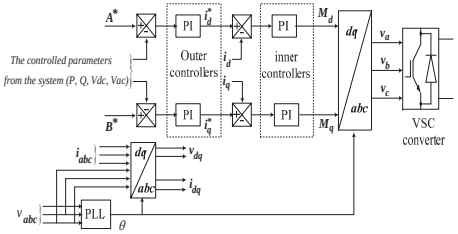

Control Strategies – Inner Controller

$$v_{cd} = -u_d + \omega L i_q - v_{sd}$$

$$v_{cq} = -u_q - \omega L i_d - v_{sq}$$

Inner Controller

Responsible for controlling the current in order to protect the converter from overloading during system disturbances

$$u_d = k_{pi}(i_d^* - i_d) + k_{ii}\int(i_d^* - i_d)dt$$

$$u_q = k_{pi}(i_q^* - i_q) + k_{ii}\int(i_q^* - i_q)dt$$

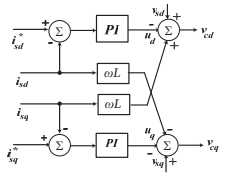

Control Strategies – Outer Controller

$$i_{sd}^* = \frac{P^*}{v_{sd}}$$

$$i_{sq}^* = \frac{-Q^*}{v_{sd}}$$

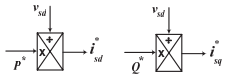

$$i_{sd}^* = k_{pdc}(V_{dc}^* - V_{dc}) + k_{idc}\int(V_{dc}^* - V_{dc})dt$$

$$i_{sq}^* = k_{pac}(V_{ac}^* - V_{ac}) + k_{iac}\int(V_{ac}^* - V_{ac})dt$$

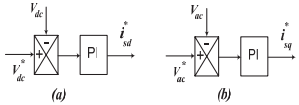

Outer controller

Responsible for providing the inner controller with the reference values, where different controllers can be employed, such as:

DC and AC voltage controllers

The Active and reactive power controllers

The frequency controller

Controllers Schematics

Wind farm side VSC

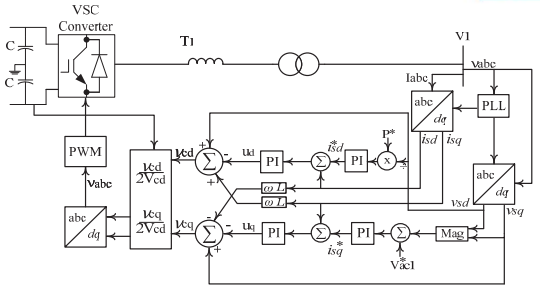

Active power and AC voltages control

Controllers Schematics

Onshore grid side VSC

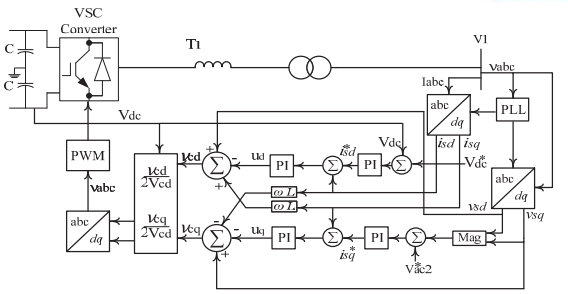

DC and AC voltages control

Test System Configuration – AC regional grids

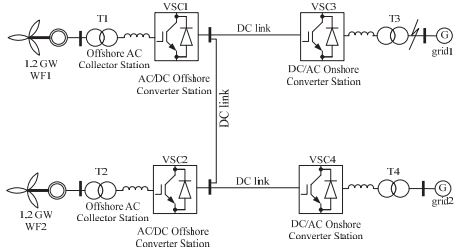

In this model, the VSC-HVDC system controls are as follows:
VSC1,2 converter controls active power flow and AC voltage control,
VSC3,4 converter controls DC and AC Voltages.

Results – active & reactive power, AC voltages

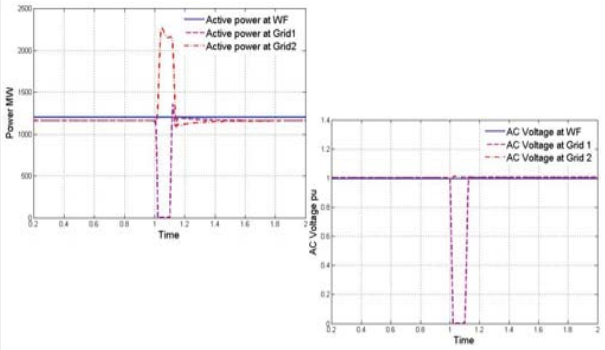

Results – DC Voltages

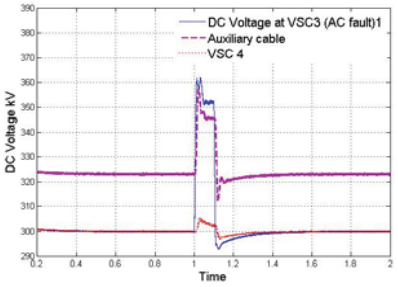

Test System Configuration - slack bus

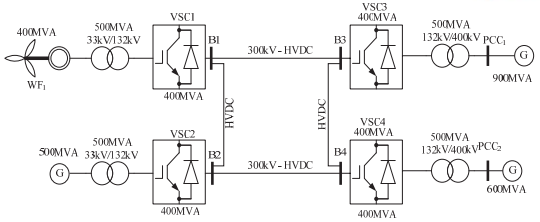

In this model, the VSC-HVDC system controls are as follows:
VSC1,2,4 converter controls active power flow and AC voltage control,
VSC3 converter controls DC and AC Voltages, slack bus

$$P_{slack\ bus} = P_{VSCWF} + P_{VSC2} + P_{VSC4} + P_{Losses}$$

Results – active & reactive power,

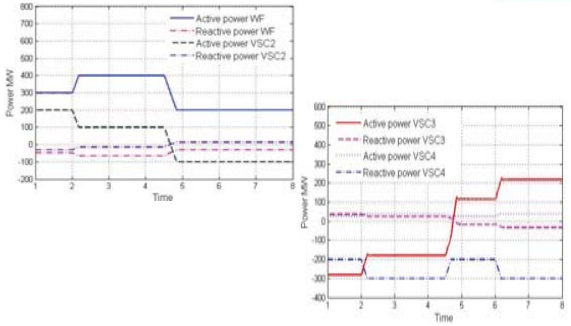

Results – DC Voltages

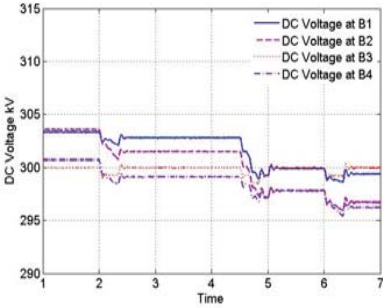

Test System Configuration – droop control

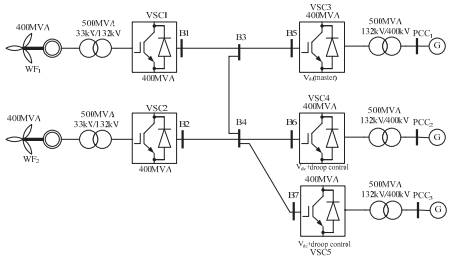

DC Voltage Droop Control

$$V_{dc} = \frac{1}{2}V_{dcj} + \frac{1}{2}\sqrt{V_{dcj}^2 - 4R_{ji}P_i}$$

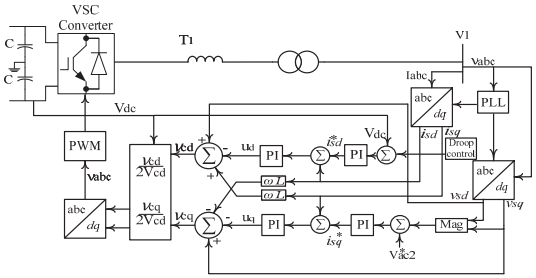

DC Voltage Droop Control

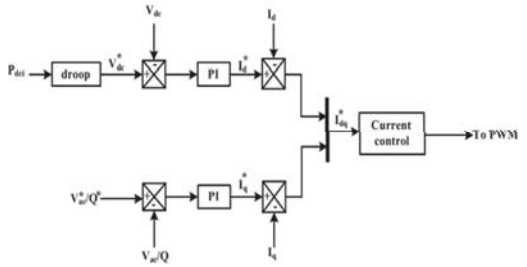

DC Voltage – Droop Control ON

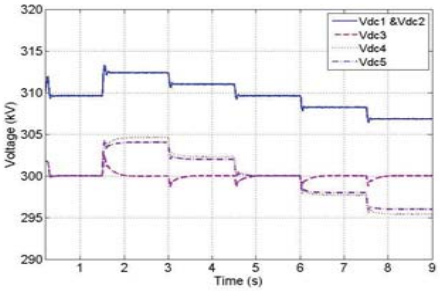

Power Balance – Droop Control ON

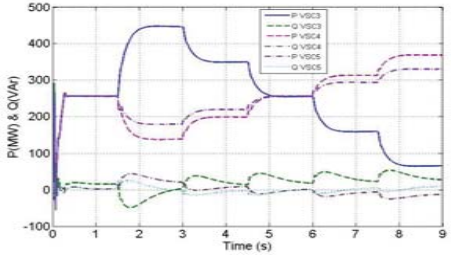

Time	0 - 1.5	1.5 - 3	3 – 4.5	4.5 - 6	6 – 7.5	7.5 - 9
VSC3	255	450	350	255	160	65
VSC4	255	175	220	255	295	330
VSC5	255	140	195	255	310	370

Conclusions

- The controllers can respond to any power demand
- There are significant advantages in terms of power flow controllability
- This can prove to be very advantageous for connection of variable wind generation and assist in the power balancing of interconnected networks.


University of
Strathclyde
Glasgow
The University of Strathclyde is a charitable body, registered in Scotland, with registration number SC015263

SINTEF NOWITECH Norwegian Research Centre for Offshore Wind Technology NTNU

Upon the Improvement of the Winding Design of Wind Turbine Transformers for Safer Performance within Resonance Overvoltages

Amir Hayati Soloot
Hans Kristian Høidalen
Bjørn Gustavsen

10th Deep Sea Offshore Wind R&D Seminar
24-01-2013- Trondheim-Norway

Contents

Challenges for wind farms

- Different challenges
  - Financial
  - political
  - Environmental
  - **technological challenges: can be better understood by observing the failures in wind farm which has occurred up to now.**

Breakdown of component failures for on/offshore wind farms (Nitschke et al., 2006)

Component damages	
Tower	18%
Blades	17%
Gearbox	16%
Generator	13%
Transformer	10%
Nacelle	8%
Control eq.	5%
Others	13%

SINTEF report, "HSE challenges related to offshore renewable energy", 15-02-12

Transient phenomena in Offshore wind farm

1. Switching transients → Energization and Deenergization
2. Lightning transients
3. Earth fault

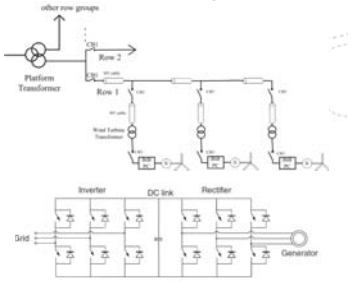

Back to Back power converter

Resonance Overvoltages

1. It may occur during earth fault or energization transients if:
   a. The quarter-wave frequency of cable is close to one of resonance frequencies of transformer, especially the dominant resonance frequency.
   b. The surge impedance of cable is much lower than transformer input impedance and much higher than source impedance
2. It leads to the highest overvoltage amplitudes with high du/dt compared to normal energization overvoltages.

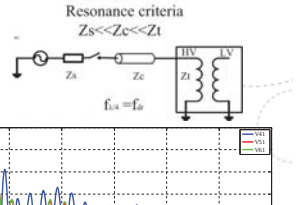

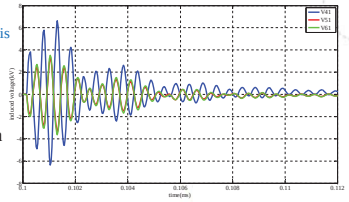

LV voltages for energization at peak of phase A on HV side of no load 300 kVA 11/0.230 kV transformer

Prototype wind turbine transformer 500kVA 11/0.230 kV

7

The winding designs

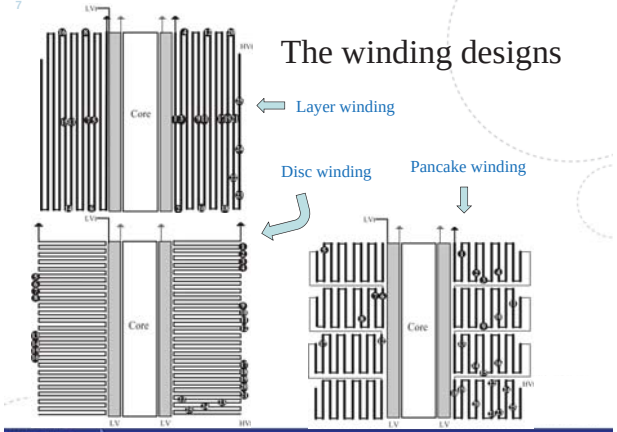

Layer winding

Disc winding

Pancake winding

8

Measurement on 500 kVA transformer

Agilent E5061B-3L5 Network Analyzer

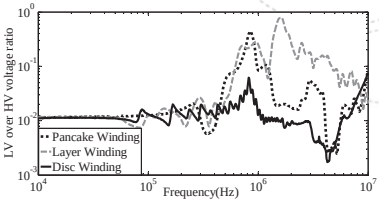

The Diagnosis of resonance frequencies in 500 kVA transformer to select the less critical **winding design** for fixed-length cable energization in wind farms

9

Measurement Results for voltage drop

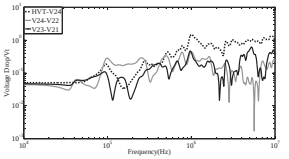

Voltage drop in taps near to HV terminal of the **layer** winding

The frequency response of the three windings for voltage drop near to HV terminal can be observed and compared in these figures.

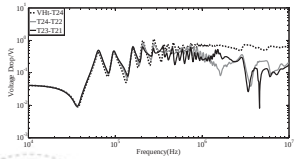

Voltage drop in taps near to HV terminal of the **disc** winding

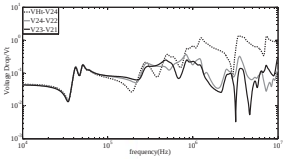

Voltage drop in taps near to HV terminal of the **pancake** winding

10

Measurement Results for voltage drop

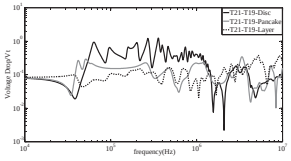

Voltage drop between taps 21 and 19 in three windings

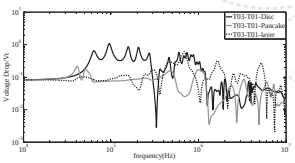

Voltage drop between taps 3 and 1 in three windings

11

Measurement Results for voltage to ground

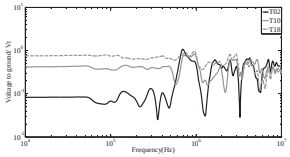

Voltage to ground for tap 2,10 and 18 in **layer** winding

The frequency response of the voltage to ground at the specific taps in the three windings

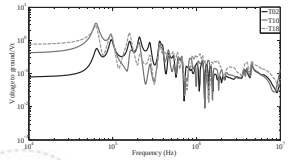

Voltage to ground for tap 2,10 and 18 in **disc** winding

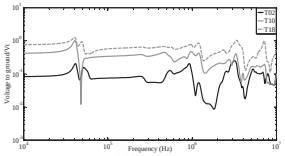

Voltage to ground for tap 2,10 and 18 in **pancake** winding

12

Measured voltage-to-ground distribution in layer winding

The dominant resonance frequency in the layer winding is approximately 1 MHz, which means the energization of the transformer with about 50 meter cable is not recommended (see the equation). The voltage ratio can be maximum mainly in the taps near to HV terminal. But, there is also one voltage ratio peak near to ground. Higher cable length is less critical.

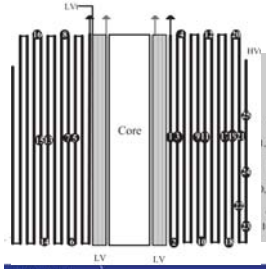

$$f_{\lambda/4} = \frac{surge\ speed\ in\ cable}{4 \times cable\ length} \approx \frac{2 \times 10^8}{4 \times 50} = 1\text{MHz}$$

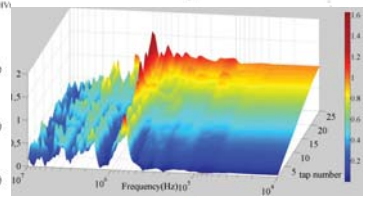

13

Measured voltage-to-ground distribution in disc winding

The dominant resonance frequency in the disc winding is approximately 70 kHz and there are many resonance peaks between 100 and 500 kHz , which means the energization of the transformer with cables more than 100 meter is not recommended. The reason is that the voltage ratio peaks appeared in all the taps (see the right figure).

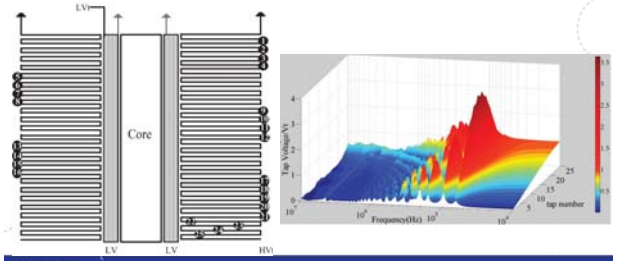

14

Measured voltage-to-ground distribution in pancake winding

The frequency response of the pancake winding is combination of layer and disc winding, i.e. resonance peaks in both 10kHz < f < 1MHz and f> 1MHz. According to the frequency response, the energization can be performed with 100-500 meter cables considering the installation of the protective devices in the taps near to the HV terminal.

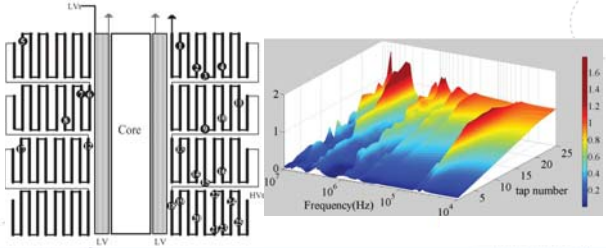

15

Conclusions

- Resonance overvoltages at LV terminal for 500 kVA:

  The dominant resonance frequency for layer winding is 1.6 MHz which the amplitude of transferred voltage is around 80 p.u.. The dominant resonance frequency for disc and pancake is 800 kHz which the amplitude is 6 and 38 p.u., respectively.

- Resonance overvoltages inside windings for 500 kVA:

  1. The voltage drops for taps near to HV terminal of the three windings, have high amplitudes (25 p.u.) at dominant resonance frequencies.
  2. The layer and pancake windings have lower values further down in the middle of winding and near to ground. But, the disc winding keeps the high value of voltage drops at resonance frequencies which means more potential of internal stresses.
  3. The Voltage to the ground in near to HV terminal has low values at resonance frequencies (2 p.u.). But, taps near to ground show high value of voltage to ground at resonance frequencies (about 10 p.u.) for disc and layer winding.

16

Future plan

- Developing analytical model of the 500 kVA transformer: 1-verification with the measurements, 2-study the effect of various design parameters on the frequency response
- Modifying the analytical model with transformer kVA scaling equations in order to observe resonance frequency shifts in 8 MVA transformer compared to 500 kVA one.

17

SINTEF

NOWITECH
Norwegian Research Centre for Offshore Wind Technology

NTNU

Thanks for your attention
Any question?

B2 Grid connection

Planning Tool for Clustering and Optimised Grid Connection of Offshore Wind Farms, Harald G. Svendsen, SINTEF

The role of the North Sea power transmission in realising the 2020 renewable energy targets - Planning and permitting challenges, Jens Jacob Kielland Haug, SINTEF Energi AS

Technology Qualification of Offshore HVDC Technologies,
Tore Langeland, DNV KEMA

Evaluating North Sea grid alternatives under EU's RES-E targets for 2020,
Ove Wolfgang, SINTEF Energi AS

Harald G Svendsen
10th Deep Sea Offshore Wind R&D conference
Trondheim, 24 – 25 Jan 2013

Planning Tool for Clustering and Optimised Grid Connection of Offshore Wind Farms

- Background
- The Net-Op DTOC tool
- Example: Kriegers Flak area
- Conclusions

The problem

Background

- NOWITECH – Norwegian Research Centre for Offshore Wind Technology
  - Has supported development of Net-Op → Applied on North Sea offshore grid analyses
  - www.nowitech.no
- EERA-DTOC – EU FP7 project
  - Aims to establish and integrated Design Tool for Offshore wind farm Clusters, including electrical grid design
  - www.eera-dtoc.eu

Net-Op

- Offshore grid expansion optimisation (planning tool)
  - **Input**: allowable connections + cost parameters + time series for wind power, demand and power prices
  - **Output**: Optimal design (number + capacity of cables)
  - Ref: *Trötscher & Korpås*, dx.doi.org/10.1002/we.461

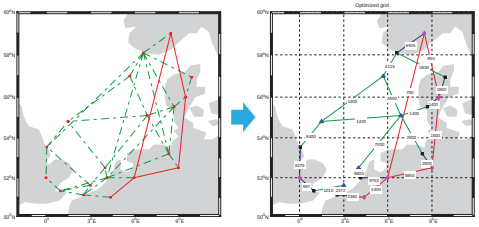

Net-Op approach

- Optimisation
  - Mixed integer linear programming (MILP) problem formulation
  - Cost function = cost of investment + operational costs (net present value)
    - Cost = fixed cost + cost per MW × rating
    - 'fixed cost' may be distance dependent
- Sampling of operational states to account for variable wind, demand and prices
- Need to limit number of allowable connections
- MATLAB implementation

$$\text{possible combinations of } B \text{ branches} = 2^B$$
$$\text{possible connections of } N \text{ nodes, } B = \tfrac{1}{2}N(N-1)$$

Applicable to wind farm cluster level?

Net-Op DTOC – an upgraded version

- Modifications
  - Multiple cable types (AC, DC)
  - Pre optimisation processing
    - Clustering algorithm
    - Automatic generation of allowable connections
  - Interface to external MILP solvers
  - Result export to PSSE, Google Earth plot (KML)
  - Command-line tool

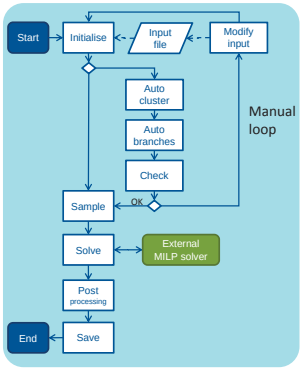

Pre-processing: Generate allowable set of connections

1: Clustering

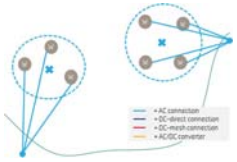

2: Add cluster branches

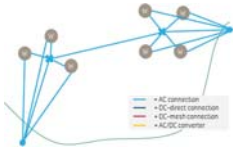

3: Replace AC by DC

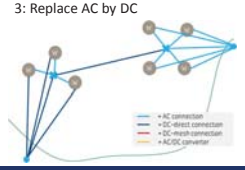

4: Add DC mesh

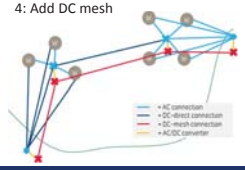

Case study: Kriegers Flak

- Wind farms:
  - Kriegers Flak (DK+DE+SE), Baltic 1 (DE), Ventotec (DE)
- Cost parameters
  - Based on Windspeed project (D2.2 – Garrad Hassan)
- Time series
  - 2010 hourly values for
    - wind production (from DTU's CorWind model – N. Cutululis)
    - demand (daily and seasonal profile as used in TradeWind & OffshoreGrid projects)
    - area prices (from Nordpool & EEX)

Input data

Wind farms:

P	Name	Country
640	Kriegers Flak	SE
288	Baltic 2	DE
600	Kriegers Flak III	DK
48	Baltic 1	DE
500	Baltic Power	DE
400	Wikinger	DE
480	Arkona Becken Südost	DE

Cost data (branches):

	Cost per branch			Cost per branch endpoint			
Type	B_{ij} M€/km	B_{ijW} M€/km/MW	B M€	C^V_{ij} M€/MW	C^- M€	C^V_{ij} M€/MW	C^V_{ij} M€
AC	0	4.1	5.000	11.8	0	11.8	0
DC-direct	0	1.27	5.000	221.8	0	221.8	27.600
DC-mesh	0	1.27	5.000	70.0	0	70.0	0
converter	0	0	0	105.0	0	105.0	27.600

Branch limits and losses

Branch type	Max distance	Max power	power loss constant	power loss slope
AC	70 km	700 MW	0	0.005 %
DC-direct		1200 MW	3.2 %	0.003 %
DC-mesh		1200 MW	0	0.003 %
converter		1200 MW	1.6 %	0

Extract showing two weeks

Wind power

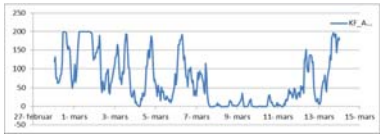

Power prices

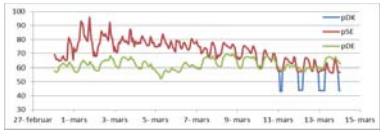

Power demand

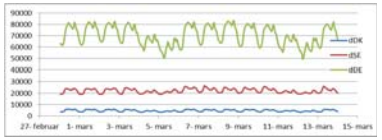

2010 power prices power demand

- Duration curves

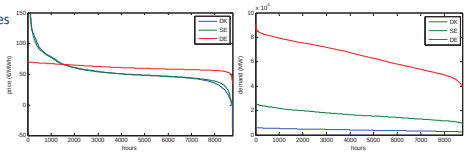

- Weekly average

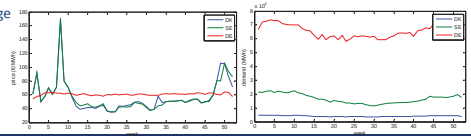

Net-Op DTOC processing

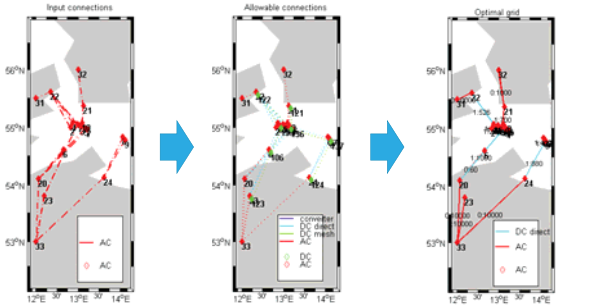

Result: Optimal grid

Additional output

- E.g. branch flow

from	to	cable type	loss fraction	distance	new cables	total capacity	cost (M€)	mean flow 1->2	mean flow 2->1
4	22	3	3.406 %	68.5	1	526	829	291.9	113.2
6	20	1	0.340 %	68.0	0	60	0	20.4	0.0
9	24	3	3.437 %	79.1	1	880	1138	380.2	0.1
10	21	1	0.169 %	33.9	1	700	348	350.6	164.7
20	33	1	0.001 %	123.0	0	10,000	0	724.8	64.2
21	32	1	0.001 %	70.1	0	1,000	0	350.0	164.7
22	31	1	0.001 %	25.3	0	10,000	0	282.0	113.2
23	33	1	0.001 %	90.3	0	10,000	0	0.0	0.0
24	33	1	0.001 %	165.6	0	10,000	0	367.1	0.1
1	35	1	0.029 %	5.9	1	200	48	92.8	0.0
2	35	1	0.034 %	6.9	1	200	55	90.2	0.0
3	36	1	0.025 %	5.0	1	200	41	92.4	0.0
4	35	1	0.021 %	4.3	1	522	53	129.8	220.5
5	36	1	0.020 %	4.0	1	288	39	134.6	0.0
7	36	1	0.037 %	7.4	1	500	79	234.7	0.1
8	37	1	0.019 %	3.7	1	400	42	196.8	0.1
9	37	1	0.015 %	3.0	1	400	36	0.1	196.8
10	36	1	0.033 %	6.6	1	700	84	257.8	142.3
36	35	1	0.081 %	16.2	1	515	156	92.1	184.2
36	20	3	3.570 %	123.3	1	1,000	1558	732.7	66.3

Conclusion

- Net-Op DTOC is a tool for clustering and grid connection optimisation of offshore wind farms
- High-level automated offshore grid planning, taking into account
  - Investment costs
  - Variability of wind/demand/power prices
  - Benefit of power trade between countries/price areas
- The tool will be integrated in the DTOC framework (www.eera-dtoc.eu)

SINTEF

Technology for a better society

The role of the North Sea power transmission in realising the 2020 renewable energy targets -

Planning and permitting challenges

Jens Jacob Kielland Haug
SINTEF Energy Research
Deep Wind seminar 24th January, Trondheim

Background

- October 19th 2011 – EC Energy Infrastructure Package
  - Measures that can affect planning and permitting practices for power transmission projects in the North Sea
- Background: Enormous investments needed in energy infrastructure to reach European energy and climate goals
- Challenges
  - Not all investments are commercially viable
  - **Building permits** takes too long to obtain
- What are the planning and permitting barriers for power transmission projects in the North Sea?
- Review of secondary literature

Challenges (1): Wind farm connections

- In most countries a permit to connect to the grid is required
- Some countries - Sweden, Germany, Belgium and the Netherlands, also require a permit to lay cables on the seabed
- Examples of permitting of wind power installations and cables being done by different authorities (Germany)
  - Can lead to more complex procedures and increased time use
- Few countries have provided information on the permitting process and the extent of coordination between authorities
- A more integrated approach between infrastructure permitting and grid connection permitting should be promoted
- Complex process - even more so for cross-border projects (hub-to-hub connections, tee-ing in of a wind farm)
- Permitting procedures for cross-border projects should be reviewed and simplified

(Sources: Seaenergy 2020 and OffshoreGrid)

Challenges (2): Interconnectors

Administrative challenges

- Different number of permits required in different countries
- Conflicts with environmental authorities represent a critical barrier
- Lack of coordination and standardisation of environmental impact assessments
  - Examples of projects being subject to an EIA in only one of the affected countries
  - Difficult for the TSOs to predict the decision made by environmental authorities
- Important not to see the one-stop shop model as the major solution
  - TSOs preferred interacting directly with the different authorities
  - One/few procedures rather than one/few authorities
- However, DK experiences show that the one-stop-shop model can be improved
  - conflicts were reduced as the Danish TSO engaged in direct dialogue with different authorities and private stakeholders

(Source: Twenties)

Challenges (3): Sea use

Shipping

- Maritime authorities routing demands with regard to shipping lanes causes major barriers
- Installation and maintenance of cables hinders shipping
- Emergency anchorages can damage cables - major economic impacts and temporary obstruction of shipping lanes during repair work

Fishing interests

- During cable installation fishing interests are denied access to areas used for fishing - recurring demands of compensation
- Fishing appliances can damage cables (trawl equipment) - cable burying reduces the risk
- Military interests, sand extraction, wind farms and other cables and pipelines can also represent barriers

Challenges (4): Onshore infrastructure

- Landfall points-overhead electricity lines and converter stations receives major public criticism
  - Demand for underground cables
- A strong onshore grid is a prerequisite for transmission of offshore power - in many European countries reinforcements are often delayed due to low public acceptance
- In addition to being an economically sound solution, moving towards a meshed grid could;
  - reduce the need for onshore transmission reinforcements
  - reduce onshore connection points
  - minimised space use as a result of more integrated infrastructure (possibly less maritime spatial conflicts) – Cobra cable bundling with wind park connectors increased acceptance

The EC's energy infrastructure package

- October 19, 2011- EC –Proposal for a regulation of the European Parliament and of the Council on guidelines for trans-European energy infrastructure and repealing Decision NO 1364/2006/EC (COM (2011) 658).
- The North Sea is one of 12 prioritised trans-European energy infrastructure corridors – projects of common interests (PCI) will be:
  - Eligible for EU funding through Connecting Europe Facility (CEF) - 9.1 billion from 2014-2020
  - Benefit from a **special permit granting procedure**

(cont.)

- Time limit -three years
- One Stop Shop
- Member States must take measures to streamline the EIA procedures
- Citizens will be involved before the project developer submits the formal application for a permit-in contrast to current practices in many member states
- Impact assessments will be taken into account at an earlier stage in the process and will be more closely connected to public and stakeholder involvement
- The Commission also acknowledges the benefits of effective upfront maritime spatial planning – impact assessment

Can maritime spatial planning facilitate power transmission permitting?

- Several studies point to the potential importance of MSP in facilitating effective permitting processes
  - Cobra cable (the Netherlands and Denmark-transit country: Germany)
- Recently enacted maritime spatial plan in German EEZ
  - positive effect as it facilitated for early identification of conflicts by early stakeholder dialogue (water and shipping authorities and nature protection authorities)
- However, the maritime plan did not reserve areas for interconnector corridors or for cable connections (OWF) – stakeholders carrying zoning rights posed some difficulties

(Cont.)

- A number of studies have pointed to the necessity to include, at some point, new developments related to offshore grid design within existing North Sea maritime spatial planning policies
- NSCOGI (Representatives from the governments, ENTSO-E, ACER, national regulators, the Commission and experts) recently published guidelines for planning and permitting procedures - recommends:
  - The use of existing MSP or sea masterplans or;
  - Overview of all planned and existing North Sea areas protected or dedicated to specific uses (military interests, shipping, fishery etc) supplied by planning or permitting authorities and the applicant/TSO
- The Seaenergy project suggests regional sea basin MSP forums - could facilitate transnational agreement on a grid connection master plan in the medium term and a could result in a more effective approach to planning
- Maritime spatial planning as a complementary strategic planning approach to a North Sea offshore grid traditionally based on a techno-economic planning approach
- The Seaenergy project has mapped a concrete grid infrastructure, including wind farm locations, against shipping routes, pipelines and cable routes and nature conservation areas in the North Sea

In conclusion

- No insuperable planning and permitting barriers to power transmission in the North Sea today, but more research is needed
- Maritime spatial planning could be important for conflict management and effective permitting procedures as different sea uses are expected to increase considerably in the North Sea
- In addition to being an economically sound solution, moving towards a meshed grid could have several benefits related to current and future planning and permitting challenges that are crucial to realise a North Sea offshore grid
- Thank you!

Technology Qualification for offshore HVDC

DeepWind 2013 - 10th Deep Sea Offshore Wind R&D Conference

Tore Langeland
24.01.2013

MANAGING RISK

Presentation outline

- Introduction to Det Norske Veritas (DNV)
- Building a position in power system transmission and distribution
- Research and innovation in DNV
- Risk based approach for development of offshore HVDC transmission technologies

Highly skilled people across the world

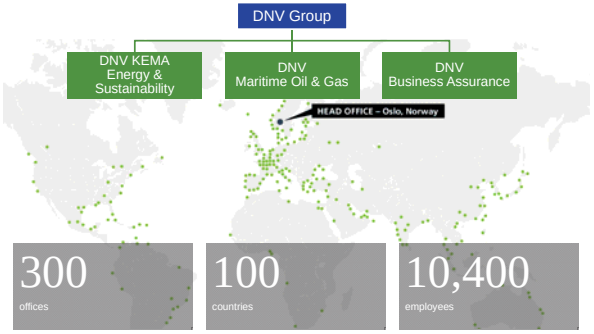

Build and share knowledge

- We invest 6% of our revenue in research and development
- We take a lead role in joint industry research and development projects
- Through our standards, rules, recommended practices and software solutions we share knowledge with the industry

Risk based approach for development of offshore HVDC transmission technologies

STRI KEMA

Outline

- Motivation
- Technology Qualification Process
- Qualification Basis
- Technology Assessment
- Other relevant initiatives
- Further work – JIP Invitation

STRI KEMA

Motivation

Motivation

Background

- 40 GW offshore wind in Northern Europe by 2020
- 150 GW offshore wind in Europe by 2030
- Grid connection of offshore oil & gas installations
- The vision of an offshore Super Grid

The challenge

- *To date there exists no operational experience with high capacity offshore HVDC transmission technologies*
- *Installations far from shore and in harsh marine environments will require high focus on Reliability, Availability and Maintainability*
- *Interoperability challenges arise with technology from multiple vendors*

Motivation

Offshore HVDC transmission

Level 1
Two converter stations
Capacity less than maximal loss of infeed

Level 2
Three or more converter stations
Capacity less than maximal loss of infeed

Level 3
Multiple converter stations
Capacity higher than maximal loss of infeed

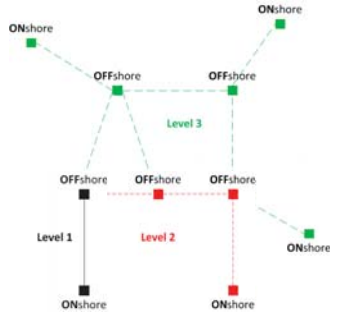

Lack of relevant standards for offshore transmission

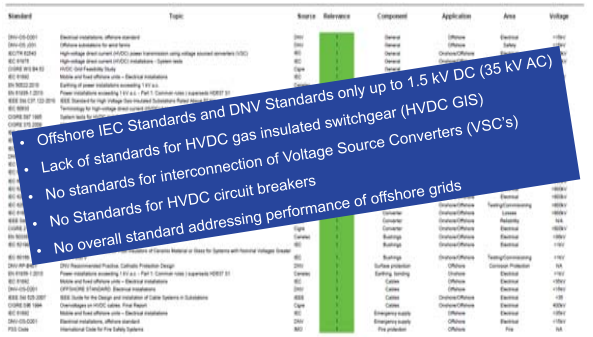

- Offshore IEC Standards and DNV Standards only up to 1.5 kV DC (35 kV AC)
- Lack of standards for HVDC gas insulated switchgear (HVDC GIS)
- No standards for interconnection of Voltage Source Converters (VSC's)
- No Standards for HVDC circuit breakers
- No overall standard addressing performance of offshore grids

Technology Qualification Process

Technology Qualification Process

DNV's Definition of Qualification:

Qualification is the process of providing the evidence that the technology will function within specific limits with an acceptable level of confidence.

Technology Qualification Process

DNV RP-A203

- First edition published in 2001
- Qualification of new technologies where failure poses risk to life, property, the environment or high financial risk.
- Qualification of technologies that are not new
  - Proven components assembled in a new way
  - Not covered by existing requirements and standards
  - Proven technology in a new environment
- Developed for the offshore oil&gas industry to increase stakeholder confidence in applying new technologies.

Technology Qualification Process

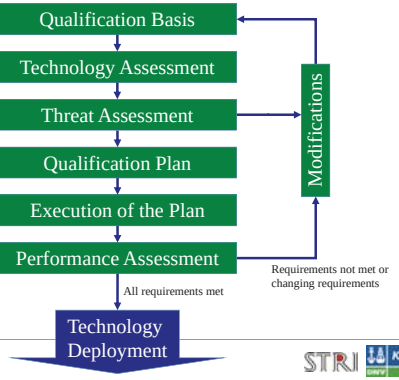

Why do we need technology qualification?

Testing is conducted according to old schemes that do not take into account new failure modes

- Equipment placed in a new environment
  - Harsh climate
  - Difficult access
- New approach to maintenance and repair strategy
- Auxiliary systems
  - Control of indoor environment
- Higher voltage, current and power ratings
  - Converter and cables
- New applications
  - Multi-Terminal DC (MTDC)
  - Meshed MTDC grid
- New design of major components
  - DC converter station and valves
  - Cables
  - DC switchgear
- System behaviour
  - Control, protection and communication

Increases the **RISK** exposure

Added value of technology qualification for offshore HVDC

- Demonstration of technology capabilities
- Address stakeholder uncertainties
  - Maturity and uncertainty of technologies
  - Feasibility of offshore HVDC transmission
- Address the risk exposure
  - Identification and categorization of technologies w.r.t. industry experience and maturity
  - Identification and understanding of failure modes and the risk picture
  - Development of methods and activities to address the risks
  - Overall reliability and availability of technologies and systems

Qualification Basis

Qualification Basis

Technology specification

- System description
- Standards and industry practice
- Maintenance and Operation strategy
- Boundary conditions

Requirements specification

- Reliability, Availability, Maintainability
- Functional requirements

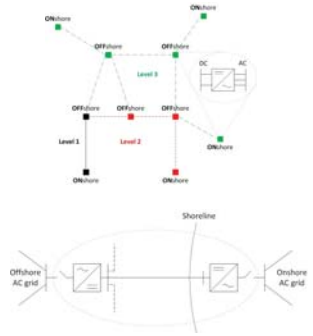

Technology Assessment

Technology Assessment

Technology breakdown

- Component
- Purpose/description
- Grid level
- Main challenges

Technology categorization

1. No new technical uncertainties
2. New technical uncertainties
3. New technical challenges
4. Demanding new technical challenges

Application Area	Degree of novelty		
	Proven	Limited field history	New or unproven
Known	1	2	3
Limited Knowledge	2	3	4
New	3	4	4

Technology Assessment

Based on STRI experience from Testing, Simulation & Studies

- Accredited high voltage testing for testing of major equipment according to relevant standards and customer requirements, e.g. CIGRE recommendations for MI DC cables and extruded DC cables. IEC 60840 and IEC 62067 for extruded AC cables.
- Simulation of HVDC and HVAC systems using most suitable program; SIMPOW, PSS-E, PSCAD-EMTDC, DigSilent etc.
- Feasibility and application studies involving users and manufacturers

Technology Assessment

Level 2-4 categorized offshore HVDC technologies

- Fast and selective detection, location and clearing of faults in a DC grid
- DC circuit breaker
- Control system for MTDC
- Polymer cable system (rating)
- Dynamic cable system
- DC Switchgear (AIS*/GIS*)
- DC/DC converter

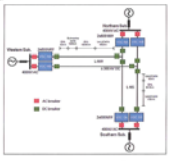

Figure 3-1 Topology of the three-terminal HVDC System.

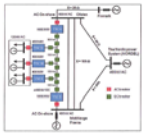

Figure 3-2 Topology of the five-terminal HVDC system.

Technology Assessment

Level 2-4 categorized offshore HVDC technologies

- Fast and selective detection, location and clearing of faults in a DC grid
- DC circuit breaker
- Control system for MTDC
- Polymer cable system (rating)
- Dynamic cable system
- DC Switchgear (AIS*/GIS*)
- DC/DC converter

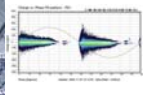

Technology Assessment

Level 2-4 categorized offshore HVDC technologies

- Fast and selective detection, location and clearing of faults in a DC grid
- DC circuit breaker
- Control system for MTDC
- Polymer cable system (rating)
- Dynamic cable system
- DC Switchgear (AIS*/GIS*)
- DC/DC converter

*AIS: Air Insulated Switchgear, GIS: Gas Insulated Switchgear

Test of UHVDC switchgear at STRI high voltage laboratory (Photo: STRI)

Test of HVDC VSC for an offshore application at STRI high voltage laboratory (Photo: ABB)

Other relevant initiatives

Relevant initiatives

Cigré

- SC B4 - HVDC and Power Electronics
  - B4-52, B4-55, B4-56, B4-57, B4-58, B4-59, B4-60
- SC B1 - Insulated Cables
  - B1.27, B1.32, B1-34, B1-35, B1.38, B1.40, B1.43

EC DG Energy

- Working group for offshore/onshore grid development

NSCOGI

- WG 1 Offshore Transmission Technology

ENTSO-E

- Regional Group North Sea (RG NS)

IEC/CENLEC

- TC 115 High Voltage Direct Current (HVDC) transmission for DC voltages above 100 kV
- CLC/SR 115 High Voltage Direct Current (HVDC) Transmission for DC voltages above 100kV (Provisional)

German commission for electrical, electronic & information technologies

- Technical guidelines for first HVDC grids - A European study group

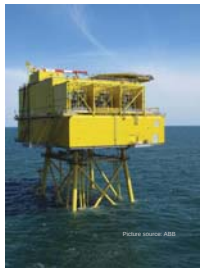
Picture source: ABB

Future work

Joint Industry Project

Why:

- Need for a faster, more efficient and more reliable deployment of offshore HVDC transmission systems.

How:

- Integrating ongoing activities and experiences of different technologies in new environments with a proven method for risk management - the DNV RP-A203.

Why DNV KEMA and STRI?

DNV KEMA

- Independent foundation with the purpose of safeguarding life property and the environment
- More than 40 years of experience in managing risk for the offshore oil and gas sector
- More than 80 years of experience in electric transmission and distribution including accredited high voltage testing facilities
- The world's second largest consulting company for wind energy projects with 30 years of wind energy experience
- Leading certifying agency for offshore wind projects
- Continuously running 30-40 Joint Industry Projects

STRI

- Independent power system consulting company with an accredited high voltage laboratory.
- Several large flexible high voltage test halls to conduct tests on products with system voltages up to 1000 kV.
- Test halls for testing of pollution, snow, ice, salt, fog and rain effects as well as chambers for multiple stress, salt fog and extreme temperatures.
- Experience in system studies for wind power integration and HVDC applications, including multi terminal VSC technology.


Test of HVDC VSC for an offshore application in STRI high voltage laboratory (Photo: ABB)

Joint Industry Project

- Scope of work
  - Activity 1 – Develop a Technology Qualification procedure for offshore HVDC transmission technologies
  - Activity 2 – Qualification examples
  - Activity 3 – Hearing process and publication
- Participants
  - Manufacturers
  - Developers
  - Operators
- Timeline
  - Kick off in October 2012
  - Industry wide hearing by Q1 2014
  - Final publication in Q2 2014

Thank you for your attention!

Safeguarding life, property
and the environment

www.dnv.com

Evaluating North Sea grid alternatives under EU's RES-E targets for 2020

Ove Wolfgang, Hans Ivar Skjelbred and Magnus Korpås, SINTEF Energy Research

DeepWind 2013, 24. – 25. January 2013, Trondheim

About study

- **Are RES-E targets important for North Sea Grid?**
  - Offshore wind-power must be connected
  - Norwegian hydropower can balance RES-E variability
  - Surplus in the Nordic area
- **Role of North Sea power transmission in realizing the 2020 renewable energy targets (2010-13)**
- **For North Sea grid configurations:**
  - Quantify energy system effects
  - Evaluate costs and benefits

Content

Tool for calculation of benefits

- EMPS model
  - No: Samkjøringsmodellen
  - Hydropower scheduling
  - Energy system planning
  - Forecasting
  - SDP
- Minimizes operational cost for a given system
- Benefit of a cable: reduced system costs

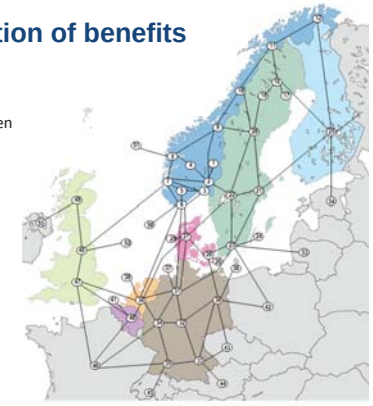

EMPS inputs

North Sea nodes

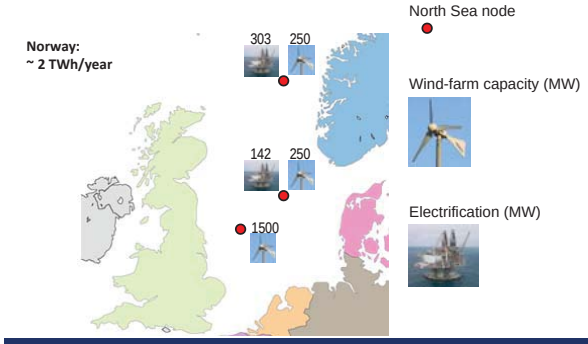

EMPS inputs

Main inputs for stage 2020

Input	Major reference
RES-E	National action plans
Thermal power capacity	ENSO-E, 2020 forecast
Consumption	National action plans
Transmission capacity	ENTSO-E, Dena II, SINTEF
Prices (fuel, CO2, …)	EC Roadmap, 2020-forecast

EMPS outputs

Power prices (average)

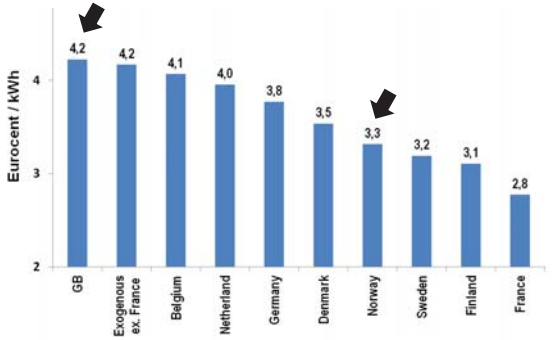

EMPS outputs

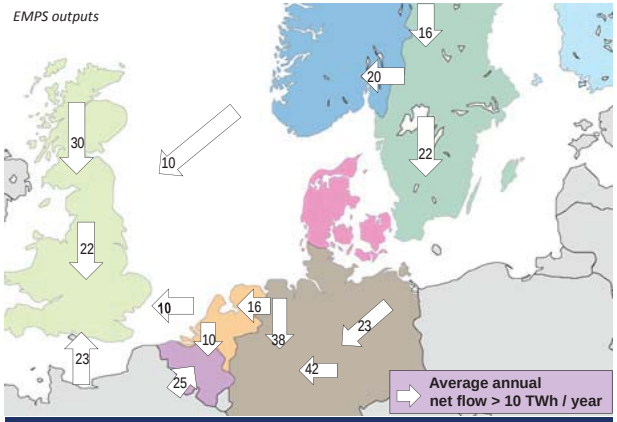

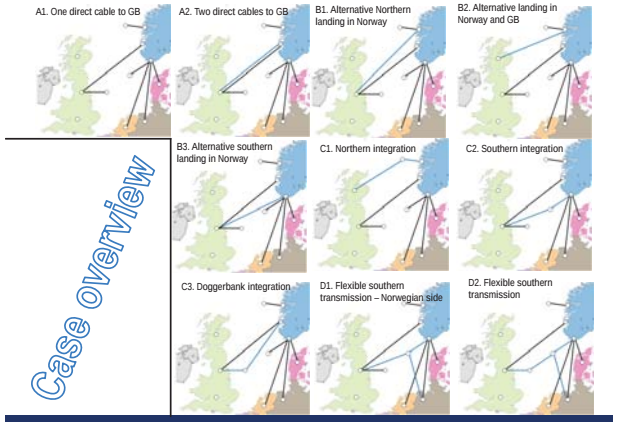

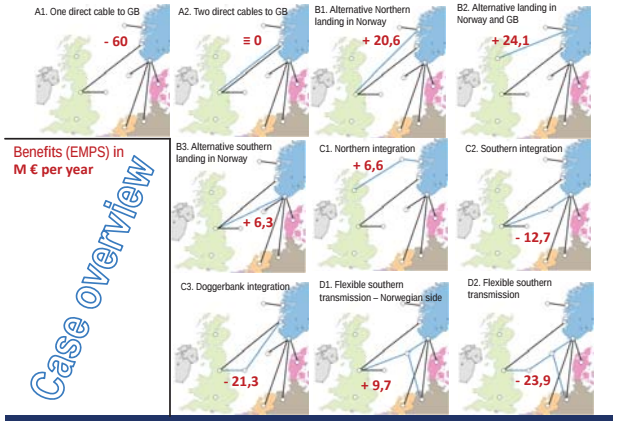

Costs: inputs

Investment costs

Table: Costs for 600 MW modules (PV)

Component	Cost	Unit
Trench/laying cost	0,76	M€/km
Cable cost, fixed charge	5,0	M€
AC/DC converter station onshore	136,1	M€
AC/DC converter station and platform offshore	167,2	M€
DC breaker and switching gear onshore, per cable	45,3	M€
DC breaker and switching gear offshore, per cable	55,7	M€

Source: Windspeed project: http://www.windspeed.eu

- Scaling, e.g. 600 MW → 1400 MW

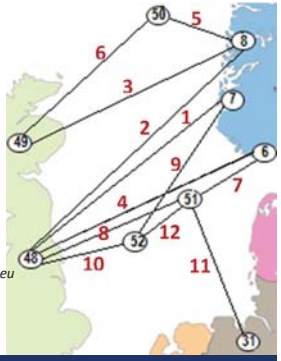

Evaluation

Cost-benefit for 2nd 1400 MW direct connection

- Benefits: 60 M € / year
- Costs: 123 M € / year

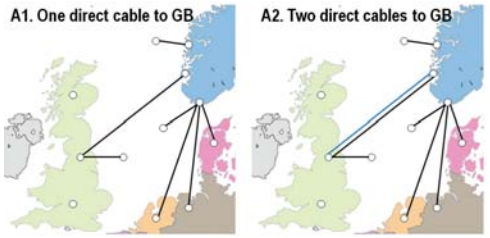

Evaluation

Cost-benefit for alternative landing of 2nd cable

(relative to A2)

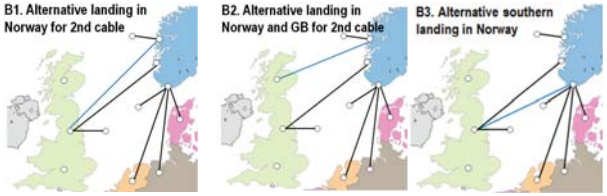

+20/+14/+6 +24/-11/+35 +6/-8/+14

Benefits / Costs / Total (in M € per year)

Evaluation

Higher prices in NOR-VESTSYD

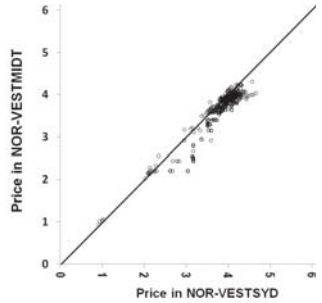

Evaluation

GB-North prices are lower but volatile

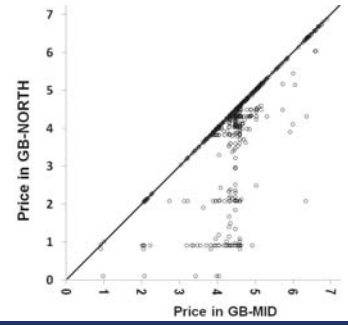

Costs: technologies

Offshore integration technologies

- **Integration**
  - North Sea nodes
  - 1400 MW NO-GB cable
- **Investment costs**
  - Saved cable meters
  - Extra offshore equipment

1) **T-junction**
   - Optimized for 2020 wind power
   - Non-flexible
   - Least expensive
2) **Flexible setup**
   - Preparation for future
   - 1400 MW infrastructure
   - DC breakers: Flexible
   - High cost
3) **"DC case"**
   - 1400 MW
   - Fewer DC breakers
   - Intermediate costs

C1. Northern integration

Table: Relative to direct Northern connection (M € per year)

	Flex	DC	T-Junction
250 MW wind			
Benefits	-18	-18	-18
Costs	12	3	-5
Total	-30	-21	-13
1000 MW wind			
Benefits	-13	-13	-13
Costs	1	-12	-19
Total	-14	-1	6

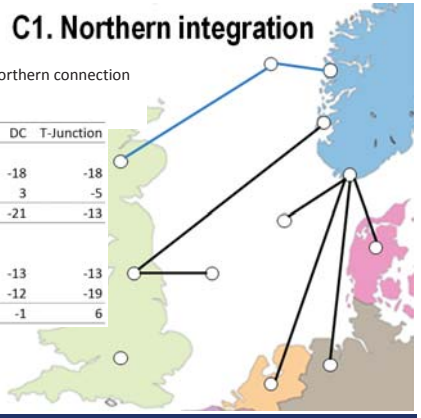

Evaluation

Northern: Direct vs. integrated connection

All simulated cases 2004

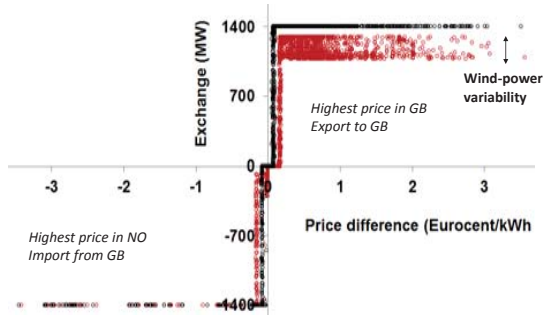

Offshore integration gives reduces transmission

Example: Wind 200 MW, electrification 300 MW

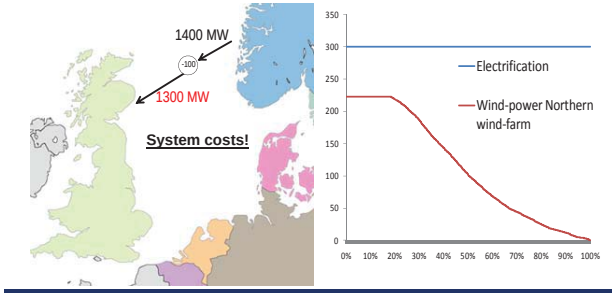

C2. Southern integration

Table: Relative to direct Southern connection (M € per year)

	Flex	DC	T-Junction
250 MW wind			
Benefits	-19	-19	-19
Costs	10	2	-8
Total	-29	-21	-11
1000 MW wind			
Benefits	-9	-9	-9
Costs	-8	-21	-27
Total	-1	12	18

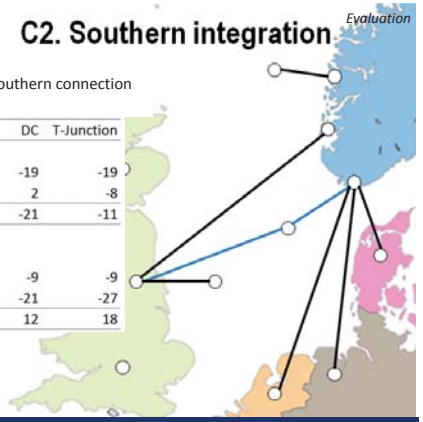

D1. Flexible southern transmission – Norwegian side

Table: Relative to Southern Integration (M € per year)

	Flex / DC
Benefits	22
Costs	72
Total	-50

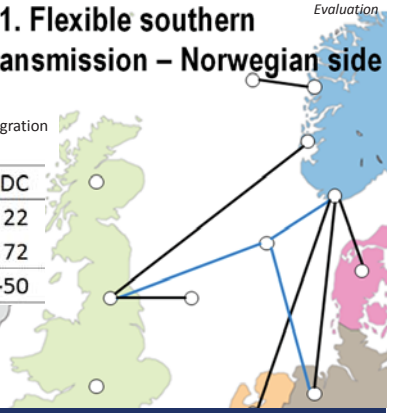

Additional cases

- No nuclear power in Germany
- No exchange with exogenous countries

Major findings

1) **Cables between GB and NO: mostly used for export to GB**
2) **2nd direct connection GB – NO in 2020**
   a) Not profitable
   b) Northern route gives highest benefits and lowest costs
3) **Offshore integration relative to direct connections**
   a) Benefits: Lower because of reduced flexibility
   b) Costs: Lower for T-junction, higher for full flex
   c) Cost/benefit: 250 MW / 1 TWh wind: direct connections
      1000 MW / 4 TWh wind: integrated solutions
4) **Leg to Germany: Extra costs > Extra benefits**

Limitations & uncertainties

- **Many**
  - Mathematical model vs. real world (limitations)
  - Energy system in 2020 (uncertainties)
- **Uncertainties**
  - RES-E implementation
  - Economic development
  - EU policies (RES-E, GHG)
  - Nuclear power
  - Technology developments
  - *… and many others*
- **Limitations**
  - Beyond 2020 developments
  - Balancing markets
  - Competition
  - Failures
  - Price variation
  - Not-considered uncertainties
  - *… and many others*

Exact geographical locations of nodes

Renewable electricity generation

Based on EU directive and national plans for 2020

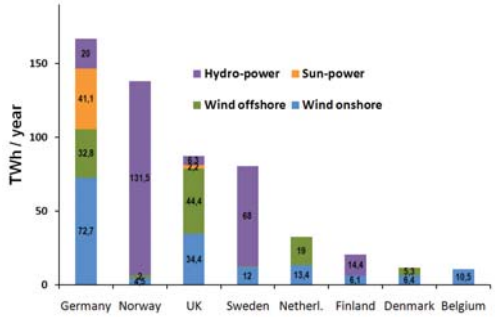

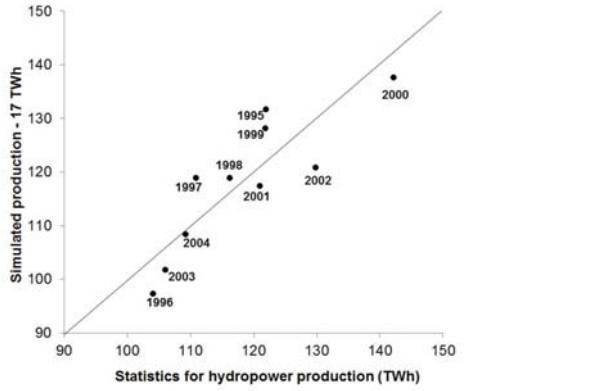

Figure 4.5 Actual annual hydropower variability for Norway 1995 – 2004, and simulated values minus 17 TWh.

Sun-power: Within-day profile area 34

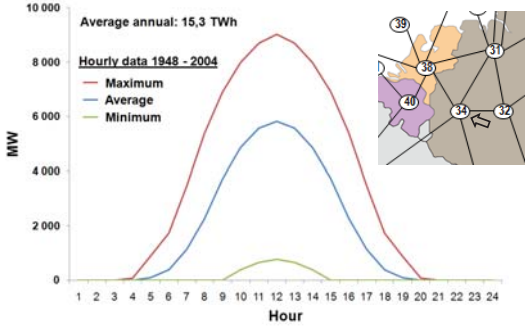

Wind-power: Within-day profile area 52

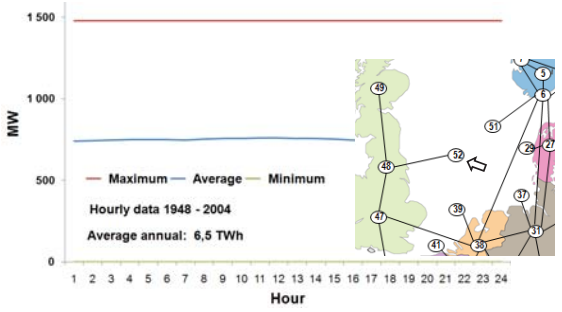

(A) The 34 within-week sequential time-steps in model
(B) Relative load-profile for area 34

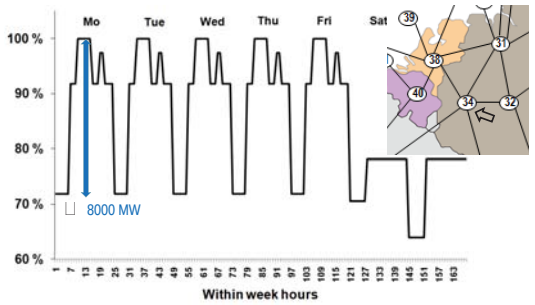

EMPS inputs

Thermal power capacity change 2008 - 2020 (ENTSO-E forecast)

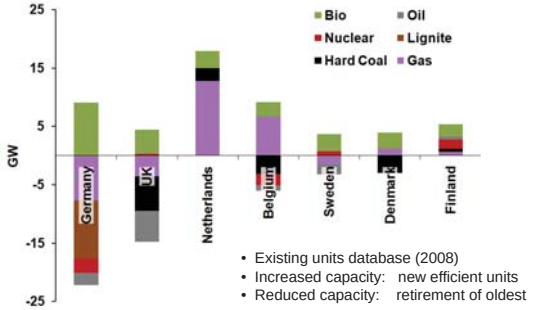

- Existing units database (2008)
- Increased capacity: new efficient units
- Reduced capacity: retirement of oldest

North Sea transmission cables in basecase

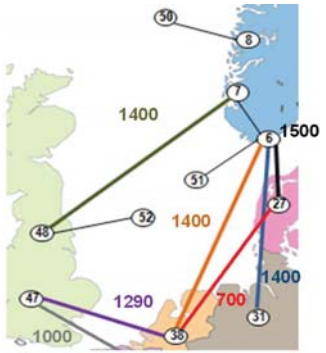

ENTSO-E forecast for thermal power capacity

Table 3.3 Forecasted 2020-capacity (MW) for thermal power generation

	Denmark	Sweden	Finland	Belgium	Netherlands	Germany	UK
Hard coal	700	100	2900	200	7500	26000	17800
Lignite						14000	
Bio	2805	2914	2920	2470	2892	9062	4210
Gas	2000	900	2300	10300	21800	18000	32300
Nuclear		10100	5900	4120	500	18800	11200
Oil	600	2400	1200		200	1000	
Mixed/unid.	1900	500	2200		1200	5000	1400
Total	8005	16914	17420	17090	34092	91862	66910

Unit aggregation
(for handling of problem-size with start-up costs)

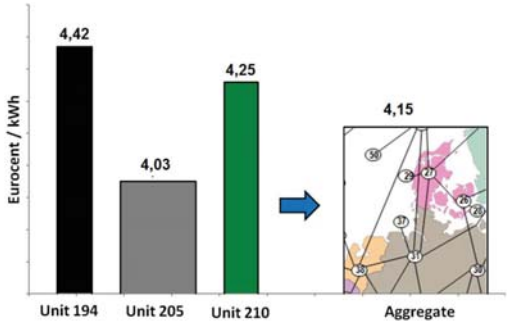

Fossil-fuel price forecast

- Reference: A Roadmap for moving to a competitive low carbon economy in 2050
- Primes model simulation
- Reference scenario (Includes 20/20/20 policy)

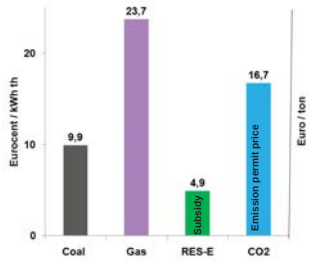

Coal-power cheaper than gas-power

$$mc^{coal}_{40\%}(€/MWh\ el) = \frac{\overbrace{9,9(€/MWh\ th)}^{coal\ price} + \overbrace{16,5(€/ton)}^{permit\ price} \cdot \overbrace{0,37(ton/MWh\ th)}^{emission\ coefficient}}{\underbrace{0,4(MWh\ el\ /\ MWh\ th)}_{efficiency}} = 40,0$$

$$mc^{gas}_{60\%}(€/MWh\ el) = \frac{23,7(€/MWh\ th) + 16,5(€/ton) \cdot 0,2(ton/MWh\ th)}{0,6(MWh\ el\ /\ MWh\ th)} = 45,0$$

Consumption

Mostly based on ENTSO-E forecast

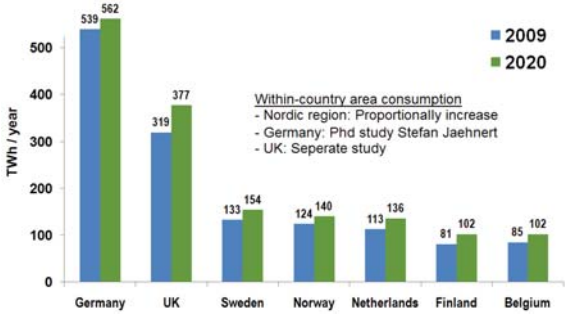

EMPS inputs

Transmission capacity matrix

	Endogenous countries								Exogenous countries							
To\From	NO	SW	DE	FI	GE	GB	NL	BE	IR	FR	SWZ	AU	CZ	PO	LI	ES
NO	-	5100	1550	150	1400	1400	1400									
SWE	5100	-	2440	2450	600									100	1000	
DE	1550	1980	-		2035		700									
FI	100	2850		-												600
GE	1400	600	2600		-		6500			2700	4400	2000	2300	1200		
GB	1400					-	1290	1000	500	3000						
NL	1400		700		6100	1290	-	2400								
BE						1000	2400	-		996						
IR						1000										
FR					2700	3000		996								
SWZ					2060											
AU					2200											
CZ					800											
PO		600			1200											
LI		1000														
ES				650												

Evaluation

Doggerbank: Direct vs. integrated connection

All simulated cases 2004

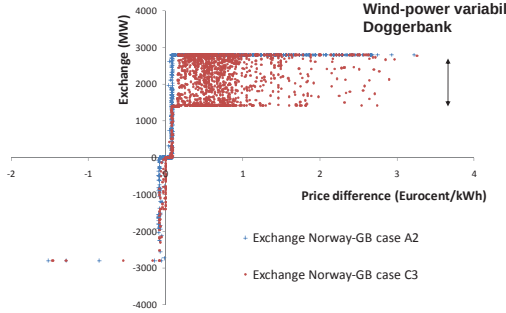

Duration curves German 2004-prices

A2_G: No exogenous trade. A2_GA: G + no nuclear in Germany

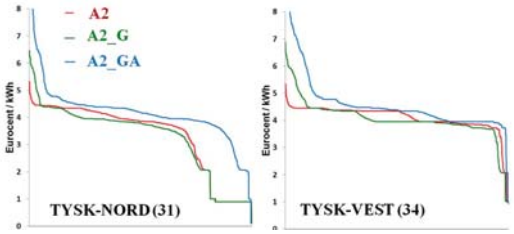

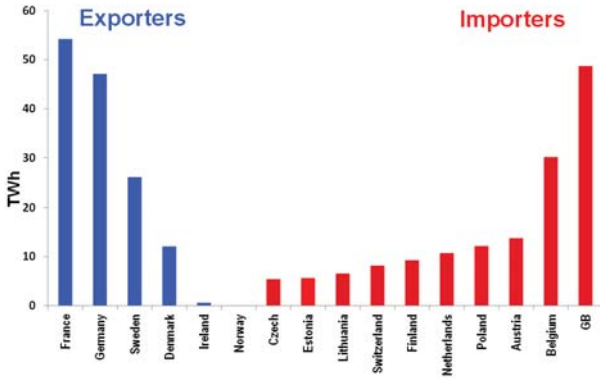

Table 4.1 Simulated energy balances for 2020 (TWh). Annual average for climate years 1948 – 2004.

	Norway	Sweden	Denmark	Finland	GB	Germany	Netherlands	Belgium
Gross consumptio	140,1	154,6	38,7	102,3	378,1	562,7	136,7	102,3
Export	30,9	42,1	23,3	8,1	3,4	81,2	29,7	6,0
Total use	171,0	196,7	62,0	110,5	381,5	643,9	166,4	108,3
Hydro ex. pumped	133,1	68,5		14,1	6,3	19,9		
Wind and solar	6,5	12,6	11,5	6,1	79,9	146,3	32,4	11,3
Bio		18,4	18,5	17,1	28,6	59,2	19,6	16,5
Coal			16,0	8,8	105,6	226,4	55,3	
Gas	0,5	2,1	3,2	2,3	25,4	21,6	14,9	12,5
Oil		3,8	1,5	0,4		1,7		
Nuclear		75,2		44,3	83,6	134,8	3,8	31,7
Other								
Total generation	140,0	180,7	50,7	93,1	329,4	609,9	126,0	72,1
Import	31,0	16,0	11,2	17,4	52,1	34,1	40,5	36,2
Curtailment								
Total available	171,0	196,7	62,0	110,5	381,5	643,9	166,4	108,3
Net export	0,0	26,1	12,1	-9,3	-48,7	47,1	-10,7	-30,2
RES-E	139,6	99,6	30,1	37,3	114,8	225,4	52,0	27,9

Table 4.2 Change 2009 – 2020 (TWh). IEA's annual energy balances are used for 2009.

	Norway	Sweden	Denmark	Finland	GB	Germany	Netherlands	Belgium
Gross consumptio	18,6	16,6	3,9	21,0	20,9	25,7	22,9	18,5
Export	16,3	33,0	12,4	4,7	-0,3	27,1	19,1	-5,3
Total use	34,9	49,6	16,3	25,8	20,6	52,8	42,0	13,2
Hydro ex. pumped	8,3	3,1		1,5	2,2	3,2	-0,1	0,2
Wind and solar	5,5	10,1	4,8	5,8	70,6	101,1	27,8	10,1
Bio		6,8	14,8	8,7	16,6	26,2	12,3	11,4
Coal		-1,5	-0,6	-6,3	3,4	-11,9	29,8	-5,9
Gas	-3,7	0,6	-3,1	-7,0	-134,3	-51,5	-50,9	-15,8
Oil		3,1	0,4	-0,1	-4,2	-7,2	-1,4	-0,3
Nuclear		25,2		21,7	20,8	7,1	-0,2	-13,3
Other				-0,3		-6,4	-0,1	-0,1
Total generation	9,5	47,5	16,3	24,0	-25,0	60,6	17,1	-13,6
Import	25,3	2,2	0,0	1,9	45,5	-7,8	25,0	26,7
Curtailment								
Total available	34,8	49,7	16,4	25,9	20,5	52,7	42,0	13,1
Net export	-8,9	30,8	12,4	2,8	-45,8	34,9	-5,8	-32,0
RES-E	13,5	20,0	19,6	16,0	89,4	130,5	40,0	21,8

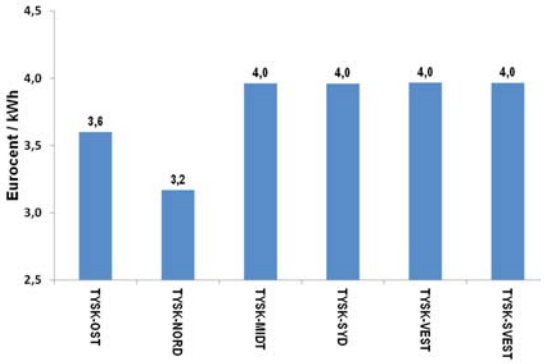

Figure 4.7 Average prices in German areas

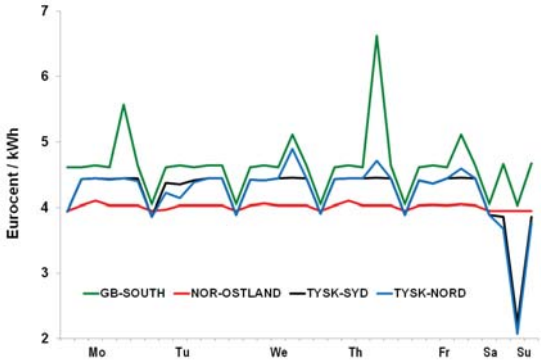

Figure 4.14 Example of simulated prices for one week

Figure 4.17 Transmission between GB-NORTH and GB-MID. All simulated time-steps in 2004.

C1 Met-ocean conditions

Wave-induce characteristics of atmospheric turbulence flux measurements, Mostafa Bakhoday Paskyabi, UiB

Experimental characterization of the marine atmospheric boundary layer in the Havsul area, Norway, Constantinos Christakos, UiB

Buoy based turbulence measurements for offshore wind energy applications, Martin Flügge, Univ of Bergen

Effect of wave motion on wind lidar measurements - Comparison testing with controlled motion applied, Joachim Reuder, Univ of Bergen

Turbulence analysis of LIDAR wind measurements at a wind park in Lower Austria, Valerie-Marie Kumer, Univ of Bergen

Wave–induced characteristics of atmospheric turbulence flux measurements

Mostafa Bakhoday Paskyabi

Geophysical Institute, University of Bergen, Norway
Mostafa.Bakhoday@gfi.uib.no

and

M. Flugge, J. B. Edson, J. Reuder

Wind and Wave energy distribution in period

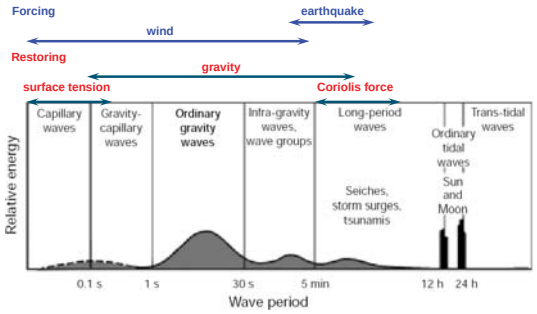

Outline

- In Situ wind data sources and uncertainties.
- **Particular problems on buoys and ships measurements.**
- The air-sea fluxes: Definitions, parameterizations, and measurements.
- **Sea Surface.**
- Field work.
- **Wave-dependent hydrodynamic properties.**
- Results.

In Situe wind data sources and uncertainties

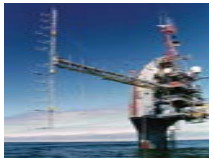

Upper: R/V Roger Revelle and WHOI Flux buoy.

Lower left: R/P FLIP. Lower right: direct flux sensors.

The air-sea fluxes

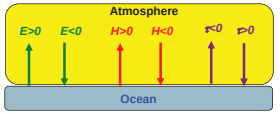

- *Turbulent fluxes*
- *Radiative fluxes*
- *Freshwater flux*
- *Net surface fluxes*

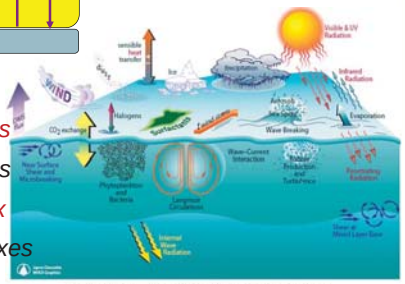

(Illustration by Jayne Doucette, Woods Hole Oceanographic Institution)

Why accurate air-sea fluxes are important

- Sensitive indicators of changes in the climate system, integrating changes in the:
  - Wind Speed
  - Air/Sea temperature difference
  - Vertical moisture differences
- Reducing large uncertainities on currently air-sea fluxes (Validation against measurements is rare and of limitation in space. Cross checks of different products (NOAA/NESDIS/NCEP and NODC/COADS, European ECMWF, British SOC, etc.) reveal large differences, but cannot tell which one is better)
- Concistency of air-sea fluxes with the ocean dynamics and energetics.

Turbulent fluxes

- Momentum flux is expressed as

$$\tau = -\rho_a(\overline{u'w'}\,\hat{\mathrm{i}} + \overline{v'w'}\,\hat{\mathrm{j}}),$$

- Estimated via:
  - direct method (Eddy Correlation),
  - Bulk parameterizations,
  - indirect technique (Inertial Dissipation)

Eddy correlation

- **Statistical meaning:**
  $u'w'$ can be considered as the second mixed moments, i.e. co-variances of variables
- **Requirements**:
  - Time resolution should be high (10-20 Hz).
  - Time of record should be relatively long (more than 20 min).
  - Stable platform.
- **Instrumentations:**
  - Sonic anemometer.
  - Fast-response thermometer.
  - Fast-response infrared hydrometer.

Eddy correlation for moving platforms: Particular Problems

- *Wind flow distortion*
- *Sea spray and salt contamination*
- *Ship and buoy motion*
- *Other contaminations*

Bulk parameterizations

Conventionally, Eq.

$$\tau = -\rho_a(\overline{u'w'}\,\hat{\mathrm{i}} + \overline{v'w'}\,\hat{\mathrm{j}}),$$

is parameterized by the following bulk formula

$$\tau = \rho_a C_D U(z)^2,$$

where U is the horizontal mean wind speed at height z meters above the ocean surface.

the vertical velocity profile is given based on Moninon–Obukhov similarity theory by

$$U(z) = \frac{u_*}{\kappa}\left|\ln\frac{z}{z_0} - \psi_m\right|,$$

Bulk parameterizations

where κ is the von kármán constant, z_0 is the aerodynamic roughness length, and ψ_m denotes the integrated non–dimensional wind gradient (ϕ_m) that is an empirical function of the stability parameter:

$$\xi = \frac{z}{L} = \frac{zg\kappa(\overline{\theta'w'} + 0.61T\overline{q'w'})}{u_*^2 T},$$

where L is the Obukhov length and $\overline{\theta'w'}$ is the buoyancy flux, T denotes the mean potential temperature in the surface layer, and g denotes acceleration due to gravitational force. The air–side friction velocity, u_* introduced in Eqs. (3) and (4) is defined through the wind stress magnitude as

$$u_* = \frac{|\tau|}{\rho_a} = \sqrt{(\overline{u'w'})^2 + (\overline{v'w'})^2},$$

Using dimensional analysis, Charnok 1955 [1] proposed that z_0 can be described as

$$z_0 = \phi\frac{u_*^2}{g},$$

Field Work

- During 13 April to 29 June 2010.
- Air-Sea Interaction Tower (ASIT).
- A moored buoy about 600 meters away from ASIT.

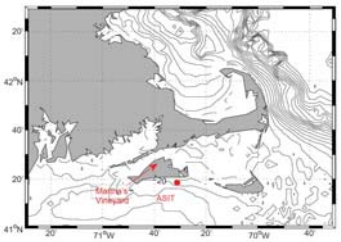

Wind forcing and wave condition

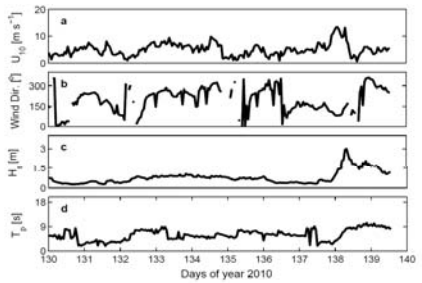

Fig. 2. Environmental conditions at the observation site between days 130 to 140, 2010. a) Wind speed at 10-m height, b) Wind direction, c) significant wave height Hs, and d) peak wave period T_p.

Wind speed: correction scheme

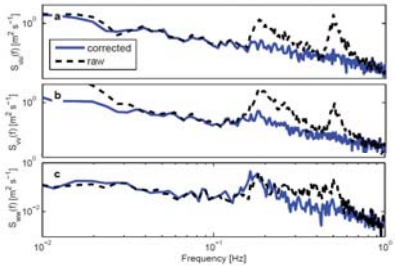

Fig. 3. Power spectral density of raw (dashed) and corrected (solid). a) u–component, S_{uu}, b) v–component, S_{vv}, and c) w–component, S_{ww}, of wind speed vector on 1 am, 11 May 2010 .

Wind speed: correction scheme

the corrected wind velocity using motion package sensors is expressed by the following basic equation:

$$\mathbf{V}_{true} = \mathbf{TV}_{obs} + \Omega \times \mathbf{TL} + \mathbf{TV}_{plat},$$

where $\mathbf{V}_{true}$ is the corrected wind vector in the Earth reference frame, $\mathbf{V}_{obs}$ denotes the measured wind velocity vector relative to the buoy coordinate system, $\mathbf{T}$ is the transform matrix from buoy coordinate to the Earth reference fixed frame of coordinate, $\mathbf{L}$ represents the position vector of the wind sensor with respect to the motion package, and $\mathbf{V}_{plat}$ is the buoy translational velocity vector with respect to the buoy coordinate system. Before starting EC technique, the corrected velocity vector is rotated into the streamwise wind·

Inertial motion unit

Wind speed: correction scheme

- 6DOF motion correction for wind speed vector using accelerometer, gyroscope, and compass:

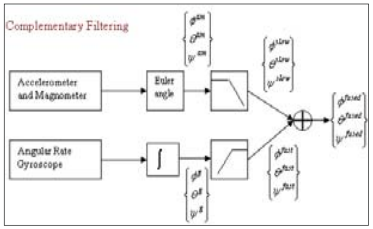

Wind speed: correction scheme

- There is a modified universal spectrum that will confirm skill of correction

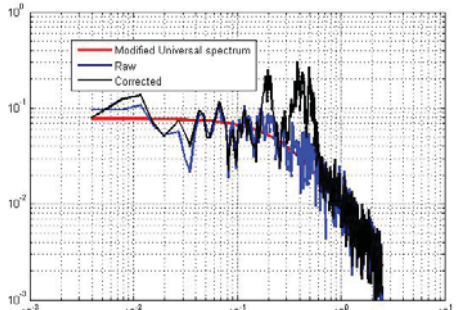

Wind speed: wave-dependent surface hydrodynamic properties

Total wind stress can be written as

$$\tau = \tau_v + \tau_t + \tau_w.$$

Following Janssen 1991, the wave–dependent total wind velocity is given by

$$U_{10}^{w}(z) = \frac{u_*}{\kappa}\left[\ln\left(\frac{z+z_1}{z_0+z_1}\right) - \psi_m\right].$$

where z_1 is the wave stress contribution in the effective roughness ($z_e = z0 + z_1$).

Wind speed: wave-dependent surface hydrodynamic properties

The wave stress is expressed as

$$\tau_w = \rho_w \int_0^{2\pi} \int_0^{\infty} \sigma S_{in}(\sigma,\theta) d\sigma d\theta, \quad |\theta_{wind} - \theta| \le \pi/2,$$

where θ_{wind} is the wind direction, θ and σ denote the direction and the angular frequency, respectively. The wind energy input source term is expressed as

$$S_{in}(\sigma,\theta) = \sigma \frac{\rho_a}{\rho_w} \left[\frac{1.2}{\kappa^2} \epsilon \ln^4(\epsilon) \right] \left(\frac{u_* \cos(\theta)}{c_p} \right) E(\sigma,\theta) = \beta_* E(\sigma,\theta),$$

with

$$\epsilon = \left(\frac{u_* \cos(\theta)}{c_p} \right)^2 \left(\frac{g\kappa^2 z_r}{u_*^2} \right) \exp\left(\frac{\kappa c_p}{u_* \cos\theta} \right),$$

$$z_r = \frac{z_0}{\sqrt{1 - c_0 \tau_w / \tau}} \text{ and } z_0 = \frac{\beta_0 u_*}{g\sqrt{1 - c_0 \tau_w / \tau}},$$

The drag coefficient is then extracted by assuming a bulk relation for wave-induced momentum

wave-dependent surface hydrodynamic properties for days 130-140

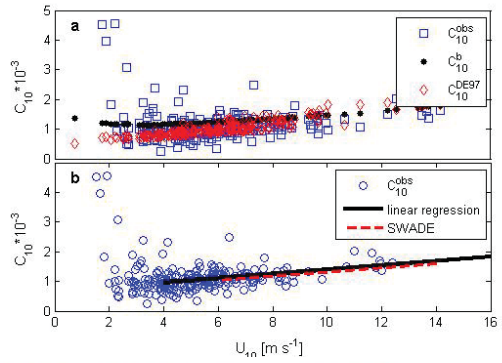

wave-dependent surface hydrodynamic properties for days 160-170

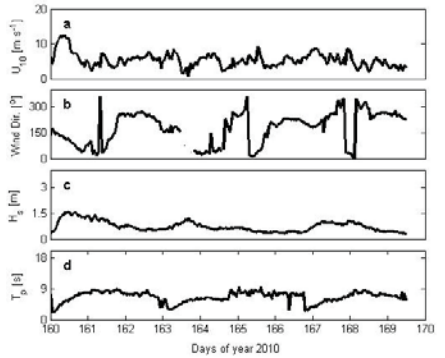

wave-dependent surface hydrodynamic properties for days 160-170

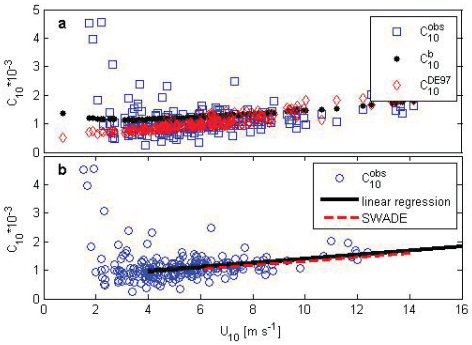

wave-dependent surface hydrodynamic properties (days 160-170)

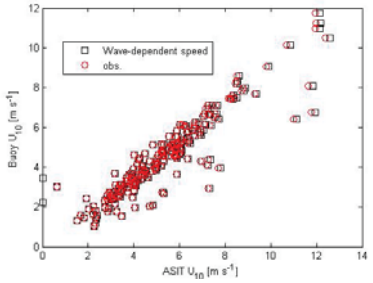

wave-dependent surface hydrodynamic properties

$$\tau = \tau_v + \tau_t + \tau_w.$$

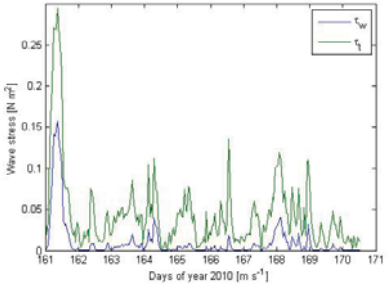

wave-dependent surface hydrodynamic properties

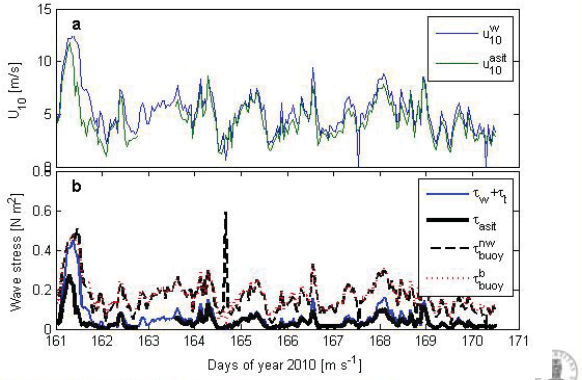

wave-dependent surface hydrodynamic properties

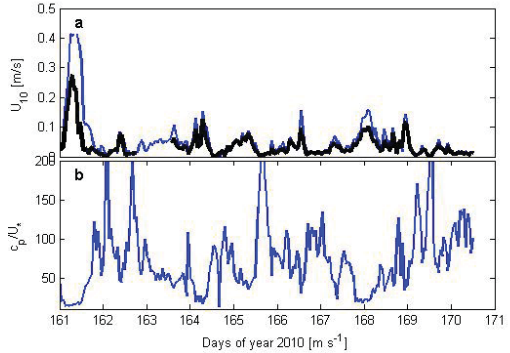

wave-dependent surface hydrodynamic properties

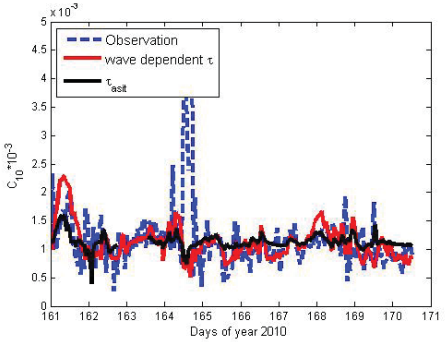

wave-dependent surface hydrodynamic properties

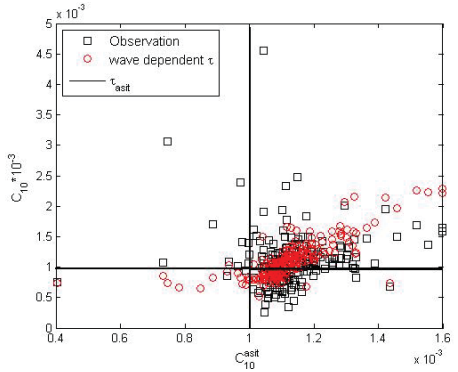

Conclusions

We presented breifly:

- Hydrodynamic properties of water surface.
- Motion correction,
- Wave-induced momentum stress,
- Comparisons made between fixed and moving platforms.

Thank you

Experimental characterization of marine atmospheric boundary layer in the Havsul area, Norway

Konstantinos Christakos[a], Joachim Reuder[a], Birgitte R. Furevik[a,b]
[a] Geophysical Institute, University of Bergen, Norway
[b] Norwegian Meteorological Institute, Norway

10th Deep Sea Offshore Wind R&D Conference , 24./25.01.2013, Trondheim

Outline

- Introduction
- Data overview
- Results
- Outlook

Source: Norcowe

Marine Atmospheric Boundary Layer (MABL)

- Average wind profiles
- Wind shear over the rotor disk
- Turbulence
- Atmospheric stability
- Wind-waves interactions

the main problem:

- the lack of observational data in the relevant altitude range (sea surface to 200m)

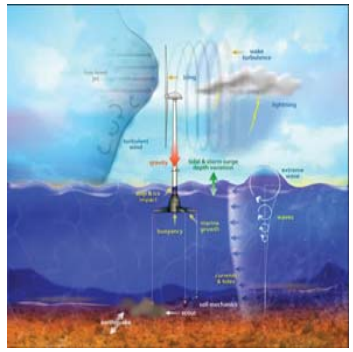

Source: http://www.ieawind.org/GWEC_PDF/GWEC%20Annex23.pdf

Marine Atmospheric Boundary Layer (MABL)

- Average wind profiles
- Wind shear over the rotor disk
- Turbulence
- Atmospheric stability
- Wind-waves interactions

the main problem:

- the lack of observational data in the relevant altitude range (sea surface to 200m)

Remote sensing instruments (i.e LIDAR)

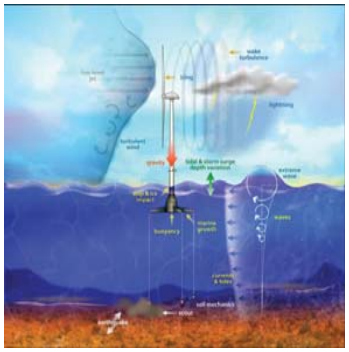

Source: http://www.ieawind.org/GWEC_PDF/GWEC%20Annex23.pdf

LIDAR (LIght Detection And Ranging)

Advantages:

- Simultaneous measurements in several heights (up to 200 m)
- 3D wind velocity vector (u, v, w)

Disadvantage :

- absence of temperature measurements (vertical gradient).

Atmospheric stability?

Stability and turbulence affect wind energy production [1], [2]

Source: VestaVind Offshore

How can atmospheric stability be estimated?

Wharton and Lundquist (2012) suggested different turbulence parameters for classifying wind profiles by stability [2] ,[3], based on onshore data (in western North America)

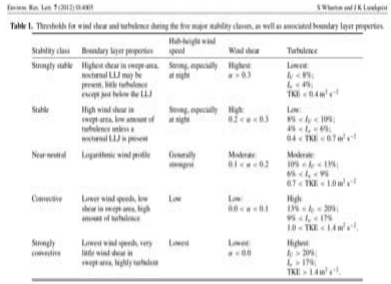

Table 1. Thresholds for wind shear and turbulence during the five major stability classes, as well as associated boundary layer properties.

Stability class	Boundary layer properties	Hub-height wind speed	Wind shear	Turbulence
Strongly stable	Highest shear in swept area, nocturnal LLJ may be present, little turbulence except just below the LLJ	Strong, especially at night	Highest: $\alpha > 0.3$	Lowest: $I_T < 8\%$; $I_k < 4\%$; $TKE < 0.4\ m^2\ s^{-2}$
Stable	High wind shear in swept area, low amount of turbulence unless a nocturnal LLJ is present	Strong, especially at night	High: $0.2 < \alpha < 0.3$	Low: $8\% < I_T < 10\%$; $4\% < I_k < 6\%$; $0.4 < TKE < 0.7\ m^2\ s^{-2}$
Near-neutral	Logarithmic wind profile	Generally strongest	Moderate: $0.1 < \alpha < 0.2$	Moderate: $10\% < I_T < 13\%$; $6\% < I_k < 9\%$ $0.7 < TKE < 1.0\ m^2\ s^{-2}$
Convective	Lower wind speeds, low shear in swept area, high amount of turbulence	Low	Low: $0.0 < \alpha < 0.1$	High: $13\% < I_T < 20\%$; $9\% < I_k < 17\%$ $1.0 < TKE < 1.4\ m^2\ s^{-2}$
Strongly convective	Lowest wind speeds, very little wind shear in swept area, highly turbulent	Lowest	Lowest: $\alpha < 0.0$	Highest: $I_T > 20\%$; $I_k > 17\%$; $TKE > 1.4\ m^2\ s^{-2}$

Turbulence parameters

- The horizontal turbulent intensity is dimensionless parameter which is defined as the standard deviation of horizontal velocity fluctuation divided by the mean horizontal wind speed:

$$I_U = \frac{\sigma_U}{U}$$

- The TKE is defined as the sum of the velocities variances in latitudinal (u), longitudinal (v) and vertical (w) direction divided by 2 :

$$TKE = \frac{1}{2}\left(\sigma_u^2 + \sigma_v^2 + \sigma_w^2\right)$$

Data overview

- 4 years(2008-2012) wind profile data were collected at the small island of Storholmen which is located 8 km northwest of the island of Vigra on the west coast of Norway.

Fig.1. *Location of Storholmen island (black square) in Ålesund, Norway. Source: Google Maps*

Data overview

- The wind speed was measured by WindCube v.1 LIDAR at 8 height levels between 60 m and 200 m a.s.l. (above sea level)
- For higher levels the data availability was reduced due to low aerosol concentration in the air which leads to a low SNR.

Only complete 10 min. average wind profiles (75249) between 60 m and 150 m a.s.l. have been used for the presented analysis.

Source: Vestavind Offshore

Investigation of Turbulence Intensity and Wind Speed

- Log-normal distribution is applied to describe the turbulence intensity distribution for different classes of wind speed at 100 m a.s.l.

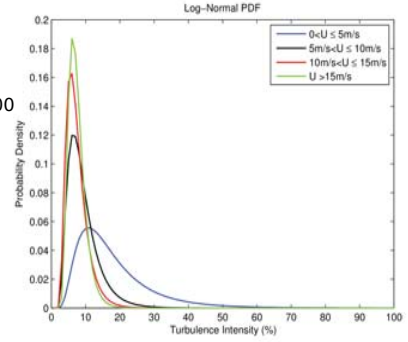

Results:

For increasing wind speed:

1. the center of distribution moves towards to lower turbulence intensities
2. The probability density for the peak value increases

Turbulence Intensity and Wind Profiles

- Average wind profiles for different classes of horizontal turbulence intensity (at 100 m a.s.l.).
- The number of profiles for each class is given in parenthesis

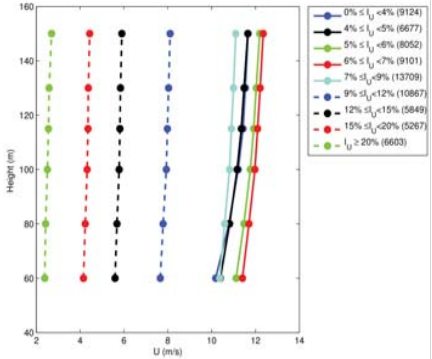

Results :

- Clear dependency between turbulence intensity and wind profiles
- For turbulence intensities greater than 6%, increase of U is related to decrease of turbulence intensity.
- For turbulence intensities below 9% the average profiles are closely grouped between 10m/s and 12m/s

Turbulence Intensity and Wind Shear

- The wind profiles have been normalized to 1 at 100m a.s.l.

Result:

- A general increase in wind shear for decreasing turbulence intensities.

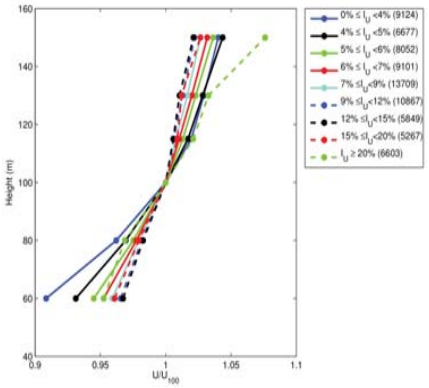

TKE and Wind Profiles

- Average wind profiles for different classes of TKE (at 100 m a.s.l.).
- The number of profiles for each class is given in parenthesis

Results :

- Clear dependency of TKE on wind profiles
- The higher the TKE, the higher the wind speed
- TKE is mainly generated by wind shear in MABL

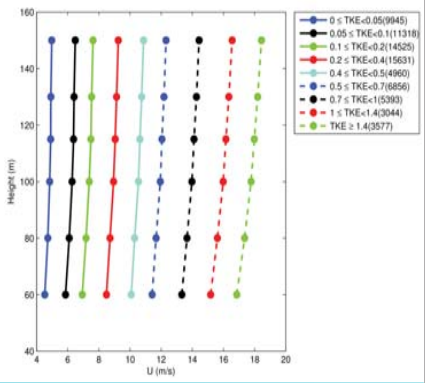

TKE and Wind Shear

- The wind profiles have been normalized to 1 at 100m a.s.l.

Result:

- For lower levels:
  for increasing TKE, the wind shear decreasing
- For higher levels:
  very little variation between TKE and wind shear

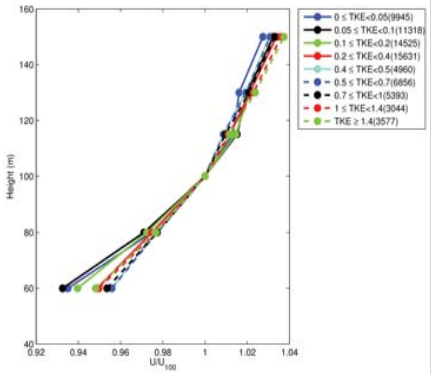

Summary and outlook

- Measurements of offshore wind conditions are essential for the accurate characterization of MABL
- Remote sensing instruments can provide a rich of source data for a better understanding of turbulence of the wind field
- Turbulence parameters such as turbulence intensity and TKE are strongly related to the wind profiles
- For offshore conditions turbulence intensity seems more promising for the classification of stability
- Need for simultaneous measurements of temperature gradient and turbulence parameters for the classification of stability

Thanks for your attention !

Source: Norcowe

References

[1] B J Vanderwende and J K Lundquist (2012) The modification of wind turbine performance by statistically distinct atmospheric regimes, Environ. Res. Lett. 7

[2] Wharton S and Lundquist J K (2012) Atmospheric stability affects wind turbine power collection, Environ. Res. Lett. 7

[3] Wharton S and Lundquist J K (2012) Assessing atmospheric stability and its impacts on rotor-disk wind characteristics at an onshore wind farm, Wind Energy 2012 15:525–546

Acknowledgements

The authors express appreciation to Vestavind Offshore AS for sharing the wind data. The leader author expresses his gratitude to NORCOWE and Statoil ASA for received travel grant.

Application of the NORCOWE DCF System for Ship based measurements

Martin Flügge[1],
Joachim Reuder[1]
[1]Geophysical institute, University of Bergen, Norway

January 24th, 2013

Background

- Offshore wind farms located close to shore line and/ or in shallow water → jacket or monopile foundations
- Increased demand for sustainable energy → developement of floating turbines that can be moored in deep water

Figure: Top 25 offshore wind farms currently operational. *Source:* http://en.wikipedia.org/wiki/List_of_offshore_wind_farms

Results from Sullivan et al. (2008) suggest that surface waves influence the lower part of the MABL in horizontal and vertical directions

↓↓

Increase of loads and fatigue on turbine rotor blades!

Figure: Hywind turbine outside Karmøy, Norway. *Source:* http://www.offshore.no

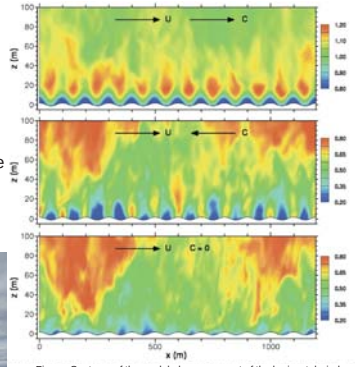

Figure: Contours of the modeled u component of the horizontal wind field for cases with moving and stationary waves. The nondimensional field shown is ũ/Ug. *Source: Sullivan et al. (2008)*

Average wind speed and turbulence structure in MABL is of outermost importance

→ has to be addressed under aspect of tolerable structural loads and potential damage

Figure: Hywind turbine outside Karmøy, Norway. *Source:* http://www.offshore.no

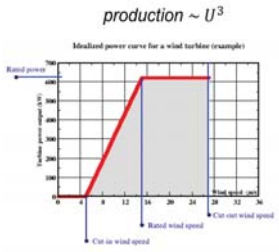

Figure: Idealized power curve from a wind turbine. Source: http://www.windatlas.ca/en/faq.php

Main challenge

- Turbulent air-sea exchange processes are not fully understood
- Most research sites are located close to shore and on small islets close to shore
- For real offshore conditions, only a few measurement sites are available in shallow waters → FINO platforms, ASIT, FLIP

↓↓

Contineous measurements in deep water are needed for the highly required characterization of the MABL

Measurements from floating platforms

Platform motion and flow distortion will conataminate measurements from floating platforms

Solution: Measurements taken by means of the Direct Covariance Flux Method → removal of platform motion in postprocessing of the data

$$\mathbf{U}_{true} = \mathbf{T}(\mathbf{U}_{obs} + \mathbf{\Omega}_{obs} \times \mathbf{R}) + \mathbf{V}_{mot}$$ (Edson et al. 1998)

$\mathbf{U}_{true}$ – desired wind vector in the reference coordinate system

$\mathbf{T}$ – coordinate transformation matrix for rotation from platform to the reference coordinate

$\mathbf{U}_{obs}$ – measured wind velocity in the platform frame

$\mathbf{\Omega}_{obs}$ – angular velocity vector of the platform coordinate system

$\mathbf{R}$ – position vector of the wind sensor with respect to the motion package

$\mathbf{V}_{mot}$ – translational velocity vector

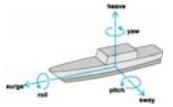

The NORCOWE DCF-system

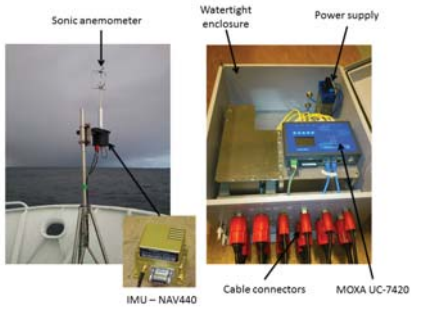

The NORCOWE DCF-system

Gill R3A sonic anemometer:

- sampling rate up to 100 Hz
- provides 3D wind speed components (U, V, W) and sonic temperature T_S → direct computation of turbulent heat and momentum fluxes
- Measurements have to be rotated from anemometer reference frame to earth frame

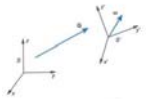

Source: Lien and Løvholden 2001

The NORCOWE DCF-system

Crossbow NAV440:

- integrated GPS and Attitude & Heading reference system (AHRS)
- Measurement of 3-axis angular rates and accelerations up to 100 Hz internally integrated to velocity and position
- Internal coordinate transformation provides attitude and velocity information in earth frame

$$\mathbf{U}_{true} = \mathbf{T}(\mathbf{U}_{obs}) + \mathbf{\Omega} \times \mathbf{TR} + \mathbf{V}_{IMU}$$

$$\mathbf{V}_{IMU} = \mathbf{V}_{acc} + \mathbf{V}_{GPS}$$

The NORCOWE DCF-system

MOXA UC-7420:

- Data logging and control unit
- RISC-based ready-to-run industrial LINUX computer
- 8 RS-232 / 422 / 482 serial ports and PCMCIA interface for WLAN
- 1 CF slot and 2 USB2 ports for external memory storage

The system is powered by 230 V AC or 12 V DC and can easily be attached to a mast or any kind of frame

Cruise to Marstein Fyr November 28th to 30th 2012

Source: http://www.bing.com/maps/

- Data presented for November 29th 16:00h – 17:00h
- Moderate winds from southwest - southeast

System performance

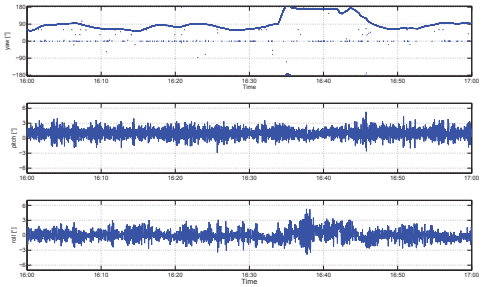

Figure: Attitude angles in Earth frane computed from integrated angular rate sensor output. The IMU was mounted below the sonicanemometer at the front bow of R/V Håkon Mosby.

cmr Instrumentation

Effect of wave motion on wind lidar measurements - Comparison testing with controlled motion applied

DeepWind 2013 – 10th Deep Sea Offshore Wind R&D Conferance
24-25 Janyary 2013, Trondheim, NORWAY

Prepared by: Jon O. Hellevang (CMR)
Presented by: Joachim Reuder (UiB)

Outline of presentation

- We will presented the key results from a comparison test between a pulsed and continuous wave (CW) lidar systems subject to controlled wave motion
  - Background/aim
  - Test site/setup
  - **Results**
  - Summary
- *Note: Results from offshore field test will be given by Jan-Petter Mathisen, Fugro OCEANOR at 16:15 "Measurement of wind profile with a buoy mounted lidar".*

[Picture from lidar comparison test (CMR)]

Background

- Mapping of offshore wind potential is of high economic importance for the power companies with respect to bankability and profitability of the investments
- Building, installing and operating offshore wind mast is very expensive
- Using autonomous measurement system on floating buoy could be a very cost efficient solutions if found sufficient accurate and reliable

[Picture of FINO 1, Courtesy of Bilfinger]

[Picture of lidar buoy, Courtesy of Fugro OCEANOR]

Project aim/organisation

- **Aim:** Demonstrate autonomous measurement system using floating buoy
- Part of the project: "**Autonomous measurement** of wind profile, current profile and waves for mapping of offshore wind potential, design and operation of offshore wind turbines".
- Comparison test presented here is part of WP2: **Concept for wind profiling** (with CMR as work package coordinator)
- Financed by the Research council of Norway (NRC) and Statoil (in addition to in-kind from Fugro OCEANOR, CMR and UiB)
- Fugro OCEANOR as project owner

Test Site / Setup

- University in Agder, Grimstad capus
- Reasonable flat within a radius of 1km
- Sea to the south and east, while there are hills further to the west
- Motion platform placed 10 meter west of a 9 meters tall building
- Motion platform: Bosch Rexroth Boxtel 6-DOF E-motion 1500 Motion System
- Lidars compared during test:
  - Wind Cube V.1 (pulsed)
  - ZephIR 300 (CW)
- Two similar lidars fixed on the ground used as reference measurement

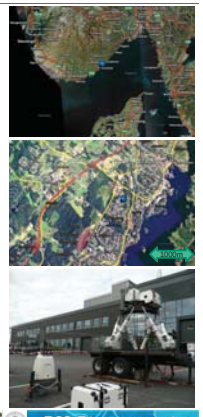

[Map test site: www.gulesider.no Picture: Test setup Grimstad (CMR)]

Motions applied

Play video

(YouTube link)

- 55 motions tested:
  - 9 baseline (no motion through the night)
  - 9 roll; A=3, 5, 10 and 15° | f=0.1 and 0.2Hz (tilt east-west)
  - 6 pitch; A=3, 5, 10, 15 and 20° | f=0.1 and 0.2Hz (tilt north-south)
  - 6 «random» pitch (based on Pierson-Moskowitz spectrum)
  - 5 yaw; A=39° | f=0.025, 0.005, 0.1, 0.15 and 0.2Hz
  - 3 surge; A=40cm | f=0.1 and 0.2Hz
  - 5 heave; A=20 and 40cm | f=0.1, 0.15, 0.2 and 0.4Hz
  - 11 vertical circle; r=30cm | A=3, 5, 10 and 12.5°, 3 and 5° offset
- Approximately 3 hours for each motion (total of 10 days)
- Pure sine-wave, except "random" motions
- Results presented are horisontal wind speed at 85 meter based on 10 minute average data (NB: No motion compenstaion applied)

Results - Horizontal wind speed

- Slight bias observed during baseline measurements
- Average of all tests with motion show very small deviation between reference and moving units
- Only yaw motion with Wind Cube shows significant deviation
- Note the higher reading with circle motion with offset pitch angle compared to the one without any offset in pitch angle
- The average wind speed is about 5m/s
- Next slides show more details

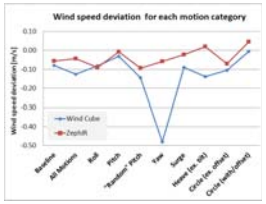

Results – Std. dev and regression

- Gradients (A) and coefficient of deterministic (R^2) are quite good for all tests
- High increase in standard deviation for Wind Cube during circle w/offset and pitch might be related to lower average wind speed (3.6m/s) compared to the other tests (5.4m/s)
- Note: The regression is forced through origin (Y=Ax), reference lidar on x-axis and moving lidar on y-axis. Based on 10 minute data obtained during each test

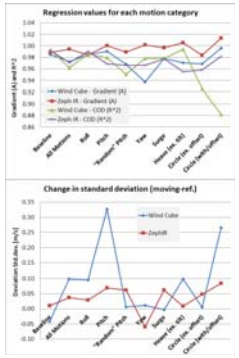

Results – Yaw motion

- Increasingly underestimation of the wind speed with yaw frequency for Wind Cube (A=39° for all tests)
- We believe that the Wind Cube wind speed calculation algorithm is somehow failing when subjected to such fast yaw motion, as the lidar only measure four points in about four seconds (ZephIR measure 50 points in one second)
- R^2 is very good throughout all tests
- Note: Such fast yaw motion might not be realistic during operation

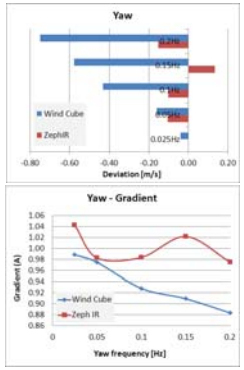

Results – Roll motion

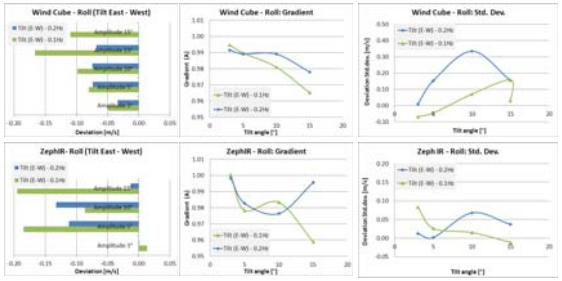

- The results indicate an decrease in horizontal wind speed and increase in standard deviation with increasing roll angle

Results – Pitch motion

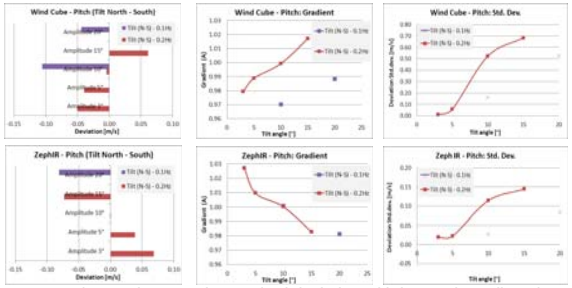

- We observe increase in standard deviation with increasing roll angle
- Average wind speed and gradient indicate different trend for the two lidar systems

Results – Vertical Circle

- It seems as the test with offset angle has higher reading compared to the other tests, especially for the Zeph IR lidar (we expect an opposite trend)
- Possible explanations might be:
  - Measurement with an offset angle has in general lower wind speed (3.3m/s) compared to the tests without any offset (4.8m/s)
  - Higher standard deviation and poorer R^2 during testing with offset angle
  - Somewhat different wind direction during the two types of motion (130-180° vs. 206-328°)
  - Different wind profile

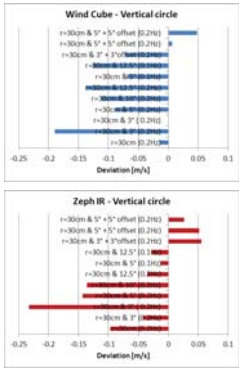

Results – Wind direction

- Very small impact of motion on wind direction measured
- Bias can be explained by offset during setup
- We observe that the ZephIR lidars shows a 180° deviation compared to Wind Cube during many of the tests
- ZephIR has a 180° wind direction unambiguity, which is solved using a local met station on the lider
- Structural disturbance at the ground level where ZephIR has the local met station can explain the errors with ZephIR
- This might also be a problem in open areas if the buoy is rotating

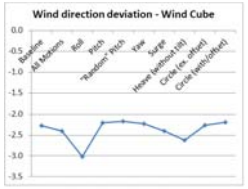

Summary

- Relatively small deviation between moving and reference lidars
- Most measurements are with the measurement uncertainty

- Increasingly underestimation of the wind speed with yaw frequency for Wind Cube
- The standard deviation is increasing with tilt angle
- In general the deviation seems to increase somewhat with tilt angle (as expected by theory)
- ZephIR measure 180° wrong wind direction during many of the test (probably due to nearby structures and setup)

- *Note: Results from offshore field test with ZephIR lidar will be given by Jan-Petter Mathisen, Fugro OCEANOR at 16:15 "Measurement of wind profile with a buoy mounted lidar"*

Acknowledgment

- University of Agder, campus Grimstad, especially Eivind Arne Johansen and Geir Hovland, for helping out with the practicalities of setting up this test
- Martin Flügge (UiB) and Stiand H. Stavland (CMR) for assisting with running the test
- Joakim Reuder (UiB) and Ivar Øyvind Sand (CMR) for valuable input to the test
- NORCOWE and NOWITECH for renting us the Wind Cube lidars and NORCOWE for renting us the motion platform used
- The project owner Fugro OCEANOR for allowing the results to be published
- The Reseach Council of Norway and Statoil as exernal funder of the project

- For more information: jono@cmr.no

[Picture: Lidar comparison test Grimstad (CMR)]

System performance

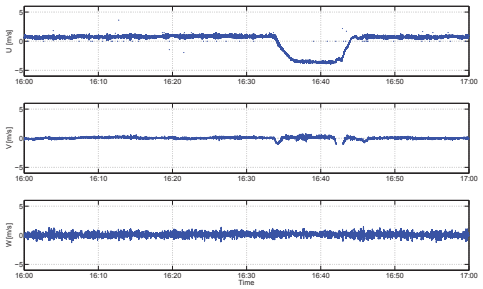

Figure: IMU ooutput of corrected velocity components in earth frame. The Imu was mounted below the sonic anemometer atb the front bow of R/V Håkon Mosby.

System performance

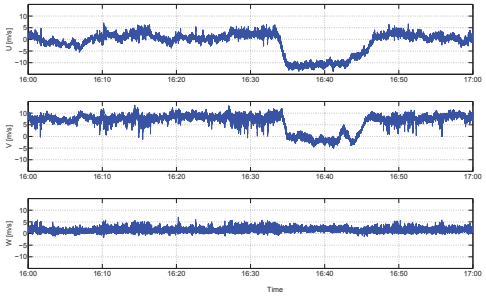

Figure: Uncorrected wind components from the sonic anemometer mounted at the front bow at R/V Håkon Mosby.

Summary

- The Norwegian Center for Offshore Wind Energy has two state-of-the-art DCF-systems
- The first offshore deployment took place in November 2012
- Preliminary results show that the system is able to provide all nessecarry attitude and velocity information needed to correct for platform motion
- The system is easy to transport and can be mounted on any kind of platform, i.e. ships, bouys, masts, etc.
- The system can easily be extended with additional instrumentation

Thank you for your attention!

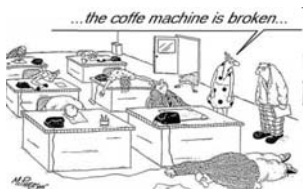

References

- Edson, J.B., A. A. Hinton, K. E. Prada, J. E. Hare and C. W. Fairall, 1998: Direct covariance flux estimates from mobile platforms at sea. *Journal of Atmospheric and Ocean Technology*, **15**(2), 547-562
- Lien J.R. and G. Løvhøiden, 2001: Generell fysikk for universiteter og høyskoler, *Universitetsforlaget*
- Sullivan, P. P., J. B. Edson, T. Hristov and J. C. McWillams, 2008: Large-eddy simulations and observations of atmospheric marine boundary layers above nonequlibrium surface waves. *Journal of the Atmospheric Sciences*, **65**(4), 1225-1245

Turbulence analysis of LIDAR wind measurements at a wind park in Lower Austria

DeepWind 2013
Valerie Kumer

Verbund imgw

Overview

- Data
  - Measurement campaign
- Methods
  - TKE calculations
- Results
  - Case study
- Outlook
  - WindCube 100S

Verbund imgw

DATA

DATA – measurement campaign

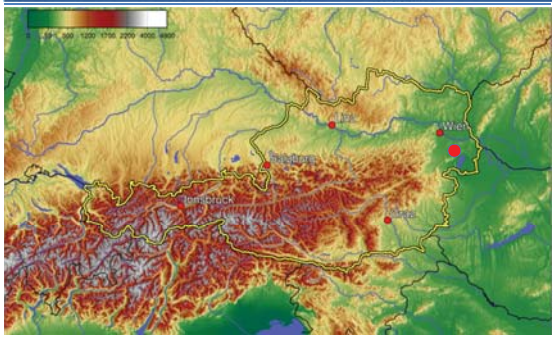

DATA – measurement campaign

DATA – measurement campaign

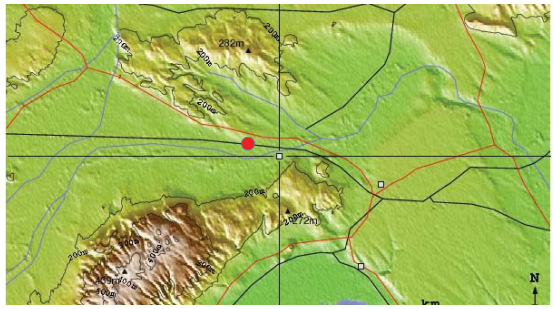

DATA – measurement campaign

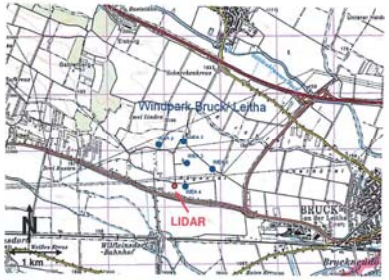

- Summer 2010
- WindCube v1 (Leosphere)

DATA – WINDCUBE™ v1

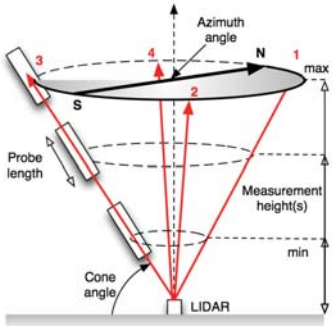

- 4 positions 0/90/180/270
- 9 altitudes 40/65/70/85/ 100/135/160/ 185/200m

DATA – WINDCUBE™ v1

$$\begin{bmatrix} V_{LoS,1} \\ V_{LoS,2} \\ V_{LoS,3} \end{bmatrix} = \begin{bmatrix} \sin\theta_1\cos\phi_1 & \cos\theta_1\cos\phi_1 & \sin\phi_1 \\ \sin\theta_2\cos\phi_2 & \cos\theta_2\cos\phi_2 & \sin\phi_2 \\ \sin\theta_3\cos\phi_3 & \cos\theta_3\cos\phi_3 & \sin\phi_3 \end{bmatrix} \cdot \begin{bmatrix} u \\ v \\ w \end{bmatrix}$$

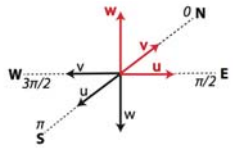

u = -v
v = -u
w = -w

Meteorology
WINDCUBE

DATA – WINDCUBE™ v1

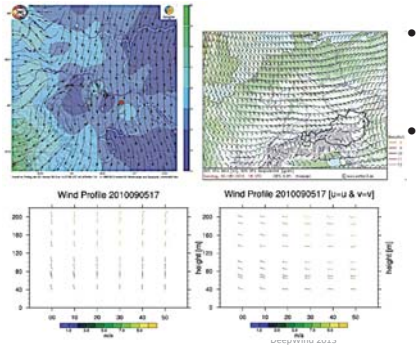

- 10m stream-lines (VERA)
- 950 hPA wind field (GFS analysis)

DATA – WINDCUBE™ v1

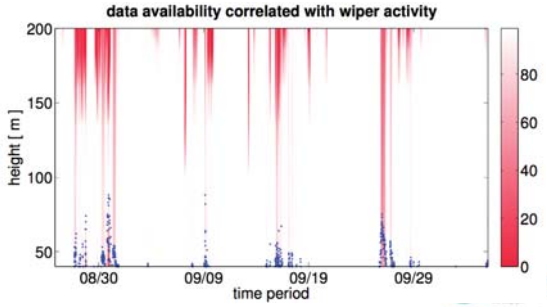

Verbund
imgw

METHODS

METHODS – TKE calculation

- Turbulence Intensity *TI*

$$TI = \frac{\sigma(v_h)}{\overline{v_h}}$$

- Turbulent kinetic energy *TKE*

$$TKE = \frac{1}{2}\left(\overline{u'^2} + \overline{v'^2} + \overline{w'^2}\right)$$

  – TKE generation due to wind shear

$$-\overline{u'w'}\frac{\partial \overline{u}}{\partial z} - \overline{v'w'}\frac{\partial \overline{v}}{\partial z} - \overline{w'w'}\frac{\partial \overline{w}}{\partial z}$$

  – TKE redistribution due to vertical advection $\overline{w}\frac{\partial TKE}{\partial z}$

METHODS– TKE calculations

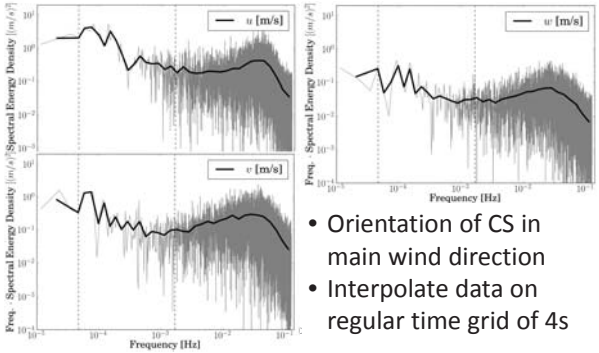

- Orientation of CS in main wind direction
- Interpolate data on regular time grid of 4s

Verbund imgw

RESULTS

RESULTS – wind rose

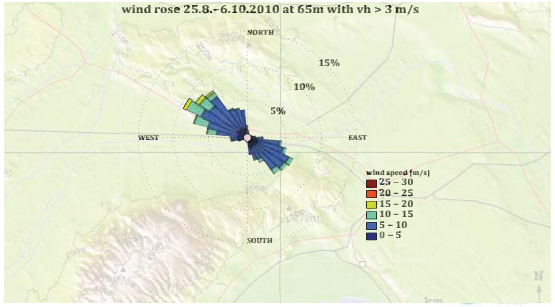

RESULTS – TI/TKE distribution

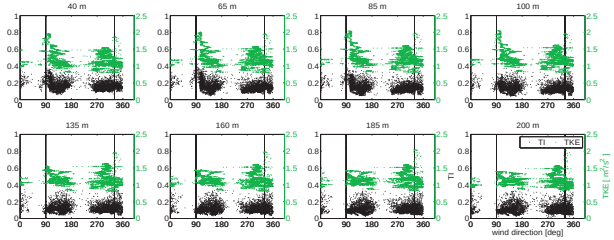

- Two wake signals at 90° and 330°, with visible wake expansion at 330°

RESULTS – case study

- September 25th 2010
- Contour plots of wind direction, horiz. wind speed and TKE

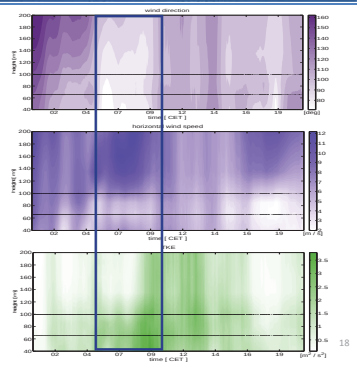

RESULTS – case study

- September 25th 2010
- Contour plots of the wind components u, v and w

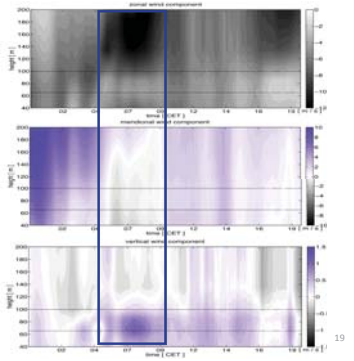

RESULTS – case study

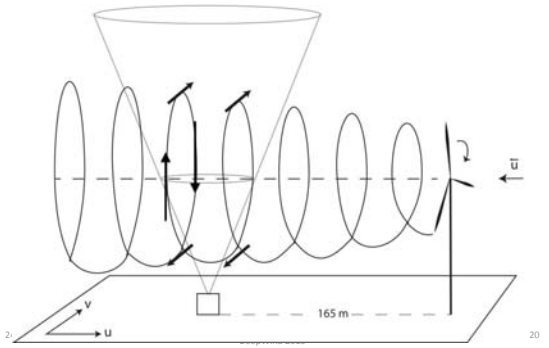

RESULTS – case study

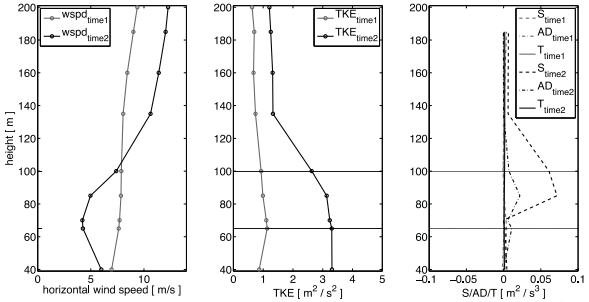

RESULTATE – Vergleiche

- TKE Profile

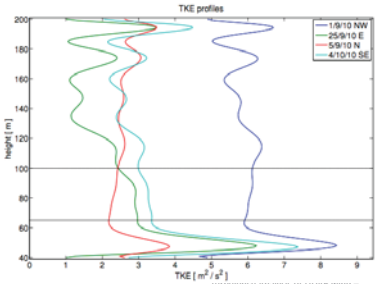

NW:
TKE = 6 m^2/s^2
SO :
TKE = 3.5 m^2/s^2
O:
TKE = 3 m^2/s^2

RESULTATE – Vergleiche

- TKE Anteil an gesamter kinetischer Energie

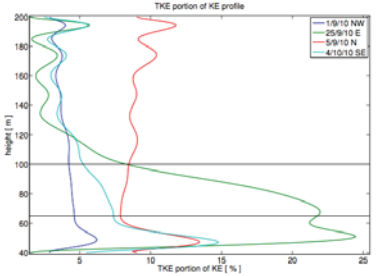

O: 21%
SO: 7%
NW: 5%

CONCLUSION

- Windcube v1 captures nicely wind regimes of region
- Windcube v1 can resolve wake effects of wind turbine
- Generated turbulence is unisotrope
  - Irregular loads to following wind turbines
- Gained information could help layout design and optimize efficiency of already existing parks

Verbund
imgw

OUTLOOK

OUTLOOK – WindCube100s

- Work will be continued with the scanning WindCube 100s
- Test deployment February 2013 at Sola Airport
- Develop and improve scanning patterns and measurement strategies for turbine and park related wake deployments

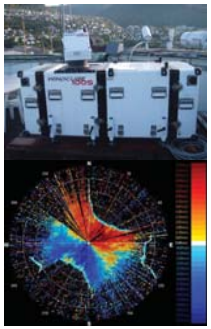

OUTLOOK – WindCube100s

- 16.8.2012 15:00
- South-westerly winds

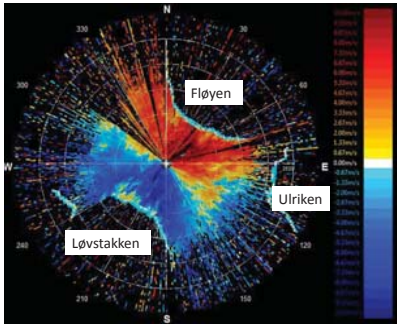

OUTLOOK – WindCube100s

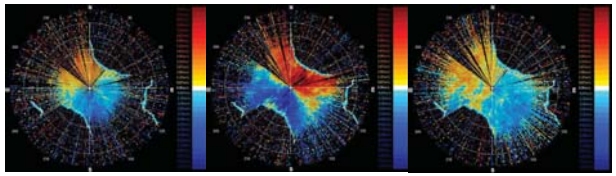

14:21 UTC SE | 14:54 UTC SW | 15:27 UTC SE

OUTLOOK – WindCube100s

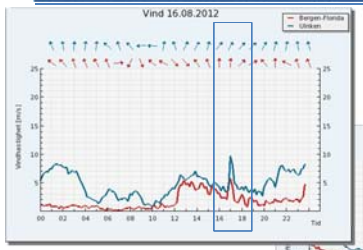

Increase in wind speed

Drop in temperature

Thanks for your attention ☺

C2 Met-ocean conditions

Wave driven wind simulations with CFD, Siri Kalvig, University of Stavanger / StormGeo

New two-way coupled atmosphere-wave model system for improved wind speed and wave height forecasts, Olav Krogsæter, StormGeo / University of Bergen

Measurement of wind profile with a buoy mounted lidar (presentation and paper) Jan-Petter Mathisen, Fugro OCEANOR

Numerical Simulation of Stationary Microburst Phenomena with Impinging Jet Model, Tze Siang Sim, Nanyang Technological University

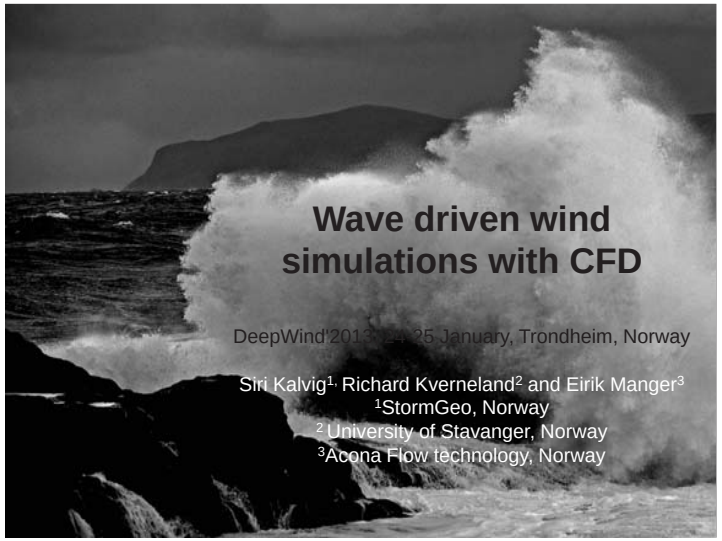

Wave driven wind simulations with CFD

DeepWind'2013, 23-25 January, Trondheim, Norway

Siri Kalvig[1], Richard Kverneland[2] and Eirik Manger[3]
[1]StormGeo, Norway
[2] University of Stavanger, Norway
[3]Acona Flow technology, Norway

Introduction

StormGeo
Control in a changing environment

- Motivation
- Wave-wind interactions
- Method
- Results
- Conclusions & comments

Industrial PhD of Stormgeo and UiS and PhD is part of NORCOWE.

Motivation

StormGeo
Control in a changing environment

Statoil's Hywind Norway, Photo; Lene Eliassen

A typical offshore wind picture….

How does a "non-flat" sea affect the wind fields?

Motivation

StormGeo
Control in a changing environment

- Will wave induced wind at an offshore wind site result in different wind shear and more turbulence than expected ?
- And if so, how will this affect the turbines?

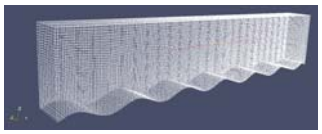

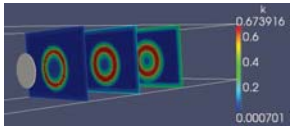

Wind wave interaction

StormGeo
Control in a changing environment

Wind sea and swell influences the atmosphere different!

Wind sea - waves generated by local wind
Swell - long period waves generated by distant storms

Most common is a mixture of wind sea and swell, and this makes the picture even more complicated.

Wind wave interaction

StormGeo
Control in a changing environment

• Field experiments and numerical simulations show that during swell conditions the wind profile will no longer exhibit a logarithmic shape and the surface drag relies on the sea state (i.e. Smedman et al. 2003 & 2009, Semedo et al. 2009).

• There is a gap between "best knowledge" (science) and "best practice" (codes, standards) and there is a need for improved guidance on the impact atmospheric stability and wave-wind interaction in the MABL can have on the offshore wind industry (Kalvig et al 2013, Wiley Wind Energy, in press)

• Swell can result in both higher and smaller effective surface drag and it is likely that swell can create different wind shear and turbulence characteristics so that a wind turbine site will be exposed to other external environmental condition than it was designed for.

Wind wave interaction

• Sullivan et al. (2008) developed a large-eddy simulation (LES) with a two-dimensional sinusoidal wave and identified flow responses for three cases; wind opposing swell, wind following swell and wind over a swell surface with no movement.

• The flow responses in the different cases where very different and 'fingerprints' of the surface wave extended high up in the MBL.

Aim at develop a wave-wind simulation set up with open source CFD and with more computational effective methods.

Method

Need to simulate wave movements!

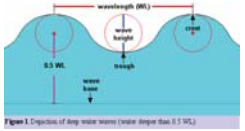

From: Grand Valley State University, http://faculty.gvsu.edu/videticp/waves.htm

Need a new boundary condition that take into account the sinusoidal movement of the "ground".

Solution:
Transient OpenFOAM simulation with pimpleDyMFoam. New boundary condition implemented with mesh transformations.

Method

Need to simulate wave movements!

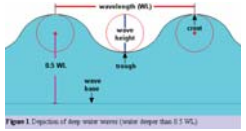

From: Grand Valley State University, http://faculty.gvsu.edu/videticp/waves.htm

Need a new boundary condition that take into account the sinusoidal movement of the "ground".

Solution:
Transient OpenFOAM simulation with pimpleDyMFoam. New boundary condition implemented with mesh transformations.

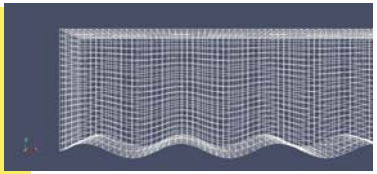

Method

• The open source CFD toolbox OpenFOAM is used for both mesh generation and CFD computations.

• Wave speeds (c), wave amplitude (a), wave length (L) are input parameters to the model.

• To start with a relatively small domain with length of 250 m and a height of 50 m was established. Various sensitivity analyses were performed where different wind velocities and sea states where studied in detail (Kverneland, master theses UiS 2012).

• Temperature and the Coriolis effect are not taking into account and only uniform wind is studied. The calculations use a Reynolds averaging Navier-Stokes (RANS) approachs and since the wave moves it is necessary with a transient (time varying) simulation. The turbulence closure model used is the standard k-epsilon model.

Method

• NORCOWE & NOWITECH organized a wind turbine blind test in 2011-2012, BT1 & BT2.

• BT1: Eight independent modelling groups submitted 11 sets of simulations. No obvious "winner" and large spread of results (Krogstad et.al. 2011).

Currently working with the Actuator disk and actuator line method.

Aiming at coupling the wave set up with a turbine wake model.

Results

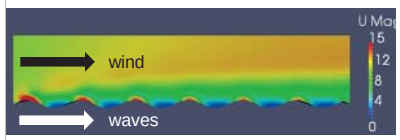

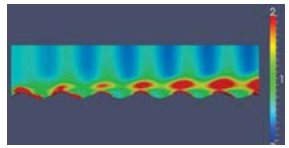

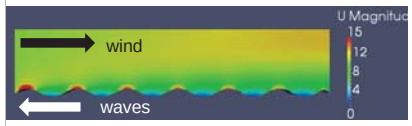

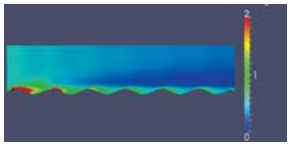

In general:

The wind speed profile and the turbulent kinetic energy pattern far above the waves will be different depending on the wave state and wave direction.

Results

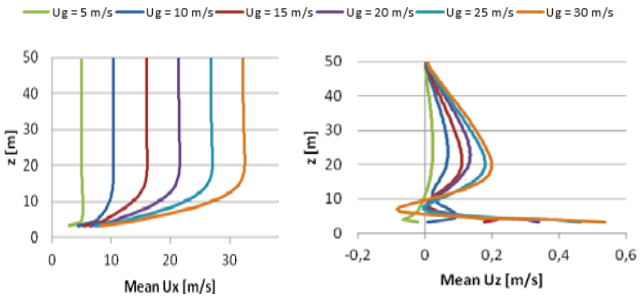

Wind aligned with waves: Vertical profile (at x=210 m) of mean values of the horizontal and vertical component of the wind flow for six cases with different inlet velocity (openFOAM f"ieldAverage" is used for mean values).

Results

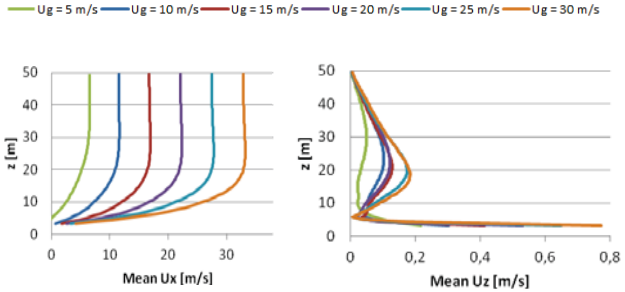

Wind opposing waves: Vertical profile (at x=210 m) of mean values of the horizontal and vertical component of the wind flow for six cases with different inlet velocity.

Results

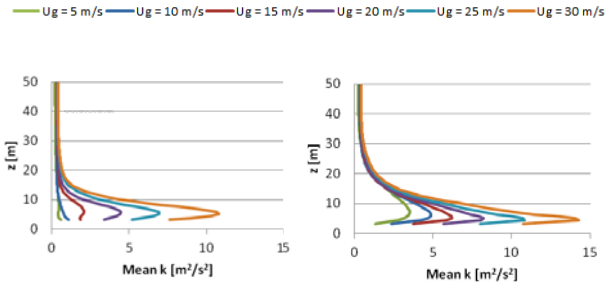

Mean turbulent kinetic energy for wind aligned with the waves and wind opposing the wave.

Results

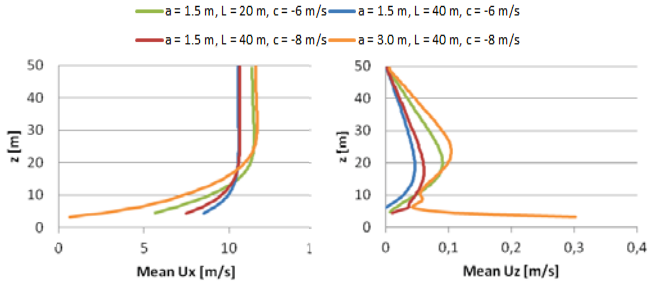

Various wave states opposed with wave propagation. Vertical profile of horizontal wind speed and mean horizontal wind speed .

Results

Uniform wind
of 5 m/s at the inlet.

Wave with;
c=8 m/s,
a=3 m,
L=40 m

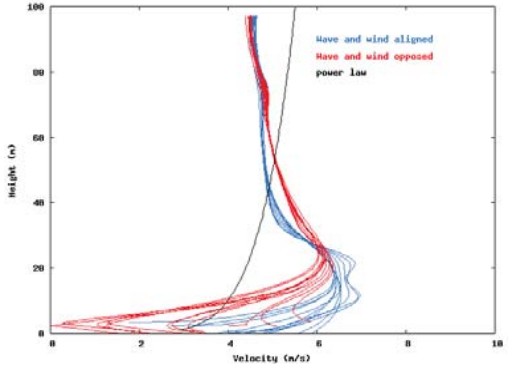

"Instant" velocity profiles over the wave surface. Lines for every 5 m in the interval of 145-200 m (over one whole wave length). Wind aligned and wind opposed the wave propagation result in very different response in the wind field.

Results

Uniform wind
of 5 m/s at the inlet.

Wave with;
c=8 m/s,
a=3 m,
L=40 m

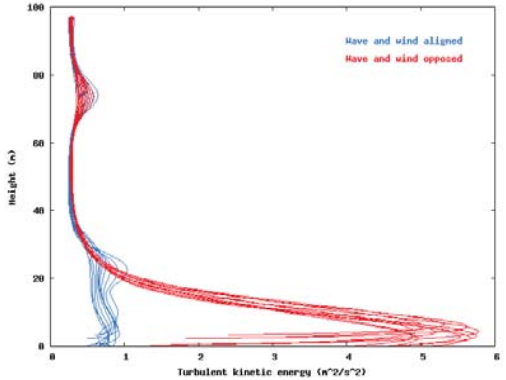

"Instant" turbulence profiles over the wave surface. Lines for every 5 m in the interval of 145-200 m (over one whole wave length). Wind aligned and wind opposed the wave propagation result in very different response in the wind field.

StormGeo

norcowe
Norwegian Centre for Offshore Wind Energy

UNIVERSITY OF BERGEN

New two-way coupled atmosphere-wave model system for improved wind speed and wave height forecasts for offshore wind energy applications

PhD-stud. Olav Krogsæter
olav.krogsaeter@stormgeo.com

Dr. Knut Lisæter
knut.lisaeter@stormgeo.com

Control in a changing environment

Outline

StormGeo
Control in a changing environment

- WRF, SWAN, and the coupled system
- Results
  - Three cases:
    - Stormy weather.
    - Cold air outbreak.
    - Inversion.
  - Yearly statistics.
- Summary

WRF Model

StormGeo
Control in a changing environment

Non-hydrostatic mesoscale weather prediction system

Weather **R**esearch and **F**orecasting model

Large and growing set of parameterization options

- Surface layer schemes
- Boundary layer schemes
- Microphysics schemes
- Cumulus schemes
- Radiation schemes

Nesting capability

Nudging capability

Assimilation capability

Open Source project

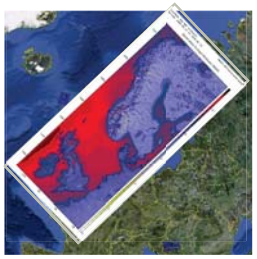

The SWAN wave model

StormGeo
Control in a changing environment

- Simulating WAves Nearshore
- Simulates the wave spectrum
- Includes effects such as
  - Shoaling
  - Refraction
  - Whitecapping
  - Bottom friction
- Has been modified at StormGeo to read 2D-spectra from Grib files
- Run operationally for N. Europe

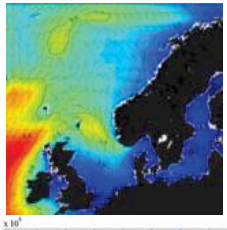

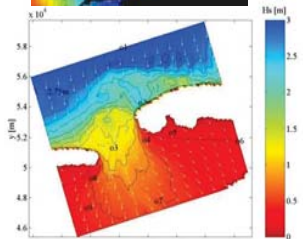

Coupled model

StormGeo
Control in a changing environment

- The most difficult part was how the SWAN model should influence the WRF model.
- Parameterizing the effect that the ocean surface has on the atmosphere is still an active field of research.
- The key parameter the SWAN model modifies is the roughness length, z_0, seen by the WRF model. This is communicated through the Charnock parameter, z_{ch}:

$$z_0 = z_{ch} (u_*)^2/g$$

where u_* is the friction velocity and g the gravitational constant.

Coupled model

StormGeo
Control in a changing environment

Stand alone WRF: Charnock parameter is a constant.

Coupled WRF-SWAN model:

i) HEXOS parameterization: The Charnock parameter depends on wave age.
   * Developing waves: Increasing roughness with wave age.
   * Swell: Decreasing roughness with wave age.

---> Charnock parameter becomes a variable

ii) Janson parameterization: The Charnock parameter is a function of wave growth.

Coupled model

- Technical work is done
  - WRF and SWAN are set up to run within Earth System Modelling Framework, ESMF
- Information exchanged every hour
  - SWAN receives 10 m winds from WRF
  - WRF receives a new roughness parameter, (z_0), from SWAN
- One year run with both the MYNN2 and MYJ Planetary Boundary Layer (PBL) scheme in WRF, coupled with SWAN and the HiEXOS parameterization is finished.

Coupled model

- Technical work is done
  - WRF and SWAN are set up to run within Earth System Modelling Framework, ESMF
- Information exchanged every hour
  - SWAN receives 10 m winds from WRF
  - WRF receives a new roughness parameter, (z_0), from SWAN
- One year run with both the MYNN2 and MYJ Planetary Boundary Layer (PBL) scheme in WRF, coupled with SWAN and the HiEXOS parameterization is finished.

WRF and SWAN: coupled run

WRF and SWAN: coupled run

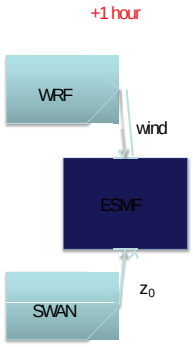

WRF and SWAN: coupled run

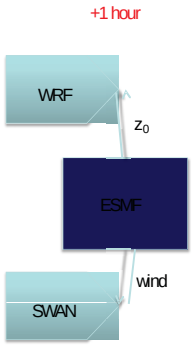

WRF and SWAN: coupled run

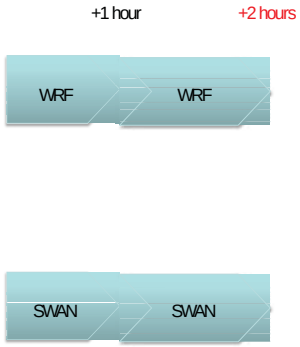

WRF and SWAN: coupled run

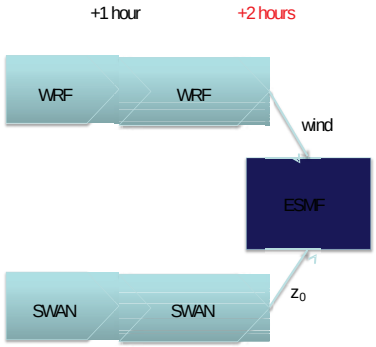

WRF and SWAN: coupled run

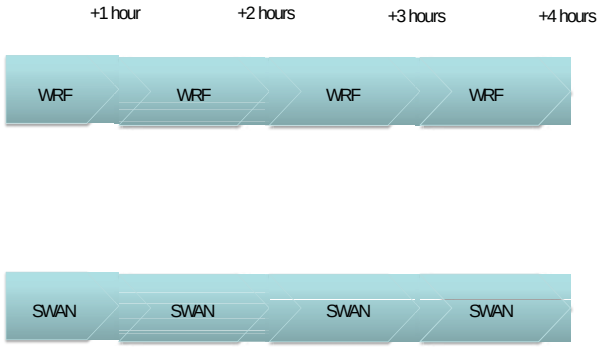

Result: Stormy case in November 2010

Wind Speed uncoupled, 40m

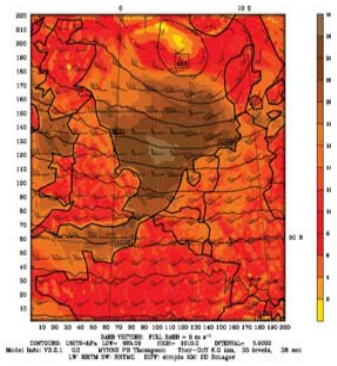

Difference wind speed, 40m, uncoupled-coupled

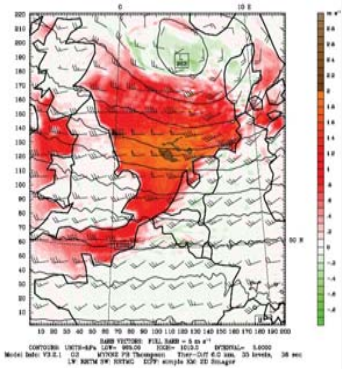

Result: Stormy case in November 2010

Wind Speed uncoupled, 40m

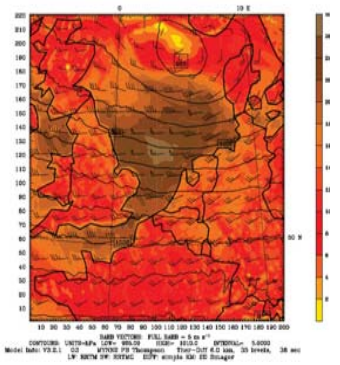

Friction velocity, u_*

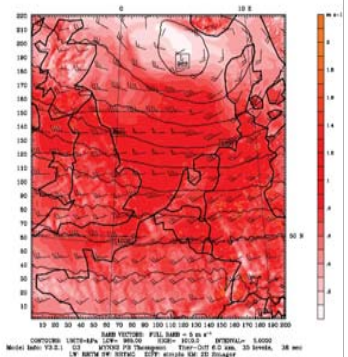

Result: Stormy case in November 2010

Friction velocity, u_*, uncoupled

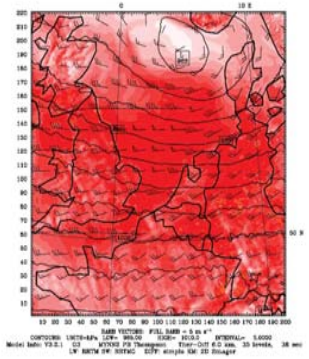

Difference, u_*, coupled-uncoupled

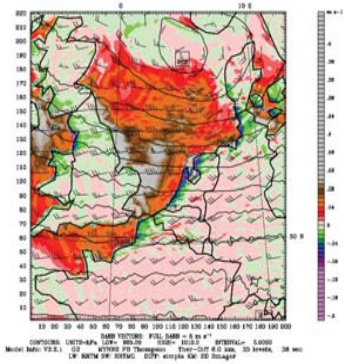

Result: Stormy case in November 2010

Wind speed, 40 m.

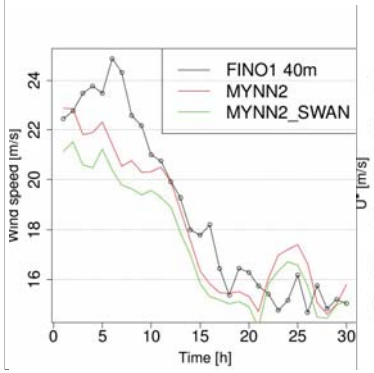

Friction velocity, u_*

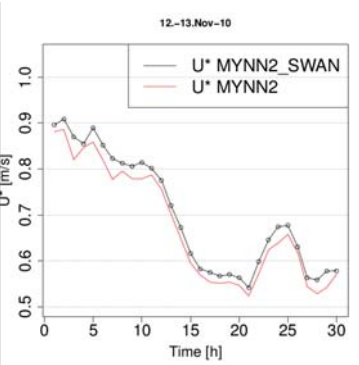

Result: Stormy case in November 2010

Vertical profiles

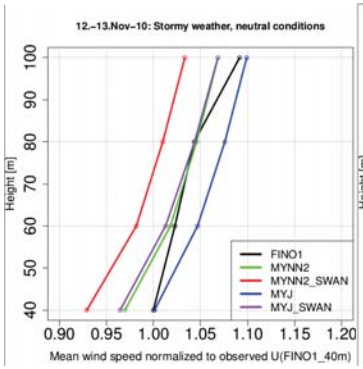

Vertical profiles

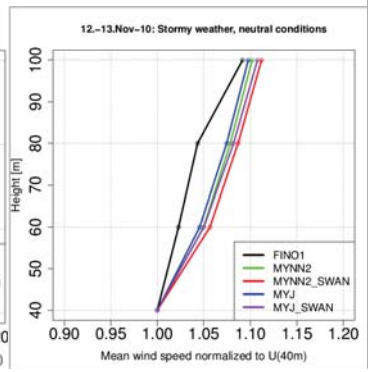

Result: Cold air outbreak, March 2010

Wind Speed uncoupled, 40m

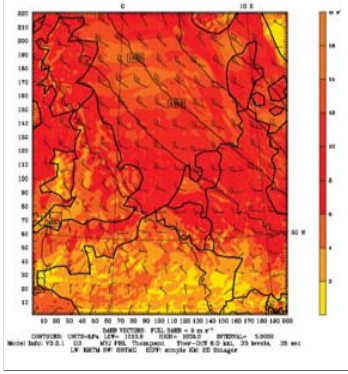

Difference wind speed 40m, uncoupled-coupled

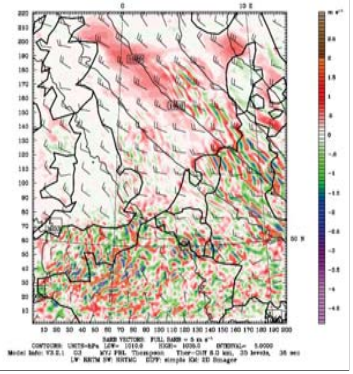

Result: Cold air outbreak, March 2010

Difference, u_*, coupled-uncoupled, MYNN2

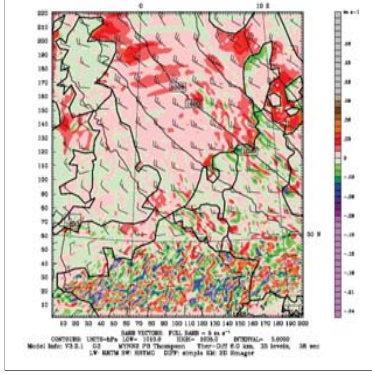

Difference, u_*, coupled-uncoupled, MYJ

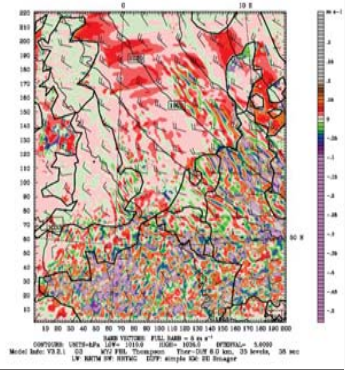

Result: Inversion, SST=18C, Ta=25C, July 2010

Wind Speed uncoupled, 40m

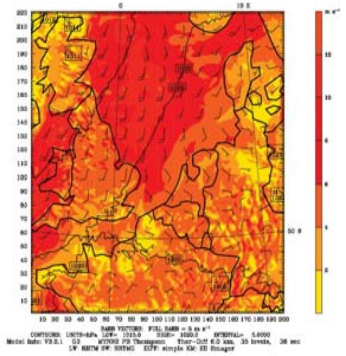

Difference wind speed 40m, uncoupled-coupled

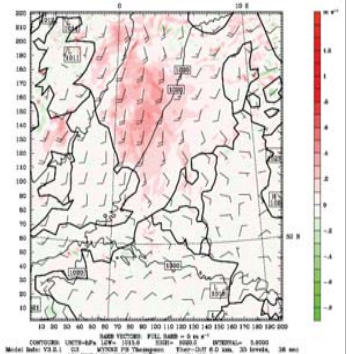

Result: Inversion, SST=18C, Ta=25C, July 2010

Wind speed, 40 m

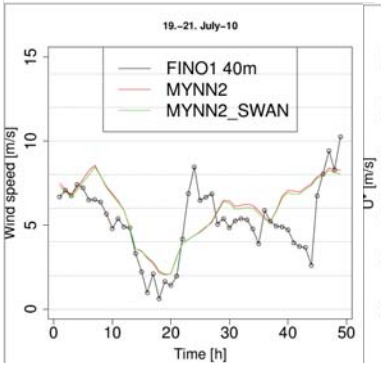

Friction velocity, u_*

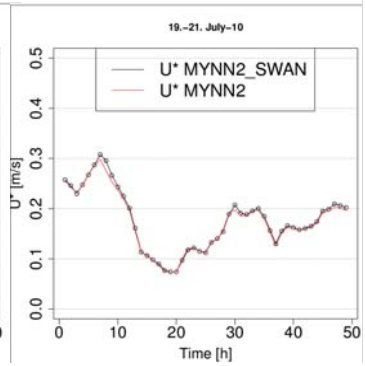

Result: Inversion, SST=18C, Ta=25C, July 2010

Vertical profiles

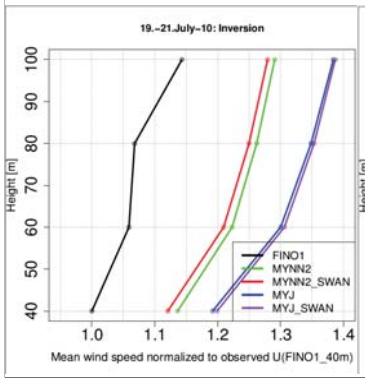

Vertical profiles

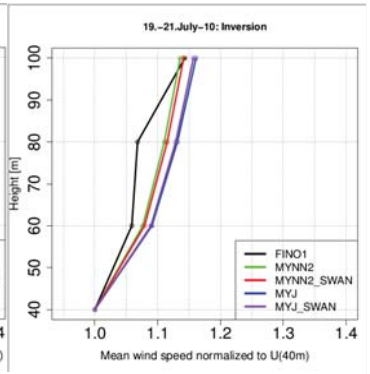

Result: qq-plot, wind speed, summary 2010

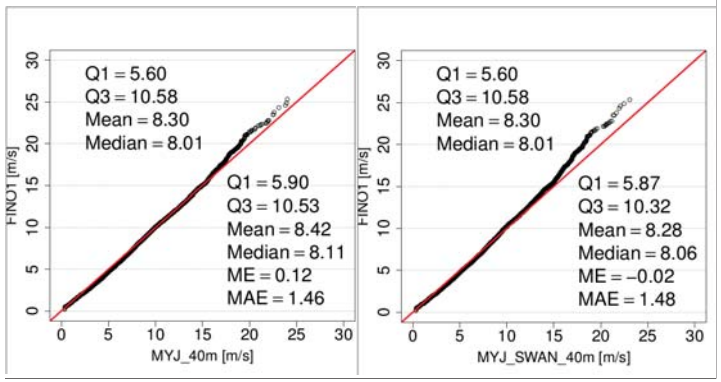

Result: qq-plot, u_*, summary 2010

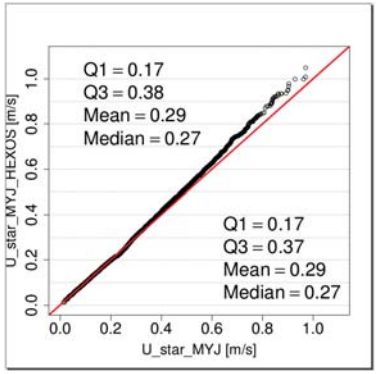

Result: 40 m wind speed, summary 2010

2010	Min.	1st Qu	Median	Mean	3rd Qu	Max	Mean error	Mean absolute error	Standard deviation
Fino1	0,18	5,60	8,01	8,30	10,58	25,33			3,85
MYNN	0,30	5,79	8,15	8,48	10,75	22,88	0,18	1,44	3,79
MYNN-SWAN	0,34	5,78	8,04	8,32	10,56	21,51	0,02	1,41	3,62
MYJ	0,35	5,90	8,11	8,42	10,53	24,01	0,12	1,46	3,69
MYJ-SWAN	0,33	5,87	8,06	8,28	10,32	23,08	-0,02	1,48	3,53

Summary

- A new two-way coupled atmosphere-wave research and forecasting system is implemented: WRF-SWAN.
- Two different PBL-schemes: MYJ and MYNN2.
- HEXOS parameterization for computing the new roughness parameter from SWAN that goes into WRF. Function of wave age.
- Janson parameterization – ongoing work. Function of wave growth.

****

- Reduces the well-known positive bias in WRF with both PBL-schemes.
- Reduces the MAE in the MYNN2-SWAN setup.
- Increases slightly the MAE in the MYJ-SWAN setup.
- Strong winds greater than 15 m/s are reduced too much in the coupled runs.

****

- From previous research on many different PBL-schemes by e.g. O. Krogsæter (2013) and A. Hahmann (2012):
  - * MYJ scheme perform best in offshore conditions with WRF stand alone.
  - * MYNN2 scheme perform slightly better in this new coupled system.

Thank you!

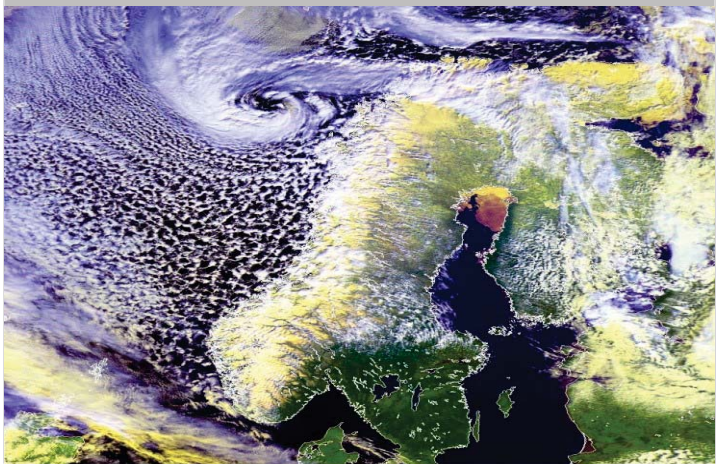

Results

Comparison with Sullivan et al. 2008:

A n openFOAM URANS set-up with a wave with a=1.6 m, L=100 m and c= 12.5 m/s on a domain of 1200 x 100 m is being compared with Sullivan et al's LES simulations. Preliminary results are promising and it looks like we are able to capture the same dynamics as Sullivan et al. But current simulations is to coarse and more refined simulations are needed.

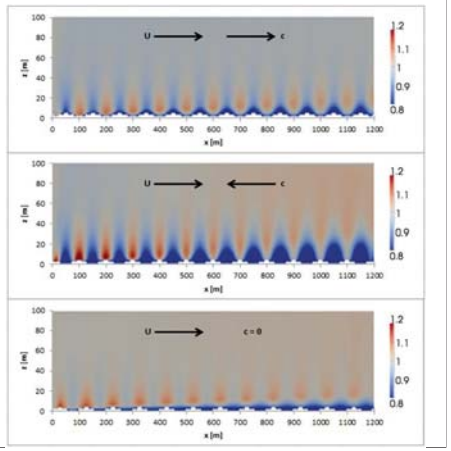

Contours of the horizontal wind field for the situation of aligned (top) and opposed with wave propagation (middle), and stationary waves (bottom) . The non-dimensional field shown is mean Ux / Ug.

Summary

✓ Wave wind simulations with openFOAM is on going PhD work at University of Stavanger /StormGeo/Norcowe.

✓ A cost efficient CFD method for flow over wave simulations, based on RANS turbulence closure is developed.

✓ The response in the boundary layer over the wave are very different for cases where the wind is aligned with the wave propagation and wind opposing the wave.

✓Case of U=5 m/s and c=10 m/s wave: A low level speed up is created in the lowest meters for wind aligned with a fast moving wave. The profiles over the wave do not exhibit a logarithmic profile (or power law profile). Turbulent kinetic energy is slightly higher for wind opposing the wave than wind aligned with the wave.

✓Preliminary result shows pattern that compares well to Sullivan et al. (2008). More detailed studies need to be performed.

✓ Next step: Test the significance and the implications of wave-wind interaction on the offshore wind turbine loads and wakes. Wave movement code and turbine modelling code need to be coupled.

References

Kalvig S, Gundmestad O-T, Winther N. A literature review on implications of wave-influenced wind and atmospheric stability for offshore wind energy. *Wind Energy 2013*, In press.

Kverneland Richard, "CFD – Simulations of wave-wind interaction", Master theses, University of Stavanger 2012.

Semedo A, Saetra Ø, Rutgersson A, Kahma KK, Pettersson H. Wave-induced wind in the marine boundary layer. *Journal of the Atmospheric Sciences* 2009; 66 : 2256-2271

Smedman A, Larsén X, Högström U, Kahma K, Petterson H. Effect of sea state on momentum exchange over the sea during neutral conditions. *Journal of Geophysical Research* 2003; 108, NO.C11, 3367. DOI: 10.1029/2002JC001526

Smedman A, Högström U, Sahlee E, Drennan WM, Kahma KK, Pettersson H, Zhang F. Observational study of marine atmospheric boundary layer characteristics during swell. *Journal of the Atmospheric Sciences* 2009; 66(9) : 2747-2763. DOI: 10.1175/2009JAS2952.1

Sullivan PP, Edson JB, Hristov T, McWilliams JC. Large-eddy simulations and observations of atmospheric marine boundary layers above nonequilibrium surface waves. *Journal of the Atmospheric Sciences* 2008; 65(4) : 1225-1245

Vincent, C. L., P. Pinson, et al. (2011). "Wind fluctuations over the North Sea." International Journal of Climatology 31(11): 1584-1595.

Acknowledgements;

Eirik Manger, Acona Flow Technology

OpenCFD, academic support agreement

E-mail: siri.m.kalvig@uis.no / siri.kalvig@stormgeo.com

Measurement of wind profile with a buoy mounted lidar

Jan-Petter Mathisen

Date: 24 January 2013

Contents Menu

History

First Automatic Wind Turbine
1887 Maykirk Scotland

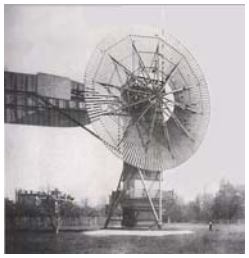

First Norwegian Wind Mill at Fram

Partisipants

- Fugro OCEANOR
- University of Bergen
- Christian Michelsen Research
- Statoil
- Marintek

Project tasks

- Formulation of requirement and specification of the system
- Concept study
- Development of a prototype including hydrodynamic simulations
- Development of a compensation algorithm for the buoy motion
- Building of a prototype buoy
- Field test of the buoy

Present technology

FINO1 German Bight

Price NOK 50 mil

Measurement system

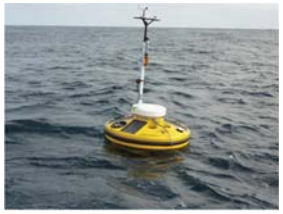

Wavescan buoy

ZephIR 300 lidar

ZephIR 300 lidar from Natural Power

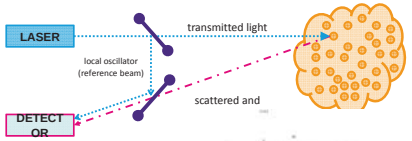

Principles of operation:

- Laser radiation scatters from atmospheric aerosols
- A laser is focussed at a point incident with the aerosols
- Aerosols movement follows the wind
- Scattered radiation is 'Doppler' shifted by the wind speed
- The 'in-line' component of wind speed is measured

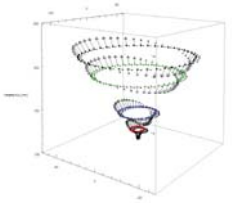

Benefits of the SEAWATCH Wind Lidar Buoy

- Wind profile, meteorological parameters, waves, current profile and other parameters can be measured from one single buoy
- The ZephIR can measure wind at 10m which is according to the WMO standard
- No recalibration is required for the ZephIR
- The Wavescan buoy is lightweight and small and is therefore easy to deploy and recover from vessels
- A standard single point mooring system is used

Test location Titran

Testing of Lidar buoy off the wind test centre

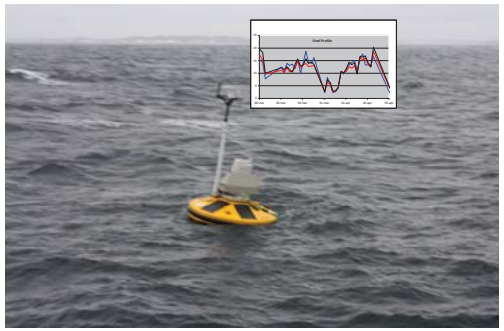

Preliminary results without compensation

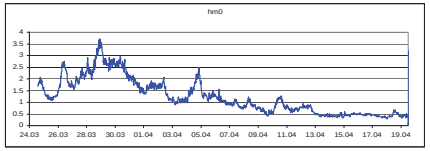

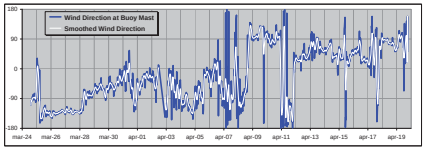

Wind speed and direction

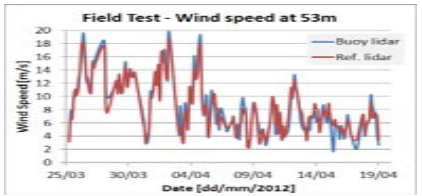

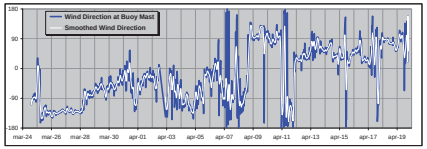

Wind speed for different heights

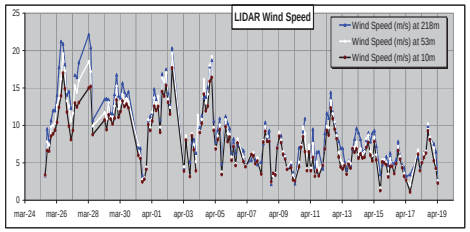

Scatter plott

All data

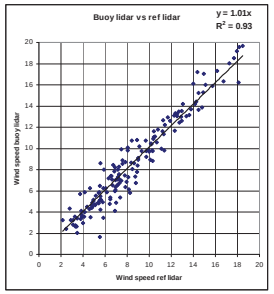

Strong wind (before 5th April)

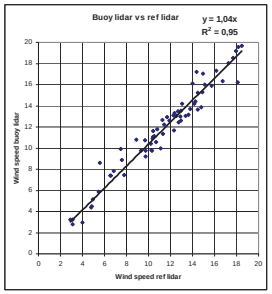

Frequency distribution

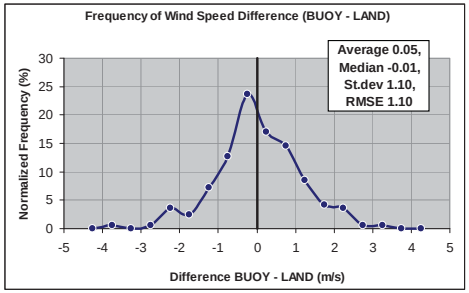

Further work

- Comparing the buoy lidar data with the wind sensors at the met mast
- Include fuel cells for powering of Lidar
  Methanol cartridges to be located in wells below the solar panels
  Consuming 2 litres of methanol per day
  8 carriages from EFOY: Operational time 112 days
  4 special designed cartridges: Operational time 180 days
- Interfacing Geni to the Lidar
- Include compensation software in Geni
- Include "slam" Lidar
- Interfacing with the small scale wind model at Kjeller Vindteknikk

Move

Fuel cell from EFOY

Available online at www.sciencedirect.com

ScienceDirect

Energy Procedia 00 (2013) 000–000

Energy Procedia

www.elsevier.com/locate/procedia

DeepWind'2013, 24-25 January, Trondheim, Norway

Measurement of wind profile with a buoy mounted lidar

Jan-Petter Mathisen

Fugro OCEANOR, Pirsenteret, Havnegt 9, Trondheim, 7462 Norway

Abstract

Traditionally wind profile measurements for offshore wind farms have been obtained by using cup anemometers mounted on wind masts. This is a very expensive method to acquire wind profile data, and the wind data will also be influenced by distortion from the mast and the sensors. A much cheaper way of obtaining offshore wind data is using a buoy mounted lidar. In addition a buoy can also measure waves, current profile and other parameters.

To be able to measure the wind profile from a buoy, a ZephIR 300 lidar from Natural Power was mounted on a Fugro OCEANOR Wavescan buoy. The Wavescan buoy is specially designed for severe environmental conditions, and has been in operation world-wide since 1985.

The buoy system was tested off Titran off the island Frøya on the coast of central Norway. This is an ideal test site as it is in a very tough environment and near to a test centre for wind measurements with 3 instrumented met masts. The wind test centre is a part of the NOWITECH infrastructure programme. A reference lidar supplied by Natural Power was also located at the wind test centre. The distance between the reference lidar and the buoy was approximately 3.5 km. The Wavescan buoy was deployed for a period of one month during March-April 2012. The buoy lidar recorded 10 minutes average wind profile at 10 heights from 11.5 to 218m every third hour, while the reference lidar measured the wind at 53 m height continuously. During the measurement period the significant wave height varied between and 0.5 and 3.6m.

The wind speed from the buoy lidar has been compared with the reference lidar showing that there is practically no bias, while there is some scatter with a correlation coefficient (R^2) of 0.93. For higher wind speeds, which are mainly towards the coast, R^2 is 0.95 with a slighter larger bias. The scatter can be explained simply by the distance between the lidars, and that the reference lidar is located on land. We are therefore planning to compare the buoy mounted lidar measurements with closer offshore wind mast data.

Keywords: Wind profile measurement; lidar; buoy

1. Introduction

The interest for offshore wind farms is increasing due to increased demand of energy world wide and that climate change has increased the interest for renewable energy.

Reliable data of the wind profile for the relevant height of recent and future wind generators (30-300m) are important both for design, estimation of wind energy potential and during operations. As the power production of wind turbines increases with the 3rd power of the wind speed, accurate measurements of the wind profile is important both with respect to financing and profitability of the investments. Up to now such measurements have been carried out on bottom mounted met mast which is expensive and stationary. By measuring the measurements from a portable buoy the cost will be decreased by a factor 10 or more.

A research project was therefore initiated for development and demonstration of an autonomous system for measuring wind profile, waves and current profile from an anchored floating buoy.

The system should be able to measure wind profile in the region from 10-300 meters above sea level, relevant for actual and future offshore wind farms. Applications for such a measurement system include:

- Mapping of wind potential
- Optimisation of wind farm during operation
- Determination of structural loads and expected fatigue
- Validation of numerical simulations of the atmospheric and oceanic boundary layer
- Measurement of wake effect

The project included the following tasks:

1. Formulation of requirement and specification of the system
2. Concept study
3. Development of a prototype including hydrodynamic simulations
4. Development of a compensation algorithm for the buoy motion
5. Building of a prototype buoy
6. Field test of the buoy

The following institutions participated in the project: Fugro OCEANOR, Statoil, University of Bergen/Uni Computing, Christian Michelsen Research (CMR) and Marintek. The project has been funded by the Norwegian Research Council, Statoil and the participants as in kind contribution except for the work carried out by Marintek which was fully financed.

2. Lidar motion test

To examining the influence of wave motion on the lidar wind profile measurements, a motion test was carried out at the University of Agder, Grimstad autumn 2011. A motion platform was rented free of charge from the University in Agder, campus Grimstad, as this infrastructure was funded by NORCOWE. A motion sensor and sonic anemometer was also rented free of charge from NORCOWE. The motion platform used had 6 degrees of freedom, with the possibility of controlling frequency and amplitude individually. The motions along the following principal axis; roll, pitch, yaw, heave and surge, in addition to the combined motions; heave, surge and pitch were applied. The objective of the setup was to simulate actual wave motion.

ZephIR 300 from Natural Power and Wind Cube from Leosphere were included in the test, being continuous wave (CW) and pulsed lidars respectively. One of each type was mounted on the moton platform, while the other two were located at the ground as reference instruments. A picture of the test setup is shown in Figure 1.

Details regarding the test are given in [1].

Figure 1. Picture of test setup in Grimstad

3. Compensation algorithm

The compensation algorithm for motion corrections has been developed by Uni Computing, University of Bergen. The algorithm can use all the 6 degree of freedom data measured by the wave sensor in the buoy, to compensate the lidar wind measurements for the buoy motion. The algorithm uses the 1 sec data from the Wave sensor to compensate the 1 sec wind measurements at each height.

4. Description of the measurement system

The Wavescan Lidar buoy includes a ZephIR 300 lidar attached to the Wavescan buoy. Below is given a description of the different elements and the ant the assembling of the system.

4.1. The Wavescan buoy

The Wavescan buoy is Fugro OCEANOR's largest buoy well suitable for rough sea condition. The horizontal diameter is 2.8 m and the weight (without mooring) is approx. 925 kg. It has large buoyancy, 2800 kg, meaning that it is well able to withstand mooring load in deep waters.

The Wavescan buoy has a discus shaped hull that can be split in two to ease transportation. A keel with counterweight is mounted under the hull to prevent capsizing of the buoy.

A cylinder in the middle of the buoy hull contains all electronic modules, the power package and the wave sensor (integrated with the data logger). The instrument container has diameter 0.7 m and height 1.46 m, giving a volume of 0.56 m^3. The different electronic modules are mounted into special splash proof compartment boxes to secure safe handling of the sensitive electronics. The buoy is equipped with a mast to support the meteorological sensors and the antennae. The meteorological parameters are measured 3.5m above sea level. This version of the buoy has a modified design with larger solar panels with a capacity of 40W each.

The buoy hull includes wells for mounting different sensors.

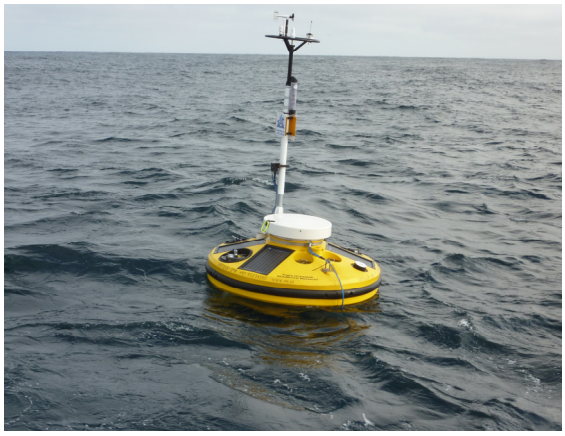

Figure 2. The Wavescan buoy. Picture of the buoy at the M-position obtained from University of Bergen.

4.2. The ZephIR lidar

ZephIR is a Continuous Wave (CW) lidar. The principle by which ZephIR measures the wind velocity is simple: a beam of coherent radiation illuminates the target (natural aerosols), and a small fraction of the light is backscattered into a receiver. Motion of the target along the beam direction leads to a change in the light's frequency via the Doppler shift. This frequency shift is accurately measured by mixing the return signal with a portion of the original beam, and sensing the resulting beats at the difference frequency on a photo detector. The essential features are readily seen in the simplified generic CLR depicted below.

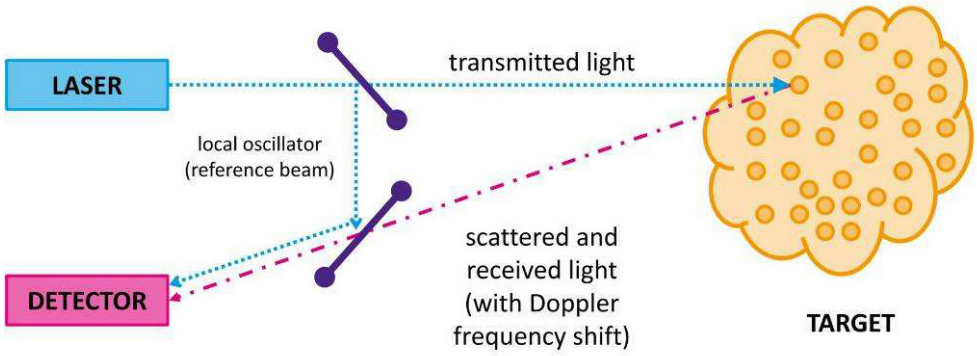

CW systems are the simplest form of Lidar and possess the advantage of reduced complexity and high reliability for long periods of autonomous and remote operation. A CW system is physically focused to the required range and it is essentially the tightness of that focus that determines the probe length: the shorter the range, the smaller this length. The latest version of ZephIR has an effective probe length of ±1m, ±6m and ±15m at 40m, 100m and 150m ranges respectively. ZephIR can measure to a minimum range of 10m or shorter if required. Wind profiling is achieved by focusing at a number of chosen ranges in turn.

As a result of physically focusing the laser at each height of interest ZephIR achieves comparable sensitivity at each height: a critical design parameter for deployments in clean air with low concentrations of natural aerosols. CW lidar is highly sensitive and, as a consequence, it can achieve an acceptable signal-to-noise ratio in a much shorter timescale than other lidar methods.

ZephIR scans its beam in a 30 degree cone and continuously gathers 50 independent line-of-sight wind speed measurements per second, from which the wind vector is derived. The rapid data rate opens up possibilities for examination of detailed flow and turbulence across the measured disk. In addition, the velocity resolution of ZephIR is very high and its accuracy is measured to be 0.003m/s against a calibrated moving belt target.

Figure 3. The ZephIR 300 lidar

5. The SEAWATCH wind lidar buoy

SEAWATCH Wind Lidar buoy consists of a standard Wavescan buoy with the ZephIR 300 mounted on the lifting ring on the central cylinder as shown in Figure 4. For measuring the current profile an Aquadop Profiler from Nortek mounted in one of the wells can be included. The laser head is located 2.5m above the sea level, so the lowest measurement height for the lidar is 12.5m. In addition a wind sensor is included on the lidar 2.5m above the sea level and a standard wind sensor mounted on the top of the met mast 3.5m above the sea level.

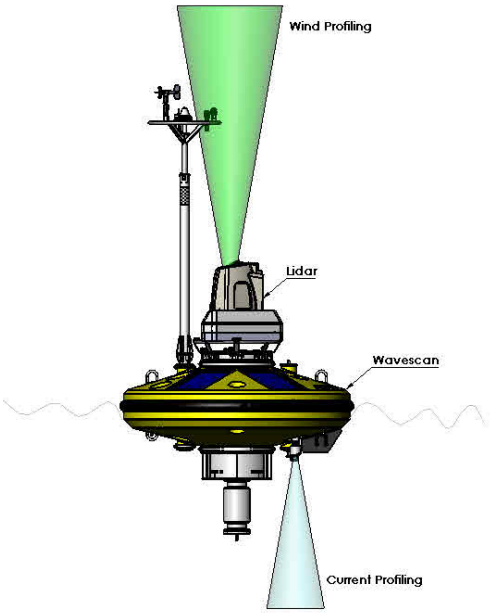

Figure 4. SEAWATCH Wind Lidar buoy with Nortek Aquadopp Profiler

6. Field test

The field test was carried out off Titran at the island Frøya, see Figure 5. This is an ideal test site since it is an exposed location and near a wind test centre with 3 instrumented met masts. The wind test centre is a part of the NOWITECH infrastructure programme. A reference lidar supplied by Natural Power was located at the wind test centre. The reference lidar is shown in Figure 6.

The Wavescan buoy with the ZephIR lidar was deployed 24 March 2012 and was recovered 19 April 2012. A picture of the buoy is shown in Figure 7**.** The distance between the reference lidar and the buoy was approx. 3.5km The buoy lidar recorded 10 minutes average wind profile at 10 heights from 12.5m to 218m every third hour, while the reference lidar measured the wind at 53 m height continuously. In addition the buoy measured waves and wind and humidity at the buoy met mast every 30 minute.

Figure 5. The location of the field test

Figure 6. The ZephIR reference lidar

Figure 7. The Wavescan buoy with the ZephIR lidar off Titran

Time series of wave height is presented in Figure 8. The significant wave height was largest during the first part of the test and reached a maximum of 3.5m on the 28th March. The wave height was below 1m after 9th April.

Time series of wind speed at 53m both for the buoy mounted and reference lidar are presented in Figure 9. As for waves the wind speed is strongest before 5th April with a maximum wind speed of 20m/s. After 5th April the wind speed is mostly below 10m/s i.e. fresh breeze (B5). The wind direction measured by the Gill ultrasonic wind sensor located on the buoy met mast 3,5m above sea level is given in Figure10. The wind direction was mainly between south-west and north until 8th April, and after then the wind direction was mainly between north and east i.e. offshore wind.

The wind speed at 3 heights measured by the ZephIR on the buoy is presented in Figure 11. There are some gradients at strong winds at the beginning of the measurement period, while there are small gradients after 1st April. During the first period the wind direction was from south-west with maritime polar air masses, while polar arctic air masses are present during northerly winds. These two air masses have different stability which will affect the wind profile. With northerly winds the air masses are transported over land over a distance of more than 3 km which has higher friction than air masses over sea, which may also affect the stability.

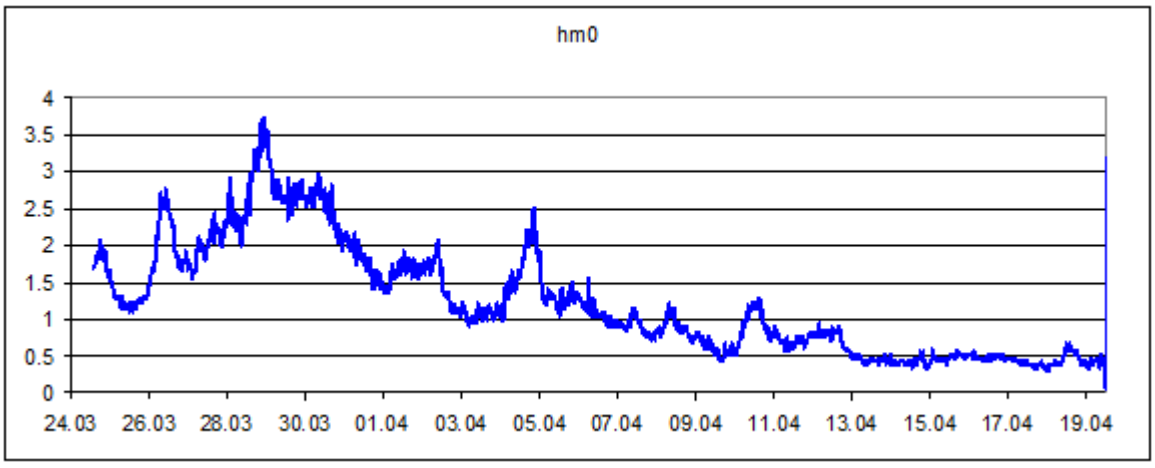

Figure 8. Significant wave height during the field test

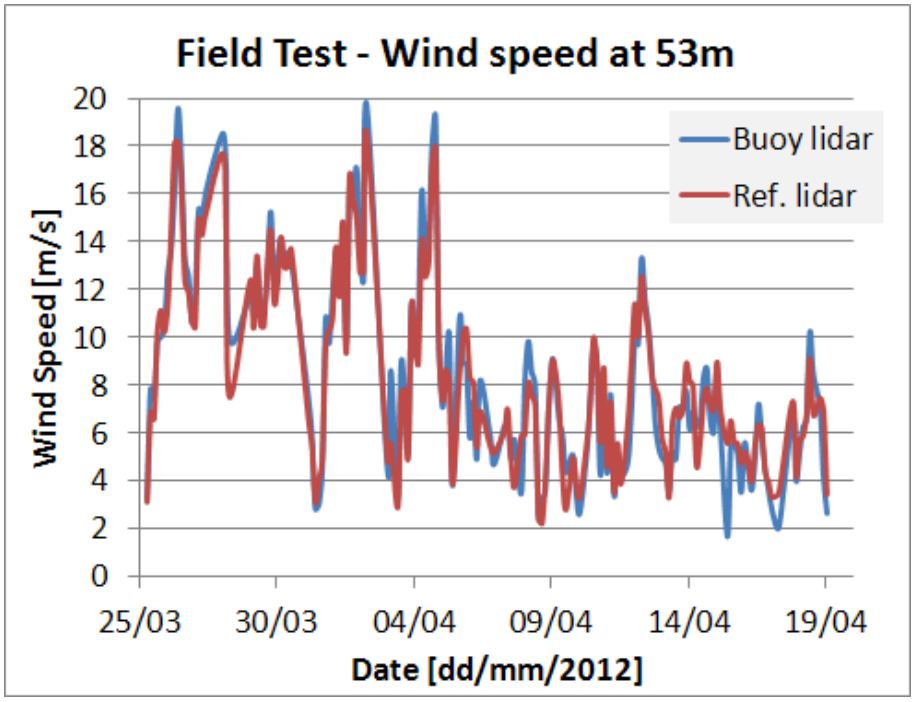

Figure 9. Time series from the onshore reference lidar and the buoy mounted lidar for the test period.

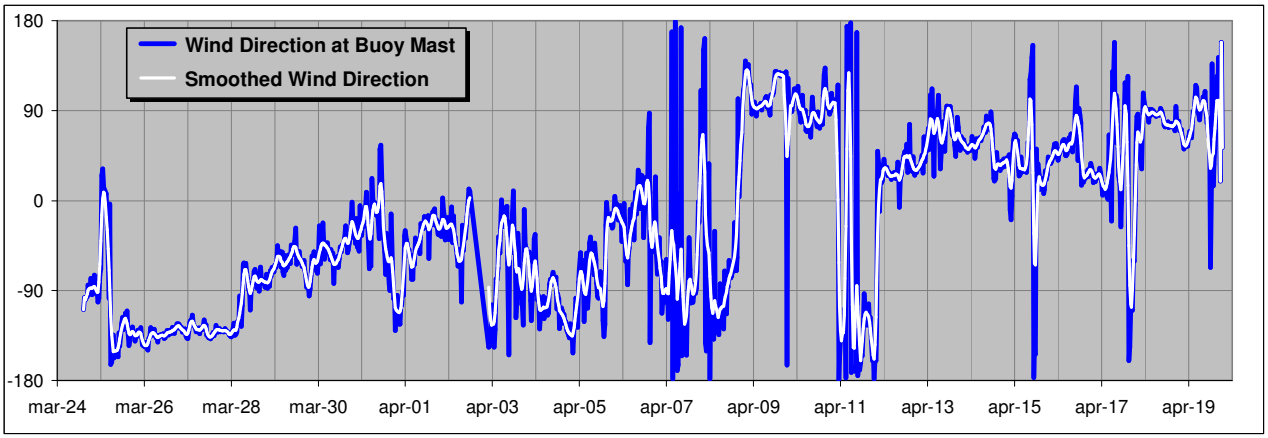

Figure 10. Wind direction measured by the buoy wind sensor 3.5m above sea level.

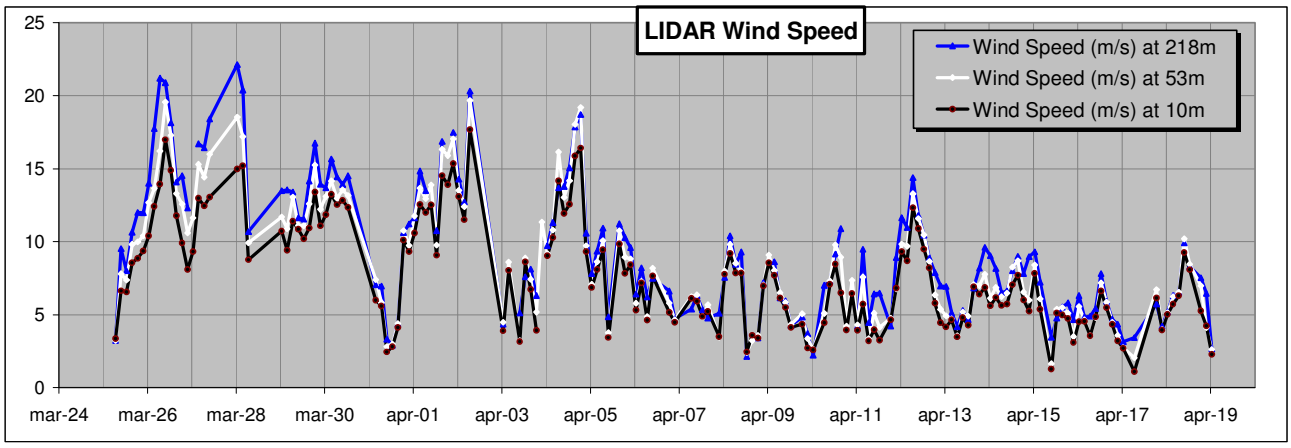

Figure 11. Wind speed at 10, 53 and 218m measured by the ZephIR at the buoy.

Scatter plot of the buoy lidar vs. the reference lidar is shown in Figure 12, which shows that there is practically no bias, while there is some scatter as indicated by a squared correlation coefficient of 0.93. Since the scatter is largest for small wind speeds, we have prepared a scatter plot for the period before 5th April. The scatter is then lower with a squared correlation of 0.95, while the bias is slightly larger. During the period after 5th April there is mainly offshore wind as discussed before, which may give larger gradients between the reference and buoy lidars.

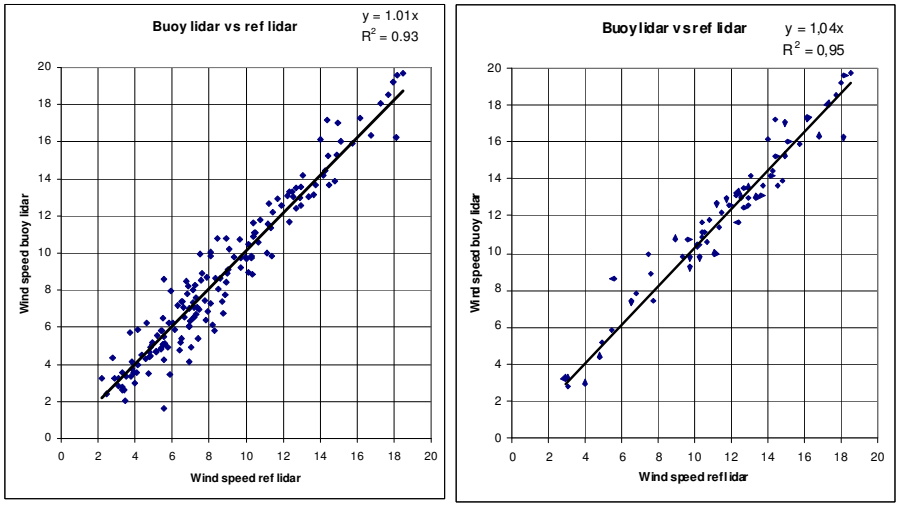

Figure 12. Scatter plot of the buoy mounted lidar vs. reference lidar for the whole period (left) and for the period before 5th April (right)

7. Conclusions

To be able to measure the wind profile from a buoy, a ZephIR 300 lidar from Natural Power was mounted on a Fugro OCEANOR Wavescan buoy. The Wavescan buoy is specially designed for severe environmental conditions, and has been in operation world-wide since 1985.

The buoy system was tested off Titran off the island Frøya on the coast of central Norway. This is an ideal test site as it is in a very tough environment and near to a test centre for wind measurements with 3 instrumented met masts. The wind test centre is a part of the NOWITECH infrastructure programme. A reference lidar supplied by Natural Power was also located at the wind test centre. The distance between the reference lidar and the buoy was approximately 3.5 km. The Wavescan buoy was deployed for a period of one month during March-April 2012. The buoy lidar recorded 10 minutes average wind profile at 10 heights from 11.5 to 218m every third hour, while the reference lidar

measured the wind at 53 m height continuously. During the measurement period the significant wave height varied between and 0.5 and 3.6m.

The wind speed from the buoy lidar has been compared with the reference lidar showing that there is practically no bias, while there is some scatter with a correlation coefficient (R^2) of 0.93. For higher wind speeds, which are mainly towards the coast, R^2 is 0.95 with a slighter larger bias. The scatter can be explained simply by the distance between the lidars, and that the reference lidar is located on land. We are therefore planning to compare the buoy mounted lidar measurements with closer offshore wind mast data.

Acknowledgements
Thanks to natural Power for supplying the reference lidar and to NOWITECH for getting access to the infra structure at the wind test centre at Titran.

References
[1] Jon Oddvar Hellevang**.** Effect of wave motion to wind lidar measurement - Comparison testing with controlled motion applied. Presented in this proceeding.

NANYANG TECHNOLOGICAL UNIVERSITY

Numerical Simulation of Stationary Downburst Phenomena with Impinging Jet Model

Tze Siang, Sim

Ph.D student
Nanyang Technological University, Singapore

24 January 2013

Content

1. Background
2. Objectives
3. Methodology
4. Results and discussion
5. Conclusion
6. Future work

Background

- What is downburst?

The famous atmospheric scientist, Fujita (1985), in his report “The Downburst- Microburst and Macroburst”, defined downburst:

as an intense, transient downdraft of air that induces an outburst of damaging wind on or near the earth’s surface.

- Fujita, T. T., (1985): "The Downburst- Microburst and Macroburst," Satellite and Mesometeorology Research Project (SMRP) Research Paper 210, Department of Geophysical Sciences, Univ. of Chicago, (NTIS PB-148880)

Background

- Where can downburst be found?

United States
Account for about 1/3 of extreme wind. (2002)

Asia
The “thunderstorm” type downburst occurs in cyclonic and non-cyclonic areas. (2004)

Australia
About ½ of downbursts in thunderstorm contribute to extreme wind gust. (2002)

- Edmund C.C. Choi, (2004),"Field measurement and experimental study of wind speed profile during thunderstorms", Journal of Engineering and Industrial Aerodynamics 92 (2004) 275-290
- C.W. Letchford, C. Mans, M.T. Chay, (2002)"Thunderstorm – their importance in wind engineering (a case for the next generation wind tunnel", Journal of Wind Engineering and Industrial Aerodynamics 90 , 1415-1433

Background

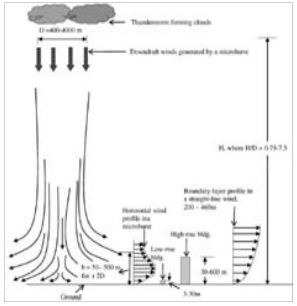

- Downburst wind starts off by travelling vertically downward.
- Upon impinging on the ground, it spreads out radially along the earth’s surface as outflow.
- Severe cases:
  The strength can be equivalent to a tornado.
- Implications:
  Wind hazard to ground structures.

Image:
- Sengupta, A., Sarkar, P.P., (2008). Experimental measurement and numerical simulation of an impinging jet with application to thunderstorm microburst wind loading. Journal of Engineering and Industrial Aerodynamics 96, 345–365.

Background

- The high speed outflow at earth’s surface is important to the ultimate load limit of structures.
- This might be a concern for large structures.
- Examples are:
  - Offshore wind turbines (2011), transmission towers

- Hieu Huy Nguyen, (2011) Lance Manuel, Paul S. Veers, "Wind turbine loads during simulated thunderstorm microburst", Journal of Renewable and Sustainable Energy 3, 053104
- Eric Savory, Gerard A.R. Parke, Mostafa Zeinoddini (2001) Norman Toy, Peter Disney, "Modelling of tornado and microburst-induced wind loading and failure of a lattice trasmission tower", Engineering Structures 23 , 365-375

Objectives

- Understand downburst outflow near the earth surface and investigate on the interaction with large structures.


Methodology

- Literature from the past 10 years from present indicates few main methods of investigating/understanding the outflow near earth surface.
  - 1. Laboratory “Impinging jet model” method (2007)
  - 2. “Cooling source” method (1992)
  - 3. Meteorological method (1993)

- Kim, J., Hangan, H., (2007). Numerical simulations of impinging jets with application to thunderstorm downbursts. Journal of Wind Engineering and Industrial Aerodynamics 95, 279–298.
- Anderson, J.R., Orf, L.G., Straka, J.M., (1992). A 3-D model system for simulating thunderstorm microburst outflows. Meteorology and Atmospheric Physics 49, 125–131
- Nicholls M., Pielke, R. Meroney R. (1993)" Large eddy simulation of microburst winds flowing around a building, Journal of Wind Engineering and Industrial Aerodynamics, 46-47, pp. 229-237

Methodology

- To help us gain a rough understanding of the flow characteristics.
- Employ the simplest laboratory “impinging jet model”.
- First proven to match closely with the downburst [illegible] Hjemfelt

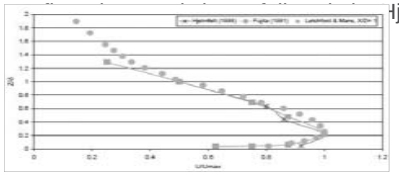

- Hjelmfelt, M.R. (1988), “Structure and Life Cycle of Microburst Outflows Observed in Colorado”, J. of Applied Meteorology, 27, 900-927

Methodology

- In the research:
  - Numerically simulate downburst, with impinging jet Model in 2D axisymmetric domain.
  - Computational Fluid Dynamics (CFD) technique. Perform steady-state Reynolds Averaged Navier Stokes (RANS) and transient RANS.
  - Characterise the flow of a stationary impinging jet and understanding the flow features.

Axi-symmetric CFD Computational domain

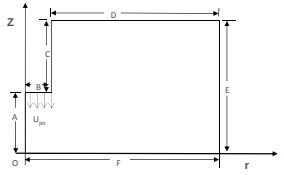

Boundary conditions

Edges	Boundary conditions	Dimensions
A	Axis	4D
B	Speed inlet	0.5 D
C	Symmetry (slip wall)	6D
D, E	Pressure-outlet	10 D (edge E)
F	Non-slip wall	10D

Assumptions:
- Incompressibility
- Temperature and buoyancy effect neglected.

Legend

Re	Reynolds number based on diameter of B
and	inlet velocity at B.
U_{jet}	Inlet velocity at B (independent variable)
D	Diameter at B
H	height of A
	kinematic viscosity of air.
r/D	normalised radial distance from *O*.
H/D	normalised height of A.

Results and discussion

- Grid and domain independence test

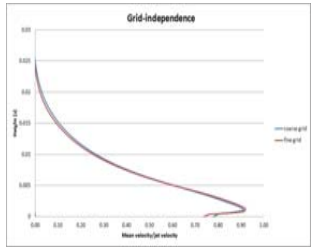

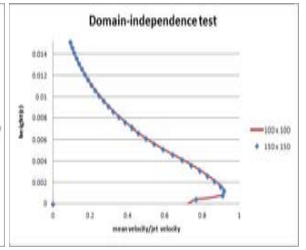

Results and discussion

- Validated with Kim and Hangan (2007) experimental data of the impinging jet at different locations along the wall (other locations are not shown.)

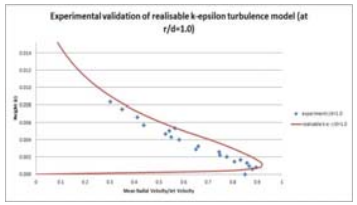

- Kim, J., Hangan, H., (2007). Numerical simulations of impinging jets with application to thunderstorm downbursts. Journal of Wind Engineering and Industrial Aerodynamics 95, 279–298.

Results and discussion
Velocity magnitude (m/s) plot contour.

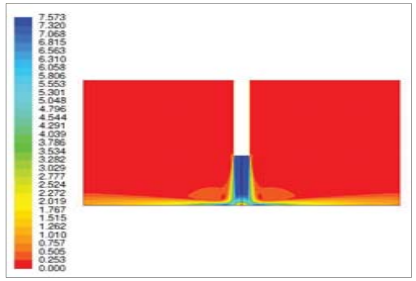

High speed flow region (close to 7.57 m/s) encountered at the "inlet" and at the "wall" region.

Results and discussion
Reynolds number dependency
Re = 20,000 ; Re=2,000,000

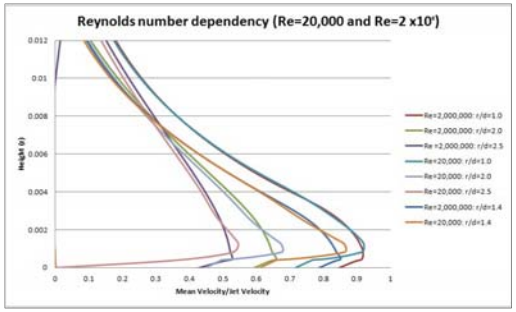

Results and discussion
At very high Reynolds number.

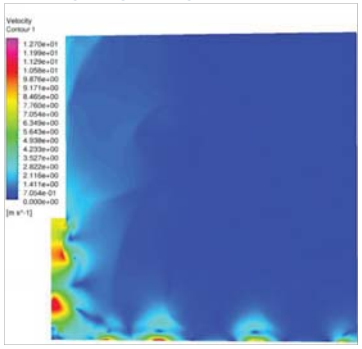

Results and discussion
Changing the diameter D of the "inlet".

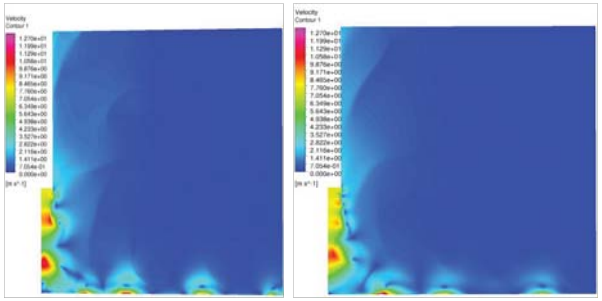

Results and discussion
Effects of changing the height H of the inlet from the wall surface (only location r/D=1.0 and r/D=2.5 shown).

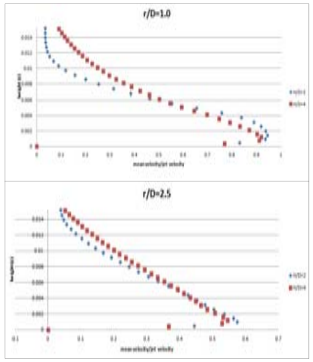

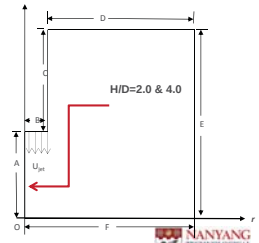

Results and discussion
Effects of gravity (in the negative axial direction)

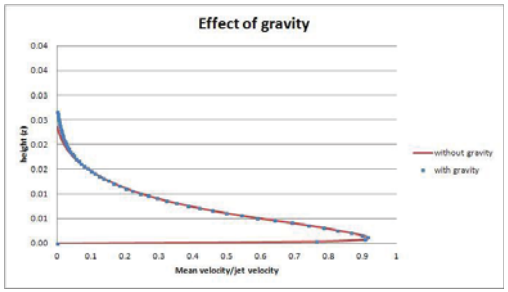

Results and discussion
Transient RANS simulation

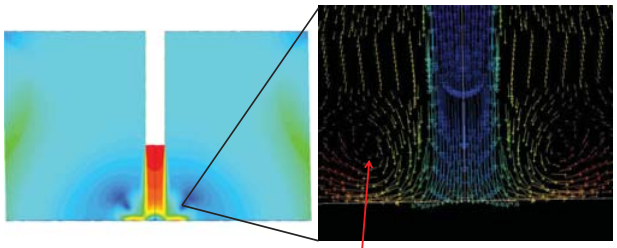

Ring vortical flow pattern near the "wall"

Conclusion

1) Maximum peak velocity magnitude in the whole computing domain occurs at r=1D.
2) As reynolds number is increased, the height at which the maximum velocity is decreased.
3) As reynolds number gets extremely large, the flow is approximately inviscid, and the flow becomes more periodic and vortices are more organised and periodic.
4) Decreasing the height H of the inlet results in increase of the peak speed of that location.
5) There is no significant effect on the flow due to gravity and changes in the diameter.

Future works

- Study effects of buoyancy and density stratification
- Performing a 3-dimensional simulation using Large eddy simulation (LES) method to study the vortices.
- Study the interaction effect of the flow with a obstacles blocking the flow.
- Study the effects due to ocean waves, where the waves are modelled as roughness elements.

SEAWATCH Wind Lidar Buoy

Posters

Magnetically Induced Vibration Forces in a Low-Speed Permanent Magnet Wind Generator with Concentrated Windings, Mostafa Valavi, PhD stud, NTNU

Stability in offshore wind farm with HVDC connection to mainland grid, Jorun I Marvik, SINTEF Energi AS

A Markov Weather Model for O&M Simulation of Offshore Wind Parks, Brede Hagen, stud, NTNU

Turbulence Analysis of LIDAR Wind Measurements at a Wind Park in Lower Austria, Valerie-Marie Kumer, UiB

Investigation of droplet erosion for offshore wind turbine blade, Magnus Tyrhaug, SINTEF

NOWIcob – A tool for reducing the maintenance costs of offshore wind farms, Iver Bakken Sperstad, SINTEF Energi AS

Long-term analysis of gear loads in fixed offshore wind turbines considering ultimate operational loadings, Amir Rasekhi Nejad, PhD, NTNU

Methodology to design an economic and strategic offshore wind energy Roadmap in Portugal, Laura Castro-Santos, Laboratório Nacional de Energia (LNEG) (poster and paper)

Methodology to study the life cycle cost of floating offshore wind farms, Laura Castros Santos,Laboratório Nacional de Energia (LNEG) (poster and paper)

Two-dimensional fluid-structure interaction of airfoil, Knut Nordanger, PhD stud, NTNU

Experimental Investigation of Wind Turbine Wakes in the Wind Tunnel, Heiner Schümann, NTNU

Numerical Study on the Motions of the VertiWind Floating Offshore Wind Turbine, Raffaello Antonutti, EDF R&D

Coatings for protection of boat landings against corrosion and wear, Astrid Bjørgum, SINTEF Materials and Chemistry

Numerical model for Real-Time Hybrid Testing of a Floating Wind Turbine, Valentin CHABAUD, PhD stud, NTNU

Advanced representation of tubular joints in jacket models for offshore wind turbine simulation, Jan Dubois, ForWind – Leibniz University Hannover

Comparison of coupled and uncoupled load simulations on the fatigue loads of a jacket support structure, Philipp Haselbach, DTU Wind Energy

Design Standard for Floating Wind Turbine Structures, Anne Lene H. Haukanes, DNV

Nonlinear irregular wave forcing on offshore wind turbines. Effects of soil damping and wave radiation damping in misaligned wind and waves, Signe Schløer, DTU

Magnetically Induced Vibration Forces In a Low-Speed PM Wind Generator with Concentrated Windings

Mostafa Valavi, PhD Candidate
Department of Electrical Power Engineering, NTNU
Supervisor: Professor Arne Nysveen

Introduction

Permanent Magnet (PM) machines with concentrated windings have been gaining importance in the last few years due to several significant advantages over machines with distributed windings. One attractive application is direct-driven wind generator where the gearbox is eliminated and this is a very effective way to increase the reliability and reduce the maintenance works. It could be a distinct advantage particularly in offshore wind farms, where the maintenance operations are difficult and expensive. The most important drawback of using concentrated windings is that the vibration level of these machines can be significantly higher than conventional machines. It is mainly due to presence of low order harmonics in the radial magnetic forces.

Generator Specifications

Rated power	50 kW
Number of phases	3
Rated frequency	50 Hz
Rated speed	51.7 rpm
Rated current	100 A_{rms}
Number of poles	116
Number of stator slots	120
Stator outer diameter	1777 mm
Stator material	M250-50A
Permanent magnets	NdFeB N35

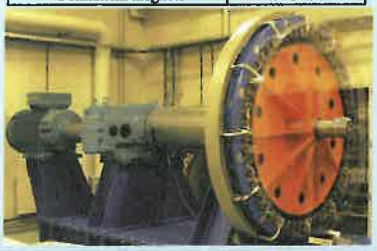

Theory

- Maxwell's stress tensor

$$f_r = \frac{1}{2\mu_0}(B_r^2 - B_t^2) \qquad f_t = \frac{1}{\mu_0}(B_r B_t)$$

- Radial magnetic force waves

$$f_r(\theta, t) = f_{r\,max}\cos(m\theta - k\omega t)$$

- Mode shapes

- Radial forces are the main cause of magnetic vibration.
- Dominant vibration mode is the lowest mode.
- In PM machines with concentrated windings, low modes of vibration can be excited.

Magnetic FEM Simulations

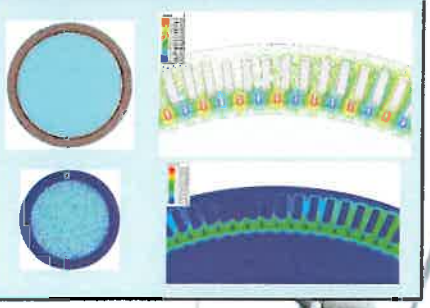

Magnetic Flux Density

PM field

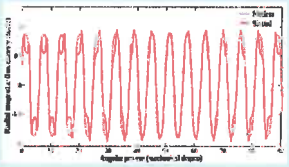

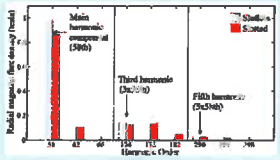

MMF field

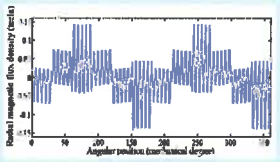

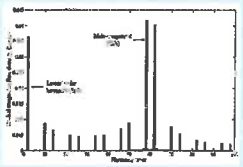

No-load Radial Force Density

Slotless

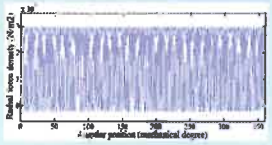

Slotted

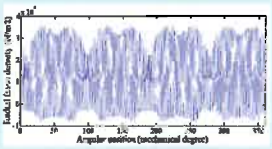

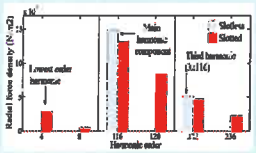

Radial Force Density at Load

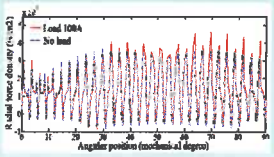

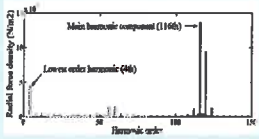

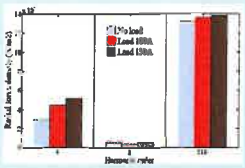

Conclusion

Radial magnetic forces in a low-speed 120-slot/116-pole wind generator are calculated using finite element method and Maxwell's stress tensor. These forces are the main cause of the magnetic vibration. Flux density distribution due to PM and MMF magnetic fields is analyzed. It is shown that slotting harmonics plays an important role in the field characteristics. Radial forces are investigated in no-load and load conditions. It is found that amplitude of the lowest spatial harmonic order (4th) is considerable even in no-load, however it increases while the machine is loaded. It is shown how slotting and MMF harmonics contribute to produce this lowest vibration mode.

Analysis of grid faults in offshore wind farm with HVDC connection

4

Jorun I. Marvik, Harald G. Svendsen

SINTEF Energy Research, Trondheim, Norway

Introduction

Future offshore wind farms are expected to be built farther away from shore and have larger capacities than today. This leads to new challenges related to grid connection. At distances longer than roughly 100 km, HVDC transmission is preferred over AC transmission due to large charging currents in AC-cables. Conventional LCC HVDC is not suited for connection to weak grids like offshore wind farms, and the less mature VSC HVDC technology is preferred instead.

A future large offshore wind farm with full power converter turbines and three-terminal VSC HVDC grid connection has been modelled in PSCAD. With three terminals the HVDC link can be used for direct transmission between the onshore terminals in addition to transmission of wind power. This work focuses on responses to faults in the collection- and transmission system. Due to the power electronics interfaces, the system has low short circuit capacity and missing inertia. Also, DC-cables are discharged very fast during faults. This leads to different fault responses than in conventional grids.

Offshore wind farm with HVDC transmission

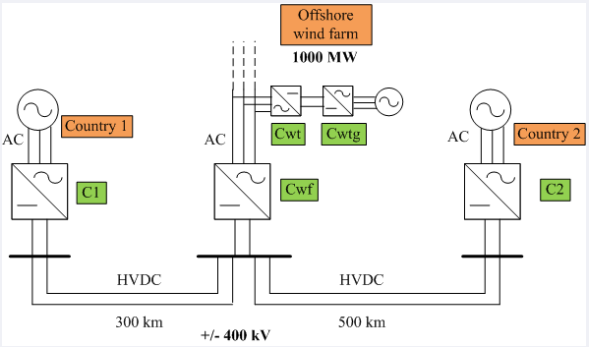

All converters are 2-level VSCs

Faults in wind farm AC collection grid

2-phase short circuit in collection grid

A) Active power on collection grid- and turbine side of one wind turbine converter
B) Wind turbine DC-link voltage and AC terminal voltage

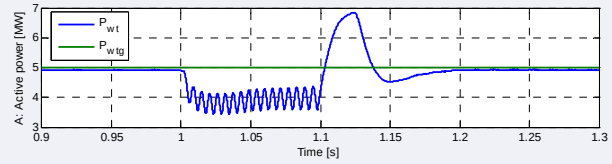

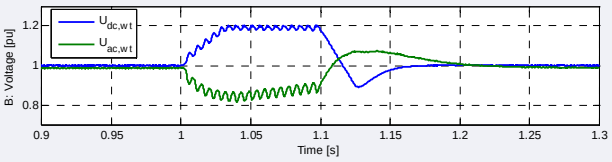

3-phase short circuit in collection grid

A) Active power on collection grid- and turbine side of one wind turbine converter:
B) Wind turbine DC-link voltage and AC terminal voltage:

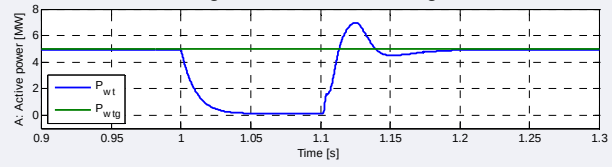

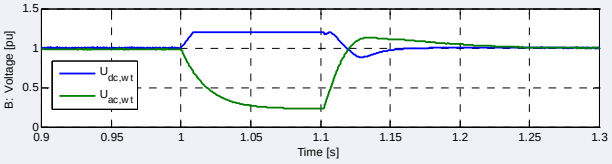

Impedance seen by relay at offshore HVDC terminal:

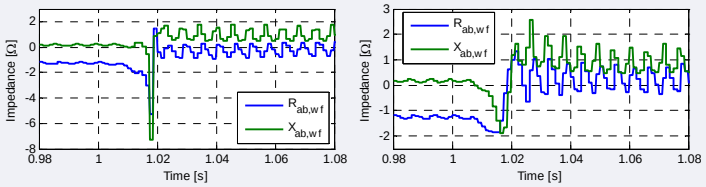

Conclusions – AC collection grid faults

- Fault detection with conventional impedance protection is difficult in the offshore AC-grid, as Impedance protection is based on impedance changing from a large value during normal operation to a small value during fault
- The surplus energy in the DC-link during the AC-voltage dip is consumed by a DC-chopper when the DC-voltage goes above 1.2 pu. The wind turbine can therefore operate undisturbed through the short-circuits.

Faults in HVDC transmission-grid

Earth-fault halfway between converters C1 and Cwf

A: HVDC cable current towards converter C1 and C2 at wind farm HVDC terminal
B: HVDC voltage at wind farm HVDC terminal

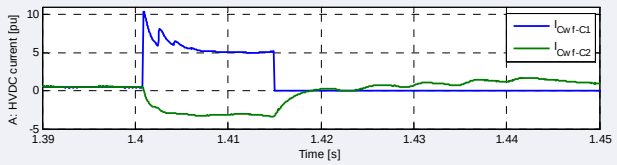

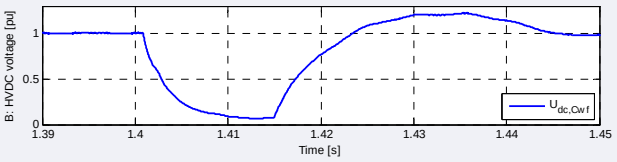

Rate-of-change of HVDC currents:

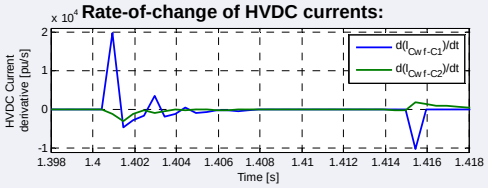

- Fast fault detection possible based on rate-of-change of current.

Active power through converters Cwf and C2:

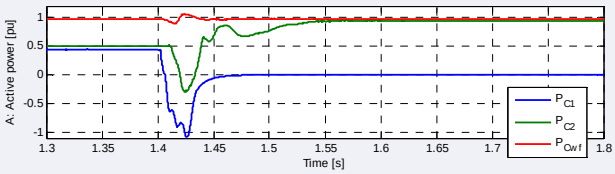

Conclusions - HVDC transmission grid faults:

- In this case, the HVDC cable between terminals C1 and Cwf has to be disconnected within 15 ms to assure stable operation (i.e. very fast).
- Fast detection is possible e.g. based on rate-of-change of current together with DC-voltage level, but fast DC breaker is required for disconnection
- When HVDC terminal C1 is disconnected, the active power delivered to HVDC terminal C2 is increased accordingly, due to the DC-voltage droop on the active power controller in the converter in C2.

A multivariate Markov Weather Model for O&M Simulation of Offshore Wind Parks

Brede Hagen (bredeand@stud.ntnu.no), Ingve Simonsen, Matthias Hofmann, Michael Muskulus
NTNU-Department of Physics, SINTEF Energy Research , NTNU-Department of Civil and Transport Engineering

Abstract

A multivariate Markov chain model is presented for generating sea state time series based on observed time series. Two ways of capturing the seasonal variation in the sea state parameters resulted in two distinct models which quality was assessed by comparing their statistical properties to what was obtained from observed time series. Two different sea state data sets were considered in the validation, and it was found that both models compared favorably to those empirical data. It was concluded that Model 1 worked best for the longest data set considered, but was challenged by the shorter time series, where Model 2 worked best.

Objectives

Main objective: Create a stochastic weather model for the sea state conditions based on observed time series which can be used in an O&M simulation tool.

A Markov chain model has recently been created by Scheu et. al. [1], and used in an operating tool for an Offshore wind farm. This model generated time series for significant wave height and wind speed and was concluded to be suitable. However, other sea state parameters such as wave period, and wind- and wave direction may also be important in an O&M simulation tool.

For this purpose a more flexible model is needed.

Method

Two multivariate Markov chain models were implemented:

Model 1 is a generalization of the weather model mentioned . This model estimates transition probabilities separately for each month. The generalization lies in the discretization procedure, where multivariate weather states were constructed. The weather state is represented by an integer which reflects the values for all sea state parameters with uncertainties corresponding to the resolutions.

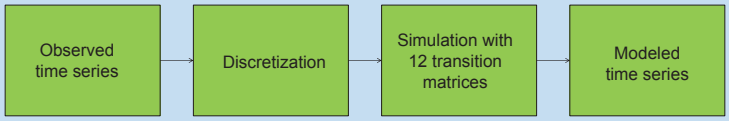

Structure of Model 1

In Model 2 an other approach of dealing with the seasonal variation for the sea state parameters was used:

The seasonal variation in the mean value and standard deviation for wave height, wind speed and wave period were assumed to be deterministic functions with a period of one year. This seasonal variation were removed from the observed times series with a transformation. The transformed time series were assumed to be stationary by estimating only one transition matrix.

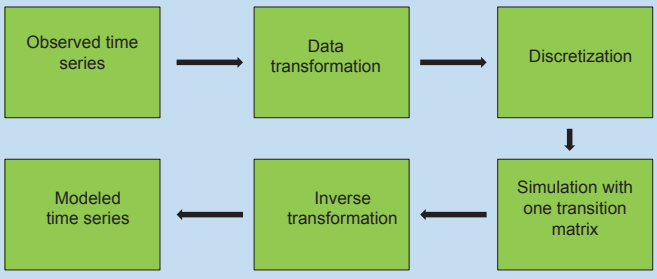

Structure of Model 2

Both models were assed by comparing statistical properties such as first and second order moments, correlations, marginal distributions, persistence of good weather windows and waiting time between these weather windows. Weather windows were characterized by small waves with a large period combined with calm wind. Statistical parameters were calculated for whole time series and on a monthly scale and both visual comparison and calculation of test statistics were performed

Results

The figures below shows how some of the statistical parameters considered were reproduced by Model 1 for the longest data set.

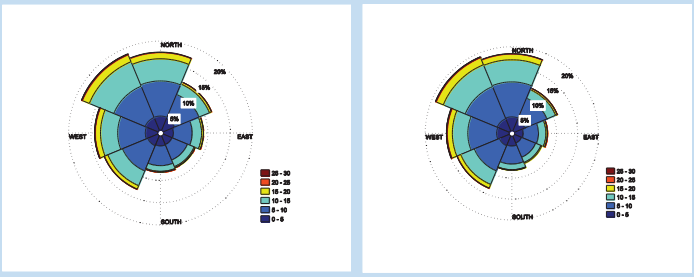

Observed (left) and modeled (right) wind roses

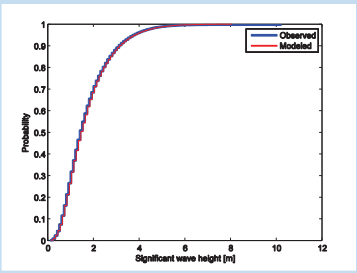

Empirical CDF- Wave height

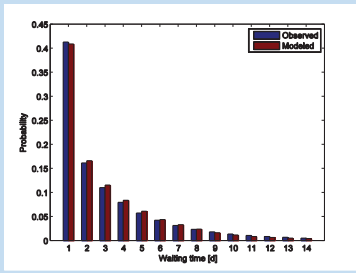

Waiting time for weather windows

Conclusions

Both models reproduce the statistical parameters well, especially the results for persistence and waiting time for weather windows were promising. Both models were therefore concluded to be suitable for O&M simulation of Offshore Wind parks. Due to a high number of weather states both models need long datasets sets to ensure that the simulated time series is different from the observed one. It has also been demonstrated that Model 1 is most restrictive to short datasets.

References

1. M. Scheu, D. Matha, M. Muskulus, Validation of a Markov-based weather model for Simulation of O&M for Offshore Wind Farms, International Offshore and Polar Engineering Conference (2012) 463-468
2. V. Monbet, P. Aillot, M. Prevosto, Survey of stochastic models for wind and sea state time series, Probabilistic Engineering Mechanics, Vol 22, (2007), 113-126
3. J. Z. Jim, C. R. Chou, A Study on Simulating the Time Series of Significant Wave Height near the Keelung Harbour, Proc. ISCOPE Conf., Vol. 3, (2002), 92-96

TURBULENCE ANALYSIS OF LIDAR WIND MEASUREMENTS AT A WINDPARK IN LOWER AUSTRIA

Valerie-Marie Kumer[1,2], Vanda Grubišić[1,3], Manfred Dorninger[1], Stefano Serafin[1], Lukas Strauss[1], Rudolf Zauner[4]

[1]Department of Meteorology and Geophysics, University of Vienna. Austria, [2]Geophysical Institute, University of Bergen, Norway, [3]National Center for Atmospheric Research, Boulder, Colorado, [4]Verbund Renewable Power GmbH, Vienna, Austria

LIDAR

An increase in nacelle height and rotor diameter of wind turbines in recent years have made measurements of wind profiles via meteorological masts difficult. In response LIDAR remote sensing has become increasingly important. With this technique, wind information at different heights is easily accessible and enables an analysis of boundary layer processes.

Figure 1: Measurement principal of the Doppler LIDAR WINDCUBE™ V1 [1]

Measurement Campaign

In this study we analyzed Doppler LIDAR measurements conducted in a field campaign at a wind park operated by VERBUND Renewable Power GmbH, near Bruck-an-der-Leitha (Lower Austria). A WINDCUBE™ V1 (WLS7) Doppler LIDAR collected data over a three-month period in summer 2010.

Measurement (analyzed) period	7.7. (25.8.) – 6.10.2010
Scanning technique	VAD
Data availability	70%

The device was located 2.5 rotor diameters (165 m) west of the wind turbine WEA4 (WindEnergieAnlage) and around 10 rotor diameters (~ 660 m) southeast of the wind turbine WEA5 (figure 2a). As the wind rose in figure 2b shows, the device is capable of capturing the ambient flow, which is influenced by the large and small scale topography.

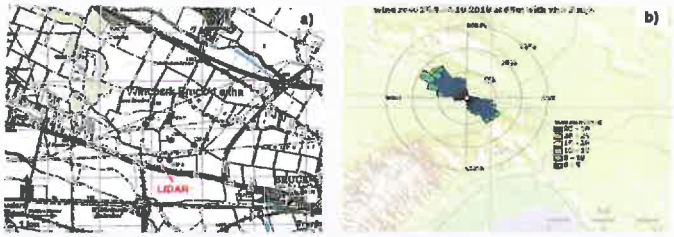

Figure 2: a) Map of the wind farm in Bruck an der Leitha with the location of the WINDCUBE™ in red and the wind turbine sites WEA1-WEA5 in blue [2]. b) Wind rose of horizontal wind speeds greater than 3 m/s collected by the WINDCUBE™, representing the analyzed period at the measurement height of 65 m

Methods

Due to a high sampling rate of 0.25 Hz, so that calculations of variances and covariances of wind parameters are possible. This allows an analysis of turbulence through derived parameters such as turbulent kinetic energy (TKE) or turbulence intensity (TI), calculated as the following

$$TKE = \frac{1}{2}\left(\overline{u'^2} + \overline{v'^2} + \overline{w'^2}\right) \qquad TI = \frac{\sigma(v_h)}{\overline{v_h}}$$

where u, v and w are the wind components, v_h is the horizontal wind speed and $\sigma(v_h)$ its standard deviation. The spectral energy gap [3] of u, v and w times series is used for a correct estimation of the turbulence scale (figure 3). On the basis of the momentum equations it is possible to calculate the tendency *T* of TKE [4]

$$T = -AD + B + S + TT + P - D$$

These terms are representing advection *AD*, buoyancy *B*, shear *S*, turbulent transport *TT*, pressure correlations *P* and dispersion *D* as the sources and sinks of TKE.

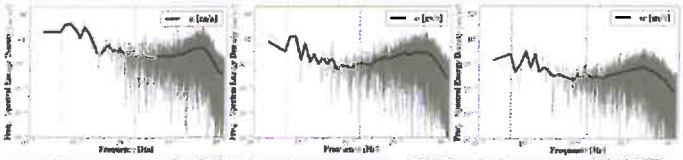

Figure 3: Spectral energy density times frequency plots of the wind components u, v and w on logarithmic axes at 65 m on September 25th 2010. The vertical black lines indicate the frequency of 6 h and 10 min

Results

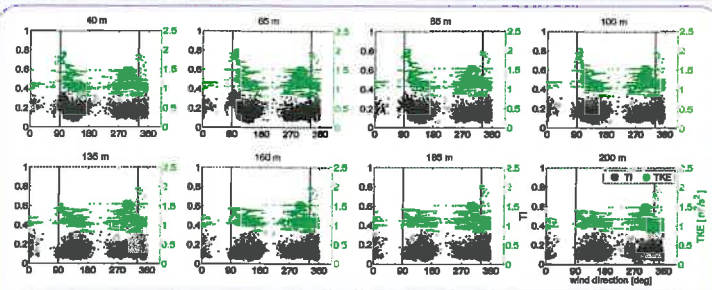

Figure 4: TI and TKE plotted in blank and green as a function of wind direction, using the turbulence processed data set for wind speeds > 3 m/s. The vertical black lines at 90° and 330° indicate disturbed winds due to the wakes of WEA4 and WEA5

- The turbulence distribution shows two wake signals for easterly and northwesterly winds (figure 4). These are consistent with the location of the WINDCUBE™ (figure 2a). The peaks at 90° vanish at measurement altitudes above blade tip height (100 m) in contrast to the ones at 330°. This indicates the wake expansion of WEA5.
- As TKE reproduces the same information as TI, it enables due to its tendency equation a more detailed analysis of turbulence.

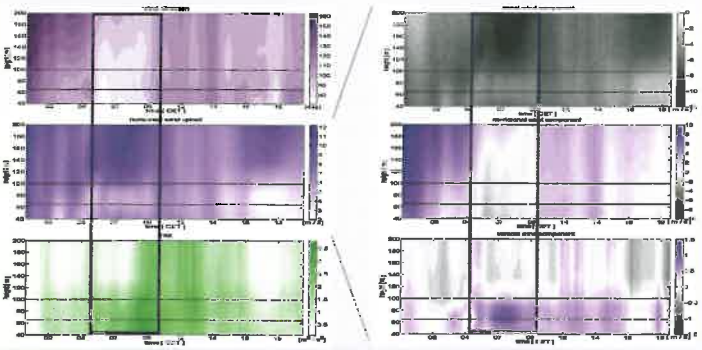

Figure 5: Contour plots of wind direction, horizontal wind speed, TKE (left) and wind components u, v and w (right) profiles during the wake case of September 25th 2010. The purple boxes and black horizontal lines indicate the period during which the device was inside the wake region and hub and blade tip height respectively

- A case study of September 25th 2010 proofs, LIDAR data is capable of resolving wake effects downstream of the wind turbine WEA4, indicated through a wind speed deficit and increased values of TKE (figure 5). Upwelling motion of the order of 1 m/s, as well as flow reversal in the meridional wind component above the blade tip height support the theoretical approach of helicoidally wake structures [5] and are comparable to results provided by laboratory experiments published by Zhang et al. [6].
- In terms of turbulence generation a maximum in vertical shear generation around the blade tip height shows compared to the other end of the rotor disk irregular loads. This turbulence maximum at blade tip height was also captured by field experiments by Iungo [7].
- The wake represents a high energy loss as TKE takes almost 22% of the whole available kinetic energy in the considered case study [8].

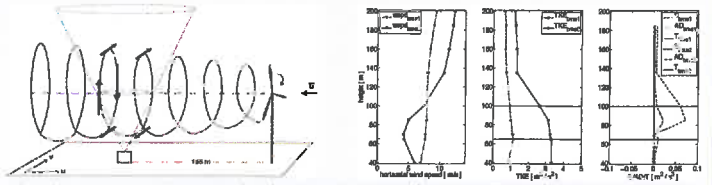

Figure 6: a) Sketch of the wake structure and derived wind pattern captured by the device. b) Vertical profiles of wind speed, TKE and TKE budget terms for time1 = 00 CET and time2 = 09 CET on September 25th 2010. Horizontal heights indicate the blade tip and hub height

Conclusion & Outlook

A detailed turbulence analysis is possible with LIDAR wind data from a WINDCUBE™ V1, leading to a quantitative description of the wake region. Anisotropic turbulence distribution indicates a dominating shear generation. The maximum shear induced turbulence is located around blade tip height an leads to irregular loads on the rotor blades. Considering this knowledge in the operation of wind parks is crucial for the operators as it could lead to more efficient lifetime power production of wind farms. Moreover the gained information can be used for optimizing layouts of new wind farms as well as for intelligent operation of already existing ones. This work will be continued at the University of Bergen, using a scanning Doppler LIDAR for further investigations.

References

[1] Clifton A. et al (2012), 1. Ground-Based Vertically-Profiling Remote Sensing for Wind Resource Assessment. IEA wind. [2] Koller S. (2010), Technical Report. Meteotest. [3] Van der Hoven I.(1957), Power spectrum of horizontal wind speed in the frequency range from 0.0007 to 9000 cycles per hour. Journal of Meteorology. [4] Markowski P. et al (2010), Mesoscale Meteorology in Midlatitudes. Wiley-Blackwell. [5] Tong W. (2010), Wind Power Generation and Wind Turbine Design. WIT Press. [6] Zhang W. et al (2012), Near-wake flow structure downwind of a wind turbine in a turbulent boundary layer. Experimental Fluids. [7] Iungo G.V. (to be published), Field measurements of wind turbine wakes with LIDARs. Journal of Atmospheric and Oceanic Technology. [8] Kumer V. (2012), Analysis of Lidar Wind Measurements at a Bruck an der Leitha Wind Park. Diploma thesis at University of Vienna

DeepWind 2013
10th Deep Sea Offshore Wind R&D Conference
DeepWind 2013
24. – 25.1.2013, Trondheim, Norway

Kumer valerie.kumer@gfi.uib.no Grubišić vanda.grubisic@univie.ac.at
Reuder joachim.reuder@gfi.uib.no Zauner rudolf.zauner2@verbund.com

Investigation of droplet erosion for offshore wind turbine blades

SINTEF

NTNU
Norwegian University of Science and Technology

Etienne Cheynet (ENSMA) and Magnus Tyrhaug (NTNU)

Supervisors: Sergio Armada(Sintef), Mario Polanco-Loria(Sintef) and Astrid Bjørgum(Sintef)

Isae ENSMA

Introduction

Droplet erosion as one type of leading edge erosion on wind turbine blades, has been studied, in order to obtain a better understanding of the mechanisms and a resistance surface treatment. The target is to develop tools helping the industry to achieve a 20 year lifetime of blades.

Different coatings were investigated by erosion tests, material characterization and numerical modeling.

Methods and materials

Droplet erosion test facility
- Sample velocity 180 m/s
- Changeable nozzles

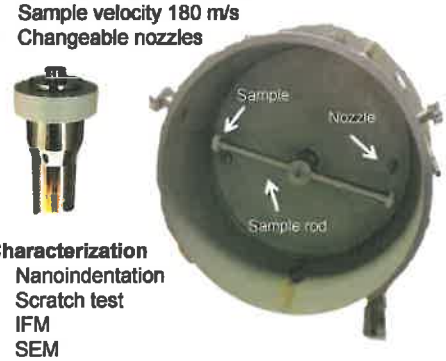

Characterization
- Nanoindentation
- Scratch test
- IFM
- SEM

Modelling of droplet impact
- Evaluation of a numerical model to simulate rain erosion
- Rain is modelled using the Smoothed Particle Hydrodynamics (SPH) formulation
- Coating is modelled with Finite Element Method (FEM)

Materials investigated

Dummy samples for erosion test facility
- HDPE
- PVC

Protective surface coatings
- 3M™ Wind Protection Tape
- Polyurethane composite coatings
  - 100% PUR
  - PUR with SiC additives (15µm and 20nm)
  - PUR with FunzioNano® additives

Experimental Results

Characterization of TS Polyurethane
Nanoindentation, IFM of scratch test and cross sections.

Sample	Modulus (MPa)	Hardness (MPa)
100% PUR	273.5	20.8
2.5% FunzioNano	108.8	9.8
2.5% nanoSiC(20nm)	122.3	10.9
5.0% coarseSiC(15mm)	115.0	9.8

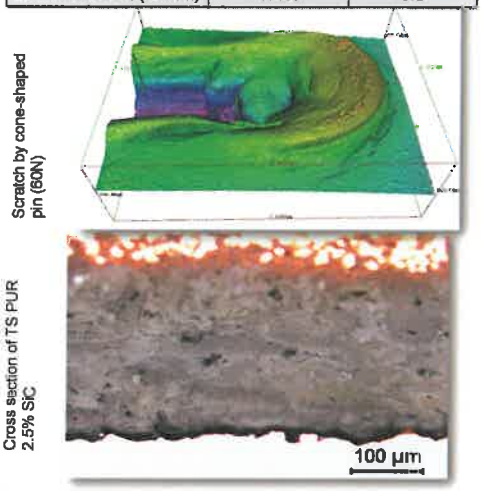

Erosion test
Erosion pattern obtained at 180 m/s with rain droplets for HDPE.

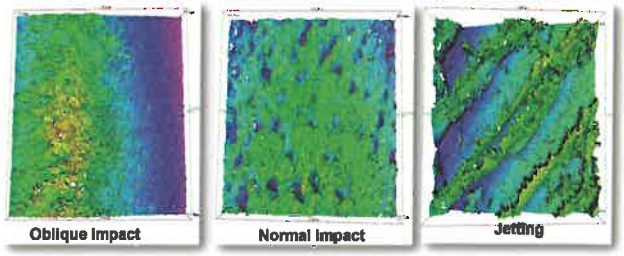

Erosion rate
The erosion resistance of the sample is evaluated through the erosion rate (loss of mass per time).

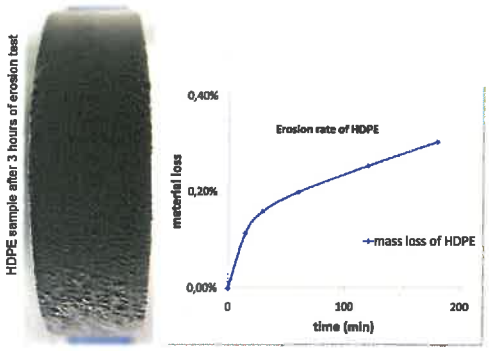

Numerical results

The discretisation of the rain field into particles moving independently is limited by the SPH formulation. The particle field is still considered as a continuum medium despite minimized interaction between particles.

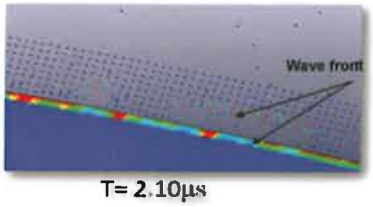

After the first impact, a shockwave propagate inside the particle field, disturbing it, spoiling the results.

Conclusions

Experimental
- Test facility provides suitable conditions to perform droplet erosion.
- Thermal sprayed Polyurethane composite coatings shows promising mechanical properties as a protective coating.
- Further characterization of materials are required.

Modelling
- Discrete Element Method (DEM) must be considered as an alternative formulation to simulate the droplets flow.
- A study of single droplet impacts, comparing the stress and pressure distribution with theoretical data to rank the coatings susceptibility to wear can be an alternative study.

Acknowledgements

We would like to thank the people of SINTEF Dept. of Applied Mechanics and Corrosion for great help and advices during our work.

Contact information

Etienne Cheynet
Mail:
Tel: +0033643731179

Magnus Tyrhaug
Mail:
Tel: +47 98023968

NOWIcob – A tool for reducing the maintenance costs of offshore wind farms

Matthias Hofmann (matthias.hofmann@sintef.no), Iver Bakken Sperstad,
SINTEF Energy Research

Abstract

One of the goals for the NOWITECH research project is to develop a scientific foundation for implementation of cost-effective operation and maintenance (O&M) concepts and strategies for deep-sea offshore wind farms. One task towards fulfilling this goal is the development of a framework and model for optimizing the maintenance and logistics activities. This model aims to help decision makers choosing the right maintenance strategies and logistic support.

Objectives

Main objective: reduce the cost of energy of far-offshore wind farms by implementation of cost-effective O&M concepts and strategies.

As basis for this objective, a decision support tool (NOWIcob) is under development that simulates the operational phase of an offshore wind farm with all maintenance activities and costs:

- analysing the profit of the wind farm from a life cycle perspective
- understanding sensitivities of the wind farm availability and the O&M costs due to changes in the maintenance strategy

Cost-benefit model for offshore wind farms (**N**orwegian **o**ffshore **wi**nd power life cycle **co**st and **b**enefit model – **NOWIcob**)

Method

The scientific approach for the model is based on a time-sequential event-based Monte Carlo technique. As illustrated in the figure below, the model takes into account both controllable options, as the logistics and maintenance choices made for the wind farm, and a number of external factors. The availability, life cycle profit, and other performance parameters are the output of the model.

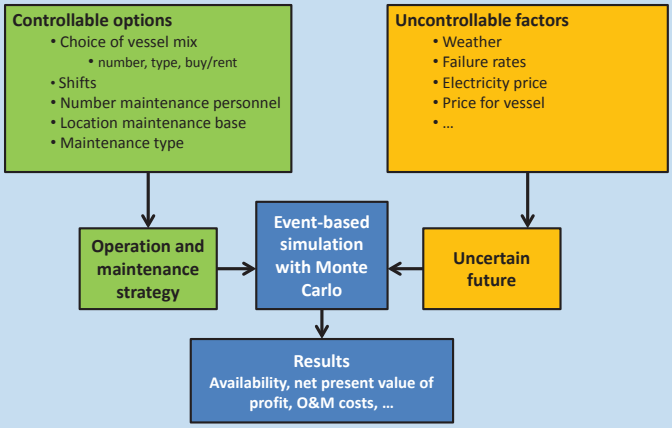

A main focus is on the representation of weather and the access criteria. Weather is represented by values of the significant wave height and the wind speed. Based on historic data, a Markov transition matrix is generated and used for generating random weather with hourly resolution. These modelled time series have the same statistical properties as the historic data, such as correlation between wind and wave, persistence, and seasonal variations.

Another focus is on the vessels and the possibility to include future vessel concepts in the model. Examples of such are mother/daughter vessel concepts, offshore accommodation platforms, and crew transfer vessels that are offshore several shifts. In addition, the weather limitations for the various capabilities and operations of the vessels are considered.

The sequence of steps in the simulation is illustrated in the simplified flow scheme to the right.

For each case, the model runs through the entire life time of the wind farm with hourly resolution. In each shift, maintenance tasks are scheduled to repair any random component failures as well as performing periodic or condition-based maintenance, taking the availability of weather windows into account.

The simulation is repeated a number of times with new generated weather and failures, and the spread of the results reflects the inherent uncertainties in uncontrollable factors.

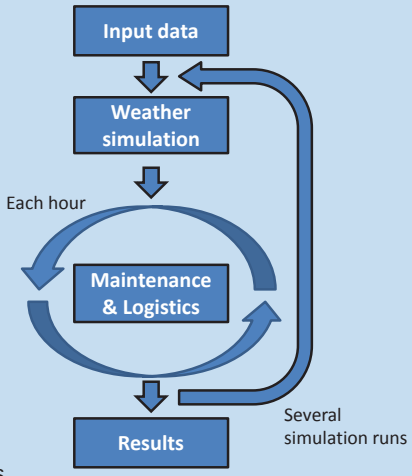

Results

The NOWIcob model is tested on some first cases. The following figure shows the availability, calculated as the ratio of produced electricity to the theoretical production without downtime, for the case of a far-offshore wind farm where a mother/daughter vessel concept is compared with the possibility of an offshore accommodation platform. The results are given as estimated probability distributions based on 100 simulation runs.

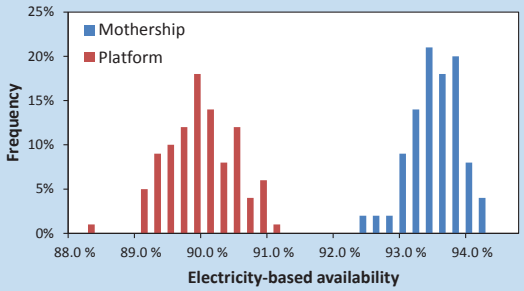

Conclusions

The NOWIcob model aims to help reducing the cost of energy for offshore wind farms. Consequences of different decisions related to the maintenance and logistic strategy can be analysed and the most effective solution can be chosen taking uncertainties into account. The model can also be used to minimize and understand the uncertainty of a wind farm project by evaluating different risk mitigation measures.

For future work, it is planned to extend the weather model to several weather parameters as for example wave period.

References

1. Hofmann, M.; Heggset, J.; Nonås, L. M.; Halvorsen-Weare, E. E. (2011): A concept for cost and benefit analysis of offshore wind farms with focus on operation and maintenance. *Proceedings of the 24th International Congress on Condition Monitoring and Diagnostics Engineering Management (COMADEM 2011)*.
2. Hofmann, M. (2011): A Review of Decision Support Models for Offshore Wind Farms with an Emphasis on Operation and Maintenance Strategies. *Wind Engineering 35 (1)*.
3. Hofmann, M.; Sperstad, I. B. (2012): User manual and documentation NOWIcob model (D5.1-32). SINTEF report.

Methodology to design an economic and strategic offshore wind energy Roadmap in Portugal

Laura Castro – Santos[a], Geuffer Prado García[a], Paulo Costa[a], Ana Estanqueiro[a]

e – mail: laura.castro.santos@udc.es

[a]National Energy Laboratory (LNEG), Solar, Wind and Ocean Energy Unit (UESEO), Estrada do Paço do Lumiar, 22, 1649-038, Lisbon, Portugal

Abstract. The main objective of this paper is to establish a roadmap for offshore wind energy in Portugal. It will determine the best sea areas to install fixed and floating offshore wind farms in this region, using spatial analysis of four economic indexes: Internal Rate of Return (IRR), Net Present Value (NPV), Discounted Pay-Back Period (DPBP) and Levelized Cost Of Energy (LCOE). Several economic parameters will be considered (Portuguese offshore tariff, investment and O&M costs, credit values, etc.).Three different discounted rates were used into the sensitivity analysis. Several types of physical restrictions will be taking into account: submarine electrical lines, bathymetry, seabed geology, environmental conditions, protected areas in terms of heritage, navigation areas, fault lines, etc. Moreover, location settings as proximity to shipyards or ports will be considered to complement the strategy. All of them will define the resulting area to install offshore wind farms along Portuguese coast. Spatial operations, considering economical, physical and strategic issues, have been carried out using Model Builder of GIS (Geographic Information Systems) software. Results indicate the Portuguese areas economically suitable for installing offshore wind farms.

METHODOLOGY

ECONOMIC DEVELOPMENT

- **Levelized Cost of Energy (LCOE)**: the approach of the International Energy Agency defines the costs as a summation of the total cost of the initial investment and annual operating and maintenance costs.
- **Net Present Value (NPV)**: it is the net value of all revenues (cash inflows – sale of electricity) and expenses (cash outflow – financial costs and O&M costs) of the project, discounted to the beginning of the investment.
- **Internal Rate of Return (IRR)**: it is a measure of a project's magnitude in the financial markets evaluation scale.
- **Discounted Payback Period (DPBP):** it uses the cash flow of each year with the respective discount rate and adds it to all previous cash flows with respective discount rate. The year when this sum is greater or equal than the initial investment is the year of the payback.

INPUT DATA

Economic parameters

- Spatial distribution for the number of hours at full capacity production (**NEPs**) in each point of the Portuguese coast.
- **Total power of the farm**: 50 MW.
- **Costs of installed system**: 3315 €/kW per fixed turbine and 16575 €/kW per floating turbine .
- **O&M costs**: 21.43 €/kW/year for 7 MW wind turbine
- **Lifecycle**: 20 years.
- **Tax**: 30%.
- **Inflation**: 2.35%/year.
- **Discount rate**: 5%, 7.5% and 10% (different scenarios)
- **Fixed tariff**: 168 €/MWh, as in WindFloat
- **Market tariff**: 50.66 €/MWh
- **Credit**: 70% investment, 15 years, 5.4 % interest

GIS parameters

- **Bathymetry**: up to 40 m (fixed offshore wind) and 40 – 200 m (floating offshore wind)
- **NEPs**: 3000 h/year
- **Wind speed**: 7 m/s
- **Ports**: 10 m of draft
- **Shipyards**: 15120 m^2 of area
- **Docks**: 120 m of length

SELECT ECONOMIC MAP: IRR, NPV, DPBP, LCOE

RESTRICTIONS

RESULTS: economic atlas with restrictions (IRR, NPV, DPBP, LCOE)

GIS DEVELOPMENT

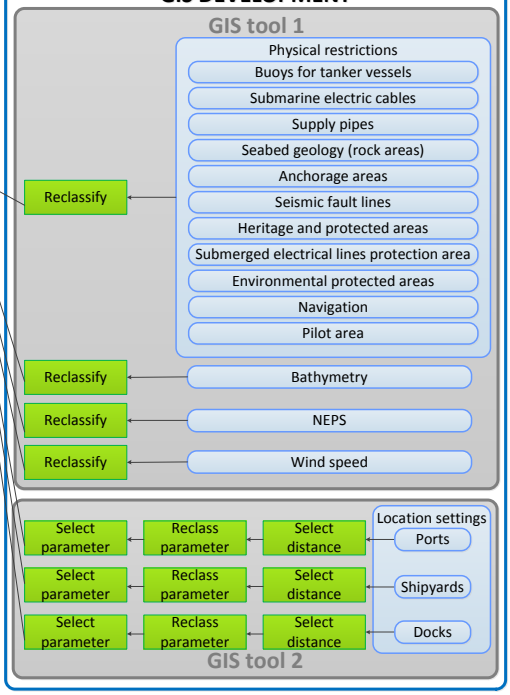

RESULTS

FIXED OFFSHORE WIND

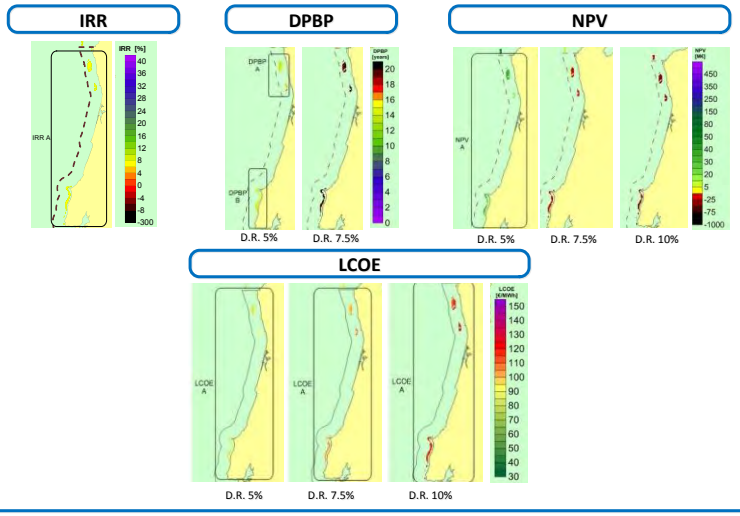

FLOATING OFFSHORE WIND

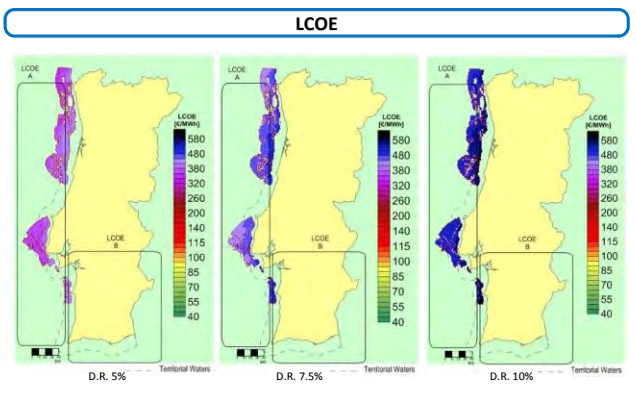

CONCLUSIONS

Fixed offshore wind

- **IRR**: 5.72% - 8.54%
- **DPBP**: 13 years – 17 years
- **NPV**: 13 M€ - 36 M€
- **LCOE**:
  - D.R. 5%: 79 – 93 €/MWh
  - D.R. 7.5%: 93 – 109 €/MWh
  - D.R. 10%: 107 – 126 €/MWh

Floating offshore wind

- **LCOE**:
  - D.R. 5%: 300 - 436 €/MWh
  - D.R. 7.5%: 340 - 519 €/MWh
  - D.R. 10%: 380 - 605 €/MWh

- This methodology could be used to analyse other offshore renewable energies, as wave energy, in future works.
- Ports selected: Leixões, Aveiro, Lisboa, Setúbal, Sines.
- Shipyards selected: Arsenal Alfeite, ENVC (Estaleiros Navais de Viana do Castelo) and Lisnave.
- The economic roadmap of offshore wind energy in Portugal gives feasible results for investors in some areas: Peniche, Viana do Castelo.
- It could improve the regional development of other parallel industries as naval construction, research clusters, maintenance industries and wind turbine developers.

Acknowledgements:

- Work funded by FCT/MTCES (PIDDAC) and FEDER through project PTDC/SEN-ENR/105403/2008

References:

- Short W, Packey D, Holt T. A manual for the economic evaluation of energy efficiency and renewable energy technologies. 1995;1-120.
- International Energy Agency (IEA). Projected Costs of Generating Electricity 2010. International Energy Agency (IEA), editor. OECD Publishing 2010;1-218.
- Costa P, Simões T, Estanqueiro A. Assessment of the Sustainable Offshore Wind Potential in Portugal. EWEC 2006;1-8.
- Ministério da Economia e da Inovação. Decree-Law n.o 225/2007 31st May. 2007;3630-8.
- ECN, MARIN, Windmaster L the, TNO, TUD, MSC. Study to feasibility of boundary conditions for floating offshore wind turbines. 2002;1-241.
- Castro R. Uma Introdução às Energias Renováveis: Eólica, Fotovoltaica e Mini-Hídrica. IST Press, editor. Portugal; 2011
- International Energy Agency (IEA). Energy Technology Roadmaps a guide to development and implementation. 2010;1-30.

Available online at www.sciencedirect.com

ScienceDirect

Energy Procedia 00 (2013) 000–000

Energy Procedia

www.elsevier.com/locate/procedia

DeepWind'2013, 24-25 January, Trondheim, Norway

Methodology to design an economic and strategic offshore wind energy Roadmap in Portugal

Laura Castro-Santos[a*], Geuffer Prado García[a], Paulo Costa[a], Ana Estanqueiro[a]

[a]*National Energy Laboratory (LNEG), Solar, Wind and Ocean Energy Unit (UESEO), Estrada do Paço do Lumiar, 22, 1649-038, Lisbon, Portugal*

Abstract

The main objective of this paper is to establish a roadmap for offshore wind energy in Portugal. It will determine the best sea areas to install fixed and floating offshore wind farms in this region, using spatial analysis of four economic indexes: Internal Rate of Return (IRR), Net Present Value (NPV), Discounted Pay-Back Period (DPBP) and Levelized Cost Of Energy (LCOE). Several economic parameters will be considered (Portuguese offshore tariff, investment and O&M costs, credit values, etc.).Three different discount rates were used into the sensitivity analysis. Several types of physical restrictions will be taking into account: submarine electrical cables, bathymetry, seabed geology, environmental conditions, protected areas in terms of heritage, navigation areas, seismic fault lines, etc. Moreover, location settings as proximity to shipyards or ports will be considered to complement the strategy. All of them will define the resulting area to install offshore wind farms along Portuguese coast. Spatial operations, considering economic, physical and strategic issues, have been carried out using Model Builder of GIS (Geographic Information Systems) software. Results indicate the Portuguese areas economically suitable for installing offshore wind farms.

Keywords: offshore wind energy, roadmap, renewable energy, economic areas, GIS

1. Introduction

A successful roadmap contains a clear statement of the desired outcome followed by a specific pathway for reaching it. This pathway should include the following components: goals, milestones, gaps and barriers, action items, priorities and timelines [1].

The development of the process ensures that a roadmap identifies mutual goals and determines specific

* Corresponding author. Tel.: +351 210924600 ext. 4345;
E-mail address: laura.castro.santos@udc.es.

and achievable actions towards realizing a common vision. The process includes two types of activities (Expert judgement and consensus and Data and analysis) and four phases (Planning and preparation, Visioning, Roadmap Development and Roadmap Implementation and revision) [1].

The main objective of this paper is to define the conditions applicable to the specific Portuguese context to design an offshore wind energy roadmap, in terms of fixed and floating wind devices.

This study determines the Portuguese coast areas which have more economic feasibility to install offshore wind structures. Several physical restrictions will be taking into account: submarine electrical cables, bathymetry, seabed geology, environmental conditions, protected areas in terms of heritage, navigation areas, seismic fault lines, etc. Furthermore, location settings as proximity to shipyards or ports will be considered to complement the strategy. All of them will define the resulting area to install offshore wind farms along Portuguese coast. Spatial operations, considering economic, physical and strategic issues, have been carried out using a GIS (Geographic Information System) tool developed in the Model Builder™ software.

On the other hand, economic indexes, such Internal Rate of Return (IRR), Net Present Value (NPV), Pay – Back Period (PBP) or Levelized Cost of Energy (LCOE), will be used to determine if it is economically feasible to install offshore wind turbines in Portugal. They will be carried out considering several economic parameters such as Portuguese offshore tariff, investment and O&M costs, credit values, etc. Finally, three different discount rates have been considered into the analysis.

2. Development of the model

2.1. Economic development

The Levelized Cost of Energy (LCOE) evaluates the economic cost of power generation system throughout its life cycle [2]. There are several approaches to the LCOE definition [2–4], for the current work the process described in IEA (International Energy Agency) has been considered. It defines the costs as a summation of the total cost of the initial investment, annual operating and maintenance costs, annual fuel and carbon costs and the cost of decommissioning. This model does not take into account extremely volatile values, like interest rates and tax rates that differ from country to country and region to region. It is very useful to compare normalized costs of energy production from different sources, regardless of the floating parameters. Since a clean renewable energy source is being analysed, the parameters "fuel costs" and "cost of carbon" were considered to be zero. The "decommissioning cost" was also considered to be zero since the site is usually reused for a new project, taking advantage of the groundwork and construction already carried out.

The Net Present Value (NPV) is the net value of all revenues (cash inflows) and expenses (cash outflow) of the project, discounted to the beginning of the investment. Essentially, revenues include cash inflows from the sale of electricity and costs include cash outflows due to the financial costs and the operation and maintenance of the offshore wind farm. For energy projects, the NPV is considered the present value of benefits subtracted from the present value of the costs. The investment decision on the project occurs when the NPV is greater than zero. If it is equal to zero, it will be indifferent for investors implement monetary resource in the project. If the NPV is negative, then the investor must discard the project, because it will bring him losses. If the investor has to choose various types of project, it will tend to choose the project with the highest NPV, since this option will provide greater return on investment.

The Internal Rate of Return (IRR) is a measure of a project's magnitude in the financial markets evaluation scale. When the IRR is above the discount rate, the project generates a rate of return higher than the discount rate of capital, thus, in principle, the project will be economically viable. When the IRR obtained is below the discount rate, the return required by investors will not be achieved [4]. The IRR calculus is a polynomial equation of N degree, where there are N different roots or solutions to the equation. However, when the investment pattern is normal (i.e., the initial investment or outflows are

followed by a stream of inflows), all the solutions are negative or imaginary, except for one positive solution. Otherwise, if the cash flow is such that the outflows occur during or near the end of project's life, then the possibility to obtain multiple positive solutions is increased. Situations where there is only one an approximate value are easy to analyze. However, when the results do not contain an approximate value rather multiple positive solutions, it is a doubtful situation and the IRR analysis should be dismissed and other economic indicators should be used [2].

Finally, the Discounted Payback Period (*DPBP*) uses the cash flow of each year with the respective discount rate and adds it to all previous cash flows with the respective discount rate. The year when this sum is greater or equal than the initial investment will be the year of the payback.

2.2. Calculating with GIS

Model Builder™ of GIS software has been used to determine the best Portuguese areas for offshore wind power development [5].

Two different tools have been designed using GIS techniques: GIS tool 1 and GIS tool 2. GIS tool 1 calculates the area allowed and introduces the economic maps for one particular case with a number of wind turbines established. On the other hand, GIS tool 2 introduces restrictions of ports, shipyards and docks taking into consideration output of GIS tool 1.

Taking into account several spatial operations, GIS tool 1 allows establishing a map which considers the physical restrictions selected by the user. This tool will give a first approximation of the areas where offshore wind farms could be installed in Portugal, without considering economic aspects, which could be added after, as **Figure 1** shows:

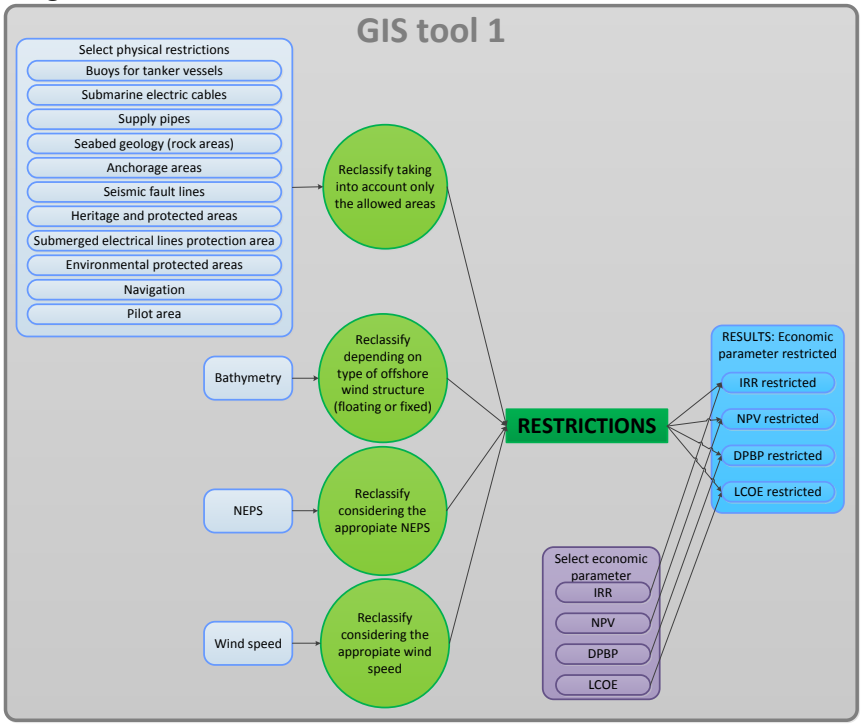

Figure 1: GIS tool 1.

Firstly, the map of all the physical restrictions will be obtained. Moreover, each of these restrictions should be reclassified. For this purpose, allowed areas will be defined as 1 and not allowed areas will be defined as 0. Therefore, all these physical restrictions reclassified should be sum up, obtaining the map of

all the physical restrictions.

Secondly, the bathymetry restriction should be added, which will be different depending on the type of offshore wind substructure (fixed or floating).

Furthermore, two physical parameters: NEPs and wind speed, will be used as part of the classification process. Their consideration is useful in terms of giving a no economic preview of the best areas in terms of offshore wind.

Finally, all the restrictions will be joined and multiplied by the economic map selected (IRR, NPV, DPBP or LCOE), obtaining the economic parameters restricted.

On the other hand, GIS tool 2 introduces restrictions of ports, shipyards and docks taking into consideration output of GIS tool 1. In this sense, the parameters which will be reclassified and the maximum distance from ports, shipyards and docks, should be defined by the user.

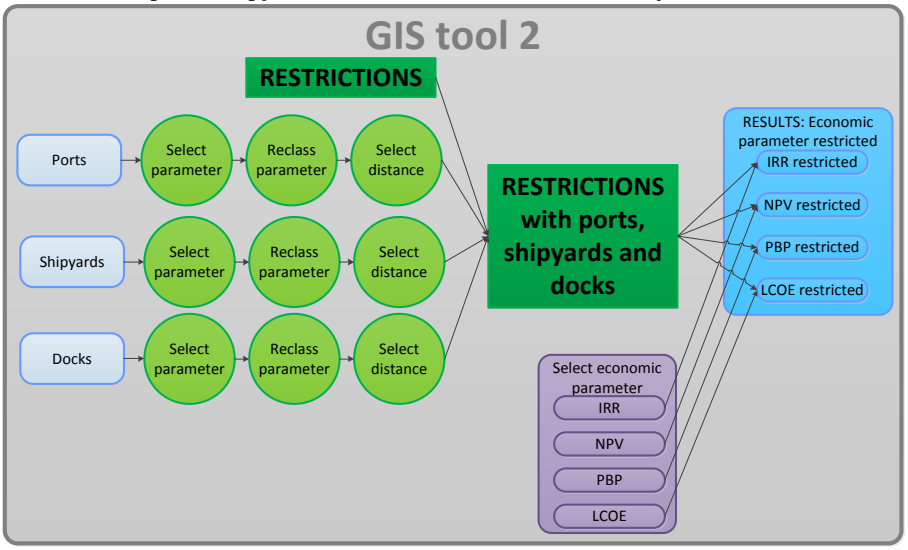

Figure 2: GIS tool 2.

3. Input data

3.1. Objectives

There are three different types of input data:

- **Physical restrictions**, which limit the strategic area using bathymetry, seabed geology, heritage protected areas and environmental conditions data.
- **Location settings**: they are related to technical infrastructure of ports, docks and shipyards.
- **Economic parameters**: they are used to map the economic results along the Portuguese coast, giving information about the feasibility of the area analysed.

3.2. Physical restrictions

Physical restrictions are defined as those that limit the strategic area taking into account geotechnical or legislative issues. Therefore, in these terms, the following physical restrictions will be defined [6] [7]: bathymetry, buoys for tanker vessels, submarine electric cables, supply lines, navigation areas, anchorage

areas, seismic fault lines, pilot area, submerged electrical lines protection area, environmental protected areas, heritage and protected areas, seabed geology (rock areas).

Otherwise, bathymetry restriction will be taken into consideration separately to the other physical restrictions because it can change when different wind substructures were considered: fixed or floating. In this sense, depths up to 40 m will involve fixed structures (monopiles, jackets, tripods and gravity foundation) [8] and depths from 40 to 200 m will be considered for floating platforms (TLP, semisubmersible, spar and barge).

Finally, two restrictions take into consideration wind resource: spatial distribution for the number of hours at full capacity production (NEPs) [9] [10] in each point of the Portuguese coast and wind speed (m/s).

3.3. Location settings

There are some factors that will not be included in GIS spatial operations, but which will also be taking into account:

- Proximity to shipyards with enough capacity to construct the platforms and with the appropriate docks.
- Proximity to ports which have surface to wind turbine storage and future maintenance.

All these factors can help us to establish a best strategy for the roadmap. In this sense, the main ports and shipyards in Portugal which can support offshore wind technology should be defined.

Firstly, shipyards location is one of the keys in designing a good strategy for the roadmap. They will be responsible for constructing floating or fixed substructures, so they should be placed close to the future offshore wind farms location. However, shipyards should have enough capacity to support these type of constructions.

On the other hand, ports also have importance for determining best area where establish offshore wind farms. Regarding installation, they should have surface enough to storage blades, gearboxes, nacelles and towers of the wind turbines. Furthermore, they should support offshore supply vessels for installation and maintenance (preventive and corrective).

3.4. Economic parameters

The economic parameters will be used as inputs to obtain economic maps with the mathematical program Matlab™. The most important ones are:

- Spatial distribution for the number of hours at full capacity production (NEPs) [9] [10] in each point of the Portuguese coast.
- Total power of the farm: 50 MW.
- Costs of installed system: 3315 €/kW per fixed turbine [11] and 16575 €/kW per floating turbine[b].
- O&M costs: 150 k€ per turbine per year or 21.43 €/kW/year for 7 MW wind turbine [11]
- Lifecycle: 20 years.
- Tax: 30%.
- Inflation: 2.35%/year.
- Discount rate: 5%, 7.5% and 10% (different scenarios)
- Fixed tariff: 168 €/MWh, as in WindFloat [12]
- Market tariff: 50.66 €/MWh
- Credit: 70% investment, 15 years, 5.4 % interest [13]

Taking into account all these previous parameters and the correspondent formulas [2] four economic maps have been developed along Portuguese coast: Internal Rate of Return (IRR), Net Present Value (NPV), Discounted Pay – Back Period (DPBP) and Levelized Cost of Energy (LCOE). Moreover, they

---

[b] The cost of the installed system for floating offshore wind has been considered as five times the cost of fixed offshore turbines.

will be developed for three different discount rates: 5% (scenario 1), 7.5% (scenario 2) and 10% (scenario 3).

4. Application and results

4.1. Allowed areas

GIS tool 2 will be required to define the allowed areas in terms of ports, shipyards and docks. Firstly, their main characteristic field should be defined. In this sense, the following parameters have been considered: 10 m of draft for ports, 15120 m^2 of area for shipyards and 120 m of length for docks.

Draft has been the parameter considerer to ports, considering the draft of the installation vessel, which could be between 3 – 8.9 m [14] [15] [16] depending on the type of ship (cargo barge, sheeleg crane, etc.). This value could be higher if a tug boat from port to wind farm was used to transport the floating platform, whose draft is, at least, 12.5 m [17]. However, the first approximation will be 10 m because in fixed offshore wind technology could not be transported using a tug boat.

Secondly, the buffers of each field are made considering 80 km of distance from ports and shipyards.

Characteristics of docks and shipyards are useful for floating platforms, which will be constructed on them. In this sense, the limits are established in relation to the dimensions of these platforms, which can vary from 12.5 m to 120 m, depending on the type of structure [18], so the maximum length considered will be 120 m and the maximum area for each platform 18x120 m^2. Moreover, the number of wind turbines considered (7) should be taken into account.

Therefore, shipyards which are suitable taking into account their area and length of dock are: Arsenal Alfeite, ENVC (Estaleiros Navais de Viana do Castelo) and Lisnave.

4.2. Economic results with restrictions for fixed offshore wind energy

If Internal Rate of Return (IRR) and the Discount Pay – Back Period (DPBP) for scenarios 1 and 2 with all the explained restrictions are analysed, the atlas of **Figure 3** will be as follows:

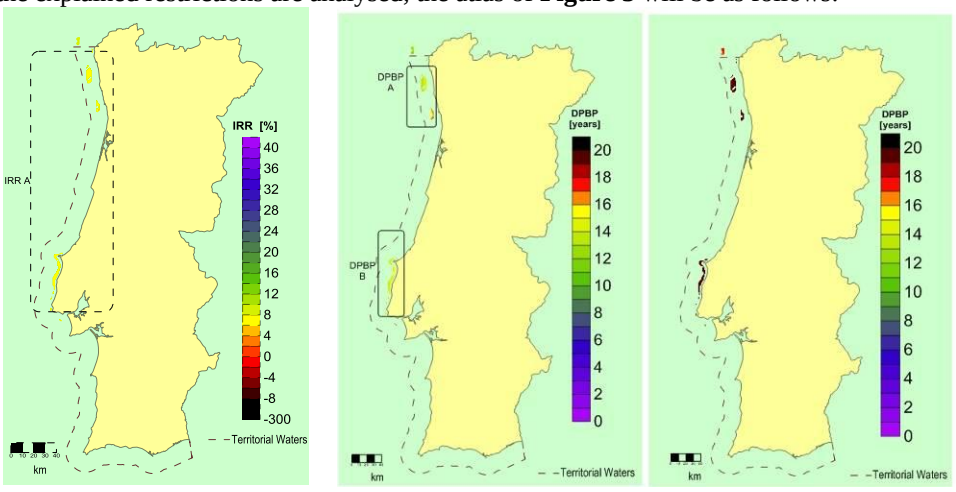

(a) (b) (c)

Figure 3: IRR (a) and DPBP with restrictions for discount rate of 5% (b) and 7.5% (c).

IRR does not depend on the discount rate considered. Therefore, there only is one scenario. **Figure 3** shows one area called as IRR A, which is characterized by Internal Rate of Return from 5.72% to 8.54%. It implies that depending on the discount rate considered, the project will or will not be viable. In fact, in terms of IRR, the project will only be economic viable for the 5% and 7.5% of discount rate scenarios.

Furthermore, **Figure 3** shows the DPBP for two scenarios: 1 and 2. Scenario 3 does not appear because

the unique areas where DPBP is different from the life cycle of the project are restricted areas (more than 40 m). Moreover, in scenario 1 there are two areas, one is next to Viana do Castelo (North), and identified as DPBP A, and the other one is close to Peniche (West), whose values go from 12.56 years to 17.43 years.

As far as LCOE maps with restrictions is concerning, a comparison between the three scenarios could be developed, as it is shown in **Figure 4**:

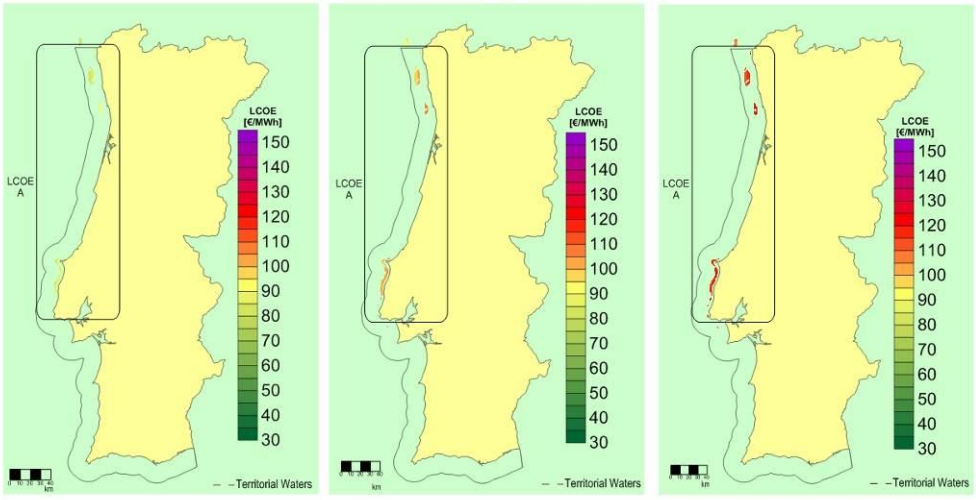

(a) (b) (c)

Figure 4: LCOE with restrictions for 5% (a), 7.5 % (b) and 10% (c) of discount rate respectively.

LCOE results are very different depending on the discount rate considered. However, one area in each map called LCOE A could be distinguished. It has values from 78.8 to 92.9 €/MWh, in the scenario 1, from 92.54 to 109.1 €/MWh in scenario 2 and from 106.95 to 126.09 €/MWh in the scenario 3.

Finally, **Figure 5** shows the results for Net Present Value (NPV) with restrictions:

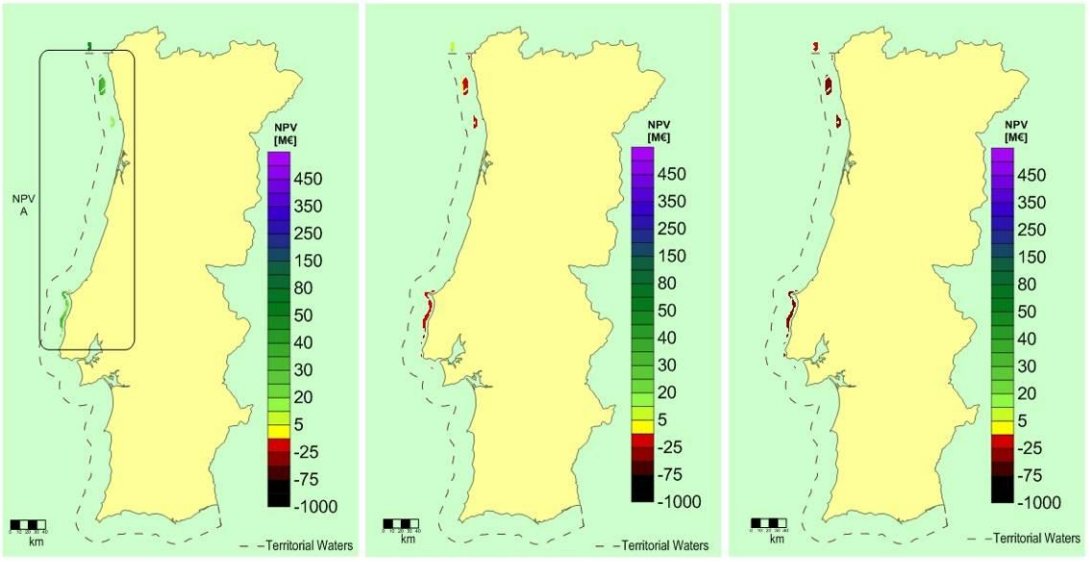

(a) (b) (c)

Figure 5: Net Present Value (NPV) with restrictions for 5% (a), 7.5 % (b) and 10% (c) of discount rate respectively.

Most of the NPV results, for all the scenarios considered, are negative, excepting region A for scenario 1, whose values go from 13 M€ to 36 M€.

4.3. Economic results with restrictions for floating offshore wind energy

In floating offshore wind farms LCOE will be the only economic parameter which will be evaluated. As in the fixed offshore case, a comparison between the three scenarios could be taken into account, as **Figure 6** shows:

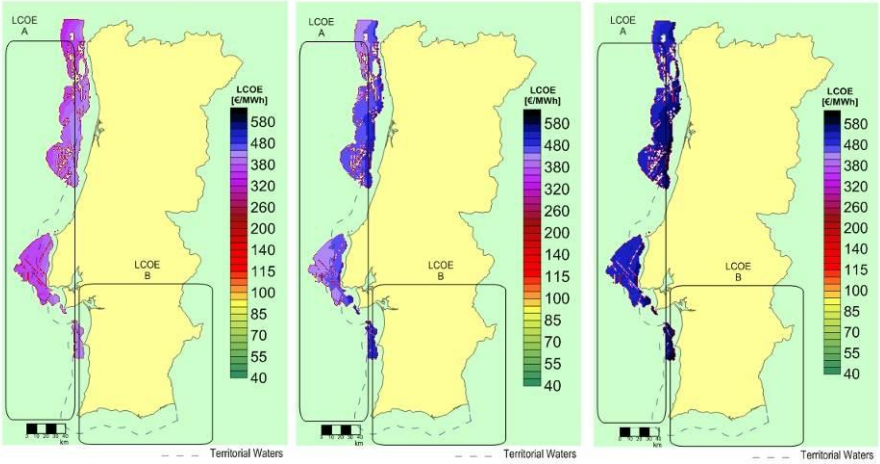

(a) (b) (c)

Figure 6: LCOE with restrictions for 5% (a), 7.5% (b) and 10% (c) of discount rate respectively.

Two areas can be distinguished: A and B. Area A has values from 300 to 435.86 €/MWh in scenario 1 (a), from 340 to 518.58 €/MWh in scenario 2 (b) and from 380 to 605.25 €/MWh in scenario 3 (c).

5. Conclusion

Values for Internal Rate of Return (IRR), Net Present Value (NPV), Discounted Pay – Back Period (DPBP) and Levelized Cost Of Energy (LCOE) have been analysed for each point of the Portuguese coast. Then, several types of physical restrictions, as bathymetry or protected areas, have been applied. This fact will reduce the region of study. In this context, one area has been obtained. It is called as A and it is located in the Centre - North of Portugal, where economic results have been much better than in other regions.

Moreover, three different discount rates (5%, 7.5% and 10%) have been taken into account, constructing a map for each of these scenarios. Regarding results, scenario 1 and scenario 2 will be the best ones. Moreover, economic indexes depend on two factors: the offshore wind device considered (fixed or floating) and the scenario analysed.

On the other hand, ports and shipyards which were well located in relation with the installation selected area have been considered.

Finally, after analysing each point of the Portuguese coast, a conclusion could be established: there are some areas in the Centre - North where offshore wind farms could be installed. It could be the beginning of a new technology market and a new economic feasible business to carry out in Portugal. The economic roadmap of offshore wind energy in Portugal gives feasible results for investors. In this sense, it could improve the regional development of other parallel industries as naval construction, research clusters, maintenance industries and wind turbine developers.

Acknowledgements

Work funded by FCT/MTCES (PIDDAC) and FEDER through project PTDC/SEN-ENR/105403/2008.

References

[1] International Energy Agency (IEA). Energy Technology Roadmaps a guide to development and implementation. 2010;1–30.

[2] Short W, Packey D, Holt T. A manual for the economic evaluation of energy efficiency and renewable energy technologies. 1995;1–120.

[3] International Energy Agency (IEA). Projected Costs of Generating Electricity 2010. International Energy Agency (IEA), editor. OECD Publishing 2010;1–218. Available from: http://www.oecd-ilibrary.org/energy/projected-costs-of-generating-electricity-2010_9789264084315-en

[4] Castro R. Uma Introdução às Energias Renováveis: Eólica, Fotovoltaica e Mini-Hídrica. IST Press, editor. Portugal; 2011.

[5] ESRI. Introduction to ArcGIS Desktop for Mining Geoscience. 2009;1–318.

[6] Fernandes M, Costa P, Estanqueiro A. Portugal, Report on the national MSP regimes and their performance. Lisbon (Portugal); 2011;1–17.

[7] Instituto da Conservação da Natureza e Biodiversidade. Web Page Instituto da Conservação da Natureza e Biodiversidade. 2012. Available from: http://www.icnf.pt/cn/ICNPortal/vPT2007/

[8] Robinson M, Musial W. Offshore Wind Technology Overview. 2006.

[9] Costa P, Simões T, Estanqueiro A. Assessment of the Sustainable Offshore Wind Potential in Portugal. European Wind Energy Conference (EWEC) 2006;1–8.

[10] Costa P, Miranda P, Estanqueiro A. Development and validation of the Portuguese wind atlas. EWEL 2006 - European Wind Energy Conference. Athens, Greece, 2006;1–9.

[11] Garrad Hassan G. Analysis on the furthering of competition in relation to the establishment of large offshore wind farms in Denmark. 2011;1–58.

[12] Ministério da Economia e da Inovação. Decree-Law n.o 225/2007 31st May. 2007;3630–8.

[13] Pordata. Web page Pordata. 2012. Available from: http://www.pordata.pt/

[14] GAC. Web Page GAC. 2012. Available from: http://www.gac.com/gac/service.aspx?id=56402

[15] Sea Trucks Group. Web page Sea Trucks Group. 2012. Available from: http://www.seatrucksgroup.com/l/library/download/9660

[16] Wayman E, Sclavounos PD, Butterfield S, Jonkman J, Musial W. Coupled Dynamic Modeling of Floating Wind Turbine Systems. Proceedings of Offshore Technology Conference. Houston, Texas (USA): The Offshore Technology Conference 2006;1–25.

[17] ECN, MARIN, Windmaster L the, TNO, TUD, MSC. Study to feasibility of boundary conditions for floating offshore wind turbines. 2002;1-241.

[18] Jonkman J, Matha D. A Quantitative Comparison of the Responses of Three Floating Platforms. European Offshore Wind 2009 Conference and Exhibition. Stockholm (Sweden) 2009;1–21.

Methodology to study the life cycle cost of floating offshore wind farms

Laura Castro – Santos[a b], Geuffer Prado García[b], Vicente Diaz-Casas[a]

e – mail: laura.castro.santos@udc.es

[a] Integrated Group for Engineering Research (GII), Naval and Oceanic Engineering Department, University of A Coruña
Edificio de Talleres, C/ Mendizábal, 15403, Ferrol, A Coruña (Spain)

[b] National Energy Laboratory (LNEG), Solar, Wind and Ocean Energy Unit (UESEO), Estrada do Paço do Lumiar, 22, 1649-038, Lisbon, Portugal

Abstract. The main objective of this paper is to determine a theoretical methodology process to study the life cycle cost of floating offshore wind farms. The principal purpose is adapting the LCC (Life-Cycle Cost Calculation) from several authors to the offshore wind energy world. In this sense, several general steps will be defined: life cycle definition, process breakdown structures, viability study and sensitivity study. Moreover, technical and economic issues and their relations will be considered. On the other hand, six life cycle phases needed to install a floating offshore wind farm will be defined: design and development, manufacturing, installation, exploitation and dismantling. They will be useful to define the majority of the steps in the process. This methodology could be considered in future works to calculate the real cost of constructing floating offshore wind farms.

METHODOLOGY

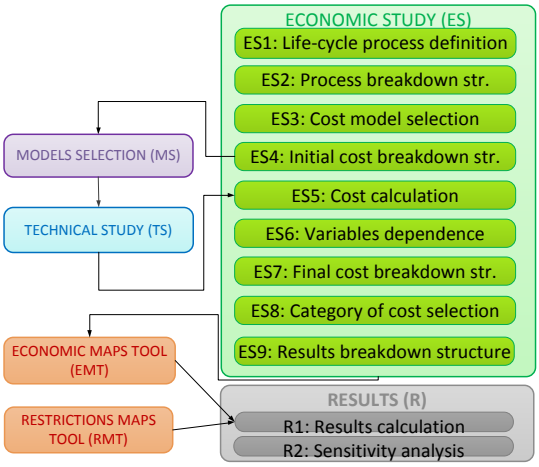

- **Economic study (ES)**: it is of utter importance in the methodology because it helps to define each of the costs involved the development of floating offshore wind farms. In fact, this article will only develop the ES step.
- **Life-cycle process definition (ES1)**: Life-cycle process has been defined modifying the recommendations of IEC 60300-3-3:2004 because this normative is focused more in a product than in a process. Therefore, the main phases of the life-cycle of a floating offshore wind farm are 6.
- **Process breakdown structure (ES2)**: it determines which are the main stages and sub-stages of the process.
- **Cost model selection (ES3)**: IEC 60300-3-3:2004 proposes several models to calculate the life-cycle cost. However, the present study will only take into account the model based on the life-cycle phases.
- **Initial cost breakdown structure (CBS) (ES4) and cost calculation (ES5)**: they are based on the disaggregation of the main costs of life-cycle: C1, C2, C3, C4, C5 and C6.

CASE OF STUDY

- Floating offshore semisubmersible platform.
- No cohesive soil.
- There is no accommodation platform.
- Synthetic fiber is the mooring material.
- Plate anchor.
- HVDC Electrical chain configuration.
- Wind turbine tower will be assembled onshore.
- Dismantling considered will be "tree falls".
- Preventive maintenance carry out with a helicopter.
- Mooring and anchoring installation are developed with an Anchor Handling Vehicle (AHV).
- Substation installation is developed with a cargo barge and a heavy lift vessel.
- Floating platform will be installed taking into account a tug boat, because draft of semisubmersible platform considered is less than shipyard draft.
- Floating offshore substation.
- Port and shipyard located in Ferrol, A Coruña (North West of Spain), close to an area of good offshore wind resource.

RESULTS

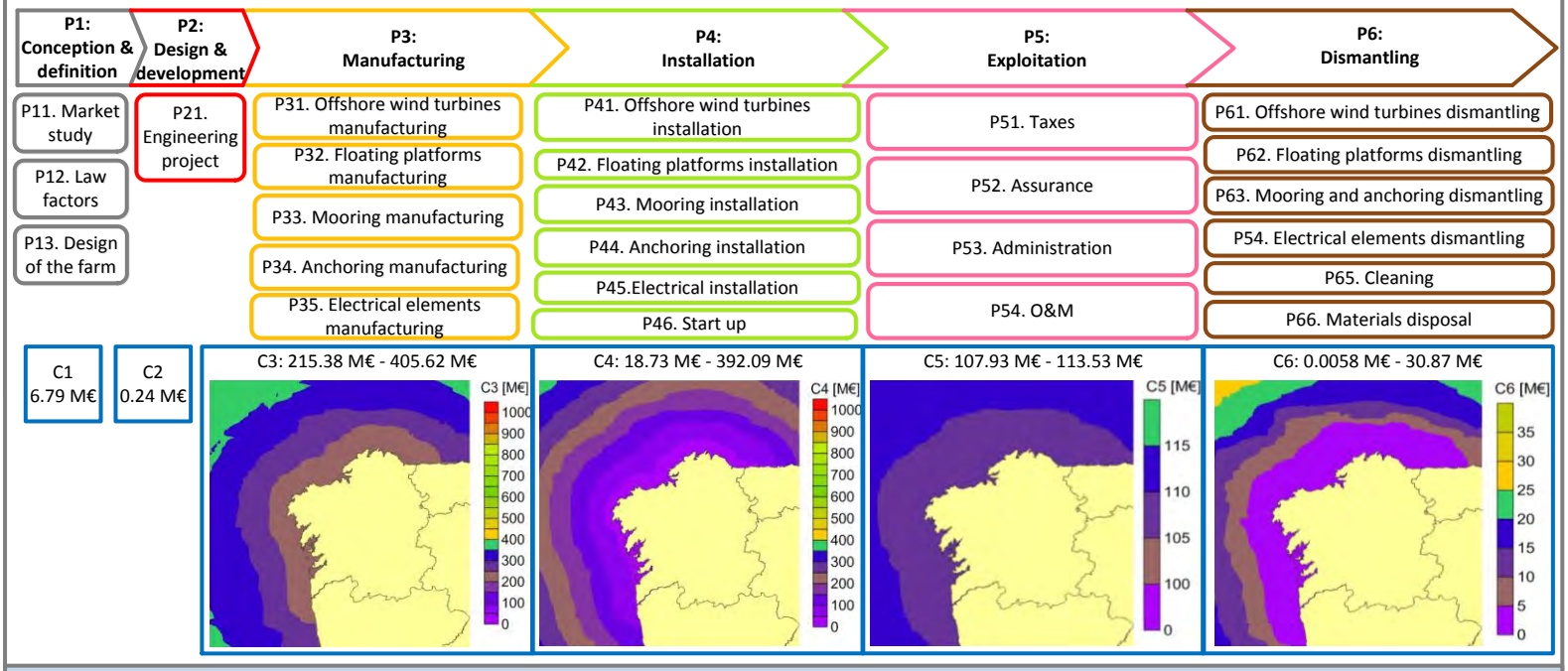

$$LCS_{FOWF} = C1+C2+C3+C4+C5+C6$$

CONCLUSIONS

Main dependences

- **Wind Turbines**: number, power, cost per MW, mass, diameter.
- **Floating platforms**: mass, cost in shipyard (steel, direct labor, direct materials, no direct activities (management, amortization of the machines, etc.).
- **Climate**: height and period of waves, wind speed at anemometer height, wind parameters (shape and scale).
- **Location**: depth, distances (to shore, to port, to shipyard).
- **Anchoring and mooring**: weight, cost per kilogram, number of mooring lines.
- **Electrical systems**: cost per section of electrical cable, number of electrical cables, grid and cable voltages.
- **Installation**: number, speed and fleet of vessels used in installation phase.
- **O&M**: failure probability.

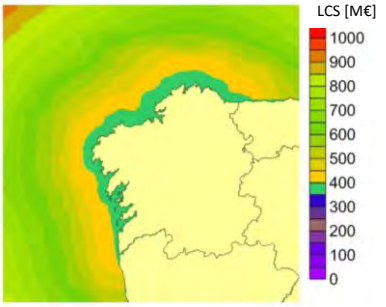

LCS_{FOWF}
365.50 M€ - 945.62 M€

- Methodology LCS_{FOWF} has been established.
- Development of the Economical Study
- Phases Economical Study
- Definition of the life-cycle phases
- Most important costs: manufacturing and installation
- Calculation of the costs for an specific location

References:

- Fabrycky WJ, Blanchard BS. Life-cycle Cost and Economic Analysis. Prentice Hall; 1991.
- Castro-Santos L, Ferreño González S, Martínez López A, Diaz-Casas V. Design parameters independent on the type of platform in floating offshore wind farms. RE&PQJ 2012;10:1-5.

Available online at www.sciencedirect.com

ScienceDirect

Energy Procedia 00 (2013) 000–000

Energy Procedia

www.elsevier.com/locate/procedia

DeepWind'2013, 24-25 January, Trondheim, Norway

Methodology to study the life cycle cost of floating offshore wind farms

Laura Castro-Santos[a b*], Geuffer Prado García[a], Vicente Diaz-Casas[b]

[a]*National Energy Laboratory (LNEG), Solar, Wind and Ocean Energy Unit (UESEO), Estrada do Paço do Lumiar, 22, 1649-038, Lisbon, Portugal*

[b]*Integrated Group for Engineering Research, Naval and Oceanic Engineering Department, University of A Coruña, Edificio de Talleres (Campus Esteiro), C/ Mendizábal, s/n, 15403, Ferrol, A Coruña, Spain*

Abstract

The main objective of this paper is to determine a theoretical methodology process to study the life cycle cost of floating offshore wind farms. The principal purpose is adapting the LCC (Life-Cycle Cost Calculation) from several authors to the offshore wind energy world, providing a new method which will be called LCS_{FOWF}. In this sense, several general steps will be defined: life cycle definition, process breakdown structure, viability study and sensitivity study. Moreover, technical and economic issues and their relations will be considered. On the other hand, six life cycle phases needed to install a floating offshore wind farm will be defined: conception and definition, design and development, manufacturing, installation, exploitation and dismantling. They will be useful to define the majority of the steps in the process. This methodology could be considered to calculate the real cost of constructing floating offshore wind farms.

Keywords: Life Cycle; Wind Turbine ; Economical Evaluation

1. Introduction

Due to fossil fuels have a limited life span [1] [2], the use of renewable energies, whose use is unlimited, will be of utter importance. Furthermore, the European goals for promoting the renewable energy sector have been established in 2009. In fact the 20% of final energy consumption should be from this type of energies in 2020 [3].

In this context, ocean energy could help to achieve this objective. In particular, floating offshore wind energy could be developed taking into account some traditional industries, as naval or industrial sectors.

However, this development will not be carried out without a preliminary study of the main costs which

* Corresponding author. Tel.: +34 981337400 ext. 3890;
E-mail address: laura.castro.santos@udc.es.

this type of farms involves.

The main objective of this paper is defining a methodology to study the Life-Cycle Cost System of Floating Offshore Wind Farm (LCS_{FOWF}). However, life cycle cost will not be understood as the cost of environmental issues [4] and emissions [5], as in other publications [6]. LCS_{FOWF} will be considered as the cost necessary to deal with each of the phases of the life cycle.

Firstly, a general methodology with several steps will be put forward. However, only the Economic Study will be considered in this paper. Several of the most important phases of which it is composed are: the life-cycle definition, the process breakdown structure, the cost model selection, the initial cost breakdown structure and the cost calculation.

This methodology will be applied to the particular case of Galicia (North-West of Spain), where wind resource has good values in deep waters.

Nomenclature

C1	Cost of conception and definition
C2	Cost of design and development
C3	Cost of manufacturing
C4	Cost of installation
C5	Cost of exploitation
C6	Cost of dismantling

2. Methodology

2.1. General structure

Methodology put forward for calculating the costs of a floating offshore wind farm is based on two different methods of life-cycle cost calculation [7] [8]. This new methodology will be named as Life-Cycle Cost System of a Floating Offshore Wind Farm, LCS_{FOWF}, and it will be developed in several steps:

- Economic Study (ES).
- Models Selection (MS).
- Technical Study (TS).
- Economic Maps Tool (EMT).
- Restrictions Maps Tool (RMT).
- Results (R).

MS will define each of the models which will be taken into consideration in the study according to offshore wind turbines, floating offshore wind platforms, mooring lines, anchors, electric system, installation, accommodation, maintenance, seabed and dismantling. These aspects will be explained in future works.

TS consists in all the engineering calculation related to electrical cables, mooring and anchoring dimensions and feasibility of mooring lines.

EMT will implement the ES using numeric calculation, which will originate the maps of the economic indexes and the maps of the different types of models taking into account the main characteristics of the location.

Results obtained from EMT will be processed with the RMT, which has been developed using a GIS (Geographic Information System) software whose results are the allowed areas considering the geographical restrictions of the site.

Consequently, not only EMT results but also RMT results will be used to determine the R for a particular geographic case.

A detailed description of the model has been presented in [9]. A general scheme could be seen in Figure 1:

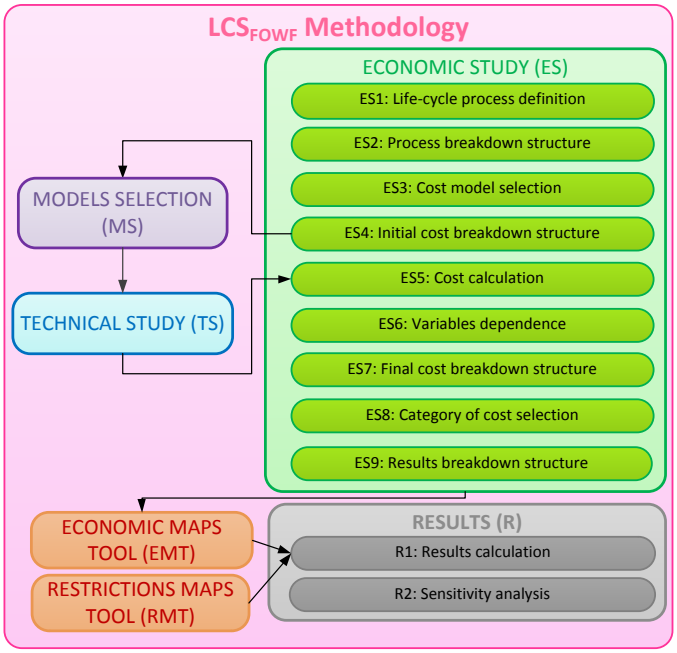

Figure 1: General methodology.

However, this preliminary study will only take into consideration the first four parts of the ES. Thus, maps with restrictions and sensitivity analysis will not be developed.

2.2. Economic Study

The ES is of utter importance in the methodology because it helps to define each of the costs involved in the development of floating offshore wind farms. In this sense, ES bears in mind the following phases:

- Phase ES1: life-cycle process definition.
- Phase ES2: process breakdown structure.
- Phase ES3: cost model selection.
- Phase ES4: initial cost breakdown structure.
- Phase ES5: cost calculation.
- Phase ES6: variables dependence.
- Phase ES7: final cost breakdown structure.
- Phase ES8: category of cost selection.
- Phase ES9: results breakdown structure.

However, this paper will be explained the first four phases because the others will be explained more in detail in the future.

2.3. Life-cycle process definition

Life-cycle process has been defined modifying the recommendations of IEC 60300-3-3:2004 [7] because this normative is focused more in a product than in a process. Therefore, the main phases of the life-cycle of a floating offshore wind farm are:

- Phase 1: Conception and definition.
- Phase 2: Design and development.
- Phase 3: Manufacturing.
- Phase 4: Installation.
- Phase 5: Exploitation.
- Phase 6: Dismantling.

All of them could be represented as Figure 2 shows:

Figure 2: Life-cycle of a floating offshore wind farm.

2.4. Process breakdown structure

Process breakdown structure determines which are the main stages and sub-stages of the process. A floating offshore wind farm will be composed by several main components: offshore wind turbines, floating offshore platforms, moorings, anchorages and electrical elements. Thus, each of the phases of the life-cycle process definition will be developed for each of these elements, as Figure 3 shows:

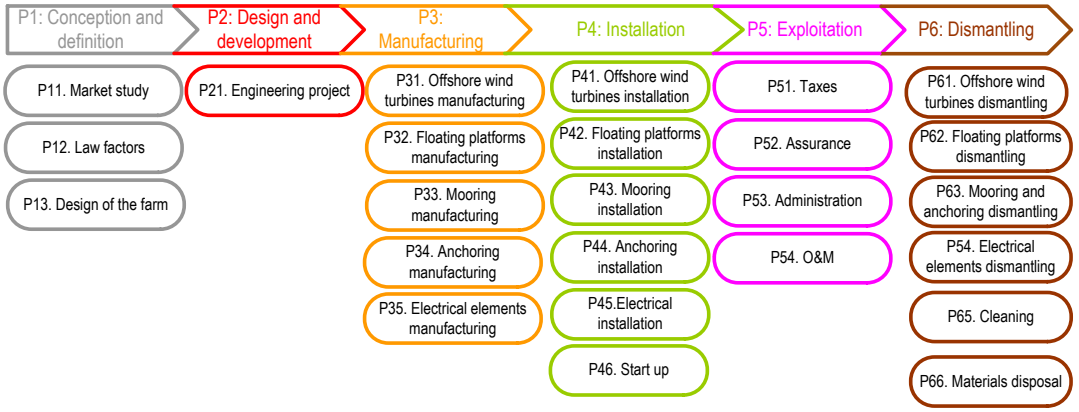

Figure 3: Breakdown structure of a floating offshore wind farm.

2.5. Cost model selection

IEC 60300-3-3:2004 [7] proposes several models to calculate the life-cycle cost. However, the present study will only take into account the model based on the life-cycle phases.

2.6. Initial cost breakdown structure and cost calculation

Initial Cost Breakdown Structure (CBS) of a floating offshore wind farm is based on the disaggregation of the main costs of life-cycle. In this sense, the costs will be: C1 is the cost of conception and definition, C2 is the cost of design and development, C3 is the cost of manufacturing, C4 is the cost of installation, C5 is the cost of exploitation and C6 is the cost of dismantling.

Thus, the LCS_{FOWF} could be formulated as:

$$LCS_{FOWF} = C1 + C2 + C3 + C4 + C5 + C6$$

However, in order to obtain their main dependences, each of these costs should be subdivided in sub-costs dependent that should be analyzed separately. This subdivision is too complex to be analyzed in the present study so it will be explained in a future paper, where phases from E55 to E59 will be described. Nevertheless, in order to give a notion of the main dependences in costs, the following parameters could be considered:

- Number of wind turbines.
- Power of wind turbines.
- Cost (in €) per MW of wind turbine.
- Mass of the floating platform.
- Mass of the wind turbine.
- Cost of steel necessary to build the floating platforms at shipyard.
- Cost of direct labor at shipyard.
- Cost of direct materials at shipyard.
- Cost of no direct activities (management, office materials, amortization of the machines, etc.) at shipyard.
- Height and period of waves.
- Wind speed at anemometer height.
- Wind shape and wind scale parameters.
- Depth.
- Weight of anchoring and mooring.
- Anchoring and mooring cost per kilogram.
- Number of mooring lines.
- Cost per section of electrical cables.
- Number of electrical cables.
- Wind turbine diameter.
- Distance to shore.
- Grid and cable voltages.
- Distance to port.
- Distance to shipyard.
- Number, speed and fleet of vessels used in installation phase.
- Failure probability.

3. Case of study

The models considered for developing this paper have been:

- Floating offshore semisubmersible platform.
- No cohesive soil.
- There is no accommodation platform.
- Synthetic fiber is the mooring material.
- Plate anchor.
- HVDC Electrical chain configuration.
- Wind turbine tower will be assembled onshore.
- Dismantling considered will be “tree falls”.
- Preventive maintenance will be carried out with a helicopter.
- Mooring and anchoring installation are developed with an Anchor Handling Vehicle (AHV).
- Substation installation is developed with a cargo barge and a heavy lift vessel.
- Floating platform will be installed taking into account a tug boat, because draft of semisubmersible platform considered is less than shipyard draft.
- Floating offshore substation.

Moreover, a port and a shipyard (Navantia) located in Ferrol, A Coruña (North West of Spain), closest to

a very good area of wind resource in deep waters, have been considered.

4. Results

Firstly, C1 and C2 will be constant and independent on the location considered. Thus, their atlas cannot be defined. Their values are 6.79 M€ and 0.24 M€ respectively.

However, C3, C4, C5 and C6 will basically be dependent on the distance to shore and the depth of the location. Therefore, they can be calculated for each point of the geography considered (coast of Galicia), giving the correspondent map for each cost.

C3 values range from 215.38 M€ for the closest areas to the Galician shore to 405.62 M€ for the most remote areas. Furthermore, C4 values range from 18.73 M€ to 392.09 M€. As it is shown in Figure 4, the cost of installation grows in a different way of manufacturing, whose increases depth by depth are lower.

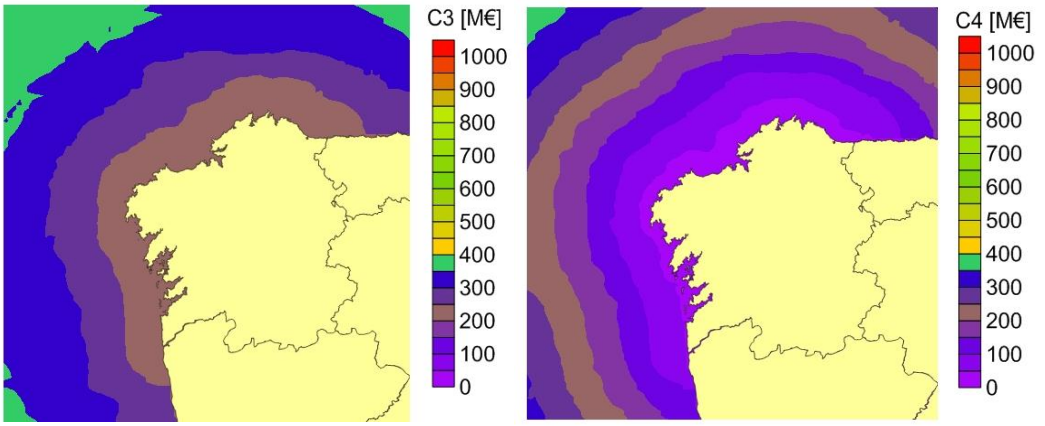

Figure 4: Values for C3 and C4.

Secondly, C5 values from 107.93 M€ to 113.53 M€ and C6 values from 0.0058 M€ to 30.87 M€, as Figure 5 shows. The value of exploitation basically is composed by the cost of operation and maintenance and it does not change a lot with the number of trips of the maintenance vessels, as it was expected. In fact, it oscillates between 105 M€ and 115 M€ depending on the location of the farm: nearshore or farshore respectively.

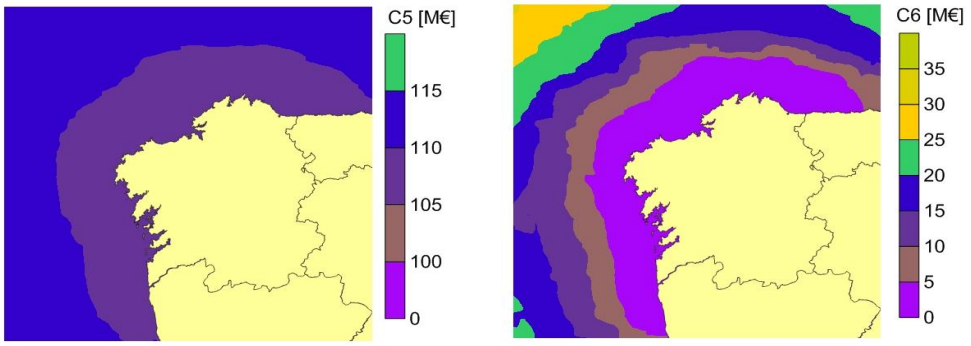

Figure 5: Values for C5 and C6.

Finally, the total cost value from 365.50 M€ and 945.62 M€, as Figure 6 shows:

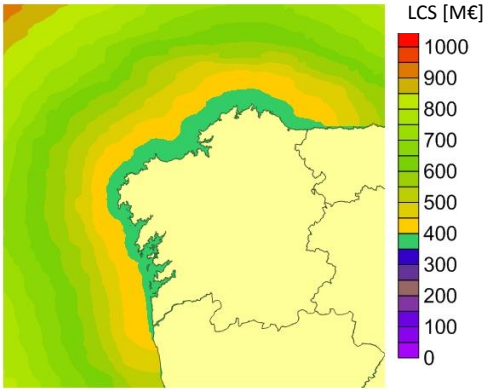

Figure 6: Values for the total cost.

5. Conclusions

The methodology of Life-Cycle Cost System of a Floating Offshore Wind Farm (LCS_{FOWF}), which is based on the study of the costs of each of the phases of the life-cycle, has been proposed. It is composed by five steps: Economic Study, Models Selection, Technical Study, Economic Maps Tool, Restrictions Maps Tool and Results. However, only the Economic Study has been developed in the present paper.

EE is composed by nine phases which will help to carry out the cost of each phase of the life-cycle of a floating offshore wind farm. The life-cycle phases considered are: conception and definition, design and development, manufacturing, installation, exploitation and dismantling.

Results show how one of the main dependences on costs are the distance to shore and the depth of where the farm will be installed. Furthermore, manufacturing cost and installation cost absorb the maximum percentage of the total costs, directly followed by maintenance.

Finally, they give an approximation to the real costs in this type of constructions. This first step could be used to calculate the economic viability of a floating offshore wind farm in the future.

References

[1] Fernandez L. A diversified portfolio: joint management of non-renewable and renewable resources offshore. Resour Energy Econ 2005;27(1):65–82.

[2] Considine TJ, Heo E. Price and inventory dynamics in petroleum product markets. Energ Econ 2000;22(5):527–48.

[3] Official Journal of the European Union. Directive 2009/28/EC of the European Parliament and of the Council of 23 April 2009 on the promotion of the use of energy from renewable sources and amending and subsequently repealing Directives 2001/77/EC and 2003/30/EC. 2009 page 16–60.

[4] Pehnt M. Dynamic life cycle assessment (LCA) of renewable energy technologies. Renew Energ 2006;31:55–71.

[5] Weule H. Life-cycle analysis - A strategic element for future products and manufacturing technologies. CIRP Annals - Manufacturing Technology. 1993;42(1):181 – 184.

[6] Benda J, Narayan R, Sticklen J. Use of expert systems for life cycle analysis. SAE SPEC PUBL1993;1–6.

[7] European Committee for Electrotechnical Standardization. IEC 60300-3-3:2004. Dependability management. Part 3-3: Application guide. Life cycle costing. 2009;1–70.

[8] Fabrycky WJ, Blanchard BS. Life-cycle Cost and Economic Analysis. Prentice Hall; 1991.

[9] Castro-Santos L, Ferreño González S, Martínez López A, Diaz-Casas V. Design parameters independent on the type of platform in floating offshore wind farms. RE&PQJ 2012;10:1–5.

Two-dimensional fluid-structure interaction simulation of NACA0012 airfoil

Knut Nordanger, PhD Candidate, Dept. of Mathematical Sciences, NTNU
Trond Kvamsdal, NTNU and Runar Holdahl, SINTEF ICT

Problem description

Flow past an oscillating NACA0012 airfoil is simulated using the incompressible Navier-Stokes equations in ALE (Arbitrary Lagrangian-Eulerian) formulation. Structural movements are calculated using a traditional Newmark scheme.

Simulations for Reynolds number 20,000 are carried out, and the Spalart-Allmars turbulence model is employed.

The main quantities of interest in this study are the drag and lift coefficients.

Aims

- demonstate the capability of the SINTEF ICT-developed isogeometric solver IFEM to simulate flow past an oscillating object
- simulate realistic airfoil shapes
- combine mesh movement and turbulence model

Isogeometric analysis [1]

- the same set of basis functions (B-splines or NURBS) is used for both the geometry representation and the analysis

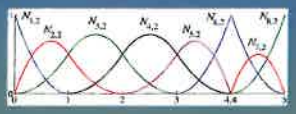

- intended to bridge the gap between design and analysis
- exactly the same geometry is used in the analysis as in the design (no approximations)
- yields higher accuracy per degree of freedom than traditional finite elements
- based on technologies from computational geometry
- allows for smooth curves and surfaces

Geometry definition

IFEM offers
- **multi-patch/block-structured meshes**
- **parallelization on patch level**

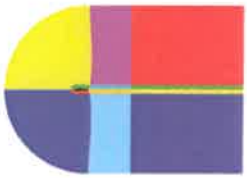

$y^+ = 1$

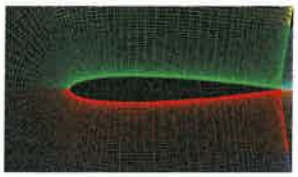

Mesh movement

Arbitrary Langrangian-Eulerian forulation

$$\rho \left.\frac{\partial u}{\partial t}\right|_{\hat{x}} + \rho(u - \hat{u}) \cdot \nabla u - \nabla \cdot \sigma(u, p) = \rho f \quad \text{in } \Omega_F(t)$$

$$\nabla \cdot u = 0 \quad \text{in } \Omega_F(t)$$

Interface condition $u = u^I(t)$ on Γ_I

Mesh update based on non-linear finite deformation analysis

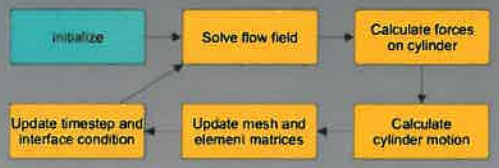

Fluid flow

Incompressible Navier-Stokes equations

$$\frac{\partial u}{\partial t} + \rho(u \cdot \nabla)u - \nabla \cdot \sigma(u, p) = \rho f \quad \text{in } \Omega$$

$$\nabla \cdot u = 0 \quad \text{in } \Omega$$

Chorin projection scheme
- **equal order approximation for velocity and pressure**
- **CG and GMRES for solving the linear systems**

Spalart-Allmaras turbulence model
- **one-equation**
- **solves a transport equation for the kinematic turbulent viscosity**

Oscillator

MCK-oscillator

$$\underline{M}\ddot{x} + \underline{C}\dot{x} + \underline{K}x = F(v_F)$$

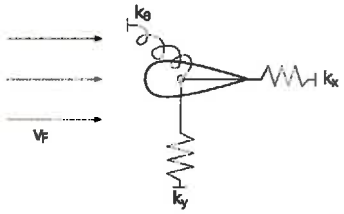

Results

Forced oscillations
- Re=20,000
- angle of attack: 0 degrees
- pitching motion h=0.0125 and h=0.025
- reduced frequency k=3.93

h=0.0125	mean CL	stdv CL	mean CD	stdv CD
Lian & Shyy (k-ω) [2]	0.01768	0.75016	0.02338	0.00396
Medjroubi (DNS) [3]	0.0098	0.7959	0.023	0.00436
IFEM (SA, Δt=0.001)	0.0000080	0.80469	0.05247	0.00426
IFEM (DNS, Δt=0.001)	0.04419	0.80679	0.02442	0.00466
h=0.025	**mean CL**	**stdv CL**	**mean CD**	**stdv CD**
Lian & Shyy (k-ω) [2]	0.0521	1.6229	0.00803	0.01624
Medjroubi (DNS) [3]	0.04572	1.5628	0.00634	0.0186
IFEM (SA, Δt=0.001)	0.0000194	1.63232	0.02231	0.01719
IFEM (DNS, Δt=0.001)	0.09434	1.69883	0.00652	0.01916

Further work

- freely oscillating airfoil shapes (e.g. NACA0012 and NOWITECH reference turbine)
- structural analysis of airfoils in flow
- coupling procedures
- 3D simulations
- aerodynamic flutter

SINTEF

NTNU – Trondheim Norwegian University of Science and Technology

References

[1] Cottrell, J. A., Hughes, T. J. and Bazilevs, Y. Isogeometric analysis: toward integration of CAD and FEA (2009), Wiley.

[2] Lian, Y. and Shyy, W. Aerodynamics of low Reynolds number plunging airfoil under gusty environment. Collection of Techical Papers - 45th AIAA Aerospace Sciences meeting (2007), 767-786.

[3] Medjroubi, W. Numerical Simulation of Dynamic Stall for Heaving Airfoil Using Adaptive Mesh Techniques. PhD thesis, Carl von Ossietzky Univeritat Oldenburg (2011)

NOWITECH Norwegian Research Centre for Offshore Wind Technology

Experimental investigation of wind turbine wakes in the wind tunnel

Heiner Schümann*, Fabio Pierella*, Lars Sætran*

*Norwegian University of Science and Technology, N-7491, Trondheim, Norway

Introduction

Wind turbines operating in the wake of an upstream turbine are exposed to conditions which are significantly different from a free standing turbine. The incoming flow field is characterized by a non-uniform velocity profile and turbulence intensities significantly higher than in the free stream. This leads to reduced power production and increased fatigue of the downstream turbine.

Detailed wake measurements under controlled conditions are indispensable for a better understanding of wake aerodynamics, in particular **wind farms**, and as **benchmark** and development basis for the further improvement of **CFD** models.

Objectives

- Provide and compare highly detailed wake measurements for the two cases :
  - a) unobstructed wind turbine, T1
  - b) wind turbine operating in the wake of an upstream turbine, T2
- Investigate wake asymmetries observed in previous measurements and evaluate the influence of the tower

Experimental Setup

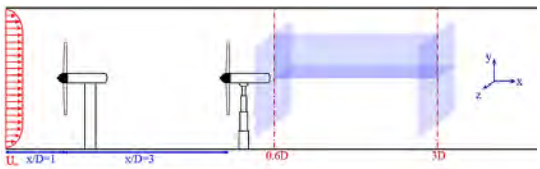

Figure 1: Tandem setup, blue areas show the measurement planes.

- Closed loop wind tunnel with closed test section (1.9m x 2.7m x 11m)
- Five-hole probe measurements (3-dim. Velocity profile)
- Hot-wire anemometry (turbulence intensity)
- Large, fully operational model turbines (D=0.9m)

Figure 2: Tandem Setup in the wind tunnel.

Operational conditions

- U_∞ = 10.5m/s
- Reynolds number based on the tip speed and the chord length, Re = 1.2 * 10^5
- $TSR_{First/Single\ turbine}$ = 6, $TSR_{Second\ turbine}$ = 4

Results

Velocity measurements

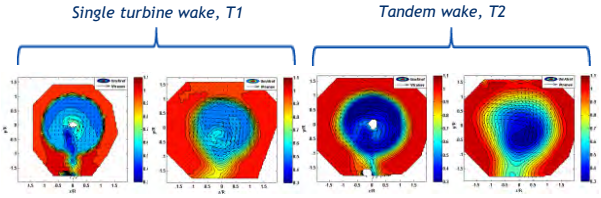

Figure 3: Normalized velocity U_m/U_∞, arrows show the transversal velocity intensity and direction, from left: T1 at x/D=0.6; T1 at x/D=3; T2 at x/D=0.6; T2 at x/D=3

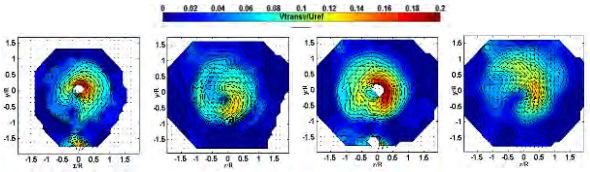

Figure 4: Normalized velocity in the cross sectional plane normal to the x-axis , from left: T1 at x/D=0.6; T1 at x/D=3; T2 at x/D=0.6; T2 at x/D=3

Turbulence measurements

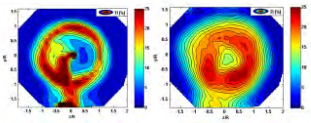

Figure 5: Turbulence intensity u'/U_m [%] , left: T2 at x/D=0.6; right: T2 at x/D=3

Wake expansion and recovery

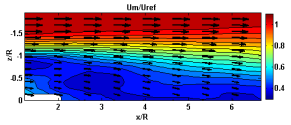

Figure 6: Normalized velocity in the x-z plane behind T2, left of the rotor axis (seen from top)

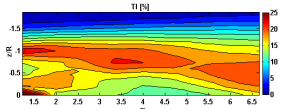

Figure 7: Turbulence intensity u'/U_m [%] in the x-z plane behind T2, left of the rotor axis (seen from top)

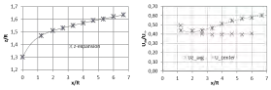

Figure 8: Wake expansion (left) and wake recovery (right) in z-direction for T2

Conclusion

- Overall wake structure, expansion and recovery as predicted by wake theory.
- Clearly observable tower wake characterized by the highest velocity deficit and turbulence intensity.
- Tower wake deflected in the direction of the wake rotation (opposite to the rotation of the rotor).
- Faster wake recovery due to the enhanced turbulence intensity by the deflected tower wake in the left part of the wake.
- Persistent asymmetries in the far-wake.

Numerical Study on the Motions of the VertiWind Floating Offshore Wind Turbine

Raffaello Antonutti – IDCORE research engineer @ EDF R&D *

Christophe Peyrard – EDF R&D #

EDF R&D LNHE – Chatou (France)

Project VertiWind

A floating offshore wind demonstrator project. One 2 MW rated unit is to be installed off Côte d'Azur, in France.

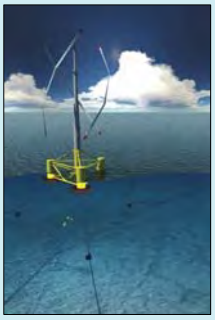

Technology developers

Nénuphar: Vertical Axis Wind Turbine design.
Technip: Floater, mooring, and installation design.

Project partners

EDF EN, Seal Engineering, Bureau Veritas, Oceanide, IFP EN, Arts & Métiers, USTV.

Governmental funding

ADEME - Agence De l'Environnement et de la Maîtrise de l'Energie.

Pseudo-quadratic viscous damping

Express the viscous damping coefficient as a linear function of motion amplitude. Iterative implementation.

A nonlinearity is introduced in the linear Equations of Motion. Dynamic response is hence linearised about each solution.

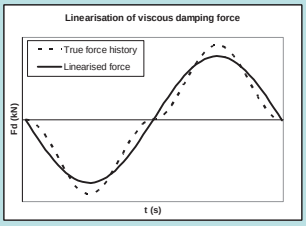

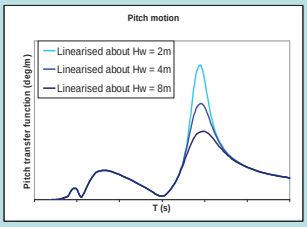

Dynamic response analysis with wind-induced trim

Static equilibrium trim angle under 50-yr return, 1-minute averaged wind speed = 12°.

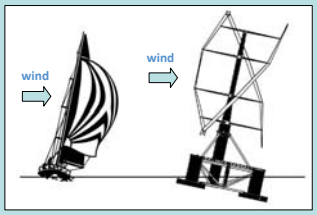

Calculate hydrodynamic loads and coefficients for new hull (linear potential BEM: *AQUA+*[1]).

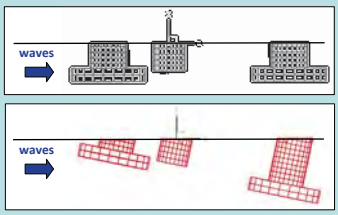

Solve Equations of Motion in the frequency domain:
- Increased hydrodynamic coupling, esp. heave & pitch;
- Increased heave and pitch excitation at low periods.

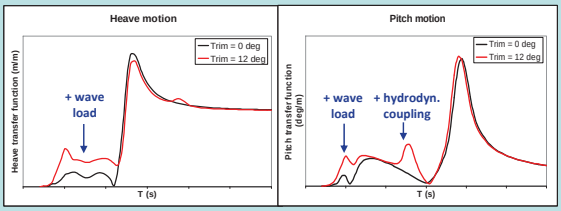

Horizontal offset and nonlinear mooring stiffness

Mooring restoring forces are nonlinear. Thus global K matrix is a function of wind/ wave/current induced offset.

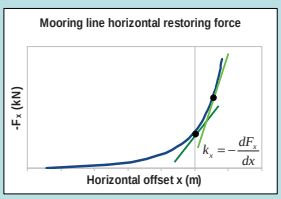

Solve Equations of Motion in the freq. domain:
- Increased surge response at large T: resonance;
- Left-shift in pitch natural period.

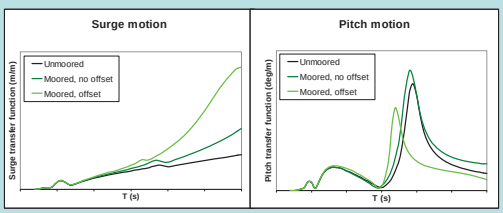

Future steps

- Moorings – FEM dynamic model using *Code_Aster*[2]
- Wind turbine aerodynamic BEM model
- Viscous excitation forces based on Morison approach
- Fully coupled time domain simulation

1. Developed by École Centrale de Nantes

2. Developed by EDF R&D

* Raffaello-externe.Antonutti@edf.fr # Christophe.Peyrard@edf.fr

Coatings for protection of boat landings against corrosion and wear

Astrid Bjørgum, Ole Øystein Knudsen and Sébastien Equey, SINTEF Materials and Chemistry and Arya P. Bastiko, NTNU

Introduction

In addition to corrosion protection boat landings need protection against impact and scour due to impact from the service boat. Coating maintenance offshore is expensive. Boat landings located in tidal and splash zones are particularly difficult to maintain due to constant wetting by seawater. Offshore oil & gas industry has reported lifetimes above 20 years for certain coating systems also in the splash zone. Offshore wind farm owners, however, have seen that protective coating systems on boat landings are damaged after few years in service.

To ensure secure access to the wind turbines for the O&M people, high friction coating systems are preferred for the boat landing.

The objective of this study has been to study abrasion and mechanical properties of different corrosion protective coating systems for boat landings.

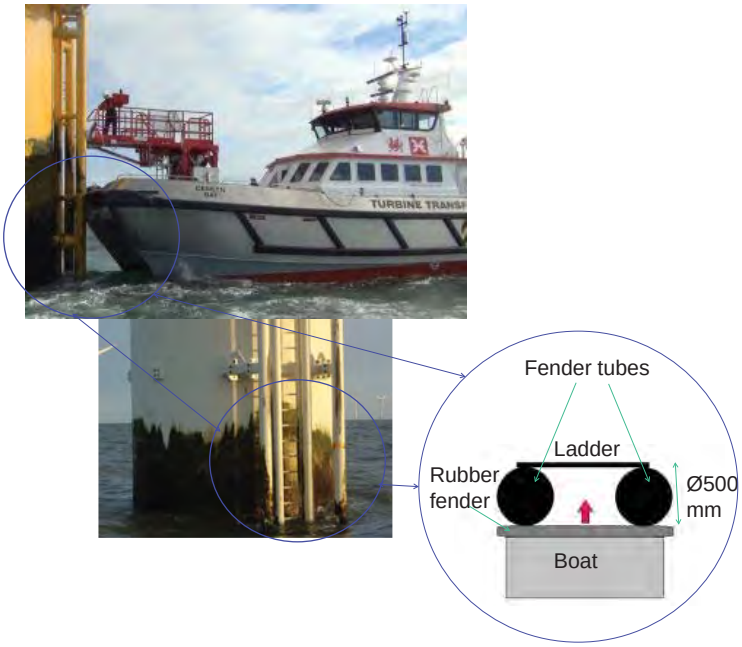

Experimental work

Coating systems used to protect boat landings and/or known to have long lifetimes in the splash zone of offshore oil & gas installations were applied on steel samples by the coating suppliers:

Coating system	Coat 1 Generic type	Coat 2 Generic type	Coat 3 Generic type	DFT [µm]
PU	Zinc rich epoxy	Epoxy	Polyurethane topcoat	310
PSO1	Zinc rich epoxy	Polysiloxane topcoat		350
PSO2	Zinc rich epoxy	Modified epoxy	Polysiloxane topcoat	280
Epoxy1a	Epoxy Alu Primer	Surface tolerant epoxy mastic	The same topcoat, Curing times 3 years (Epoxy1a) and 3 months (Epoxy1b)	450
Epoxy1b	Surface tolerant epoxy mastic	Surface tolerant epoxy mastic		500
Epoxy2	Glasflake reinforced epoxy	Glasflake reinforced epoxy		500
HDG	Hot dip galvanized			200
HDG_powder	Hot dip galvanized	Powder coating		300
Reinforced	Glasflake reinforced polyester	Glasflake reinforced polyester		1500

Vulcanised neoprene rubber applied on steel samples in approximately 4.5 mm thickness were used to simulate the fenders on service boats.

Abrasion testing was done to determine the ability of the boat landing coatings to resist wear due to contact with the rubber fender on the boats. Testing was performed by sliding the rubber sample against the coated surface, applying a 200 N weight load at a frequency of 0.1 Hz for 700 s in air and 1800 s in artificial seawater. The load used was estimated from Herz' equations assuming that the service boat acts with a propulsion force of 10,000 N against the boat landing.

Abrasion testing in (a) air and (b) artificial seawater

Mechanical properties were investigated by

- Vickers hardness according to ISO 14705
- Impact resistance according to ISO 6272
- Adhesion according to ASTM D1002-10

Results

Abrasion testing of the coating systems showed generally

- Decreasing friction coefficients with increasing testing time
- Faster degradation of Rubber than the other coating systems
- Weight loss despite some rubber settled on the coating surfaces
- educed surface roughness

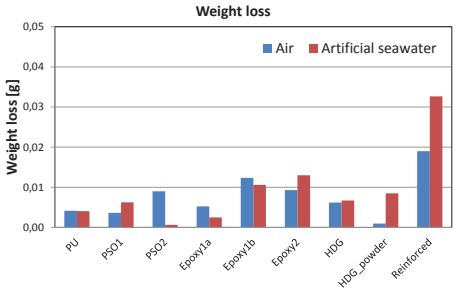

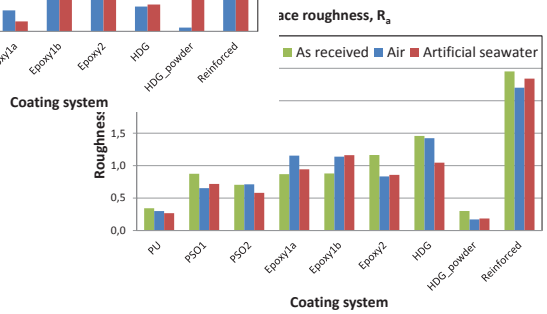

Impact testing of the coating systems showed

- Cracking of the PU, PSO and HDG-powder coatings
- No cracking of Epoxy1a, Epoxy1b, Epoxy2 and Reinforced coatings

Conclusions

- Increased roughness and low weight loss in the abrasion test indicate that the well cured Epoxy1a is suitable for boat landings
- High friction coefficients but high weight loss may question use of the Reinforced coating on boat landings
- High surface roughness and low weight loss indicate that HDG may be a compromise to organic coating systems for boat landings

Real-time Hybrid Testing of a Spar-type Wind Turbine

PhD-student Valentin Chabaud, Dept. of Marine Technology, NTNU

Real-time Hybrid Testing

Up to now scale model testing of floating wind turbines has mainly been used as a necessary step towards large scale prototype testing, but intrinsic issues prevented it from generating trustworthy data to validate numerical models upon:

- Generating good wave **and** wind conditions demands specific facilities
- Scaling effects arising from Froude/Reynolds scaling impairs accuracy

Real-time hybrid testing (RTHT) overcomes those shortcomings by performing scale model testing only on a subpart of the whole structure, the remainder being simulated numerically. The loads acting on the virtual substructure are calculated from online-measured motions of the physical substructure and actuated back on the latter in real-time. RTHT brings also the ability to focus the experimental study on a substructure and consequently to limit the sources of uncertainties.

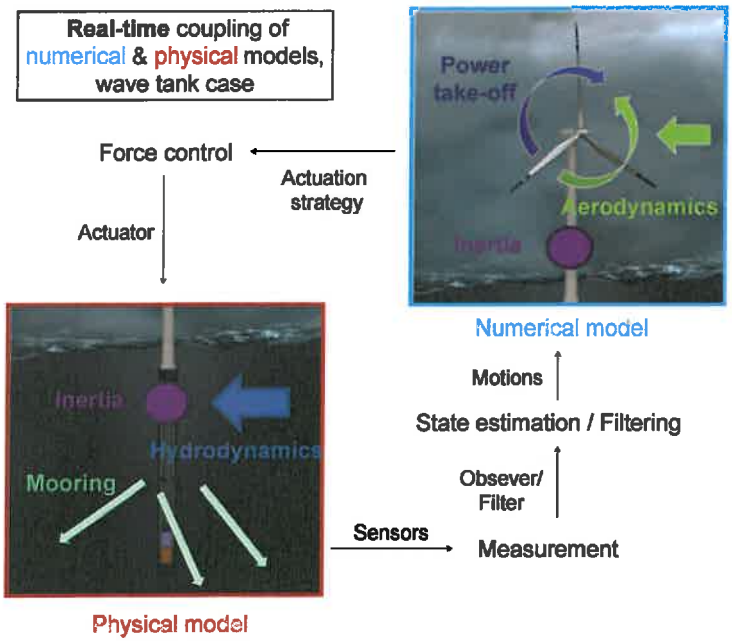

Objectives

The main objective is to make all the items of the RTHT loop fit into one time step by:

- Reducing numerical computational time
- Reducing force control delay (actuator dynamics compensation)
- Inhibiting filtering delay (observer design)
- Lengthening the time step (actuation strategy design)

While keeping an acceptable level of accuracy.

We focus at first on the wave tank case (physical hydrodynamics, mooring and inertia; numerical aerodynamics, generator and control), with 2 degrees of freedom (pitch and surge).

Reducing numerical computational time

Numerical method for aerodynamics

Advanced actuation strategies require the modeling of both substructures (numerical, but also physical for observing purposes). Aerodynamics (numerical substructure) must be modeled in a fast and accurate enough way. 3 methods are compared:

Name	Call-in-the-loop (CIL)	Look-up tables (LUT)	Analytic Actuator Disc (AAD)
Description	AeroDyn (NREL)	LUT for thrust and torque, calculated from CIL	Analytic model, empirical coefficients
Wake modeling	Dynamic	Quasi-static	Dynamic
Turbulence model	Discretized 2D field	Punctual + Shear	Punctual + Shear
Main advantage	Conventional	Simplistic	Fast and simple
Main disadvantage	Slow	Inaccurate, limited	Punctual turbulence model

Actuator disc turbulence model

- Turbsim (NREL) is used to generated full-field wind files
- Wind speed / direction is averaged over the rotor area
- The root-mean-squared wind speed is filtered in time
- The wind profile is modeled through a linear shear

Results

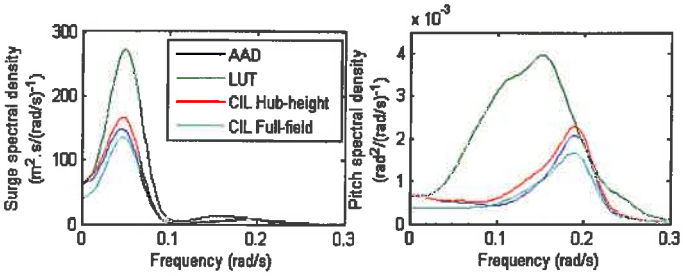

- Quasi-static wake modeling (LUT) is insufficiently accurate
- AAD and CIL methods correlate well
- Carefully reducing a 2D wind field to a punctual representation is reasonable regarding rigid body motions
- AAD allows larger (~ 2 times) time-steps than CIL
- CPU time for one iteration (ms):

CIL	AAD	LUT
0.3	0.001	0.002

➡ The AAD method appears as the most appropriate choice to model rigid body motions of floating wind turbines.

Further work

- Coarsen discretization in time and space to improve performance
- Include yaw dynamics modeling
- Move on to the next task: Observer and actuation strategy design

Advanced representation of tubular joints in jacket models for offshore wind turbine simulation

Jan Dubois*[1,2], Michael Muskulus[2], Peter Schaumann[1]
[1)]ForWind – Leibniz University of Hannover, Institute for Steel Construction[1], Hannover, Germany
[2)]Department of Civil and Transport Engineering, Norwegian University of Science and Technology, Trondheim, Norway

Motivation

Offshore wind farms are increasingly realized in water depths beyond 30m, where lattice support structures are an interesting option to withstand the severe environmental actions. One of the main tasks for the future is the optimization of support structure designs, making the exploitation of offshore wind resources more competitive. Jacket substructures show strong potentials in a broad spectrum of water depth from 25 up to 70m and this work addresses the optimization of jackets, using an advanced simulation approach specifically optimized for jackets. The ultimate goal are lighter jacket structures or improved fatigue performance. Both aspects, less material consumption as well as additional fatigue life time lead to lower cost support structures for offshore wind turbines in deeper waters.

Jacket Models with Different Level of Detail

- simple beam models
- enhanced beam models
  - consideration of chord-brace overlap (relevant for wave loads) and **local joint flexibilities** (using springs)
- sophisticated beam models with joint regions as superelements

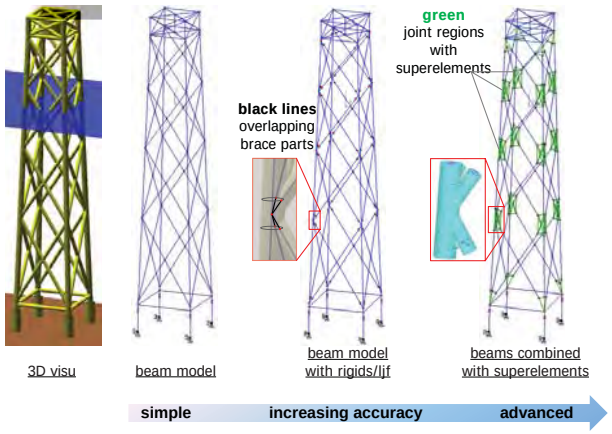

Figure 1: Jacket models with different levels of detail (shown at OC4 jacket)

Improved Superelement Application for Jackets

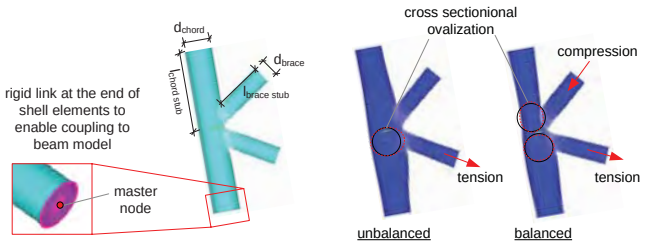

Figure 3: Superelement dimensions and unbalanced/balanced axial joint loading

- rigid link increases stiffness of detailed FEM joints (cf. Figure 3, left)
- ovalization of chord walls due to local brace loading obstructed
- a minimum ratio α of chord stub length and chord diameter is thus necessary to avoid this “artificial” stiffening due to rigid links

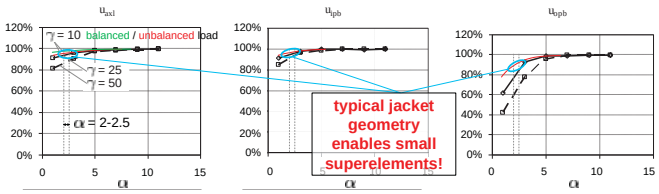

Figure 4: Normalized joint flexibility depending on α (chord stub length to chord diameter ratio) and γ (chord diameter to chord wall thickness ratio)

Superelement Approach

What about superelement size and local joint stresses?

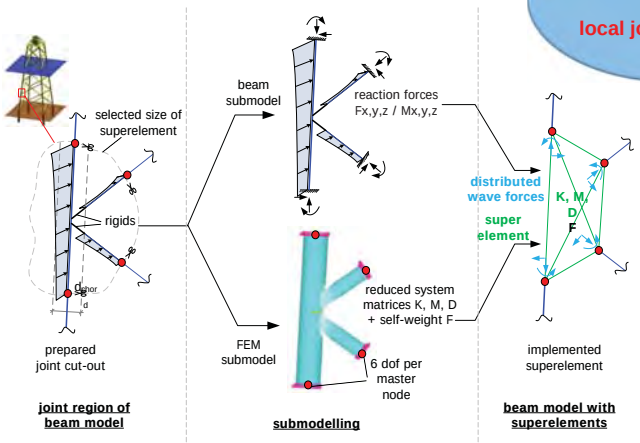

Figure 2: Implementation of a tubular jacket joint as super element

- joint geometry is cut-out of beam model (cf. Figure 1 right, green area)
- detailed FEM models of joints are generated for substructuring
- coupling of reduced system matrices of detailed joint models (superelements) with remaining beam model at interface nodes
- global wave loading considered via load submodel of joint regions
- current size recommendations do not cover typical dimensions of jacket joints and size of cut-out regions can even exceed bay height

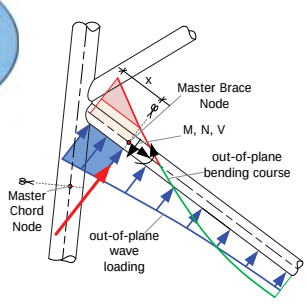

Figure 5: Joint stress extrapolation

- typical jacket geometry allows for relatively small superelements
- small cut-out regions enable a quasi-static extrapolation of member forces into local joint region (cf. Figure 5)

Improved Application
- **superelement size optimized**
- **smaller size facilitates application on OWT jackets**
- **local joint stresses calculable**

Enhanced fatigue performance of joints in OC4 jacket

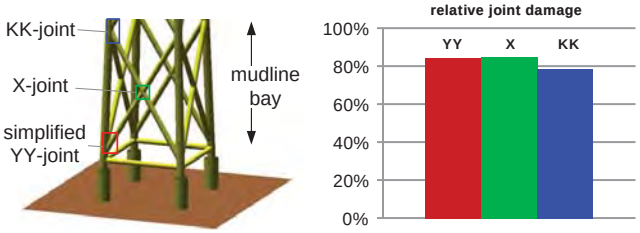

Figure 5: Predicted fatigue damage of joints at mudline using the sophisticated superelement model or the beam model - results normalized to beam model damage

Conclusions

- predicted fatigue damage of essential joints significantly reduced by ~20% (see Figure 6)
- study shows that predicted jacket fatigue life time is increased by up to 15% - enabled by optimized superelement approach!

Acknowledgements
Research work has been carried out during the project “Advanced jacket models for offshore wind turbines with superelements” (Project No: 21983/F11) financially supported in the framework of the IS-Mobil programme by the The Research Council of Norway

*E-Mail of the corresponding author:
dubois@stahl.uni-hannover.de

Comparison of coupled and uncoupled load simulations on the fatigue loads of a jacket support structure

P. Haselbach[1] , A. Natarajan[1], R. Jiwinangun[1] and K. Branner[1]
[1]DTU Wind Energy, Technical University of Denmark

Abstract

A comparison of the moments and forces at the joints of a jacket structure is made between fully coupled aero-hydro-elastic simulations in HAWC2 and decoupled load predictions in the finite elements software Abaqus. The four legged jacket sub structure is modeled in moderate deep water of 50 m and designed for the 5 MW NREL baseline wind turbine. External conditions are based on wind and wave joint distribution in the North Sea. In both simulation cases, the integrated loads acting on the jacket legs are computed as time series. The analyses of the fully coupled and decoupled simulations show that differences depending on the structural stiffness and the applied wave loads occurs. Variation in the amplitudes of the moments and forces on the jacket legs up to 25 % was observed.

Motivation

The design of offshore wind turbine structures is based on computer simulations of various load cases that the turbine is expected to experience in its life time as stipulated in the IEC 61400-3 standard [3]. The computation of the loads on the sub structure based on these design load cases requires fully coupled aero-hydro-elastic simulations. However on many occasions, the turbine design is made by a manufacturer and the sub structure (such as a jacket) design is made at another company and it is often not possible to a have a fully integrated model in a simulation platform. It is then imperative to understand the difference in sub structure internal forces and moments from those obtained in fully coupled load simulations against those determined using uncoupled load simulations where the tower top loads from the rotor are captured using an aeroelastic software and then used in a different software in which the tower, transition piece and sub structure are represented.

Approach

The tower, transition piece and jacket structure of the UpWind 5MW turbine [4] are modeled in the Abaqus [5] platform. The hydrodynamic loads are input to Abaqus using a Matlab based code that uses the Morison equation [6] based on wave kinematics obtained using a second order non linear irregular wave model. The tower top fore-aft and side to side forces and bending moments are input to the Abaqus model based on normal turbulent wind simulations conducted in the HAWC2 aeroelastic software [7] between 8 m/s and 25 m/s mean wind speeds. Wind and waves are aligned in all load simulations performed. The DLC 1.1 [3] load case simulations results are obtained in HAWC2, from which the tower top moments are transferred to the Abaqus model.

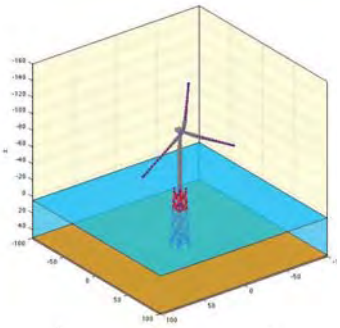

Natural frequency comparison

In order to verify the structural representation of both models (HAWC2 and Abaqus model) are identical, along with their geometrical consistency, the natural frequencies of the jacket structure are compared. The natural frequency of the coupled structure is displayed in Table 1, wherein it is seen that the structural frequencies in both software match quite well for the first and second fore-aft modes and side-to-side modes. Deviations between the HAWC2 and Abaqus mode shapes are minor. The maximum deviation is of the order of 1.25 % between both simulations. The Figures below show the corresponding eigenmodes of the natural frequencies.

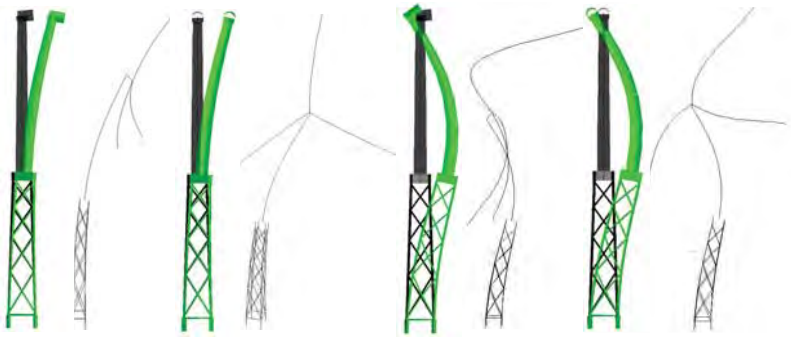

1st Fore-Aft Mode 1st Side-Side Mode 2nd Force-Aft Mode 2ndSide-Side Mode

Table 1: Natural frequencies of the jacket structures

Mode	Abaqus model	HAWC2 model
1st Fore-Aft Mode	0.3169 Hz	0.3164 Hz
1st Side-Side Mode	0.3174 Hz	0.3214 Hz
2nd Fore-Aft Mode	1.2090 Hz	1.2047 Hz
2nd Side-Side Mode	1.2145 Hz	1.2144 Hz

Investigation of tower top displacement

The tower top displacement at a height of 88.15 m (position of the yaw bearing) was studied. A constant wind speed of 10 m/s was simulated and hydrodynamic loads were ignored. The blades were assumed to be rigid in HAWC2 to minimize the aeroelastic effects in the fully coupled simulation. The tower top displacement differed by 1.5 % between the fully coupled and decoupled simulation results, which indicates both model representations are similar without aeroelastic coupling. Subsequently, the blades were made elastic and a turbulent wind input with a mean wind speed of 10 m/s was applied in the HAWC2 model. The tower top displacement in x- and y-direction for the decoupled simulation exceeded the fully-coupled simulation by around 14 % (see Fig. 1 and 2).

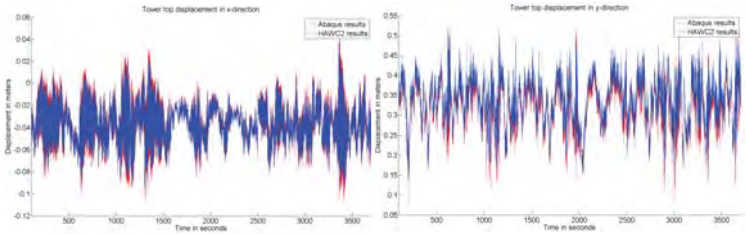

Figures 1 and 2: Tower top displacement in x- and y-direction for a turbulent wind seed and elastic blade

Loadings at the connection joint of the jacket structure

A load spectrum for turbine loads with wind speeds between 10 m/s and 25 m/s including the corresponding hydrodynamic loads were simulated and analyzed. The analyses of the shear forces and bending moments at the selected joints of the jacket support structures showed clearly differences between the fully coupled and uncoupled simulations. The magnitude reached up to the values of 25 % for the mean shear forces and bending moments (see Fig. 7 and 8). During the analysis 5 % higher deviations of the bending moments depending on the beam axis were recognized. The bending moments of the uncoupled simulation around beam axis 1, which describes the bending in wind direction, deviated stronger from the fully-coupled simulation results than the bending moments perpendicular to it.

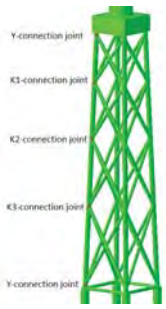

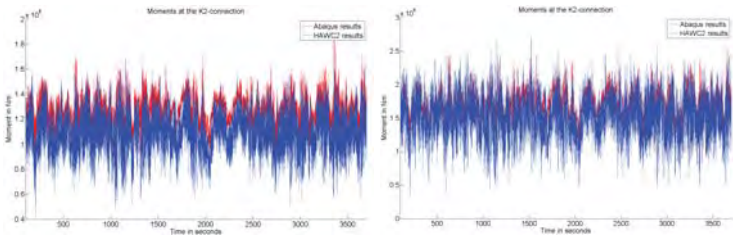

Figures 3 and 4: Bending moments around beam axis 1 (left) and beam axis 2 (right) for a wind speed of 10 m/s.

Conclusion

The comparison between the fully coupled simulation performed with HAWC2 and the uncoupled simulation shows that the extreme and fatigue loads on the jacket leg joints differed significantly between the two cases. The decoupled simulation method predicts higher extreme forces and moments in the Y- and K-connection joints of the jacket support structure. The comparison shows clearly that aeroelastic and hydroelastic coupling can account for at least 25 % of difference in loading on the jacket structure when compared to uncoupled simulations. The effects of fully coupled simulations can depict a bigger influence on larger and more flexible offshore wind turbines.

Acknowledgement

The work presented in this paper is a part of the Danish Advanced Technology Foundation (ATF) project titled, Cost-effective deep water foundations for large offshore wind turbines, contract le no.010-2010-2. The financial support is greatly appreciated.

Design Standard for Floating Wind Turbine Structures

Anne Lene Haukanes Hopstad
Knut Olav Ronold
Johan Slätte

Status of Floating Wind Turbine Technologies

Introduction

Offshore wind power is expected to play an increasingly important role in the future energy supply and floating wind turbine solutions have received considerably more attention during the last few years.

A large number of concepts are being developed, full-scale prototypes have already been installed and several are under operation in testing phases. Floating wind turbine structures have several advantages compared to their bottom-fixed peers. Much of the world's shallower waters have already been developed and/or are subject to other interests than energy production. Other areas, closer to shore, are just not suitable for bottom fixed installations due to environmental or public reasons.
The abundant wind resources available in deep waters, advancing technologies, the potential for a global market and decreasing cost levels are all parameters that have helped to create the recent momentum for the floating wind turbine industry, attracting investments and allowing for the development of demonstration projects.

The evolvement and future prospect for offshore wind, going into deeper waters and to further distances from shore have been addressed in several assessments during the last years, as shown in the below figures:

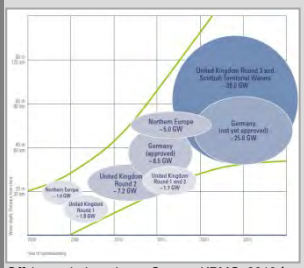

Offshore wind roadmap. Source: KPMG, 2010 [1]

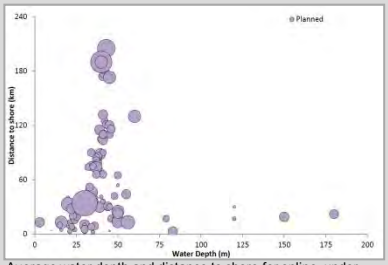

Average water depth and distance to shore for online, under construction and consented offshore wind farms. Source: EWEA, 2012 [2]

Floating wind turbine concepts

Within the floating wind turbine industry, three key design philosophies are preferred by the developers, all of them well known from the oil & gas industry, the spar buoy, the semi-submersible and the tension leg platform (TLP). The semi-submersibles with their low draft have a high site flexibility. The spar buoys are simple structures with an inherently high stability, while the tension leg platforms are low weight structures which impacts the investment costs. The most suitable design will have to be found by analyzing the actual site with associated manufacturing facilities and transport route, the metocean conditions and the actual concept's design and characteristics, to find the optimal concept with the least trade-offs.


Hywind
Source: Statoil

The **spar buoy** is typically a steel or concrete cylinder with low water plane area, ballasted with water and/or solid ballast which results in a weight-buoyancy stabilized structure with a large draft. The philosophy uses simple (few active components), well-proven technology with inherently stable design and few weaknesses.
Based on the large draft, the spar may however require towing to the deep-water site in a horizontal position. In such cases the structure needs to be up-ended, stabilized and the turbine is then installed using a crane barge. A spar is generally moored using catenary or taut spread mooring systems.

Statoil's Hywind is a 2,3 MW prototype that was deployed outside the west coast of Norway in 2009. It is the first floating wind turbine structure installed and is still in operation.


WindFloat
Source: PrinciplePower

A **semi-submersible** is a free-surface stabilized structure with relatively small draft. It is a very flexible structure thanks to its relatively low draft and high flexibility related to soil conditions. It is a heavy weighted structure with a considerable amount of steel and a relatively high manufacturing complexity due to the many welded connections. A semi-submersible structure is kept in position by the mooring lines, which typically are taut or catenary.
In 2011 the first large scale semi-sub prototype, Principle Power's WindFloat structure, was installed outside Portugal. The 2,0 MW turbine on a semi-submersible platform is the first offshore wind turbine to be installed without the use of any heavy lift vessels or piling equipment at sea. All final assembly, installation and pre-commissioning of the turbine and substructure took place on land in a controlled environment and the complete system was then wet-towed using simple tug vessels.


PelaStar
Source: Glosten Associates

The **Tension Leg Platforms (TLP)** are tension restrained structures with relatively shallow draft. The tension leg philosophy enables low structural weight of the substructure, and thus lower material costs. TLPs have high buoyancy and are held back by tendon arms connected to the anchors. This adds additional requirements with regard to soil conditions at site.

No TLP has yet been deployed as a large scale prototype, but the PelaStar concept being developed by Glosten Associates is probably the concept furthest in development. The PelaStar concept is currently being considered for a demonstration site in 60-100 m water depth outside the UK.

A Global Market

The development of deep water offshore floating systems has so far mainly been led by Northern European countries, but today a considerable amount of R&D, concept developments and testing of floating systems are performed also in the US, Japan and elsewhere within the EU, creating the potential and environment for a global market. Recent developments are described below:

- In late December 2012, The European Commission decided to provide project funding for a 27MW floating offshore wind farm, utilizing the WindFloat semi-submersible structures and the next generation multi-megawatt offshore wind turbines.
- In the UK, ETI plans to invest £25m in a 5 to 7 MW demonstrator project in 60 to100 m water depth. Considerable parts of UK Round 3 zones are in deep waters, suitable for floating wind turbine installations.
- The Japanese government are currently involved in several large national development projects with floating wind turbine platforms , e.g. the Fukushima Floating Pilot Wind Farm and the Kabashima demonstration turbine, a 1:2 spar solution with a 100 kW turbine installed in 2012. A full scale 2 MW turbine installed on a spar is planned to be deployed in 2013 as a part of the Kabashima project. In addition, in mid January 2013 Japan released a plan to build the world's largest offshore wind farm with 143 turbines mounted on floating platforms outside the coast of Fukushima.
- In late December 2012, the US Department of Energy (DOE) decided to partly fund the development of seven offshore wind projects, including three floating solutions. This is in line with the US ambition to create a momentum in their domestic wind energy industry, utilizing their vast deep-water wind resources.

Development of design standard for Floating Wind Turbine Structures

Background

Floating wind turbines is a field currently undergoing major development. Several companies and research institutes worldwide are engaged in research programs, pilot projects and even planning of commercial floating wind farms. Developing standards for design of floating wind turbine structures is crucial and necessary for the industry to continue to grow. A technical standard embodies the collective experience of an industry and contains normative requirements that shall be satisfied in design. Development of a standard for floating wind turbine structures will lead to:

- Expert consensus on reliable approaches to achieve a tolerable level of safety
- Industry consensus on practicable approaches to achieve tolerable level of safety
- Experience from the industry reflected in the contents of an industry-wide standard regarding safe design, construction and in-service inspection
- A tool to be used related to innovative designs and solutions within given acceptance criteria
- A full-fledged reference code supplementing existing offshore wind turbine structure codes that do not cover floating units

As a first step towards developing a standard for design of floating wind turbine structures, a *DNV Guideline for Offshore Floating Wind Turbine Structures* was established in 2009 as a supplement to *DNV-OS-J101 Design of offshore wind turbine structures*. The development of this guideline was based on identification of current floating wind turbine concepts in conjunction with experience from other floater applications. The guideline, which is less formal than an official standard document, addresses floater-specific issues such as stability and station keeping.

The standard DNV-OS-J101 "Design of Offshore Wind Turbine Structures" provides principles, technical requirements and guidance for design, construction, in-service inspection and decommissioning of offshore wind turbine structures. However, DNV-OS-J101 does not cover floater-specific design issues. This is also the case for other existing standards for offshore wind structures e.g. *IEC61400-3 Wind turbines - Part 3: Design requirements for offshore wind turbines* and *GL (IV Part 2) Guideline for the certification of offshore wind turbines*.

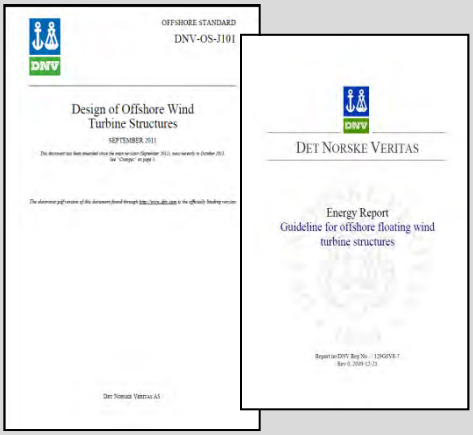
OFFSHORE STANDARD
DNV-OS-J101
Design of Offshore Wind Turbine Structures
SEPTEMBER 2011
DET NORSKE VERITAS
Energy Report
Guideline for offshore floating wind turbine structures

Joint Industry Project

As a second step, initiated in September 2011, DNV is currently conducting a joint industry project (JIP) for development of a full-fledged DNV standard for design of floating wind turbine structures. Ten of the world's leading players in the wind industry (Europe, USA and Asia) are currently participating in this JIP. The standard will be a supplement to DNV-OS-J101. The JIP is looking into floater specific design issues: suitable safety level, calibration of safety factors, global performance stability, station keeping, site conditions in relation to low frequent floater motions, necessary simulation periods, higher order responses and design of floater-specific structural components. The following technical issues will be covered in the standard:

- Safety philosophy and design principles
- Site conditions, loads and response
- Materials and corrosion protection
- Structural design
- Design of anchor foundations
- Stability
- Station keeping
- Control and protection system
- Mechanical system and electrical system
- Transport and installation
- In-service inspection, maintenance and monitoring
- Cable design
- Guidance for coupled analysis

The project secures quality assurance through a technical reference group where all participants have a representative. The standard will also go through an internal DNV and external industry hearing process. The standard is expected to be released during Q2 2013.

Assessment of acceptable safety level

An important task in the JIP is to determine which safety level that is necessary or acceptable in design of floating wind turbines structures. The target safety level of the existing standards is taken as equal to the safety level for wind turbines on land as given in *IEC61400-1 Wind turbines - Part 1: Design requirements*, i.e. normal safety class.
As the consequence of failure is primarily a loss of economic value, this is evaluated through a cost-benefit analysis. The analysis is to be used as part of the basis for selecting target safety level. This target safety level originally developed for small, individual turbines on land has been extrapolated to be used also for:

1. Larger MW size turbines on land
2. Offshore turbines
3. Support structures for offshore turbines
4. Many large turbines in large offshore wind farms

It is foreseen that the future floating wind farms will consist of a large number of turbines. Different target safety levels may be reasonable for offshore turbines in a large farm. The selected target safety level is likely to depend on the number of turbines in the wind farm.

Structural design

Another important issue is structural design. Reliability-based calibration of partial safety factor requirements for design of structural components is assessed for e.g. tendons and mooring lines. Existing design standards from other industries will be capitalized on, e.g. *DNV-OS-C101 Design of Offshore Steel Structures, General (LRFD Method)* and *DNV-OS-C105 Structural Design of TLPs (LRFD* Method) for tendons and *DNV-OS-E301 Position Mooring* for mooring lines. The JIP has access to full scale data from Hywind (Statoil) and analysis data from Pelastar (Glosten Associates) and WindFloat (Principle Power). These data will be used as part of the basis for calibrating the safety factors.

Acknowledgements and references

JIP participants:
Statoil (Hywind), Navantia, Gamesa, Alstom Wind, Iberdrola, Sasebo Heavy Industries, Nippon Steel, STX Offshore & Shipbuilding, Principle Power (WindFloat), Glosten Associates (Pelastar),

[1] EWEA : Task Force 'Deep Offshore & New Foundation Concepts', 2012; [2] KPMG, 2010: Offshore Wind in Europe, 2010 Market Report

DTU Wind Energy
Department of Wind Energy

Nonlinear irregular wave forcing on offshore wind turbines. Effects of damping in misaligned wind and waves.

S. Schløer, H. Bredmose, R. Klinkvort

AGENDA

An offshore wind turbine with a monopile foundation is considered and the importance of the damping from the soil, waves and structure is investigated in a situation with misaligned wind and waves.

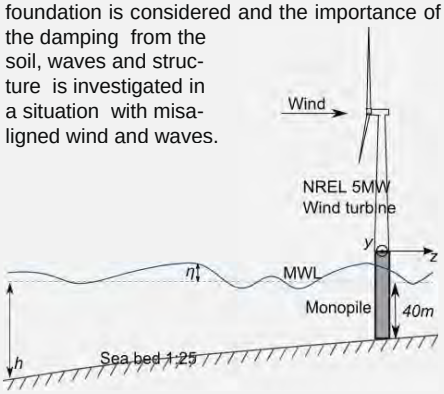

Schløer et al. (2012) investigated the effect from fully nonlinear irregular wave forcing on the fatigue life of the monopile and the tower and found that under normal conditions, where the wind and waves are aligned and the wind turbine is in operation, the aerodynamic damping is so strong that the effects from the nonlinearity of the waves become insignificant. However, in cases where the aerodynamic damping is absent, the effects from the wave nonlinearity on the fatigue life is of magnitude 30 %. It was further found that excitation of the first structural eigenmode due to the waves mainly occurred in the tower, while the response in the monopile was more static.

Model setup

The dynamic behavior of the wind turbine and foundation is calculated in the aeroelastic code Flex5, Øye (1996). The wave kinematics are calculated using a fully nonlinear potential flow wave model, Engsig-Karup et al. (2009), and afterwards included into Flex5 to form the hydrodynamic loads.

T_p (s)	H_s (m)	W (m/s)	I (%)	P_{rel} (%)	0°	30°	60°	90°	120°	150°	180°
6.8	2.3	6.7	0.22	50	6.0	12.5	9.0	7.5	6.5	5.5	3.0
7.9	3.0	8.5	0.20	37	5.9	10.0	7.8	4.8	3.7	3.0	1.8
10.5	4.5	13.4	0.16	11	3.2	4.9	1.9	0.4	0.2	0.1	0
12.3	6.8	18.1	0.15	2.2	0.9	1.2	0.1	0	0	0	0
14.2	9.3	23.5	0.14	0.23	0.1	0.1	0	0	0	0	0

Table 1

Five representative sea states combined with a corresponding wind velocity and turbulence intensity are considered . Each sea- and wind state are given a probability of occurrence and a wind-wave-misalignment-distribution, stated in table 1.

Two situations are considered: In the first case no damping is applied to the structure. In the second damping is applied to the monopile and tower so that the first structural eigenmode has a damping equal to a log. decrement of 8%. The 8 % represents all the damping which exist beside the aerodynamic damping such as soil-, radiation- and structural damping.

EQUIVALENT LOAD RANGE

Figure 1 shows the equivalent loads, L_{eq}, of the force in the bottom of the tower and monopile perpendicular (y) and aligned with the wind direction (z). L_{eq} is calculated for each sea state including the wind-wave-misalignment-distribution stated in table 1 with 0% and 8% of log. damping.

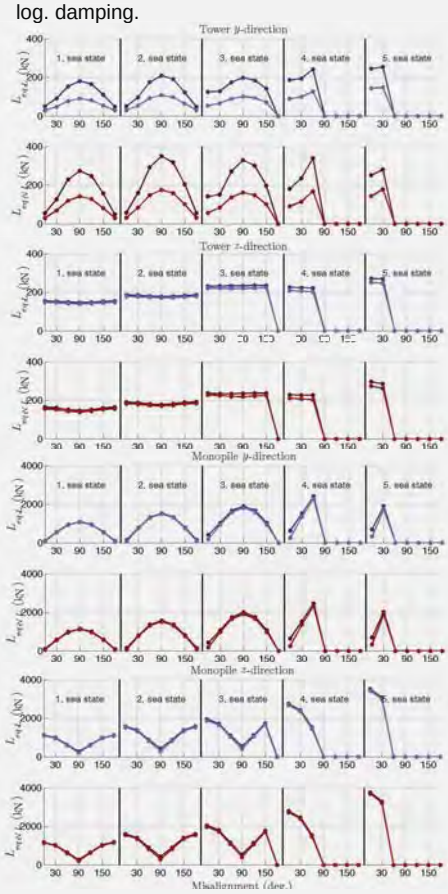

Figure 1 Linear, 0%damping; Linear, 8%damping; Nonlinear, 0%damping; Nonlinear, 8%damping

In the tower the equivalent loads perpendicular to the wind direction decrease significantly when the 8% of damping is included both for the linear and nonlinear waves. It is further seen that L_{eq} in the tower perpendicular to the wind direction due to the nonlinear waves are up to 50 % larger than L_{eq} due to the linear waves. In the monopile and in the tower aligned with the wind direction the effects from both the 8% damping and the nonlinearity of the waves are small.

ACCUMULATED FATIGUE DAMAGE

The fatigue analysis is based on the relative probability of occurrence, P_{rel}, and the probabiity of the wind-wave-misalignment-distribution.

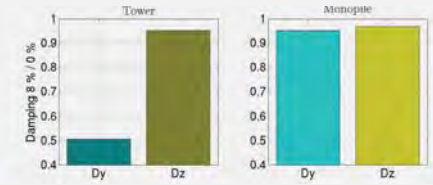

Figure 3

The ratio between the fatigue damage with and with out damping for the nonlinear waves is shown in figure 3. The fatigue damage in the tower is reduced with 50 % in the direction perpendicular to the wind direction (D_y) when the 8% of damping is included. Aligned with the wind and in the monopile the effects from the damping is less significant however the fatigue damage is still reduced with 5 %.

DISCUSSION

The analysis indicates that the nonlinearity of the waves and the damping can change the fatigue damage particularly in the tower and in the direction perpendicular to the wind. The reason that the effects are strongest in the tower is because the first structural eigenmode is excited in the tower. The monopile can more be seen as a force “transmitter”. The aerodynamic damping is the strongest damping effect but the additional damping effects can also lead to a reduction in the fatigue damage. It is therefore important to know the magnitude of the damping which can be expected at an offshore wind farm site in order not to overestimate the fatigue damage. Next to aerodynamic damping, soil damping gives the largest contribution to the overall damping.

Soil friction is currently included in FLex5 through adaption of the recent model of Hededal and Klinkvort (2010) which takes the effects of pre-consolidation and creation of gaps into account.

Figure 4

Soil damping is introduced into the model by hysteresis. Figure 4 shows an example of such a spring element. The new soil model will allow dynamic computations with more physical soil damping. The next step is to investigate the impact on the structural dynamics.

References

Engsig-Karup, A., Bingham, H. and Lindberg, O. (2008). An efficient flexible-order model for 3D non-linear water waves. *Journal of Computational Physics* 228(6), 2100–2118.

Hededal, O. and R. Klinkvort (2010). A new elasto-plastic spring element for cyclic loading of piles using the *p-y-curve concept. Numerical Methods in Geotechnical Engineering – Benz & Nordal (eds).*

Schløer, S., H. Bredmose, H. B. Bingham and T. J. Larsen (2012). Effects from fully nonlinear irregular wave forcing on the fatigue life of an offshore wind turbine and its monopile foundation. *In Proc. of the ASME 31th 2012 Int. Conf. on Ocean, Offshore and Arctic Engng. ASME. Rio de Janeiro, Brazil.*

Øye, S. (1996). Flex4 simulation of wind turbine dynamics. In 28th *IEA Meeting of Experts Concerning State of the Art of Aeroelastic Codes for Wind Turbine Calculations* (available through International Energy Agency).

Acknowledgements

This research was carried out as part of the Statkraft Ocean Energy Research Programme, sponsored by Statkraft (www.statkraft.no).This support is gratefully acknowledged.

D Operation & maintenance

Development of a Combined Operational and Strategic Decision Support Model for Offshore Wind, Iain Dinwoodie, PhD Stud, Univ Strathclyde

Vessel fleet size and mix analysis for maintenance operations at offshore wind farms, Elin E. Halvorsen-Weare, SINTEF ICT/MARINTEK

NOWIcob – A tool for reducing the maintenance costs of offshore wind farms, Iver Bakken Sperstad, SINTEF

WINDSENSE – a joint development project for add-on instrumentation of Wind Turbines, Oddbjørn Malmo, Kongsberg Maritime AS

Long-term analysis of gear loads in fixed offshore wind turbines considering ultimate operational loadings, Amir Rasekhi Nejad, PhD stud, NTNU

Development of a Combined Operational and Strategic Decision Support Model for Offshore Wind

I Dinwoodie, Y Dalgic, I Lazakis, D McMillan, M Revie
iain.dinwoodie@strath.ac.uk

Overview

Motivation and Objectives

Methodology – Knowledge, Operational Model and Decision Support Tools

Demonstration Case study

Conclusions and Future Work

Motivation & Objective

Existing models typically engineering approaches

Lack of models that help high level decision making

"To develop a methodology to allow O&M models to effectively inform developer and operators decisions"


Image: REPower

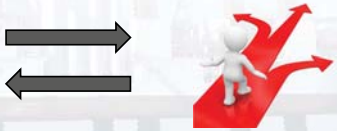

Requirements

Knowledge of offshore wind turbine and vessel market

Accurate, robust and efficient operational model

Relevant and practical decision making models

Background Expertise

Offshore costs driven by failures and accessibility

Vessel Type	Transfer	Field Support	Jack - up
Typical day rate	~ £1750	~ £9500	~ £100 – 250k
Baseline λ	1.8	0.4	0.2
Operation time	< 1/2 day	1 day	2 days
Direct cost impact	Low	Low	High


Image: Windcat


Image: Subsea 7


Image: MPI

All important, jack-up strategy currently highest impact but may change in future

Strategy Specification

Fix on fail (spot market)

Batch fix on fail (x fails before commission)

Short term (1-6) month yearly charter

Purchase

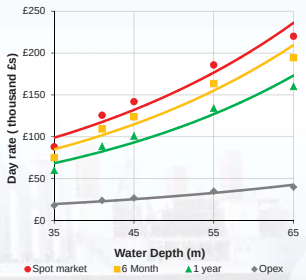

Modelling Approach

Climate Model –Correlated Auto-Regressive model

Failure Model – Markov Chain Monte Carlo simulation

Decision Models – BBN informed decision tree analysis and emulator models

Climate Model

Correlated Auto-Correlated wind and wave model

$$X_t = \mu + \varepsilon_t + \sum_{i=1}^{p} \varphi_i (X_{t-i} - \mu)$$

De-trend time series and use correlation matrix in AR simulation process

Maintains key site characteristics and computationally simple

Failure model

Markov Chain Monte Carlo failure simulation

$$\lambda(t) = \rho\beta t^{\beta-1}$$

$$R < \lambda(t) * \frac{\Delta t}{8760}$$

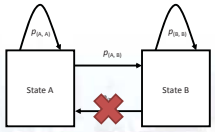

Decision Support Models

Bayesian Belief Networks – informed decision tree

Output risk profile

Modelling Approach

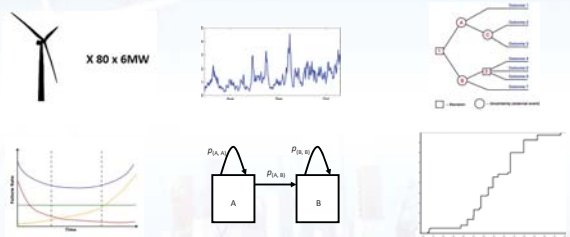

Case Study

Simple demonstration wind farm – 60 x 5 MW

Failures based on onshore observations

Identified strategies can be chosen for early life and remaining duration

Uncertainty represented by failure rate and electricity market price

Case Study - Results

Optimal strategy identified at two operation decision point using decision tree

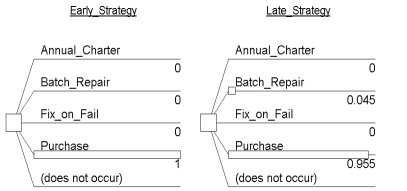

Case Study - Results

Project costs estimated including likelihood of different results

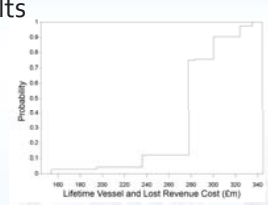

Key financial risks from uncertainties and decision consequences can be identified

Future Work

Further integrate operational and decision support models

Perform full scale analysis on existing and future wind farms

Use of emulators to perform wide ranging high level analysis based on operational model

Thanks for listening

iain.dinwoodie@strath.ac.uk

http://www.strath.ac.uk/windenergy

EPSRC

Vessel fleet analysis for operation and maintenance activities at offshore wind farms

DeepWind 2013
Trondheim 25 January 2013

Elin E. Halvorsen-Weare[1,2], Christian Gundegjerde[3], Ina B. Halvorsen[3],
Lars Magnus Hvattum[3], Lars Magne Nonås[2]

[1]Department of Applied Mathematics, SINTEF ICT, Norway (elin.halvorsen-weare@sintef.no)
[2]Department of Maritime Transport Systems, MARINTEK, Norway
[3]Department of Industrial Economics and Technology Management, NTNU, Norway

Outline

1. Motivation
2. Problem description
3. Mathematical model formulation
4. Some numerical results
5. Conclusions and further research

Motivation

- EU's 20-20-20 target – to be meet by 2020
  - A reduction in EU greenhouse gas emissions of at least 20% below 1990 levels
  - **20% of EU energy consumption to come from renewable resources**
  - A 20% reduction in primary energy use compared with projected levels, to be achieved by improving energy efficiency
- 25-30 % of the cost from producing energy from offshore wind farm comes from the **operation and maintenance (O&M) activities**
- Vessels to support O&M activities – one of the **most costly resources in the supply chain**

Motivation

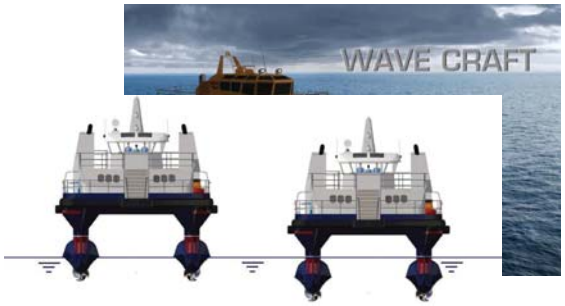

Problem description

- One or more wind farms has a number of wind turbines that require maintenance operations during a planning horizon
- Vessel resources and maintenance infrastructure can be shared between the wind farms
  - Maintenance infrastructure/bases can be onshore ports, offshore installations, mother vessel concepts…
  - Vessel resources can be purchased or chartered and can be CTVs, supply vessels, crane vessels, helicopters…

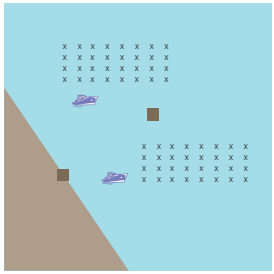

Problem description

- Maintenance bases can have investment costs and have a maximum vessel capacity
- Vessel resources are associated with a given maintenance base
- Each vessel resource has:
  - investment cost or time charter cost
  - variable cost
  - service speed
  - deck load
  - deck size
  - crew capacity
  - operational and safety weather requirements

Problem description

- Vessel fleet and maintenance infrastructure need to support the wind farm(s) need for preventive and corrective maintenance operations
- Preventive maintenance operations are executed to extend the life of a wind turbine and keep the number of failures down
  - Scheduled according to the wind farm operator's maintenance strategy
- Corrective maintenance operations are executed due to unforeseen failures to the system
- Each maintenance operation is divided into up to three maintenance activities

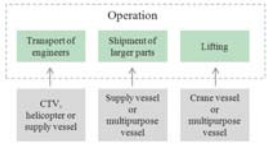

Problem description

- Preventive maintenance activities will have a soft and a hard time window for execution
- Corrective maintenance activities always have a penalty cost based on the real downtime cost the failure cases
- Activities can be delayed until next planning horizon at a penalty cost

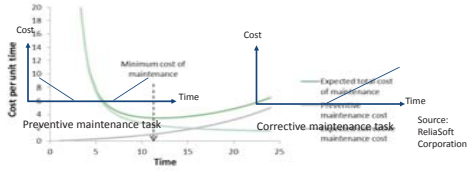

Problem description

- Several uncertain parameters:
  - Weather conditions: Wind speed and direction, wave heights and directions, current…
  - Determines when operations can be executed and when vessels need to return to a safe haven
  - Wind speed and direction also determine the power production
  - Electricity prices determine the revenue from the wind farm
  - Spot prices of time charter contracts determine the cost of charter vessels
  - Number of failures and when they occur determines the corrective maintenance activities
- Deterministic modeling approach: All uncertain parameters are treated as known

Problem description

Objective:

Determine the minimum cost fleet and maintenance infrastructure that can execute all, or most, of the maintenance activities during the planning horizon

Mathematical model formulation – objective function

Minimize

Cost of maintenance bases +
Fixed cost of vessels +
Variable cost of using vessels to execute maintenance activities +
Penalty cost for maintenance activities executed outside their soft time window +
Penalty cost for not executed maintenance activities +
Travel cost for vessels

Mathematical model formulation – constraints

Restricting the number of vessels that can be based at a maintenance base
Budget constraint restricting the investment in vessels and bases
Maintenance activities are either executed within their hard time windows or postponed until next planning horizon
Only one vessel can be used to execute a maintenance activity at the same time
Determining the number of vessels that need to be purchased or chartered
Operational constraints - weather
Safety constraints - weather
Balancing constraints and flow conservation constraints
Binary, integer and non-negativity requirements

Numerical results

- Mathematical model formulation implemented in Xpress-IVE

- 15 problem instances
- Planning horizon of one year (360 days)
- 2 maintenance bases – one port and one offshore installation
- 9 vessel types: 3 CTVs, 2 supply vessels, 2 helicopters, one multipurpose vessel, one jack-up rig
- 1-3 wind farms
- 20-200 wind turbines per farm

Numerical results

Problem instance	# wind farms	# wind turbines per wind farm	# maintenance activities	CPU [s]	Bases	Vessel types	# activities not executed
1	1	20	74	6.262	Onshore, Offshore	1,8	0
2	1	50	185	46.14	Onshore, Offshore	1,2,8	0
3	1	100	359	42.39	Onshore, Offshore	1,2,8	0
4	1	150	562	117.96	Onshore	2,3,4,8	4
5	1	200	741	86.65	Onshore, Offshore	1,2,3,4,6,8	2
6	2	20	152	10.81	Onshore, Offshore	1,2,8	0
7	2	50	365	276.16	Onshore, Offshore	1,2,3,4,8	2
8	2	100	728	700.02	Onshore, Offshore	1,4,6,9	4
9	2	150	1126	1277.00	Onshore, Offshore	1,2,3,4,6,9	4
10	2	200	1546	923.03	Onshore, Offshore	1,2,4,6,8,9	8
11	3	20	234	313.13	Onshore	2,3,4,8	3
12	3	50	574	1157.08	Onshore, Offshore	1,3,4,8	8
13	3	100	1099	5317.45	Onshore	2,3,4,9	6
14	3	150	1671	6716.62	Onshore, Offshore	1,2,3,4,6,9	6
15	3	200	2175	18000.00	Onshore, Offshore	1,2,4,6,8,9	11

Conclusions and further research

- A deterministic optimization model has been developed for the fleet composition problem for maintenance operations at offshore wind farm
- The model is implemented in commercially available software
- Numerical results show that the model can be used to provide decision support on optimal or near-optimal vessel fleet within acceptable computational time

- Future research should focus on modifying the model to capture other relevant aspects to the problem not yet discovered
- The problems underlying uncertain nature can make it relevant to investigate ways of incorporating uncertainty into the model
  - Stochastic modelling approach

Vessel fleet analysis for operation and maintenance activities at offshore wind farms

DeepWind 2013
Trondheim 25 January 2013

Elin E. Halvorsen-Weare[1,2], Christian Gundegjerde[3], Ina B. Halvorsen[3],
Lars Magnus Hvattum[3], Lars Magne Nonås[2]

[1]Department of Applied Mathematics, SINTEF ICT, Norway (elin.halvorsen-weare@sintef.no)
[2]Department of Maritime Transport Systems, MARINTEK, Norway
[3]Department of Industrial Economics and Technology Management, NTNU, Norway

NOWIcob – A tool for reducing the maintenance costs of offshore wind farms

Iver Bakken Sperstad, Matthias Hofmann
SINTEF Energy Research
Trondheim, 25 January 2013

Outline

1. Describe prototype of life-cycle profit model (NOWIcob)
2. Illustrate use by test cases
3. Possible applications

Motivation

- Estimating life-cycle O&M costs and profit
- Optimizing the maintenance strategy

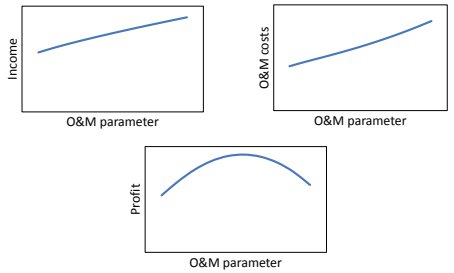

Model overview: Input and output

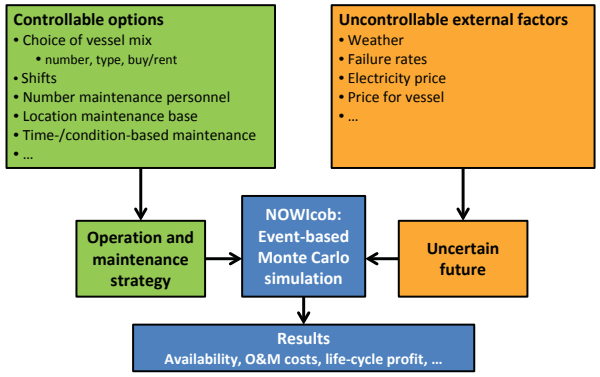

NOWIcob: Norwegian offshore wind power life cycle cost and benefit model

- Life-cycle profit model
- Event-based simulation of operational phase of an offshore wind farm
- Focus on maintenance activities
  - Weather limits
  - Weather model
  - New maintenance concepts
- Monte Carlo to take into account uncertainties
- Long-term, system-wide perspective

Model overview: Flow scheme

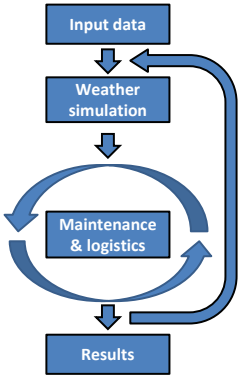

Input data

- Locations
  - Weather data
- Turbines
  - Power curves
  - Subcomponents
- Maintenance tasks
  - Failure/inspection rates
  - Maintenance type
  - Operation steps
  - Working duration
  - Cost of spare parts etc.

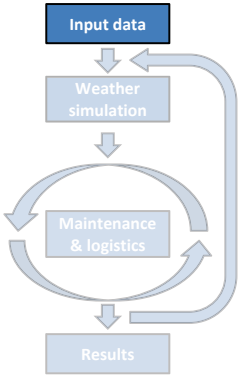

Input data

- Vessels
  - Weather limits for access etc.
  - Other abilities
  - Costs
  - Maintenance base
  - Mother ship?
  - Several shifts?
  - Order time?
- Shifts
  - Working hours
  - Shifts per day

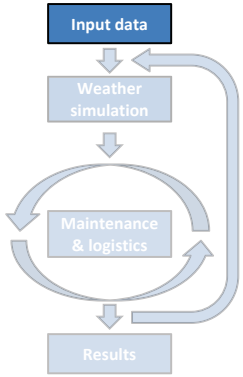

Weather simulation

- Markov chain weather model
  - Transition matrix from historic weather data
  - Generates simulated time series

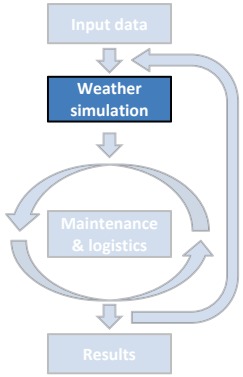

Weather simulation: Markov chain model

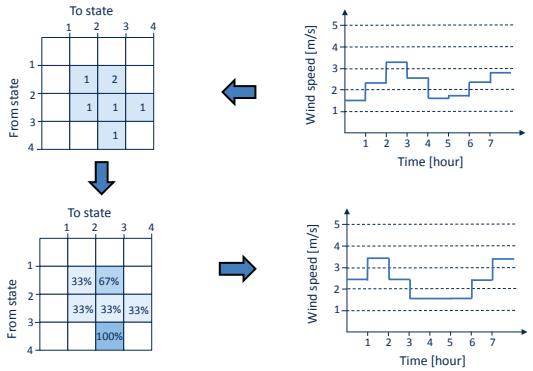

Weather simulation

- Markov chain weather model
  - Transition matrix from historic weather data
  - Generates simulated time series
- Simulated time series
  - Same statistical properties
  - Wind speed and wave height
  - Hourly resolution
  - Captures seasonal variations

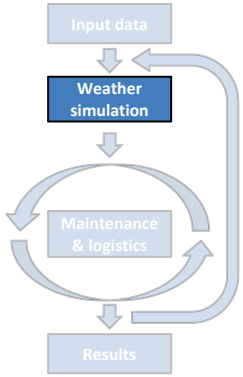

Maintenance & logistics

- Entire life time of the wind farm
- Scheduling for each shift
- Restrictions:
  - Weather
  - Personnel
  - Vessels
- Taking into account:
  - Waiting time
  - Travel time
  - Access time
  - Working time

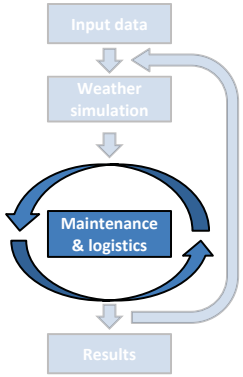

Results

- Electricity produced
- Electricity-based availability (E/E_{ideal})
- Net present value of
  - Income
  - O&M costs
  - Profit

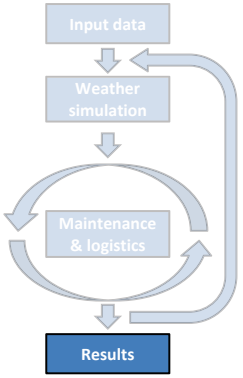

Multiple simulation runs

- New weather and new failures
- Histogram of results
  - Estimating probability distribution
  - Uncertainties / risks

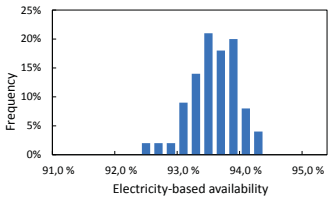

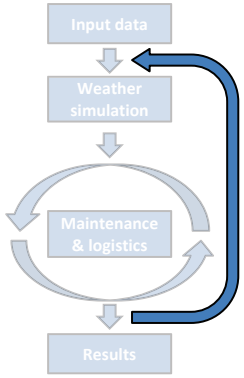

Examples of results

- Test case: Far-offshore wind farm (150 km)
  - Conventional logistics solution
  - New concepts:
    - Mother ship
    - Offshore platform

Examples of results: conventional

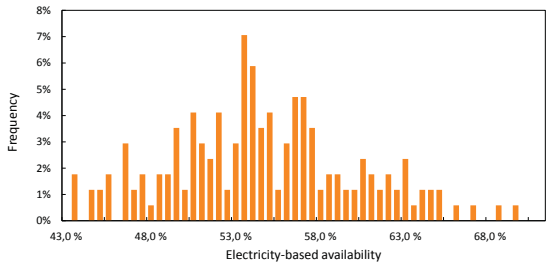

Examples of results: concepts

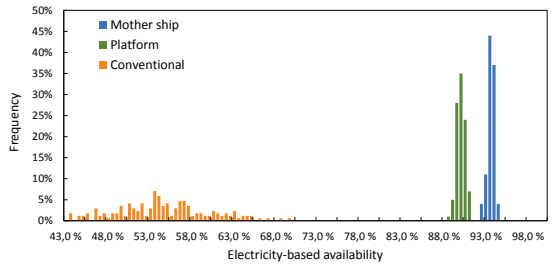

Examples of results: concepts

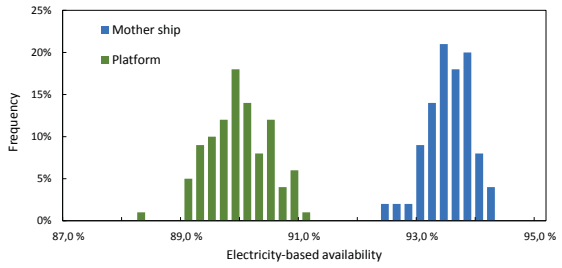

Examples of results: availability vs personnel

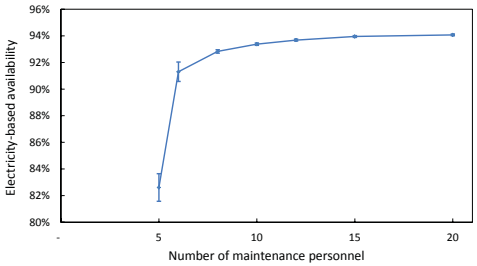

Examples of results: profit vs personnel

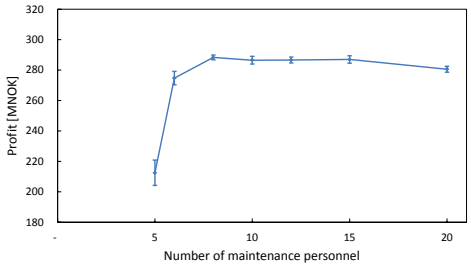

Possible applications

- Optimizing the maintenance strategy (design phase)
- Sensitivities – important parameters for offshore wind
- Estimating life-cycle O&M costs and profit
- Evaluating introduction of new technical concepts

Summary

- NOWIcob: Norwegian offshore wind power life cycle cost and benefit model
- Simulating O&M of offshore wind farm
- Focus on weather, access criteria, and novel concepts
- Output: Availability, O&M costs, profit, …

"Windsense – a joint development project for add-on instrumentation of Wind Turbines"

DeepWind 2013, 25 Jan. 2013

By Oddbjørn Malmo, Kongsberg Maritime AS

Main challenge:

CoE of wind power must be reduced by at least 30 %
Offshore even more

Indicative cost breakdown (with 3 MW WTG´s)

Key assumptions

- "*All inclusive*" engineer-procure-construct (EPC) cost .
- The cost structure for actual offshore wind projects is highly dependent on site specific conditions.
- Park size: constrained by grid capacity.

$$CoE = \frac{\text{Annualized CAPEX + Annualized OPEX}}{\text{Annual Energy Production}}$$

Source: VESTAS

O&M Costs for German Turbines (1997–2001) (Krohn et al. 2009)

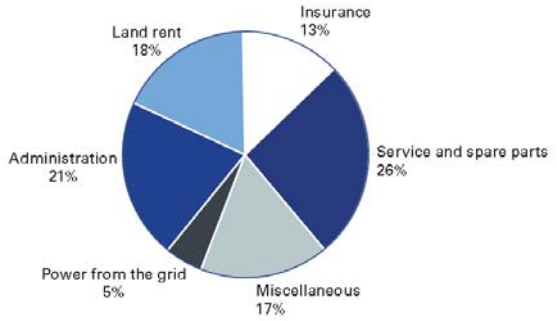

Operation & Maintenance Costs (O&M)

- Offshore O&M costs are 2-7 times higher than onshore costs[1)]
- O&M cost per produced kWh [1)]
  - Onshore: 0.05 NOK/kWh
  - Offshore: 0.1 to 0.2 NOK/kWh
- Value of lost production
  - 1% loss in a 50 MW plant at 30% capacity amounts to 1.6 MNOK /year @ 0.5 NOK/kWh

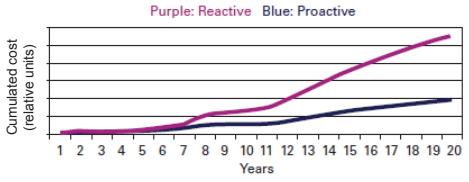

Life Cycle Cost: Pro-Active vs. Reactive Maintenance (Roeper 2009 [1)])

[1)] Source: Wind Energy OM Report 2011

Planned vs. unplanned service trips

Figures for a 240 MW wind park

- 80 turbines @ 6 MW
- 40 preventive maintenance trips
- 120 corrective maintenance trips
  - 1.5 failures per year per turbine

Source: DOWEC offshore reference wind farm case study [1)]

The absolute minimum (in red), and what you also should have (in blue)

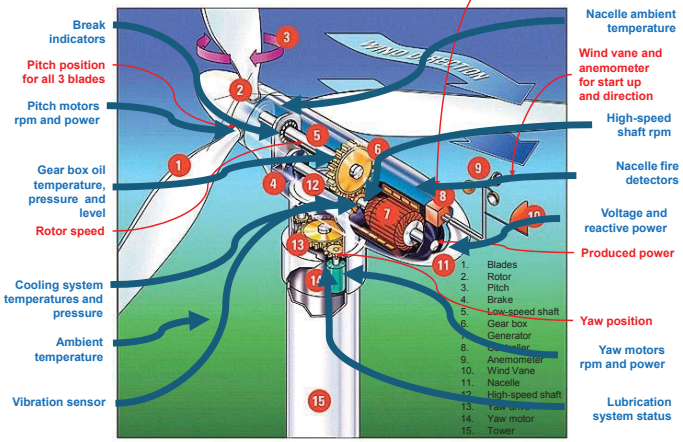

Requirements according to IEC 61400-1 ed.3

8 Control and protection system
8.1 General
Wind turbine operation and safety shall be governed by a control and protection system that meets the requirements of this clause.
Manual or automatic intervention shall not compromise the protection functions. Any device allowing manual intervention must be clearly visible and identifiable, by appropriate marking where necessary.
Settings of the control and protection system shall be protected against unauthorized interference.

8.2 Control functions
The control functions may govern or otherwise limit functions or parameters such as
- **•power;**
- **•rotor speed;**
- **•connection of the electrical load;**
- **•start-up and shutdown procedures;**
- **•cable twist;**
- **•alignment to the wind.**

8.3 Protection functions
The protection functions shall be activated in such cases as
- **•overspeed;**
- **•generator overload or fault;**
- **•excessive vibration;**
- **•abnormal cable twist (due to nacelle rotation by yawing).**

Forskningsrådet

Fremtidens rene energisystem (RENERGI)

WINDSENSE

Add-on instrumentation for Wind Turbines

3 year project (2012-2014):
Funded by NFR

KONGSBERG, Statoil, NTE, TROLLHETTA, SINTEF, MARINTEK, NTNU Det skapende universitet, HST, NCE Instrumentation

Windsense is aimed to develop

- A cost-efficient **add-on instrumentation system** for monitoring of **technical condition** and lifetime related parameters for critical components in a wind turbine
- **Analyse** these data primarily for **prediction** of **component degradation** and estimation of **remaining lifetime.**
- Develop sensors and system components that allow **on-line acquisition and analysis** of data which are currently only obtained by operator handheld equipment.

Windsense
Work packages and responsibilities

Status		Work package	Responsible
✓	WP1	GAP analysis	MARINTEK
✓	WP2	Functional requirement specification	STATOIL
✓	WP3	Evaluation of sensing methods & eq.	HIST
	WP4	Dev. data interpretation algorithms	NTNU
	WP5	Implementation in CM system	KM
	WP6	Laboratory testing	KM
	WP7	Field testing at pilot turbine(s)	STATOIL
	WP8	Development of prediction algorithms	SINTEF ER
	WP9	Implementation of CBM system	MARINTEK
	WP10	Analysis of cost saving potential	TROLLHETTA
	WP11	Administration & dissemination	KM

Windsense
Illustration of data acquisition and analysis

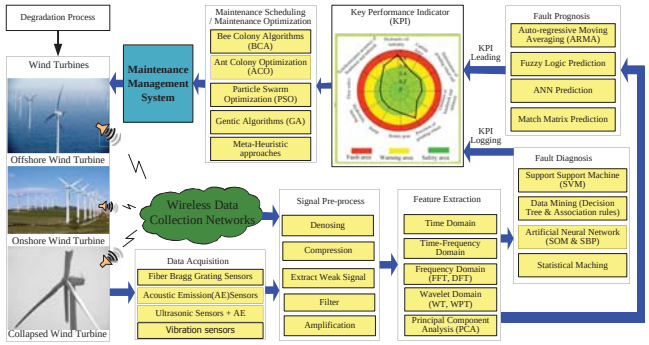

Condition monitoring (CM)
Key: Early warning and less manual inspections

- CM sensors added for real-time condition assessment of all critical Wind Turbine Components i.e.
  - Gearbox
  - Rotor blades
  - Main bearings
  - Drive shafts
  - Oil system
  - Power electronics etc.

Typically observed parameters:
- Temperature
- Oil quality
- Vibration
- Manual wear inspections

Better instrumentation required for online monitoring of Rotor Blades:
- Loads
- Local strain
- Cracks
- Delamination
- Surface defects

- Additional parameters for offshore and floating wind turbines
  - Structural loads
  - Moorings
  - Scouring
  - Corrosion

□on□ition □ase□ □aintenance □□□□□

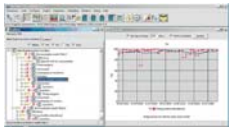

Methods and systems employed especially in the process and offshore industry provides

- An indication of degraded performance or technical condition in a plant
- Efficient drill down capability
- Triggers further investigation with analysis and diagnostics□either through CM system or by manual inspection
- Includes decision support for intervention planning

□oal

A substantial reduction in maintenance cost and increased energy production for offshore wind turbines by

- A significant reduction in number of unplanned service trips
- A reduced number of stops and less downtime
- Controlled operation at reduced load when this is safe rather than full shut down until maintenance can be performed

□□□ □nal□sis

□□□ □ault situations e□aluate□ an□ □an□e□

- System
  - Sub-system
    - □ailure mode
      - □ □ailure symptom
      - □ □ailure effect
      - □ Criticality
      - □ □requency
      - □ Downtime
      - □ CM method□s□
        - Measured parameter
        - Continuous/Batch sampling
        - While turbine is running□
        - Application of method □A-□□□
        - Ob□ective □inspection/diagnostics□

Wind Turbine Components

Annual □ailure Rate and Downtime

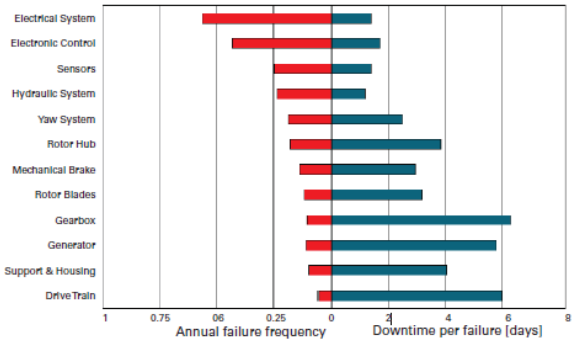

Source: □aulstich et al. 200□1□

□□□□□□ □o□in□

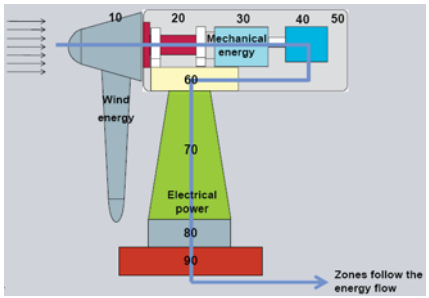

- 00-09: common/central systems
- 10-19: rotor
- 20-29: main shaft
- □0-□9: gearbox
- □0-□9: generator
- □0-□9: nacelle housing
- □0-□9: yaw section
- □0-□9: tower
- □0-□9: transition piece
- 90-99: foundation□monopole.

□pplication o□met□o□ □□□□□

A: The method is commonly used in wind turbines today and normally included in SCADA

B: The method is commonly used in wind turbines today as a manual inspection

C: The method is more advanced and is used on some turbines today, or used in special cases. It typically require special competence from the operator.

D: The method is rarely used, either because it is time-consuming, expensive or that the benefit is not well proven.

E: Experimental methods or prototypes.

F: Future ideas

□□elimina□□ □in□in□s an□ □u□t□e□□o□□

GAP analysis

- A general lack of high frequency data
- Limited use of advanced signal analysis
- Limited data for lifetime prediction
- Need for improved blade monitoring
- Need for improved monitoring of high voltage components

CM methods □to be evaluated with respect to

- Early and secure detection
- Low false alarm rate
- Reliable diagnostics
- Cost/benefit ratio

How the Windsense project can contribute to a reduced CoE

- Replace manual inspections with remote on-line measurements and analysis
- Implement automated diagnostics tools
- [illegible]

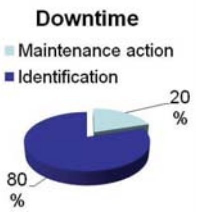

- Reduce consequential damages
- Enable delay of maintenance until proper weather window occur
- Reduce downtime by more efficient fault identification and diagnostics
- Improve maintenance planning by better diagnostics and estimation of remaining lifetime

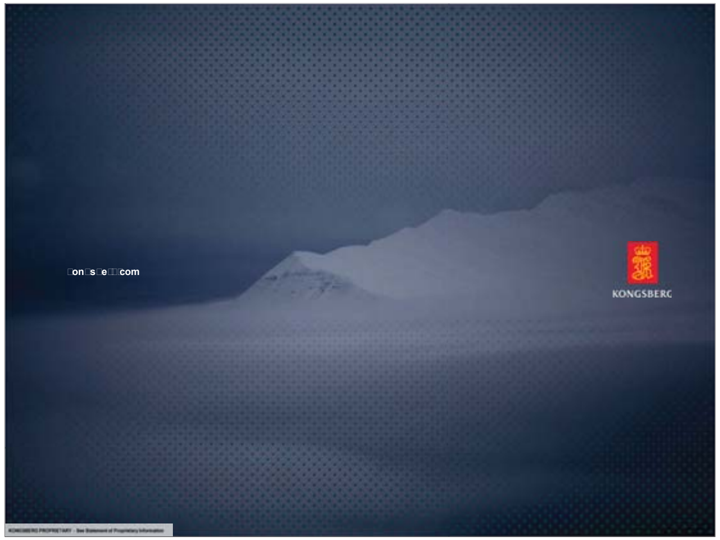

NTNU
Norwegian University of Science and Technology

DeepWind 2013
10th Deep Sea Offshore Wind R&D Conference

Long-Term Analysis of Gear Loads in Fixed Offshore Wind Turbines Considering Ultimate Operational Loadings

Note:
This is a web publication version with images removed, those were copyrighted other than NTNU. The article related to this presentation can be found at "Energy Procedia", an Elsevier journal (around June 2013).

Amir R. Nejad
Ph.D Candidate
NOWITECH / CeSOS

Amir.Nejad(at)ntnu.no

CeSOS – Centre for Ships and Ocean Structures

Outline

- Introduction
- Objectives
- Methodology
- Results: 5 MW case study
- Conclusions

Introduction

- The annual failure rate of the wind turbine gearbox assembly, reported by the EU funded ReliaWind project, is about 5% per wind turbine.

Introduction

- Gears have been around for at least 5,000 years!
- Aristotle (330 BC) writes of gears as if they were commonplace so the beginnings must go back much farther.

- With such a long history, why still problem ?

Introduction

- An overall review of the published researches indicates that the **Design process** may have the biggest contribution to this premature failure.

Objectives

- The ultimate objective of this research is to establish a reliability-based design method for gears in wind turbines.

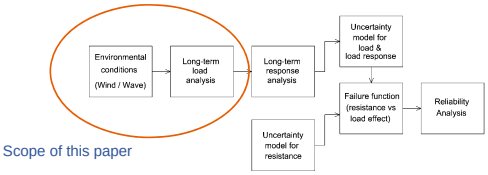

Scope of this paper

Flowchart of structural reliability analysis steps

Methodology

- A) Methods for Gear Load Calculation:
  - A-1) Multi Body System (MBS) method
  - A-2) Rigid Body, Rigid Contact (RBRC) method
- B) Methods for long-term extreme load analysis
  - B-1) Long-term extreme value analysis
  - B-2) Design state or contour line method

Methods for Gear Load Calculation

- A-1) Multi Body System (MBS) method :

In MBS method, each component is modelled as a rigid or flexible body connected with appropriate joints or stiffness to the others.

The motion equation of entire drivetrain is expressed as:

$$\mathbf{M}\ddot{\mathbf{x}} + \mathbf{C}\dot{\mathbf{x}} + \mathbf{K}\mathbf{x} = \mathbf{F}$$

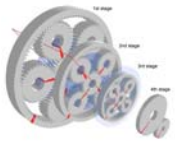

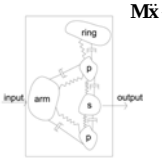

Methodology

- A-2) Rigid Body, Rigid Contact (RBRC) method:

Assumptions:

- Rigid bodies
- Internal gear dynamics is neglected
- Non-torque input loading is ignored

$$\mathbf{F}_i^i(t) = \left(\frac{2\left(m_{Gi} m_{G(i-1)} m_{G(i-2)} .. m_{G(i-n-1)}\right)}{N d_i} \right) \cdot \mathbf{T}_{LS}(t)$$

Verification of RBRC method

- The RBRC method is verified by comparison with a detailed MBS model of NREL 750 kW wind turbine, developed at CeSOS.

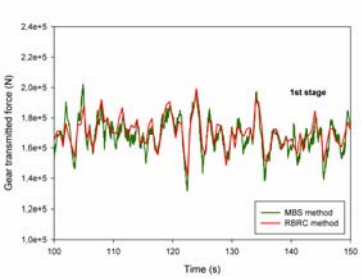

Verification of RBRC method

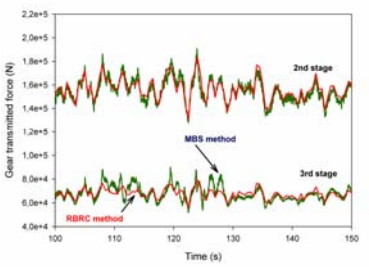

Verification of RBRC method

		mean (kN)	standard deviation (kN)
1st stage	MBS	169.4	11.18
	RBRC	171.0	10.26
2nd stage	MBS	156.1	9.99
	RBRC	157.4	9.44
3rd stage	MBS	67.7	5.69
	RBRC	68.1	4.09

Methods for long-term extreme load analysis

- B)Long-term extreme value analysis:
  - All peak values:

$$F_{Sext-1h}^{LT}(s)=\frac{1}{v_S^+(m)}\int_{cut-in}^{cut-out} v_S^+(m\,|\,u)\cdot F_{Sp}^{ST}(s|u)\cdot f(u)\cdot du$$

$$F_{Sext-1h}^{LT}(s)=\int_{cut-in}^{cut-out} F_{Sp}^{ST}(s|u)\cdot f(u)\cdot du$$

  - All short-term extremes:

$$F_{Sext-1h}^{LT}(s)=\int_{cut-in}^{cut-out} F_{Sext-1h}^{ST}(s|u)\cdot f(u)\cdot du$$

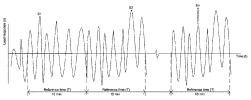

  - Up-crossing rate:

$$F_{Sext-1year}^{LT}(s)=\exp\left\{-T\int_{cut-in}^{cut-out} v_S^+(\xi\,|\,u)\cdot f(u)\cdot du\right\}$$

Methods for long-term extreme load analysis

- B) Design state or contour line method:
  - The contribution from short-term wind states near cut-out is more than the other wind conditions in long-term extreme load response analysis.

Exceedance probability :

$$Q_{Sext-1h}^{ST}(s_0\,|\,u)=1-F_{Sext-1h}^{ST}(s_0\,|\,u)$$

$$s_0=1.75\times T_{rated}$$

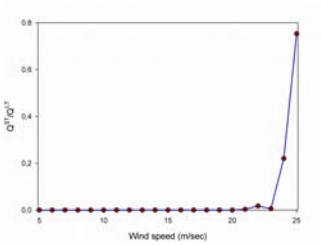

Results: 5 MW

- A floating sun concept gearbox is designed at CeSOS/Nowitech in accordance with wind turbine gearbox design codes e.g. IEC 61400-4 and based on the wind turbine data from NREL 5 MW reference turbine.

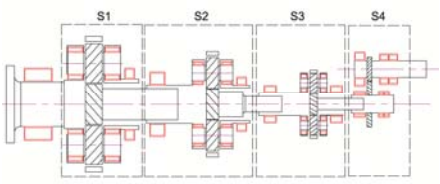

Results: 5 MW

- The aerodynamic simulation of 5 MW case study wind turbine is carried by the Hawc2 version 11.3.

Case	Wind speed	Case	Wind speed	Case	Wind speed
1	5	7	14	13	20
2	7	8	15	14	21
3	9	9	16	15	22
4	11	10	17	16	23
5	12	11	18	17	24
6	13	12	19	18	25

Results: 5 MW

$$T_{rated}=\frac{60P_{rated}}{2\pi n_{rated}}=\frac{60\times 5000}{2\pi\times 12.1}=3{,}946\ \text{KNm}$$

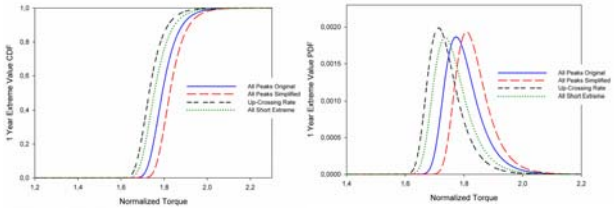

1-year extreme value CDF and PDF of main shaft torque

Results: 5 MW

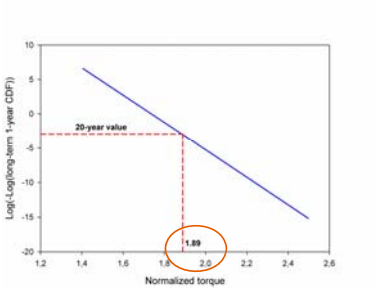

20-year extreme value of main shaft torque

Results: 5 MW

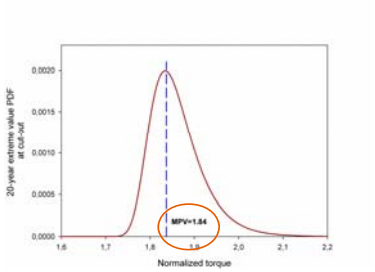

Most Probable Value (MPV) at 25 m/sec

Results: 5 MW

Gumbel parameters of the 1-year long-term distribution of gear transmitted force

F'	$\mu(kN)$	$\alpha(kN)$
1st stage	1077.23	30.36
2nd stage	443.28	12.49
3rd stage	161.19	4.54
4th stage	337.73	9.52

20-year value of gear transmitted force

F'	20-year value (kN)
1st stage	1148.23
2nd stage	472.54
3rd stage	171.83
4th stage	360.03

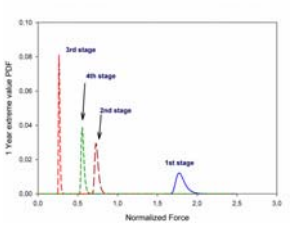

Long-term 1-year extreme value PDF of the gear transmitted force

Concluding remarks

- The 20-year expected extreme value of the 5 MW gearbox input torque is **1.89** times the rated value.
- The cut-out wind speed has the biggest contribution in the long-term gearbox extreme loads.
- 3 long-term extreme value analysis methods are described. It is found that the difference between the methods is about 5-6% of the mean value.
- The difference between Rigid Body, Rigid Contact (RBRC) method and MBS for gear load calculation is about 1% of mean value in LS stage.

E Installation & sub-structures

Structures of offshore converter platforms - Concepts and innovative developments, Joscha Brörmann, Technologiekontor Bremerhaven GmbH

Dynamic analysis of floating wind turbines during pitch actuator fault, grid loss, and shutdown, Erin E. Bachynski, PhD stud, NTNU

Use of a wave energy converter as a motion suppression device for floating wind turbines, Michael Borg, Cranfield University

Loads and response from steep and breaking waves. An overview of the ‘Wave loads’ project, Henrik Bredmose, Associate Professor, DTU Wind Energy

Effect of second-order hydrodynamics on floating offshore wind turbines, Line Roald, ETH Zürich

tkb. Technologiekontor Bremerhaven

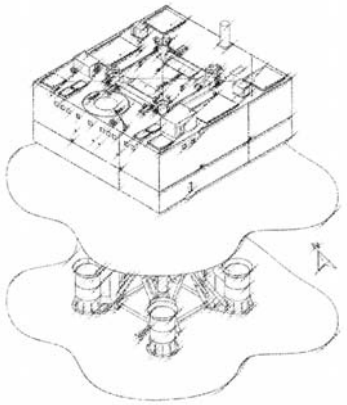

Innovative design for offshore converter platforms

DeepWind'2013

tkb. Technologiekontor Bremerhaven

Content

1. Recent designs
   a. Design & Construction
   b. Installation & Maintainability
2. Optimizations to topside designs
3. Approaches to effective designs

tkb. Technologiekontor Bremerhaven

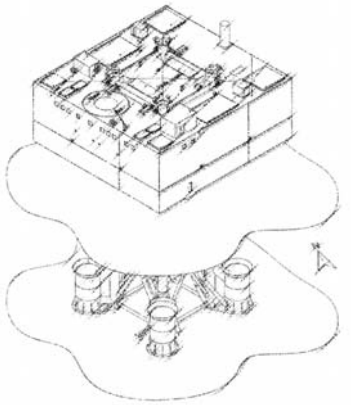

Design & Construction

RECENT DESIGNS

tkb. Technologiekontor Bremerhaven

Recent Designs

Design & Construction

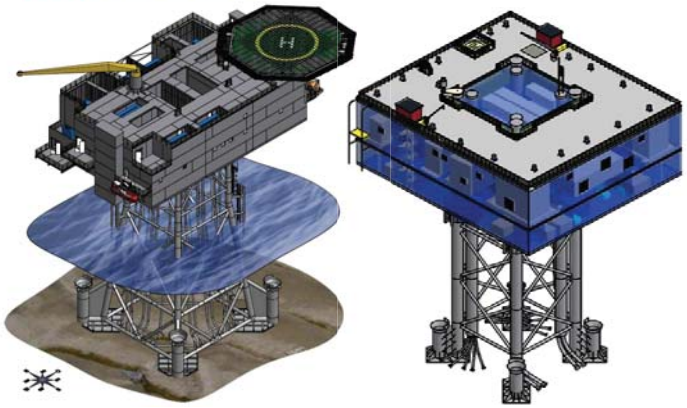

tkb. Technologiekontor Bremerhaven

Recent Designs

Design & Construction

Meerwind OSS (288MW)

- Jacket founded
- Crane Lifted
- water depth 24,7m MSL
- approx. 46m x 30.5 x 12m
- approx. 16,836m3
- 3 Decks + Cable- and Roofdeck
- Partly enclosed
- Air cooled
- External cable deck
- Centralised Design

Baltic II OSS (288MW)

- Jacket founded
- Self erecting
- water depth 32,5m MSL
- approx. 40m x 38m x 15,4m
- approx. 23,408m3
- 3 Decks + Roofdeck
- Fully enclosed
- Seawater cooled
- Internal cable deck
- Decentralised Design

tkb. Technologiekontor Bremerhaven

Recent Designs

Design & Construction

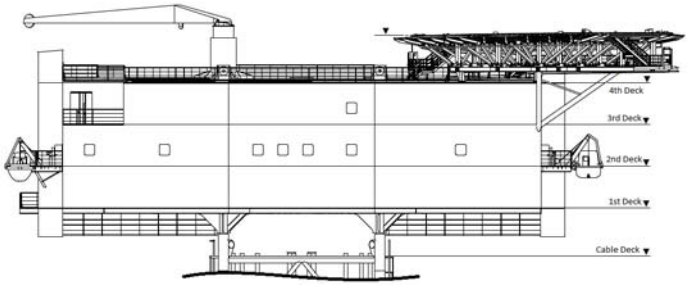

- Cable deck underneath the platform
- 1st and 2nd deck hosting main equipment and oil separator as well as shelter facilities
- 3rd deck hosts auxiliaries, control systems and auxiliary generators
- 4th deck host table heat exchanger, crane and helideck

Recent Designs
Design & Construction

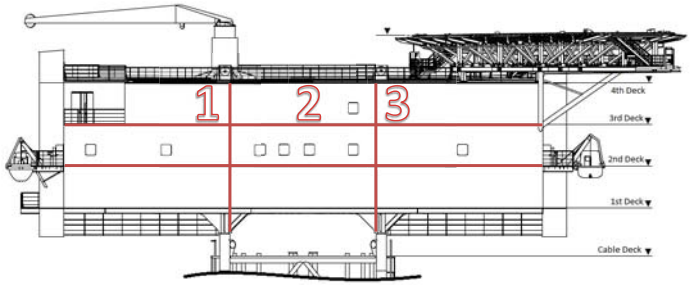

- Thematically segregation into 3 preassembled sections (HV, MV, HVAC)
- Continuous separation into 3 decks
- Further segregation into 28 smaller “container” along main axis 28

Recent Designs
Design & Construction

Equipment Weight Distribution per Deck

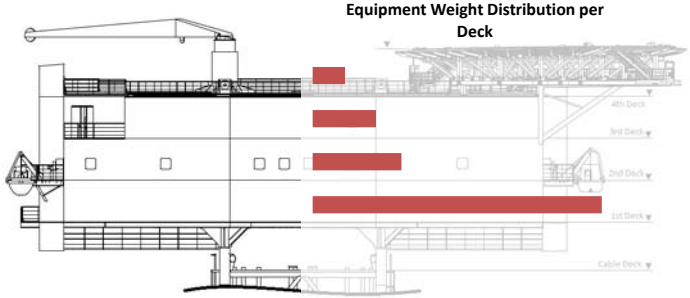

- Allocation of equipment is done with emphasis to keep the COG as low as possible
- Minimization of the extent of the cable deck is utilized by smart allocation of switchgears, transformers and shunt reactors

Installation & Maintainability

RECENT DESIGNS

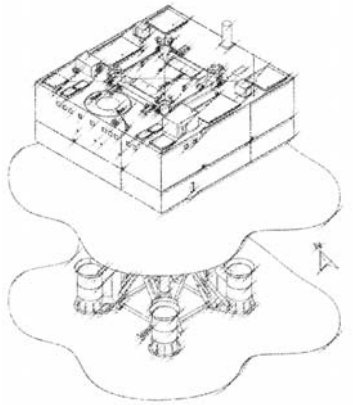

Recent Designs
Installation & Maintainability

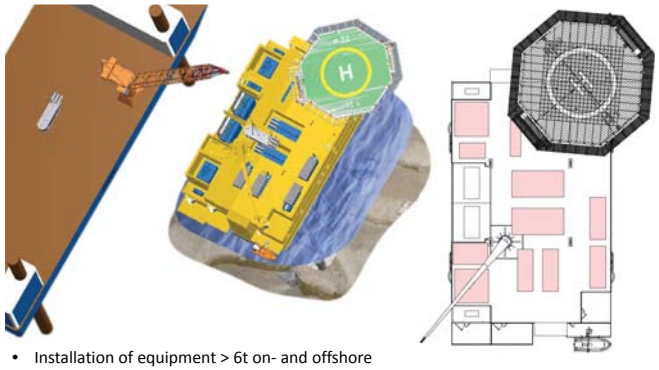

- Installation of equipment > 6t on- and offshore
- All components > 6t with hatches in roof deck

Recent Designs
Installation & Maintainability

- Equipment < 6t mounted on „equipment-tables“
- Applies to equipment located on 1st and 2nd deck having no access via hatches
- Footprint aligned with topside steel structure (multiples of deck stiffener)
- Adjacent tables share same girder
- Orientation either parallel or 90° according to deck stiffener orientation

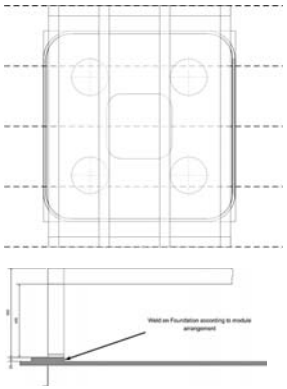

Recent Designs
Installation & Maintainability

- Low floor vehicle
- Load capacity of module table and component
- Manoeuvrable on floor and corridors without additional need for stiffening
- Rotatable around 5 vertical axis
- Storable on platform
- Capable to handle 6 module variants:
  - 2,400mm x 600mm
  - 2,800mm x 1,800mm

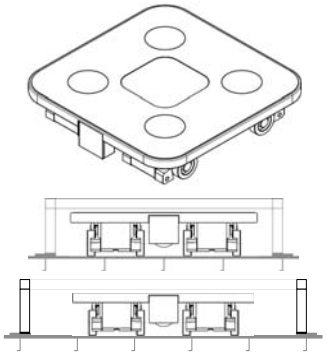

Recent Designs
Installation & Maintainability

- Lifting cart
- Lifting capacity of module and component
- Storable on platform
- Capable to handle 2 module variants:
  - 600mm x 600mm
  - 1,200mm x 600mm

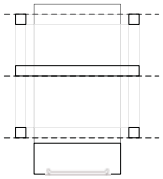

Recent Designs
Installation & Maintainability

- Wall penetration modules
- enables quick installation of equipment
- according to maximum required clear width of module tables
- bolted onto the wall

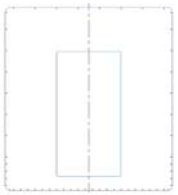
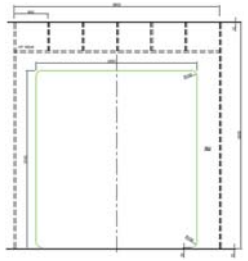

OPTIMIZATION OF TOPSIDE STRUCTURES

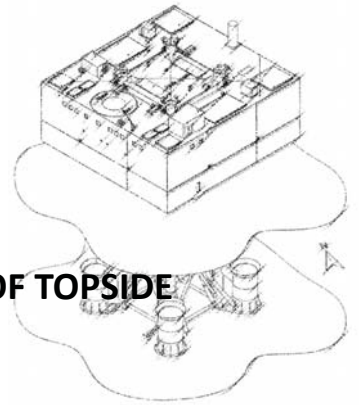

Optimization of topside designs

- Integration of equipment foundations into topside structure
- Using provided „Holland Profiles“ within deck structure
- Reduces interfering contours in lower decks

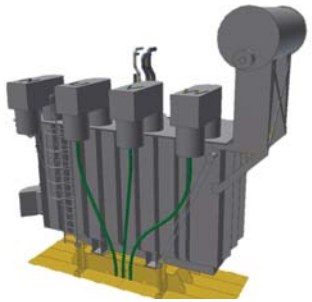

Optimization of topside designs

- superimposed crane column
- Using provided „Holland Profiles“ and walls to convey the forces into the topside structure

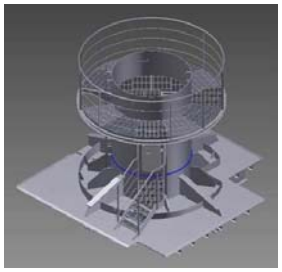

APPROACHES TO EFFECTIVE DESIGNS

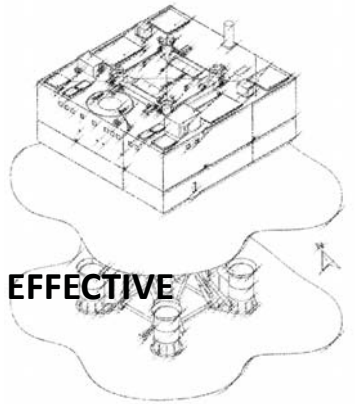

NTNU
Norwegian University of Science and Technology

Norwegian Centre of Excellence

Dynamic analysis of floating wind turbines during pitch actuator fault, grid loss, and shutdown

Erin E. Bachynski, Mahmoud Etemaddar, Marit I. Kvittem, Chenyu Luan, Torgeir Moan
Center for Ships and Ocean Structures, NTNU
NOWITECH

10th Deep Sea Offshore Wind R&D Conference
Trondheim, January 25th, 2013

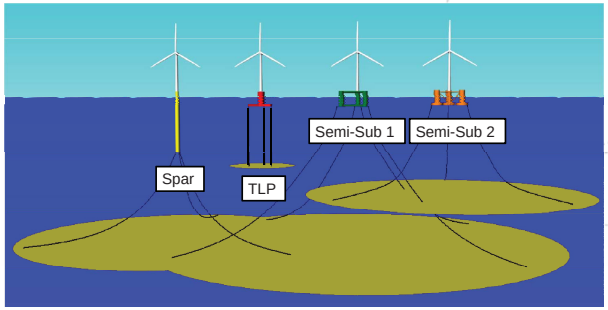

What are the consequences of control system faults?

How do the loads due to faults compare to loads due to extreme conditions?

Outline

- Floating wind turbine models
- Analysis tool: Simo-Riflex-AeroDyn
- Blade pitch and grid faults
- Floating turbine responses
- Summary

Floating Wind Turbine Models

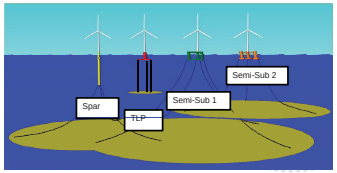

	Spar	TLP	Semi-Sub 1	Semi-Sub 2
Water depth (m)	320	150	320	200
Displacement (tonnes)	8 227	5 796	4 640	13 473
Draft (m)	120	22	17	20
Surge period (s)	129.5	41.9	99.9	115.9
Sway period (s)	129.5	41.9	159.8	115.9
Heave period (s)	31.7	0.6	20.0	17.1
Roll/Pitch period (s)	29.7	2.8	42.1	26.0
Yaw period (s)	8.2	18.0	66.7	80.2

Semi-Sub 1: Active Ballast

- Small hydrostatic restoring stiffness (C_{44}/C_{55})
- Ballast system: PID loop, 20 minutes (Roddier, 2011)

Normal operation

Sudden shutdown during normal operation

Consequent Static Angle

WS (m/s)	Angle (deg)
8	7.0
11.4	13.1
14	8.4
17	6.8
20	5.9

Fault Condition Implementation in Simo-Riflex-AeroDyn

- Nonlinear time domain coupled code
- Single structural solver
- Control code (java) modified to allow
  - Blade pitch error at a given time
  - Grid error at a given time
  - Emergency shutdown (aerodynamic braking, grid disconnect)
- Fault conditions for different platforms, including advanced hydrodynamics
- Good agreement with HAWC2 (land-based and spar, including fault)

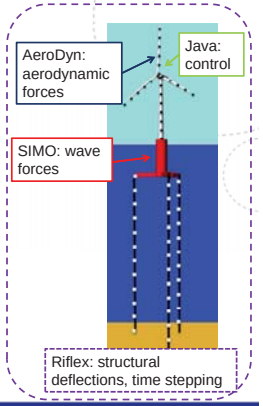

7

Fault and Shutdown

Fault	Definition
A	No fault
B	Blade seize
C	Blade seize + shutdown
D	Grid loss + shutdown

- **Blade seize (B/C)**: one blade stops pitching
- **Grid loss (D)**: generator torque drops to zero
- **Shutdown (C/D)**: generator torque drops to zero, all unfaulted blades pitch to feather (90 deg)
- Shutdown begins 0.1 s after fault occurs

Land-Based, U = 20m/s, Case C

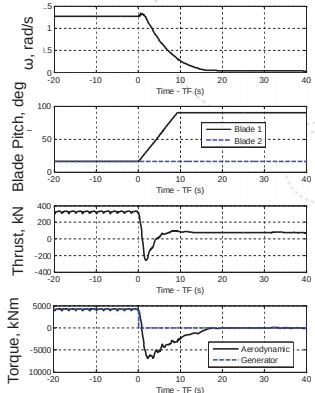

8

Environmental/ Fault Conditions

Fault	Definition
A	No fault
B	Blade seize
C	Blade seize + shutdown
D	Grid loss + shutdown

EC	U (m/s)	Hs (m)	Tp (s)	Turb. Model	Faults	# Sims.	Sim. length* (s)
1	8.0	2.5	9.8	NTM	A, B, C, D	30	16 min.
2	11.4	3.1	10.1	NTM	A, B, C, D	30	16 min.
3	14.0	3.6	10.3	NTM	A, B, C, D	30	16 min.
4	17.0	4.2	10.5	NTM	A, B, C, D	30	16 min.
5	20.0	4.8	10.8	NTM	A, B, C, D	30	16 min.
6	49.0	14.1	13.3	NTM	A (idling)	6	3 hours
7	11.2	3.1	10.1	ETM	A	6	3 hours

Max. thrust

50 yr. storm

Ext. turb.

* Simulation length after 200s initial constant wind period

9

Maximum loads

EC	U (m/s)
1	8.0
2	11.4
3	14.0
4	17.0
5	20.0
6	49.0
7	11.2 (ETM)

Fault	Definition
A	No fault
B	Blade seize
C	Blade seize + shutdown
D	Grid loss + shutdown

Absolute maximum/Expected maximum

Response	Land-based	Spar	TLP	Semi-Sub 1	Semi-Sub 2
Platform Pitch Motion	-	6A/6A	6A/6A	2D/2D	6A/6A
Platform Yaw Motion	-	6A/6A	5C/5C	5C/5C	7A/7A
Mooring System	-	6A/6A	6A/6A	6A/6A	6A/6A
Tower Base FA Moment	2C/2D	6A/6A	6A/6A	6A/2D	6A/6A
Tower Base SS Moment	5C/5C	6A/6A	5C/4C	6A/6A	6A/6A
Tower Top FA Moment	2C/2C	2C/2C	3C/2C	2C/2C	2C/2C
Tower Top SS Moment	5B/5B	4B/5B	5B/5B	5B/5B	5B/5B
(not faulted) Flapwise Moment	4B/7A	4B/7A	5B/7A	3B/7A	4B/7A
(not faulted) Edgewise Moment	2C/2D	2C/2C	3C/3D	4D/3C	6A/6A
(faulted) Flapwise Moment	3B/7A	3B/7A	3B/7A	2B/7A	3B/2B
(faulted) Edgewise Moment	3D/3D	5D/3D	2D/3D	4D/2D	4C/5C

10

Maximum loads

EC	U (m/s)
1	8.0
2	11.4
3	14.0
4	17.0
5	20.0
6	49.0
7	11.2 (ETM)

Fault	Definition
A	No fault
B	Blade seize
C	Blade seize + shutdown
D	Grid loss + shutdown

Absolute maximum/Expected maximum

Response	Land-based	Spar	TLP	Semi-Sub 1	Semi-Sub 2
Platform Pitch Motion	-	6A/6A	6A/6A	2D/2D	6A/6A
Platform Yaw Motion	-	6A/6A	5C/5C	5C/5C	7A/7A
Mooring System	-	6A/6A	6A/6A	6A/6A	6A/6A
Tower Base FA Moment	2C/2D	6A/6A	6A/6A	6A/2D	6A/6A
Tower Base SS Moment	5C/5C	6A/6A	5C/4C	6A/6A	6A/6A
Tower Top FA Moment	2C/2C	2C/2C	3C/2C	2C/2C	2C/2C
Tower Top SS Moment	5B/5B	4B/5B	5B/5B	5B/5B	5B/5B
(not faulted) Flapwise Moment	4B/7A	4B/7A	5B/7A	3B/7A	4B/7A
(not faulted) Edgewise Moment	2C/2D	2C/2C	3C/3D	4D/3C	6A/6A
(faulted) Flapwise Moment	3B/7A	3B/7A	3B/7A	2B/7A	3B/2B
(faulted) Edgewise Moment	3D/3D	5D/3D	2D/3D	4D/2D	4C/5C

11

Motions and Mooring Loads

- Largely unaffected by fault
- Exceptions:
  - Semi-sub 1: pitch motion after shutdown
  - Spar & TLP: yaw after blade seize + shutdown

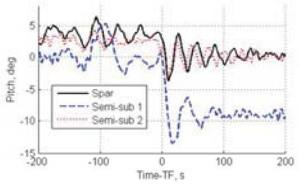

EC 3, case D

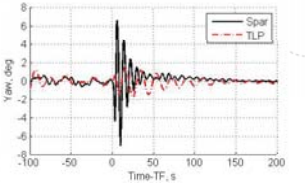

EC 2, case C

12

Maximum loads

EC	U (m/s)
1	8.0
2	11.4
3	14.0
4	17.0
5	20.0
6	49.0
7	11.2 (ETM)

Fault	Definition
A	No fault
B	Blade seize
C	Blade seize + shutdown
D	Grid loss + shutdown

Absolute maximum/Expected maximum

Response	Land-based	Spar	TLP	Semi-Sub 1	Semi-Sub 2
Platform Pitch Motion	-	6A/6A	6A/6A	2D/2D	6A/6A
Platform Yaw Motion	-	6A/6A	5C/5C	5C/5C	7A/7A
Mooring System	-	6A/6A	6A/6A	6A/6A	6A/6A
Tower Base FA Moment	2C/2D	6A/6A	6A/6A	6A/2D	6A/6A
Tower Base SS Moment	5C/5C	6A/6A	5C/4C	6A/6A	6A/6A
Tower Top FA Moment	2C/2C	2C/2C	3C/2C	2C/2C	2C/2C
Tower Top SS Moment	5B/5B	4B/5B	5B/5B	5B/5B	5B/5B
(not faulted) Flapwise Moment	4B/7A	4B/7A	5B/7A	3B/7A	4B/7A
(not faulted) Edgewise Moment	2C/2D	2C/2C	3C/3D	4D/3C	6A/6A
(faulted) Flapwise Moment	3B/7A	3B/7A	3B/7A	2B/7A	3B/2B
(faulted) Edgewise Moment	3D/3D	5D/3D	2D/3D	4D/2D	4C/5C

13

Tower Top Bending Moments

- Blade seize increases both fore-aft and side-side loads
- Side-side loads are reduced by shutdown

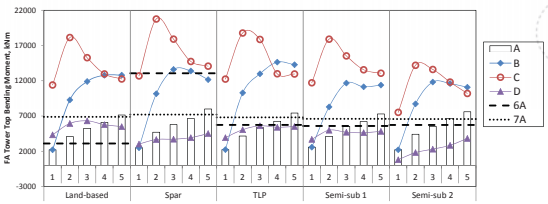

14

Maximum loads

EC	U (m/s)
1	8.0
2	11.4
3	14.0
4	17.0
5	20.0
6	49.0
7	11.2 (ETM)

Fault	Definition
A	No fault
B	Blade seize
C	Blade seize + shutdown
D	Grid loss + shutdown

Absolute maximum/Expected maximum

Response	Land-based	Spar	TLP	Semi-Sub 1	Semi-Sub 2
Platform Pitch Motion	-	6A/6A	6A/6A	2D/2D	6A/6A
Platform Yaw Motion	-	6A/6A	5C/5C	5C/5C	7A/7A
Mooring System	-	6A/6A	6A/6A	6A/6A	6A/6A
Tower Base FA Moment	2C/2D	6A/6A	6A/6A	6A/2D	6A/6A
Tower Base SS Moment	5C/5C	6A/6A	5C/4C	6A/6A	6A/6A
Tower Top FA Moment	2C/2C	2C/2C	3C/2C	2C/2C	2C/2C
Tower Top SS Moment	5B/5B	4B/5B	5B/5B	5B/5B	5B/5B
(not faulted) Flapwise Moment	4B/7A	4B/7A	5B/7A	3B/7A	4B/7A
(not faulted) Edgewise Moment	2C/2D	2C/2C	3C/3D	4D/3C	6A/6A
(faulted) Flapwise Moment	3B/7A	3B/7A	3B/7A	2B/7A	3B/2B
(faulted) Edgewise Moment	3D/3D	5D/3D	2D/3D	4D/2D	4C/5C

15

Blade Bending Moments

- Relatively small change in load magnitude
- Unfaulted blades are also affected by blade seize (flapwise)
- Edgewise loads can be large during shutdown

5B: Blade seize

5C: Blade seize + shutdown

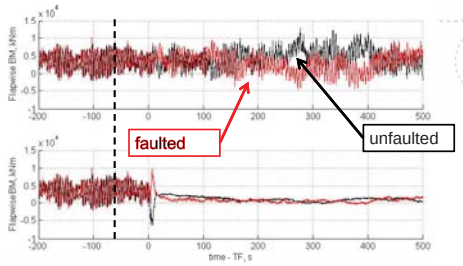

16

Summary

- Fault has relatively little effect on global motions/mooring loads
  - Exception: semi-sub 1 (pitch due to shutdown)
  - Exception: spar & TLP (yaw due to blade seize)
- Fault has relatively little effect on tower base loads for floating platforms (compared to wave-induced loads)
- Blade seize faults greatly increase tower top loads
  - Shutdown works for mitigation in high winds, less effect for lower winds
  - Shutdown less effective for spar, semi-sub
- Blade seize faults increase flapwise blade loads
- Shutdown can cause large edgewise blade loads

17

Future Work

- Azimuthal dependence
- Misaligned wind and wave conditions – with and without fault
- Fatigue due to undetected/unmitigated faults
- Sensor faults
- Different control strategies in response to blade seize
- Detailed analysis of gearbox loads due to fault

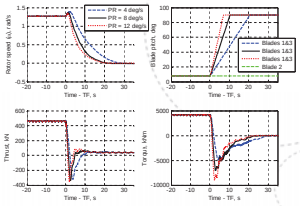

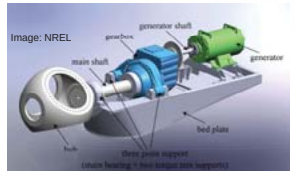

18

Approaches to Effective Designs

- Introduction of a design hierarchy with
- Breakdown the design problem into sub-problems
- Problem formulation down to single equipment level

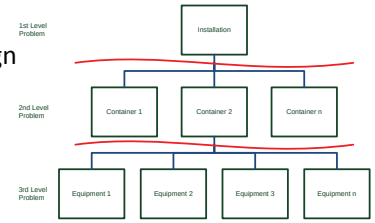

Approaches to Effective Designs

- Introduction of Generic Algorithms to solve allocation problem automatically
- Development of relevant:
  - design constraints
  - safety requirements
  - equipment requirements
  - cost functions
- Introduction of interface variants as an additional degree of freedom during design
- Development of a equipment database including variables:
  - *oilvolume*
  - *accessablesides*
  - *solascategory*
  - *massinstallation*
  - *massoperation*

Approaches to Effective Designs

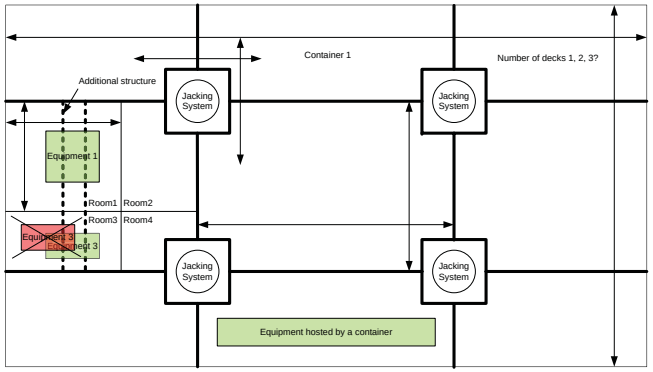

QUESTIONS?

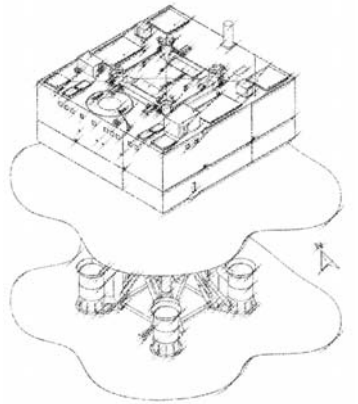

THANK YOU FOR YOUR ATTENTION

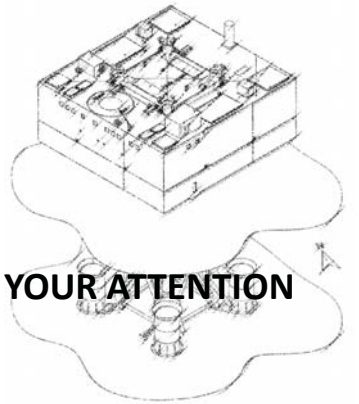

Use of a wave energy converter as a motion suppression device for floating wind turbines

25th January, 2013

Michael Borg,
Cranfield University

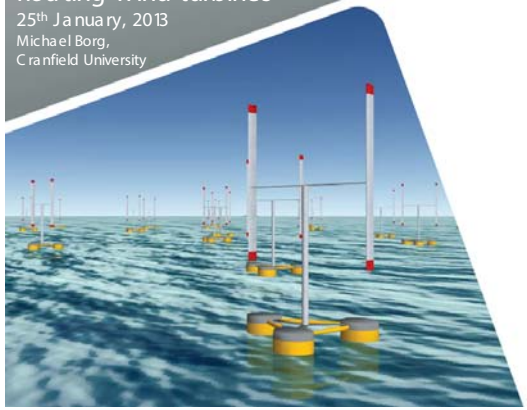

Cranfield UNIVERSITY

www.cranfield.ac.uk

Outline

- Introduction
- System Description
- Methodology
- WEC Parameters
- Numerical Model
- Results
- Conclusions

Cranfield UNIVERSITY

www.cranfield.ac.uk

Introduction

- Floating platforms subject to large-amplitude motion
  - →Increased fatigue loads
  - →Reduced aerodynamic performance

Increased cost of electricity

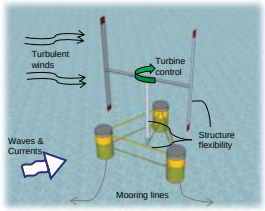

Cranfield UNIVERSITY

www.cranfield.ac.uk

Introduction

- Use of passive damping devices to reduce motion

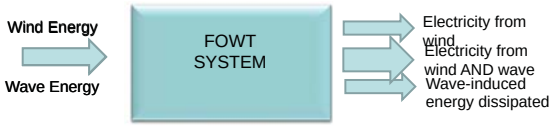

- Propose that this energy is captured using a WEC
  - →Increased system energy yield
  - →Shared infrastructure and reduced costs

Cranfield UNIVERSITY

www.cranfield.ac.uk

Methodology

- Hypothetical WEC is considered.
  - No characteristic constraints
  - No geometry considered → No hydrodynamic forces
- Assumed to move only in heave
- Connected to FOWT with spring-damper system
- Identify spring-damper characteristics for two cases:

1. Maximum Motion Reduction
2. Maximum Energy Extraction

Cranfield UNIVERSITY

www.cranfield.ac.uk

System Description

- 5MW Vertical Axis Wind Turbine mounted on Trifloater
- Dogger Bank site, North Sea
  - →JONSWAP spectrum
  - →H_s=4.9 m ; T_z=10s

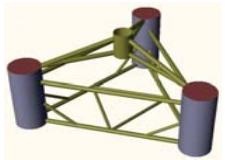

- Hypothetical WEC: additional degree of freedom in heave
  - →Connected through PTO spring-damper coupling

Cranfield UNIVERSITY

www.cranfield.ac.uk

WEC Parameters

- Mass → 3 cases: 2.5%, 5% and 10% of FOWT mass
  → based on Refs. [1], [2]
- Damping → Damping ratio (ζ) varied from 0.17 to 7.7
  → 5 cases
- Stiffness → 3 cases: WEC nat. freq.(ω_n)= FOWT ω_n
  1 cases: Varied 25% to 200% FOWT ω_n
  → constant damping

$$m\ddot{x} + 2\zeta\omega_n\dot{x} + \omega_n^2 x = F_{exc}$$

Numerical Model

- Based on Marine Systems Simulator Toolbox [3] in the MATLAB/Simulink environment
- Cummins Eqn. used with radiation-force approximation
- Aerodynamics modelled with Double Multiple Streamtube model with modifications [4]
- Gyroscopic forces also included [5]

Results
Maximum Energy Extraction

- Found to occur with largest mass and lowest PTO damping
- Shifting WEC ω_n reduces power absorbed

Absorbed Power vs. Supply Reliability

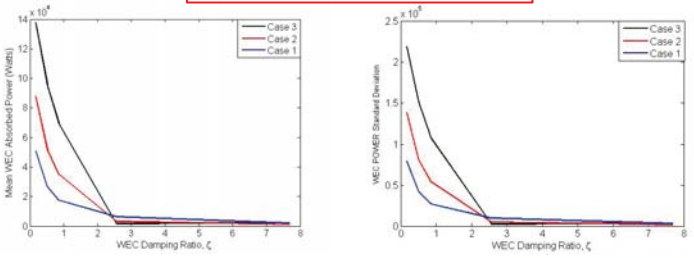

Results
Effect of WEC Damping

- Increase in PTO damping led to smaller motion reduction
- Damping ratio > 1 → RAO deteriorates

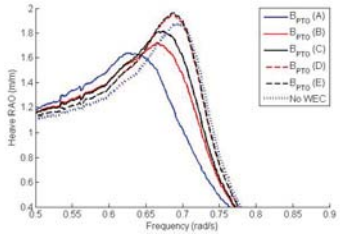

Results
Maximum Motion Reduction

- Occurs when WEC ω_n is lower than FOWT ω_n

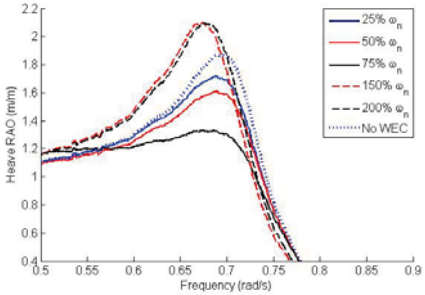

- 15% reduction in heave mean amplitude
- 29% reduction in RAO peak response

Conclusions

- Proposed concept of using a WEC to reducing FOWT motion and increase cost-effectiveness.
- Maximum energy extraction from the WEC is achieved by matching the WEC ω_n to the FOWT ω_n and using low damping ratios.
- Maximum motion reduction of the FOWT is achieved by shifting the WEC to a lower frequency than the FOWT ω_n.
- Importance of maximising energy yield per unit area of ocean utilised.

Cranfield UNIVERSITY

Thank you for your attention

References

[1] Peiffer, A., Roddier, D. and Aubault, A. (2011), "Design of a point absorber inside the WindFloat structure", *Proceedings of the International Conference on Offshore Mechanics and Arctic Engineering - OMAE, Vol. 5, pp. 247.*
[2] Muliawan, M. J., Karimirad, M. and Moan, T. (2013), "Dynamic response and power performance of a combined Spar-type floating wind turbine and coaxial floating wave energy converter", *Renewable Energy, vol. 50, pp. 47-57.*
[3] Fossen, T. I. and Perez, T. , *MSS. Marine Systems Simulator (2010), available at: http://www.marinecontrol.org (accessed*16.04.2012).
[4] Shires, A. (2013), "Design optimisation of an offshore vertical axis wind turbine", *Proc. Inst of Civil Engineers, Energy, vol.*166, no. EN0, pp. 1-12.
[5] Blusseau, P. and Patel, M. H. (2012), "Gyroscopic effects on a large vertical axis wind turbine mounted on a floating structure", *Renewable Energy.*

Loads and response from steep and breaking waves
An overview of the "Wave loads" project

Henrik Bredmose
Associate prof, DTU Wind Energy

Jacob Tornfeldt Sørensen
Head of innovation, Ports and Offshore Technology, DHI

Torben Juul Larsen
Senior Scientist, DTU Wind Energy

DTU Wind Energy
Department of Wind Energy

DHI

Wave loads on offshore wind turbines

ForskEL. DTU Wind, DHI, DTU MEK. 2010-2013. 10.5MDKK.

Statkraft

Henrik Bredmose
Signe Schløer
Torben Larsen
Taessong Kim

Jacob Tornfeldt Sørensen
Flemming Schlütter
Jesper Mariegaard
Anders Wedel Nielsen
Hans Fabricius Hansen

Bo Terp Paulsen
Harry Bingham

DTU Wind Energy
Department of Wind Energy

DHI

Wave loads on offshore wind turbines

ForskEL. DTU Wind, DHI, DTU MEK. 2010-2013.

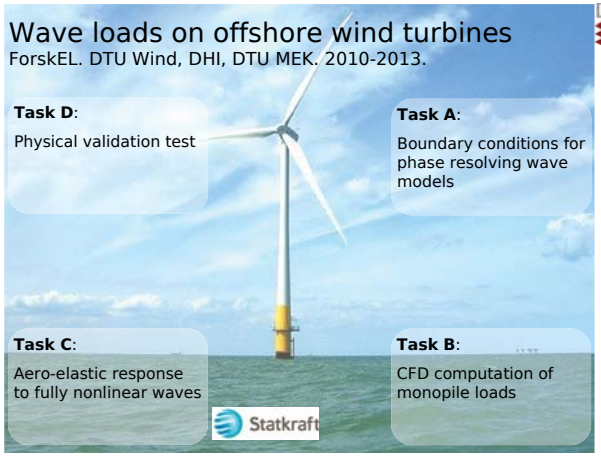

Task D:
Physical validation test

Task A:
Boundary conditions for phase resolving wave models

Task C:
Aero-elastic response to fully nonlinear waves

Task B:
CFD computation of monopile loads

Statkraft

DTU Wind Energy
Department of Wind Energy

DHI

Hydrodynamic loads

Simplest: Linear wave kinematics and Morison equation

$$F = \frac{1}{2}\rho C_D D|U|U + \rho C_M A\frac{dU}{dt}$$

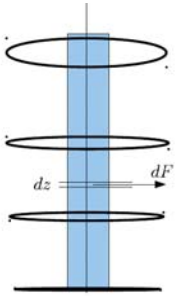

DTU Wind Energy
Department of Wind Energy

DHI

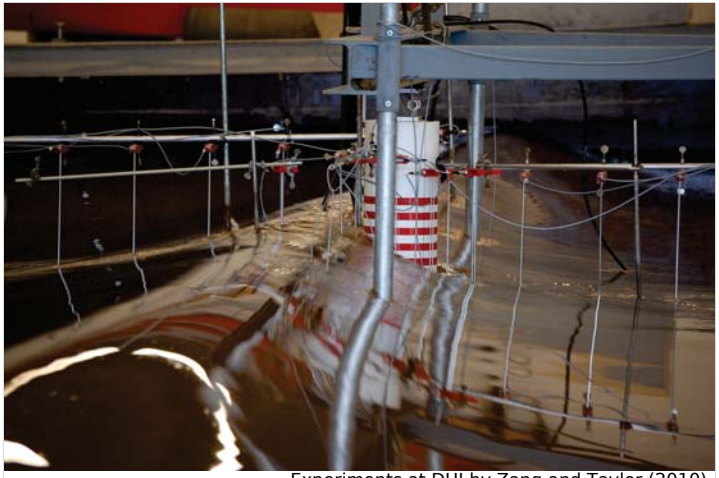

Experiments at DHI by Zang and Taylor (2010)

DTU Wind Energy
Department of Wind Energy

DHI

Hydrodynamic loads

Simples: Linear wave kinematics and Morison equation

$$F = \frac{1}{2}\rho C_D D|U|U + \rho C_M A\frac{dU}{dt}$$

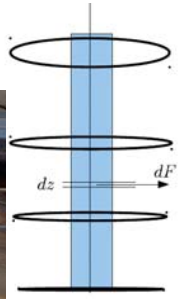

Better: Fully nonlinear wave kinematics and Morison equation

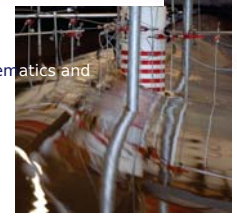

Zang and Taylor (2010)

DTU Wind Energy
Department of Wind Energy

DHI

Hydrodynamic loads

Simples: Linear wave kinematics and Morison equation

$$F = \frac{1}{2}\rho C_D D|U|U + \rho C_M A\frac{dU}{dt}$$

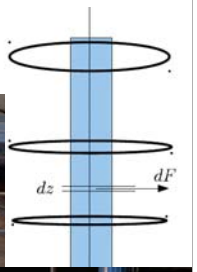

Better: Fully nonlinear wave kinematics and Morison equation

Advanced: CFD and coupled CFD

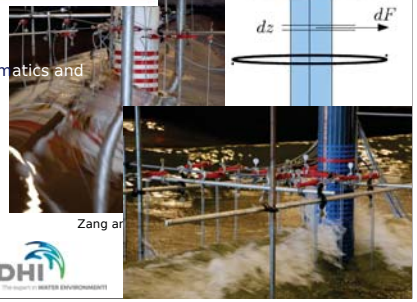

Zang ar

DTU Wind Energy
Department of Wind Energy

Forces from a fully nonlinear potential flow solver

'OceanWave3D', Engsig-Karup et al (2009)
Allan Engsig-Karup, Harry Bingham and Ole Lindberg

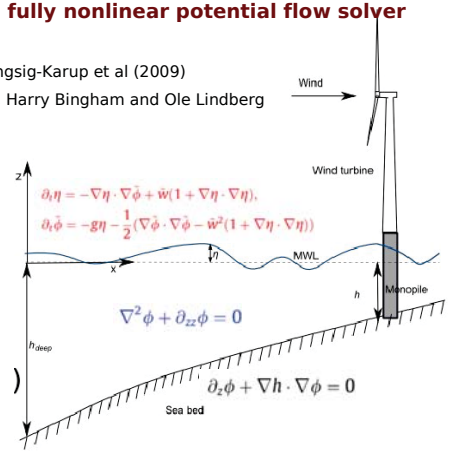

DTU Wind Energy
Department of Wind Energy

Apply within Flex5 aero-elastic model

Flex5, developed by Stig Øye at DTU
Widely used in industry
Modal approach → runs at 8 x real time

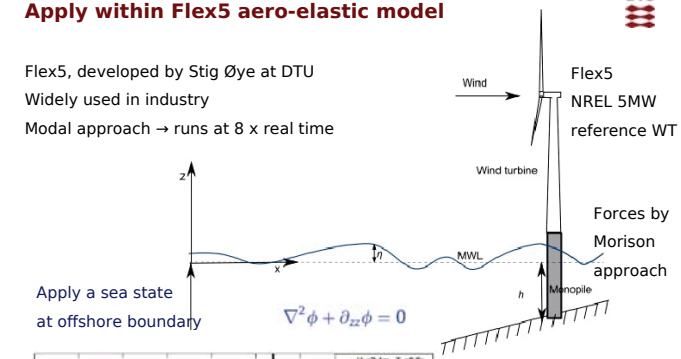

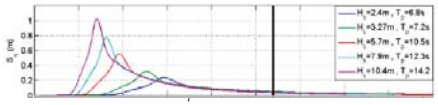

Signe Schløer

DTU Wind Energy
Department of Wind Energy

Response in bottom of tower

Fully nonlinear waves versus linear waves

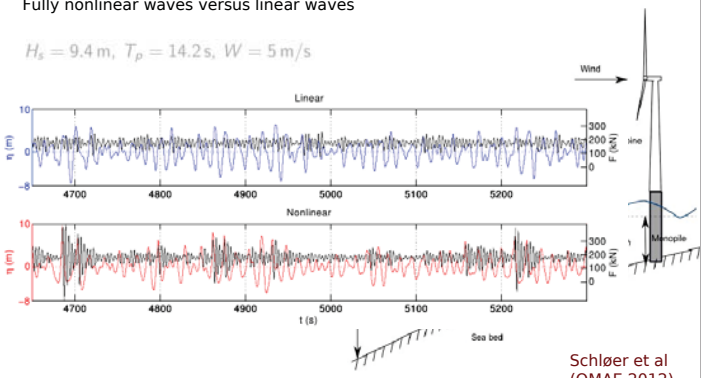

Schløer et al
(OMAE 2012)

DTU Wind Energy
Department of Wind Energy

Response in bottom of tower

Fully nonlinear waves versus linear waves

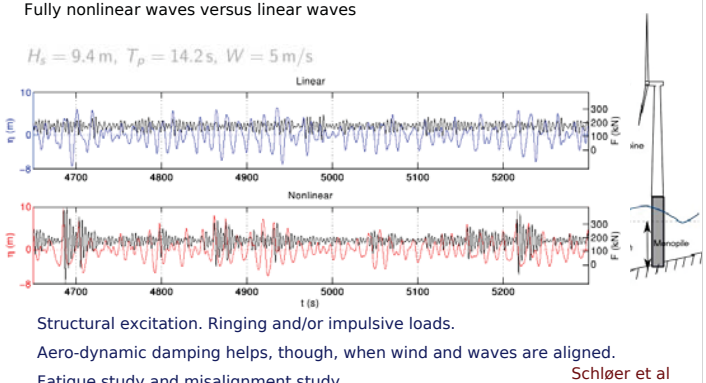

Structural excitation. Ringing and/or impulsive loads.

Aero-dynamic damping helps, though, when wind and waves are aligned.

Fatigue study and misalignment study.

Schløer et al
(OMAE 2012)

DTU Wind Energy
Department of Wind Energy

The OC4 jacket

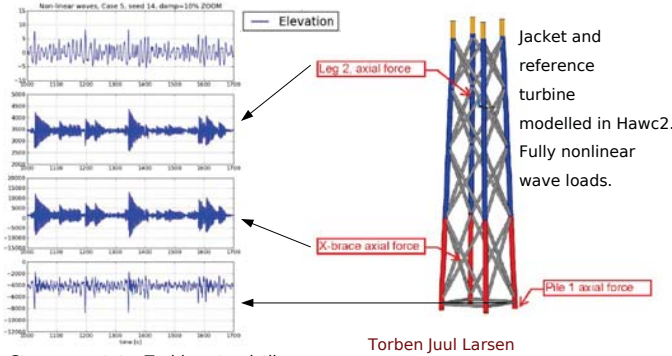

Jacket and
reference
turbine
modelled in Hawc2.
Fully nonlinear
wave loads.

Storm sea state. Turbine standstil.

Severe ringing/impulsive excitation.

Torben Juul Larsen
Taesong Kim
Larsen et al Europ. Offsh. Wind 2011

DTU Wind Energy
Department of Wind Energy

Wave loads on offshore wind turbines

ForskEL. DTU Wind, DHI, DTU MEK. 2010-2013.

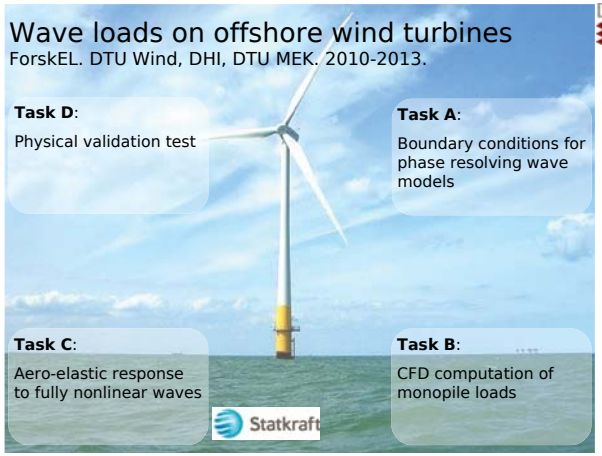

DTU Wind Energy
Department of Wind Energy

DHI

The OpenFOAM® CFD solver

Open source CFD toolbox
Vast attention during last 3 years

This study: interFoam solver
- 3D incompressible Navier-Stokes
- two phases (water and air)
- VOF treatment of free surface

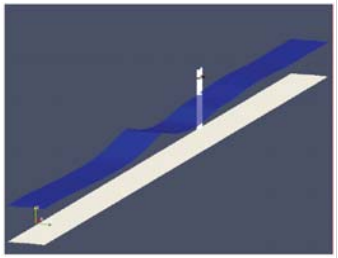

Waves2foam wave generation toolbox has been developed and validated
(Niels Gjøl Jacobsen
PhD thesis 2011; Paper in Coastal Engineering)

DTU Wind Energy
Department of Wind Energy

DHI

Second-order focused wave group

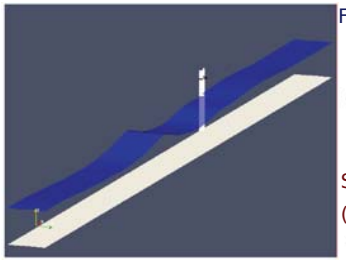

First-order wave field

$$\eta^{(1)}(x,t) = \sum_{p=1}^{N} a_p \cos(k_p(x-x_0) - \omega_p(t-t_0))$$

$$\phi^{(1)}(x,z,t) = \sum_{p=1}^{N} b_p \frac{\cosh k_p(h+z)}{\cosh k_p h} \times \sin(k_p(x-x_0) - \omega_p(t-t_0))$$

Second-order wave field
(Sharma & Dean 1981)

$$\eta^{(2)}(x,t) = \frac{1}{4}\sum_{i=1}^{N}\sum_{j=1}^{N}[\quad (3)$$
$$T_{ij}^{-} a_i a_j \cos((k_i - k_j)(x-x_0) - (\omega_i - \omega_j)(t-t_0))$$
$$+T_{ij}^{+} a_i a_j \cos((k_i + k_j)(x-x_0) - (\omega_i + \omega_j)(t-t_0))]$$

DTU Wind Energy
Department of Wind Energy

DHI

2D wave calibration

Free surface elevation

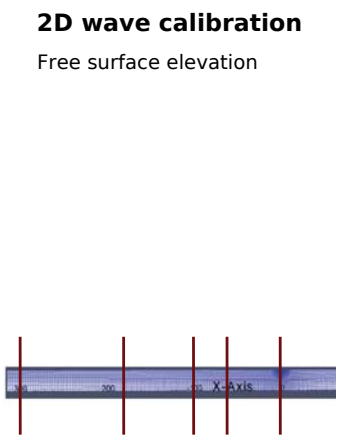

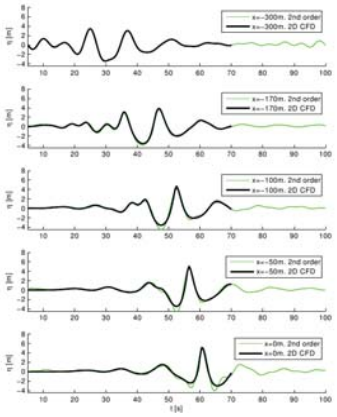

DTU Wind Energy
Department of Wind Energy

DHI

Platform height of 8.96

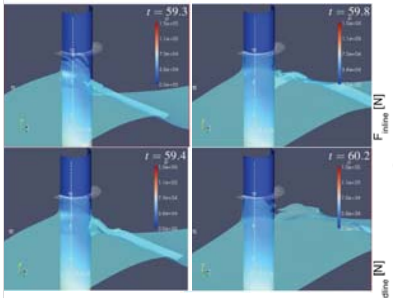

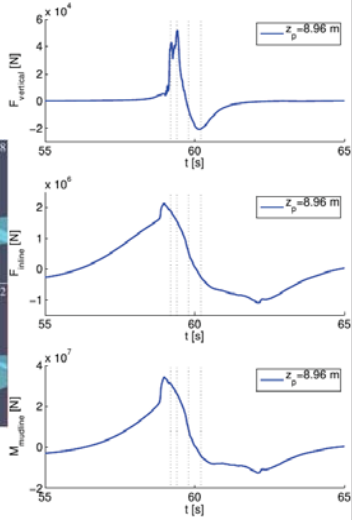

DTU Wind Energy
Department of Wind Energy

DHI

Platform height of 8.96m

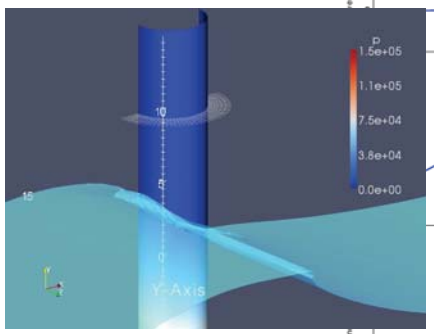

t=58.8s

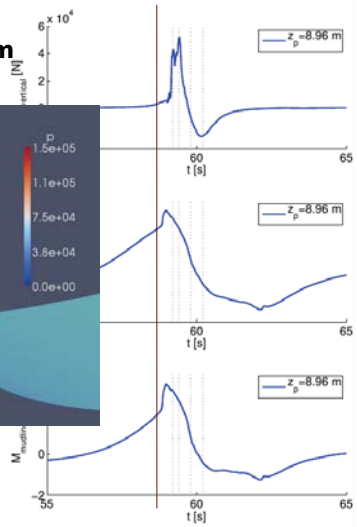

DTU Wind Energy
Department of Wind Energy

DHI

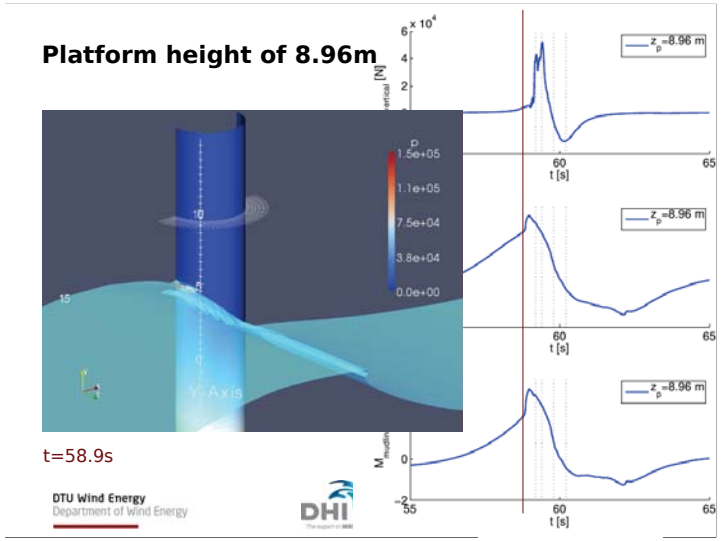
Platform height of 8.96m
t=58.9s
DTU Wind Energy
Department of Wind Energy
DHI

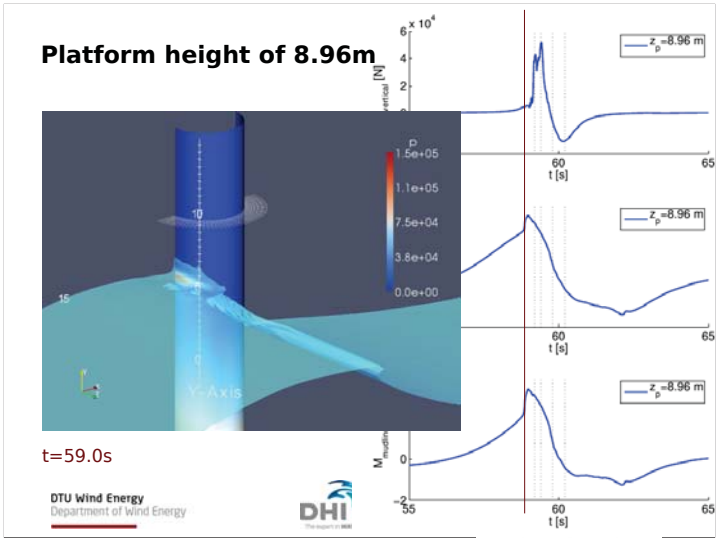
Platform height of 8.96m
t=59.0s
DTU Wind Energy
Department of Wind Energy
DHI

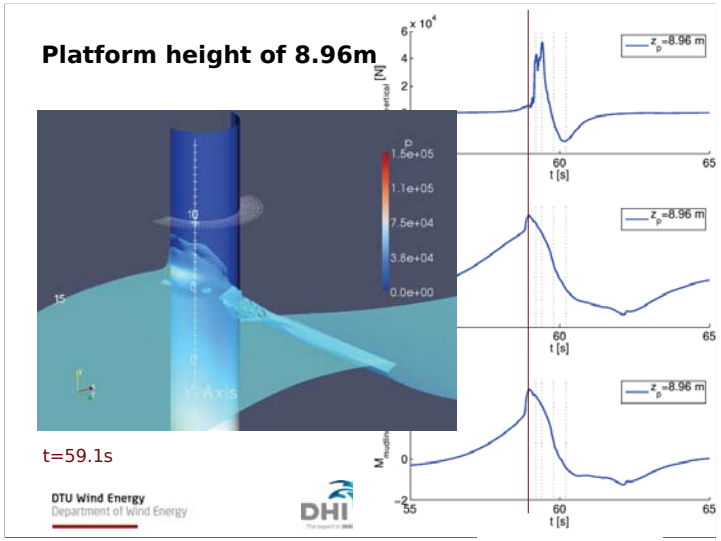
Platform height of 8.96m
t=59.1s
DTU Wind Energy
Department of Wind Energy
DHI

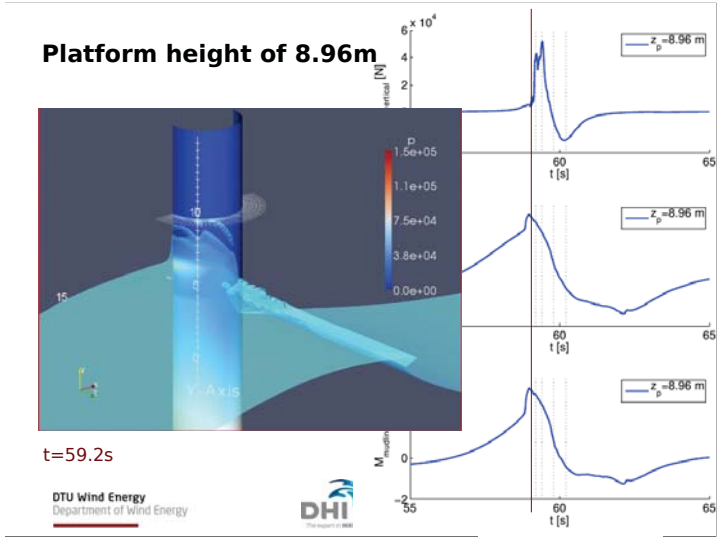
Platform height of 8.96m
t=59.2s
DTU Wind Energy
Department of Wind Energy
DHI

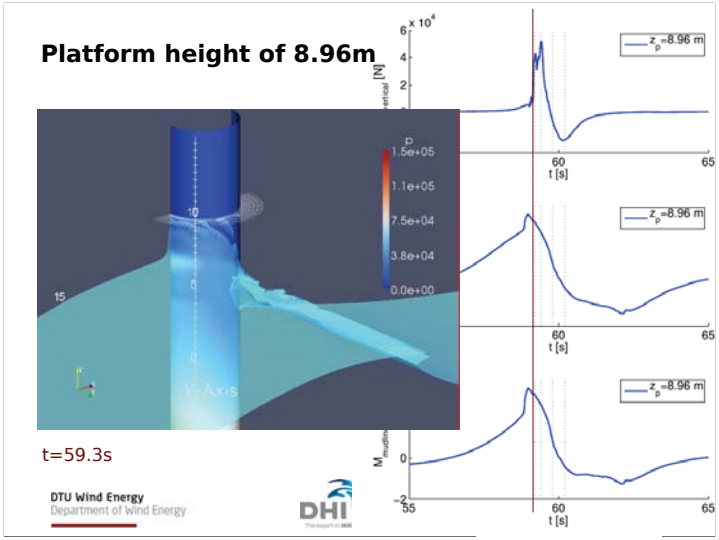
Platform height of 8.96m
t=59.3s
DTU Wind Energy
Department of Wind Energy
DHI

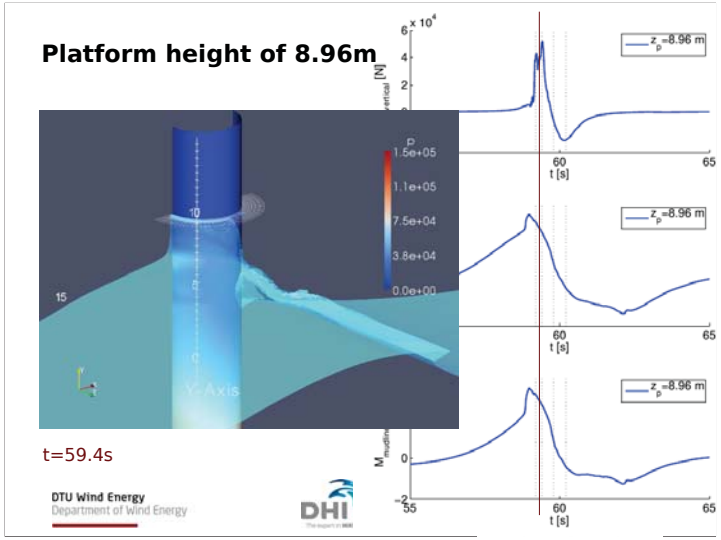
Platform height of 8.96m
t=59.4s
DTU Wind Energy
Department of Wind Energy
DHI

Platform height of 8.96m

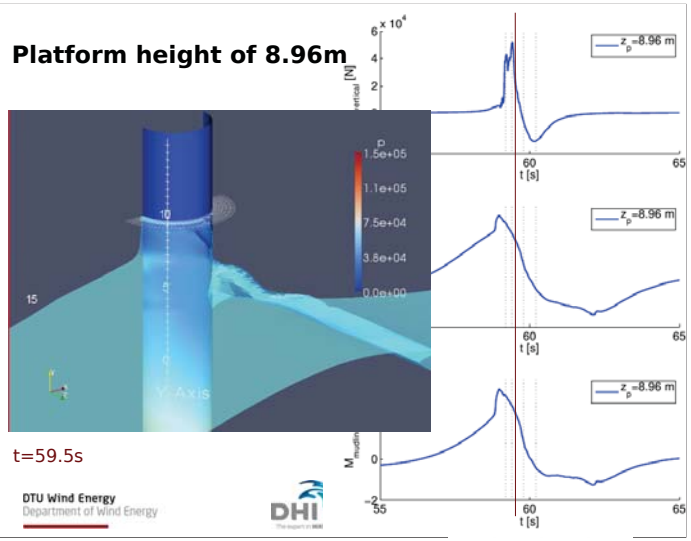

t=59.5s

DTU Wind Energy
Department of Wind Energy

DHI

Platform height of 8.96m

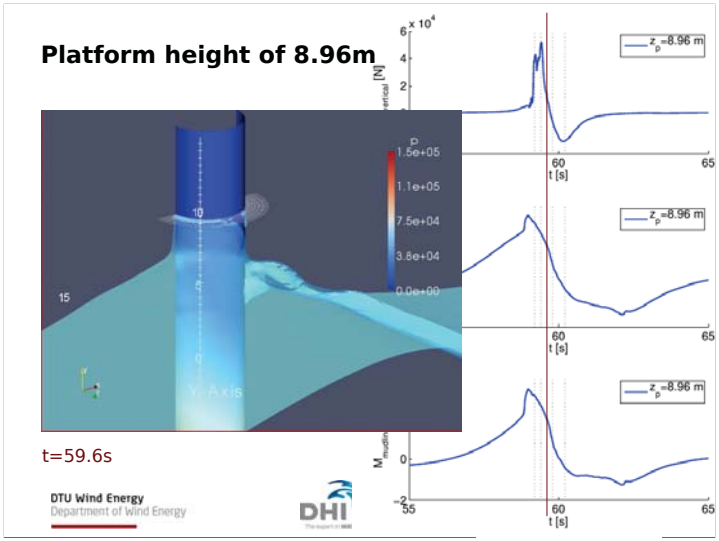

t=59.6s

DTU Wind Energy
Department of Wind Energy

DHI

Platform height of 8.96m

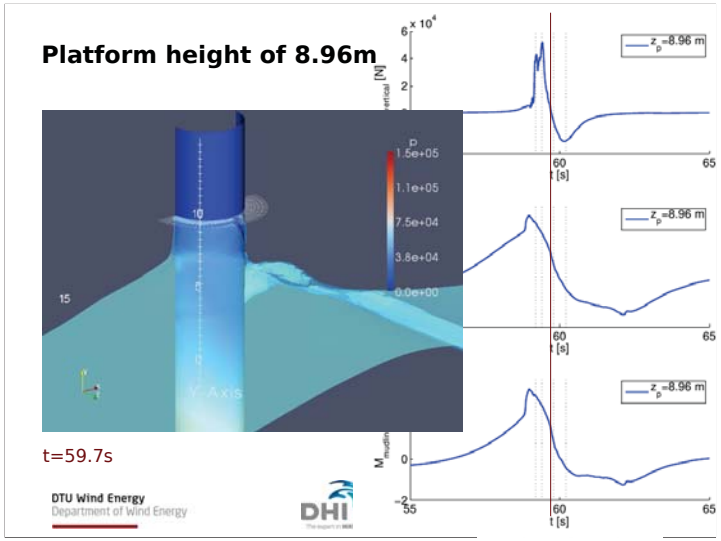

t=59.7s

DTU Wind Energy
Department of Wind Energy

DHI

Platform height of 8.96m

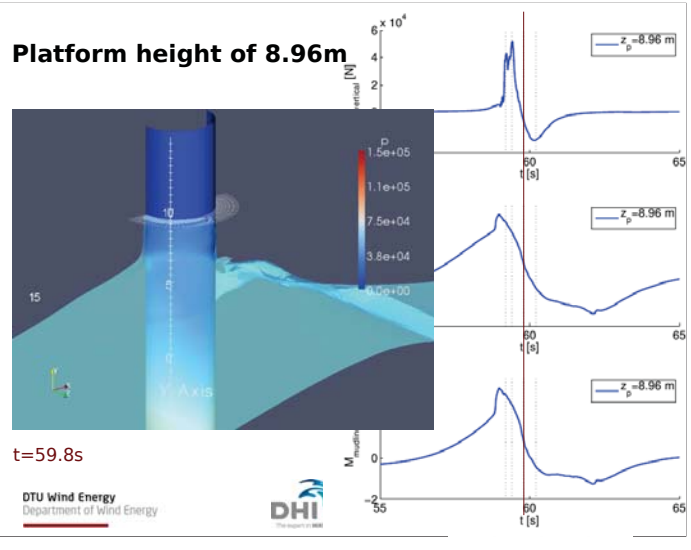

t=59.8s

DTU Wind Energy
Department of Wind Energy

DHI

Platform height of 8.96m

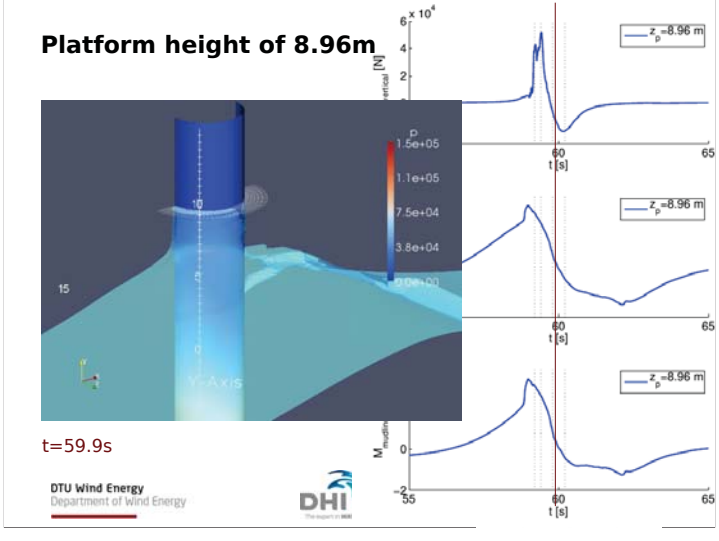

t=59.9s

DTU Wind Energy
Department of Wind Energy

DHI

Platform height of 8.96m

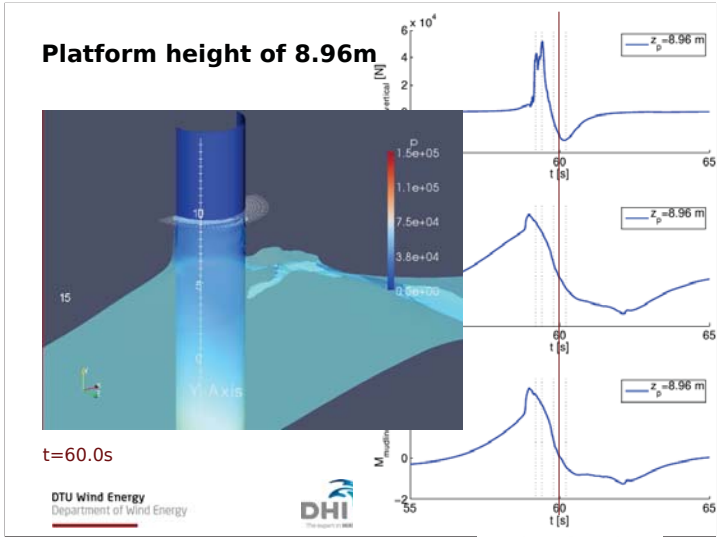

t=60.0s

DTU Wind Energy
Department of Wind Energy

DHI

Platform height of 8.96m

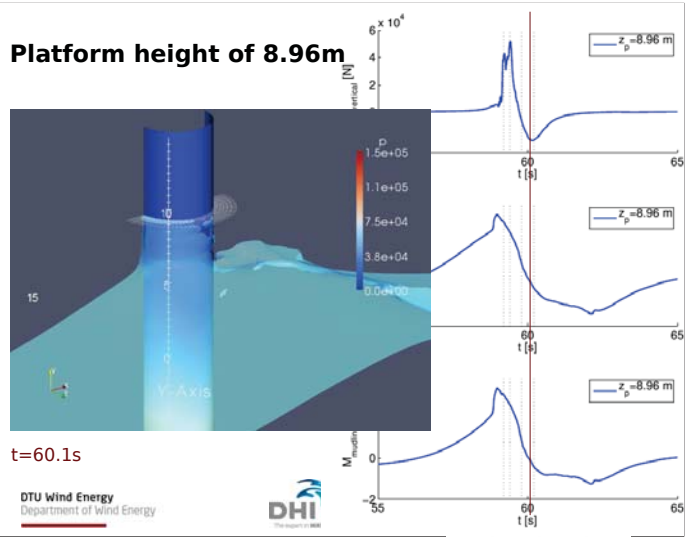

t=60.1s

DTU Wind Energy
Department of Wind Energy

Platform height of 8.96m

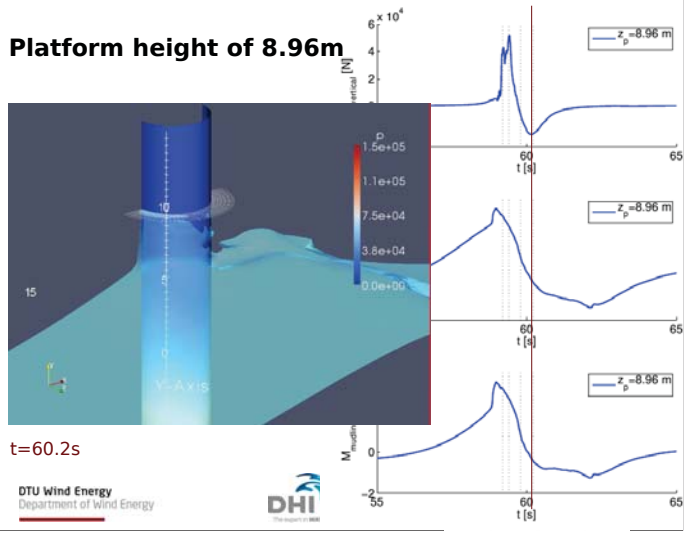

t=60.2s

DTU Wind Energy
Department of Wind Energy

Platform height of 8.96m

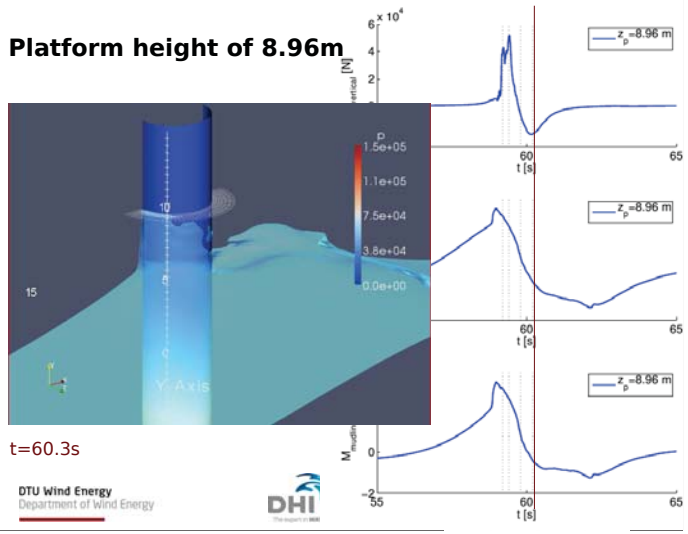

t=60.3s

DTU Wind Energy
Department of Wind Energy

Platform height of 8.96m

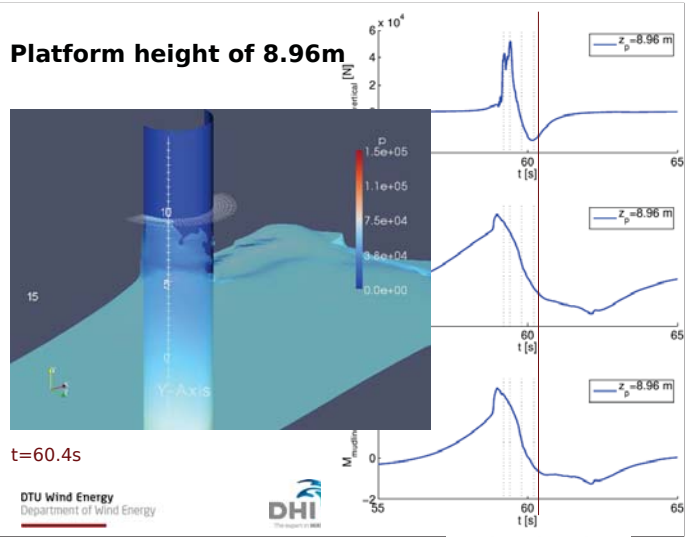

t=60.4s

DTU Wind Energy
Department of Wind Energy

Platform height of 8.96m

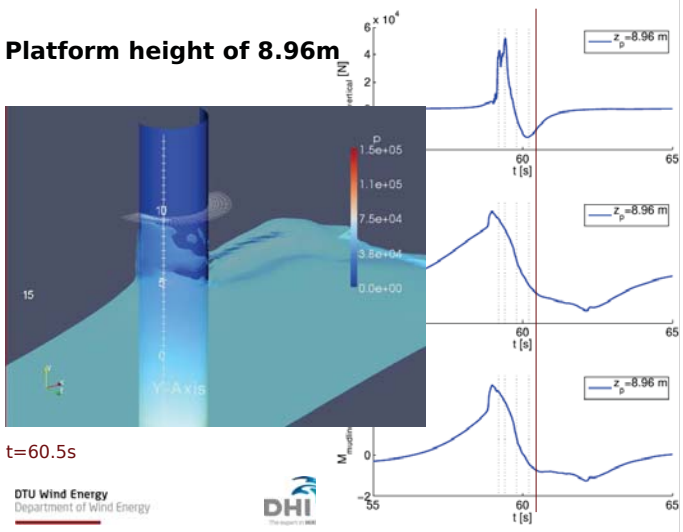

t=60.5s

DTU Wind Energy
Department of Wind Energy

Comparison for 5 platform heights

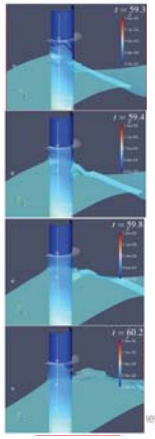

Downward force on platform Slamming

Contribution from impact with platform

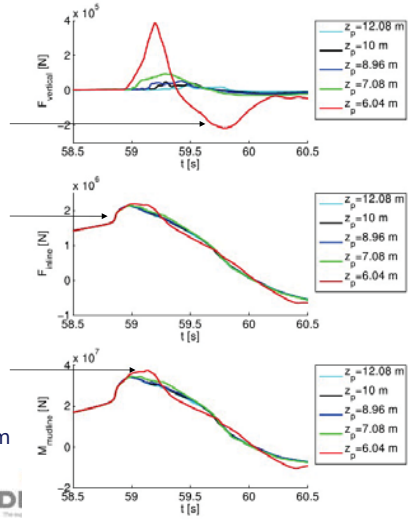

Detailed calculation of forces from steep regular waves

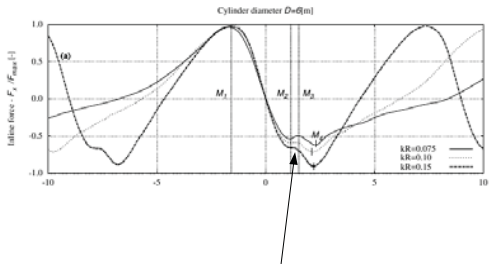

secondary load cycle

Bo Terp Paulsen

Third-harmonic force compared to FNV theory

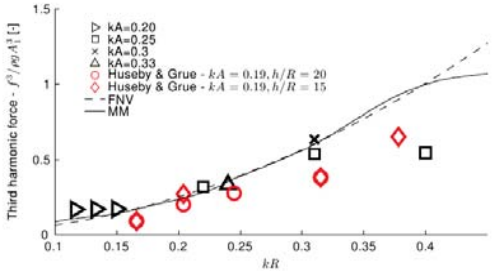

Terp Paulsen et al
Eur. Offsh Wind 2011

Coupling of OpenFOAM and OceanWave3D

- Irregular waves: JONSWAP($T_p = 12$s, $H_s = 8$m)
- Large domain⇒ Impossible to resolve with CFD alone!
- Rather trivial test case as it serves as validation

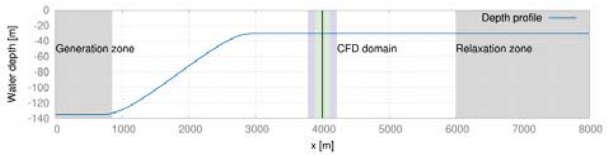

Terp Paulsen et al (2012)

Coupling of OpenFOAM and OceanWave3D

- 3hours times series of 2D irregular waves computed in hours with OceanWave3D
- Selected event analysed with OpenFOAM (~1day)

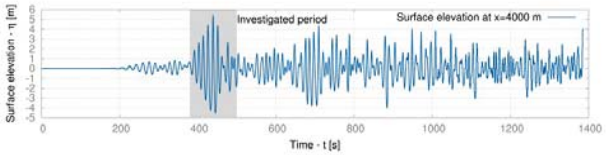

Terp Paulsen et al (2012)

Coupling of OpenFOAM and OceanWave3D

- Small "warmup" period for the CFD-computations: No initialization of pressure and pseudo air velocities
- Morison forces and CFD-computations agrees for small wave heights
- Discrepancies after passage of main event is attributed to diffraction effects

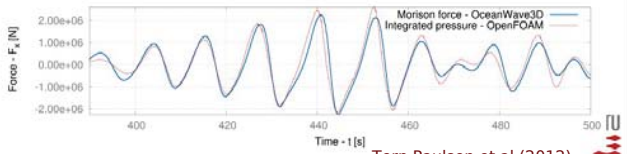

Terp Paulsen et al (2012)

Wave loads on offshore wind turbines

ForskEL. DTU Wind, DHI, DTU MEK. 2010-2013.

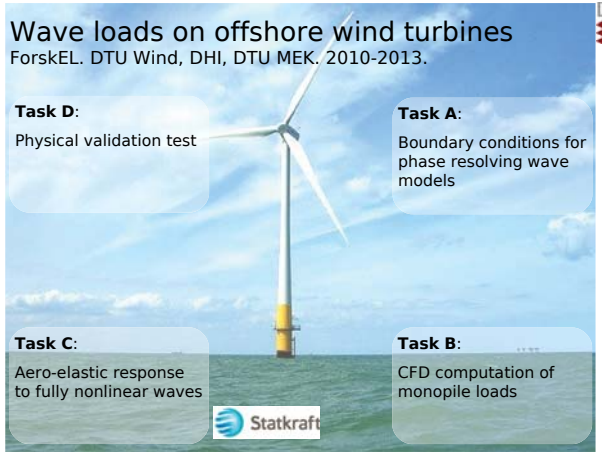

Wave loads Task D
Physical validation test

New tests at DHI with a rigid and a flexible structure

DHI:
Flemming Schlütter
Anders Wedel Nielsen
Jacob Tornfeldt Sørensen

DTU:
Henrik Bredmose
Torben Larsen
Signe Schløer
Bo Terp Paulsen
Harry Bingham

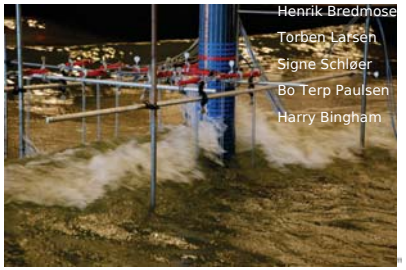

Wave loads Task D
Physical validation test

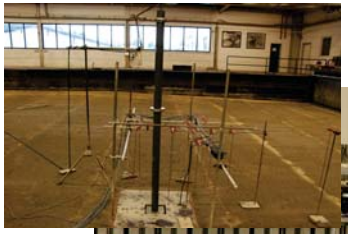

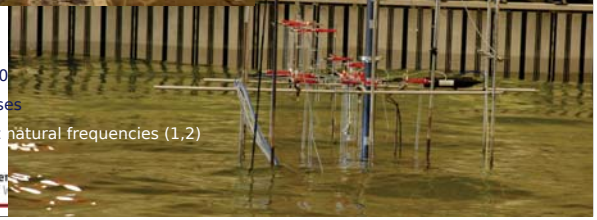

PVC pipe
Scale 1:80
Two masses
→ right natural frequencies (1,2)

Experimental setup

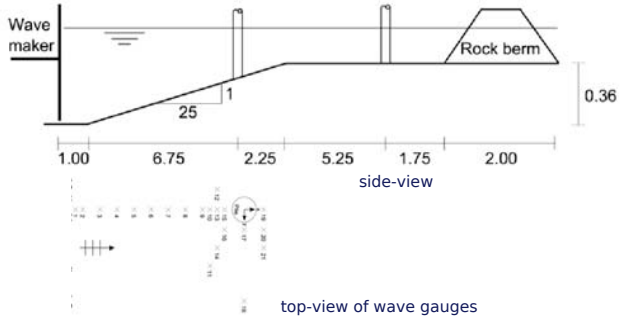

side-view

top-view of wave gauges

DTU Wind Energy
Department of Wind Energy

Results and brief analysis for flexible pile

Irregular JONSWAP waves, unidirectional
h=20m
Tp=14s
Hs=11m

Free surface elevation 0.15m from pile
Measured inline force on pile
Acceleration of top point
Displacement of top point

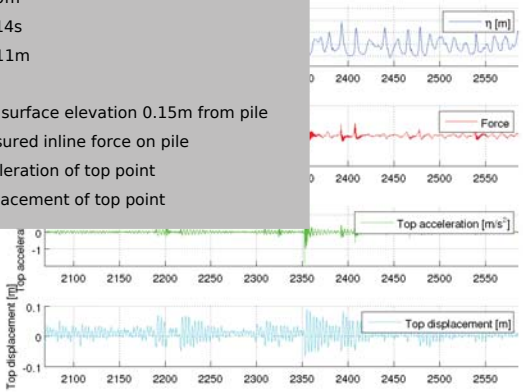

Results and brief analysis

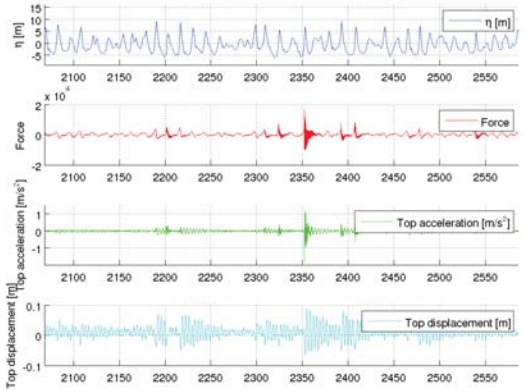

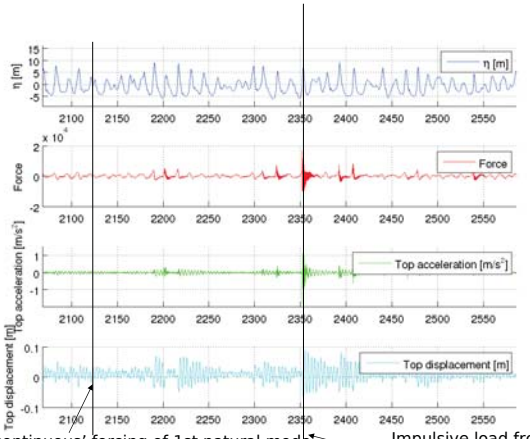

'continuous' forcing of 1st natural mode from wave-nonlinearity

Impulsive load from breaking /near breaking wave

DTU Wind Energy
Department of Wind Energy

Raw spectra

Nat freq of clamping/load cell?

Natural freqs (0.27 and 1.90 intended)

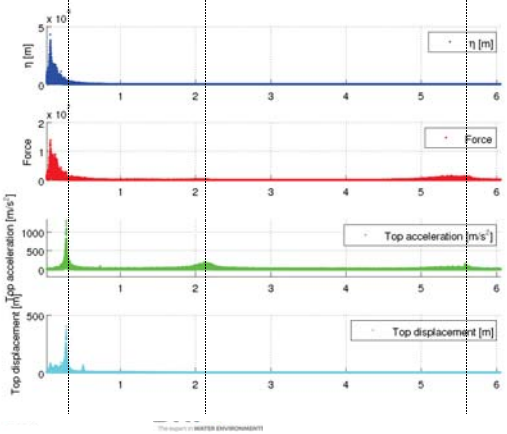

DTU Wind Er
Department o

Correlation of ringing to eta_t

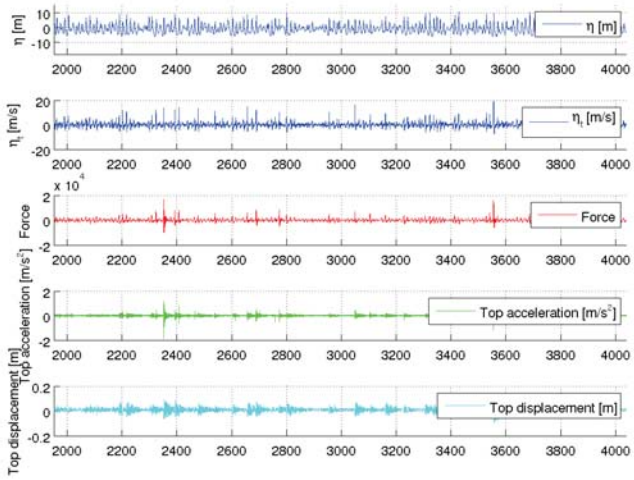

Which waves give the largest forces?

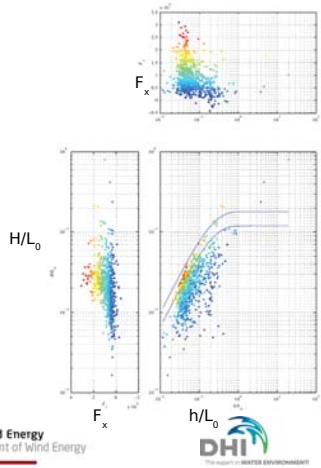

DTU Wind Energy
Department of Wind Energy

Sahlberg-Nielsen and Slabiak (2013)

Wave loads on offshore wind turbines

ForskEL. DTU Wind, DHI, DTU MEK. 2010-2013.

Task D:
Physical validation test

Task A:
Boundary conditions for phase resolving wave models

Task C:
Aero-elastic response to fully nonlinear waves

Task B:
CFD computation of monopile loads

Statkraft

DTU Wind Energy
Department of Wind Energy

DHI

Loads and response from steep and breaking waves

An overview of the "Wave loads" project

Henrik Bredmose, hbre@dtu.dk
Associate prof, DTU Wind Energy

Jacob Tornfeldt Sørensen
Head of innovation, Ports and Offshore Technology, DHI

Torben Juul Larsen
Senior Scientist, DTU Wind Energy

DTU Wind Energy
Department of Wind Energy

DHI

ETH Eidgenössische Technische Hochschule Zürich Swiss Federal Institute of Technology Zurich

LEC Laboratory for Energy Conversion

Effect of Second-Order Hydrodynamics on Floating Offshore Wind Turbines

L. Roald, J. Jonkman, A. Robertson, N. Chokani

25.01.2013, Deepwind, Trondheim

Outline

- Introduction
- Analysis approach
- Analyzed Systems
- Results
  - Comparison to first-order hydrodynamic forces
  - Comparison to aerodynamic forces
- Conclusions

Second-order hydrodynamics

- Radiation/diffraction apporach:
  - Assume potential flow
  - Assume small wave amplitude a
  - Perturbation series with respect to a
- First-order excitation force: $F_{ex}^{(1)} = Re\left(\sum_{j=1}^{N} a_j X_j e^{i\omega_j t}\right)$
- Second-order excitation force:

$$F_{ex}^{(2)} = Re\left(\sum_{k=1}^{N}\sum_{l=1}^{N} \underbrace{a_k a_l f_{kl}^{+} e^{i(\omega_k+\omega_l)t}}_{\text{sum-frequency}} + \underbrace{a_k a_l^{*} f_{kl}^{-} e^{i(\omega_k-\omega_l)t}}_{\text{difference-frequency}}\right)$$

Second-order hydrodynamics

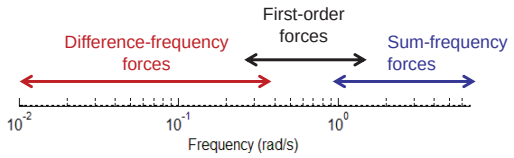

Second-order hydrodynamics

Pitch motion of spar configuration from the DeepCWind wave tank tests:

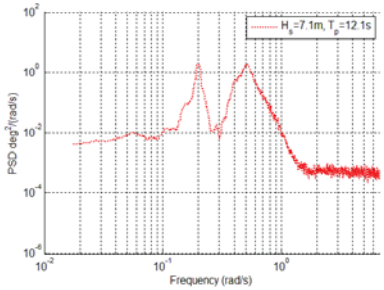

Figure: Goupee, A.J., Koo, B., Kimball, R.W. and Lambrakos, K.F., *Draft: Experimental Comparison of Three Floating Wind Turbine Concepts*, Proceedings of the 31st International Conference on Ocean, Offshore and Arctic Engineering, Rio de Janeiro, Brazil, June 10-15, 2012

Second-order hydrodynamics

Pitch motion of spar configuration from the DeepCWind wave tank tests:

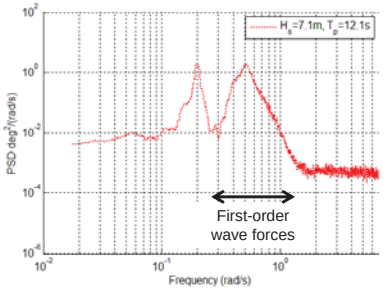

Figure: Goupee, A.J., Koo, B., Kimball, R.W. and Lambrakos, K.F., *Draft: Experimental Comparison of Three Floating Wind Turbine Concepts*, Proceedings of the 31st International Conference on Ocean, Offshore and Arctic Engineering, Rio de Janeiro, Brazil, June 10-15, 2012

Second-order hydrodynamics

Pitch motion of spar configuration from the DeepCWind wave tank tests:

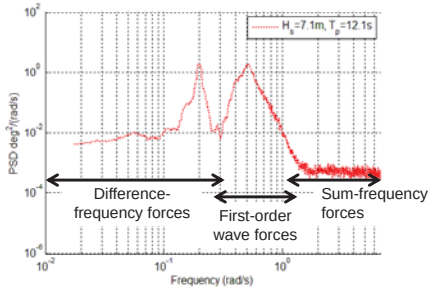

Figure: Goupee, A.J., Koo, B., Kimball, R.W. and Lambrakos, K.F., *Draft: Experimental Comparison of Three Floating Wind Turbine Concepts*, Proceedings of the 31st International Conference on Ocean, Offshore and Arctic Engineering, Rio de Janeiro, Brazil, June 10-15, 2012

1. Are second-order hydrodynamics important for floating offshore wind turbines?

1. Are second-order hydrodynamics important for floating offshore wind turbines?
2. What are the differences to second-order analysis of traditional offshore structures?

Analysis Methodology

- WAMIT: First- and second-order hydrodynamics in the frequency domain
- FAST: Aerodynamics, structural dynamics, control system properties and first-order hydrodynamics in the time domain

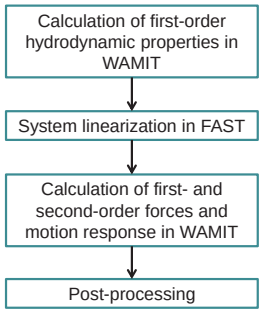

Analyzed systems

OC3 Hywind spar:

	Natural frequencies [rad/s]
Surge	0.051
Sway	0.051
Heave	0.204
Roll	0.215
Pitch	0.215
Yaw	0.761

DeepCWind TLP:

	Natural frequencies [rad/s]
Surge	0.156
Sway	0.156
Heave	5.975
Roll	3.388
Pitch	3.392
Yaw	0.374

First- and second-order results: OC3 Hywind

- Considered sea state: Hs = 3.66 m, Tp = 9.7 s

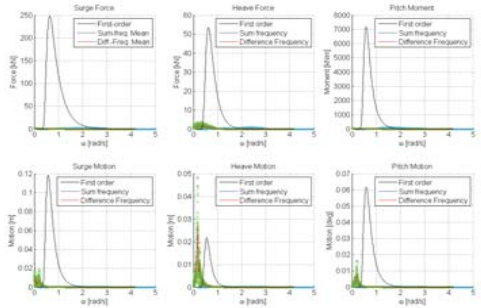

First- and second-order results: UMaine TLP

- Considered sea state: Hs = 3.66 m, Tp = 9.7 s

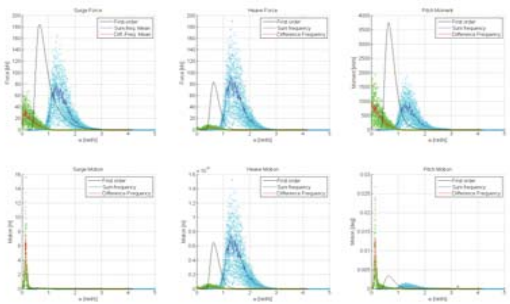

Comparison of Mean Drift Force and Mean Thrust

- Test case: OC3 Hywind
- Operating turbine:
  Mean drift force less than 1 % of mean rotor thrust
- Idling turbine:
  Mean drift force less than 15 % of mean rotor thrust

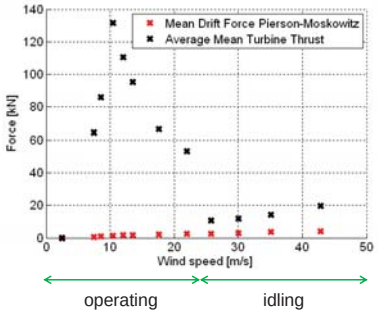

Comparison of aerodynamic and second-order response

- Test case: OC3 Hywind
- Environmental condition:
  - Hs = 3.66 m, Tp = 9.7 s
  - Wind speed = 17.6 m/s
- Simulation in FAST including aerodynamics and first-order hydrodynamics
- Simulation in WAMIT including first- and second-order hydrodynamics

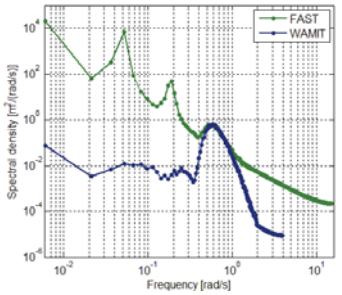

Current limitations

- Influence of turbine tower flexibility
  - Shift of the eigenfrequencies
  - Inaccurate first- and second-order response

Eigenfrequencies of UMaine TLP

	Rigid tower [rad/s]	Flexible tower [rad /s]
Surge	0.156	0.156
Sway	0.156	0.156
Heave	5.975	5.948
Roll	3.388	2.005
Pitch	3.392	2.021
Yaw	0.374	0.374

Hydrodynamic forces of the Umaine TLP

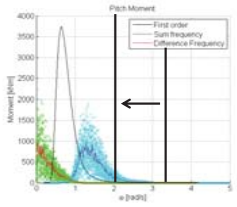

Conclusions

- Response due to **difference-frequency** forces at eigenfrequencies below frequencies of the incident waves
- **Sum-frequency** forces are quite significant for the TLP, although even though eigenfrequencies are excited
- Comparison to aerodynamic forces:
  - **Mean drift forces** are insignificant compared to mean thrust
  - **Low frequency response** seems to be dominated by aerodynamics
- Some limitations to the proposed method have been identified:
  - Eigenfrequency of the turbine tower influences TLP eigenfrequencies
  - No damping from viscosity is included in current simulations

Thank you for your attention

Line Roald
roald@eeh.ee.ethz.ch
+41 44 632 65 77

F Wind farm modelling

Wind farm optimization, Prof Gunner Larsen, DTU Wind Energy

Blind test 2 - Wind and Wake Modelling, Prof Lars Sætran, NTNU

A practical approach in the CFD simulations of off-shore wind farms through the actuator disc technique, Giorgio Crasto, WindSim AS

3D hot-wire measurements of a wind turbine wake, Pål Egil Eriksen, PhD stud, NTNU

Near and far wake validation study for two turbines in line, Marwan Khalil, GexCon AS

TOPFARM – A TOOL FOR WIND FARM OPTIMIZATION

G. C. Larsen, P. E. Réthoré

DTU Wind Energy
Department of Wind Energy

Outline

- Introduction – vision and philosophy
- Importance of wind farm (WF) flow field modeling
- Wind farm optimization
  - Optimal power production
  - Optimal economic performance
- The TOPFARM platform in brief
- Demonstration example 1
- Demonstration example 2
- Conclusion
- Future activities
- References

Introduction – vision and philosophy

- Vision: A "complete" wind farm topology optimization, as seen from an investors perspective, taking into account:
  - *Loading*- and *production* aspects in a realistic and coherent framework
  - Financial costs (foundation, grid infrastructure, …)

  … and and subjected to various constraints (area, spacing , …)
- Philosophy: The optimal wind farm layout reflects the *optimal economical performance* as seen over the lifetime of the wind farm

Importance of WF flow field modeling (1)

- Wind Farm (WF) wind climate deviates significantly from ambient wind climate:
  - Wind resource (decreased)
  - Turbulence
    - Turbulence intensity increased
    - Turbulence structure modified (… incl. intermittency)
  - … and the WF turbines interact dynamically though wakes

Importance of WF flow field modeling (2)

- WF wind climate characteristics important for:
  - Design of wind turbine (WT) control strategies
  - Wind farm optimization. Potential approaches:
    - Optimizing the power output … and ensuring that that the loading of the individual turbines is beneath their design limit
    - Optimizing wind farm topology from a "holistic" economical point of view … throughout the life time of the WF

Optimal power production – input (1)

- Ambient/undisturbed *flow conditions* on the intended WF site assumed given! – measured or modelled (with meso-scale models or others…)
  - Mean wind distribution … conditioned on wind direction (deterministic)
  - Roughness/shear … conditioned on wind direction (deterministic)
  - Turbulence parameter distributions … conditioned on wind direction (stochastic)
  - Wind direction distribution

Optimal power production – input (2)

- *Wind Turbines* (WT) strongly simplified and basically represented by characteristics as:
  - Thrust curve ("flow resistance")
  - Power curve (production)

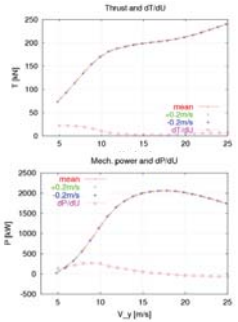

Optimal power production – WF flow field

- Typically modelled using *stationary* approaches, such as e.g.
  - The N.O. Jensen model (simple top hat model based on momentum balance)
  - Parabolised CFD models with an eddy viscosity closure (UPM model (ECN WindPRO), Ainsley model (GH Windfarmer), …)
  - Lineralized RANS model (FUGA) based on a first order perturbation approach. Numerical diffusion omitted! (mixed spectral formulation)

Optimal power production – objective function

- Relatively simple … because all elements have the *same unit*
- No cost models are consequently required!
- Objective function … to be optimized:

$$P_{tot} = \sum_{life\ time} \sum_{pdf\ \theta} \sum_{pdf\ U} \sum_{i=1}^{N} P(x_i, y_i)$$

Optimal economical performance – input

- In a "true" rational *economical optimization* of the wind farm layout, the goal is to determine the *optimal balance* between capital costs, operation and maintenance (O&M) costs, fatigue lifetime consumption and power production output … possibly under certain specified constraints
- Same input as used for optimizing power production … supplemented by
  - Wind turbine information sufficiently detailed for setting up aeroelastic model(s) of the turbines in question

Optimal economical performance – modeling

- Stationary flow fields and rudimentary WT models may suffice for optimizing wind power production … but is clearly *not* sufficient for achieving the overall economical WF optimum
  - *Non-stationary* characteristics of the WF flow field have to be considered to enable prediction of reliable WT dynamic loading … which is essential for fatigue load estimation, cost of O&M, …
  - Detailed WT modeling (i.e. *aeroelastic modeling*) is needed to obtain main component structural response in sufficient detail and of sufficient accuracy
  - Cost models are needed to aggregate different types of quantities into an objective function

Optimal economical performance – summary

- The main parameters governing/dictating WF economics include the following:
  - Investment costs - including auxiliary costs for foundation, grid connection, civil engineering infrastructure, …
  - Operation and maintenance costs (O&M)
  - Electricity production/wind resources
  - Turbine loading/lifetime
  - Discounting rate

The TOPFARM platform in brief

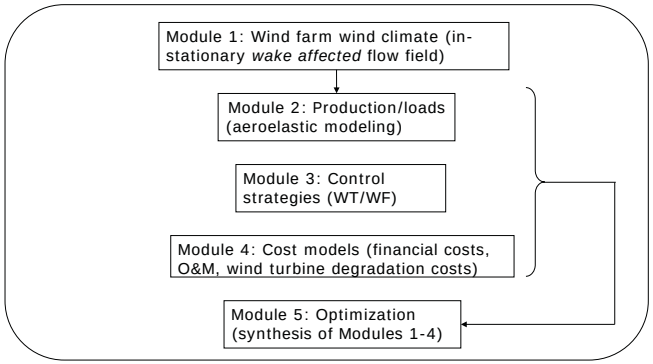

The TOPFARM platform in brief – module 1

- Multi-fidelity optimization approach requires a hierarchy of models

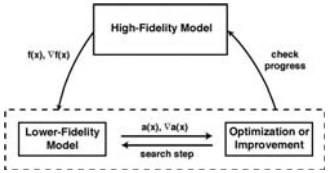

1. Stationary wake (analytical model) + Power curve
2. "Poor man's LES"; i.e. DWM (Database – generic production/load cases + interpolation)
3. DWM (Simulation)

The TOPFARM platform in brief – modules 2 / 3

- HAWC2:
  - Non-linear FE model based on a multi-body formulation
  - Aerodynamics based on Blade Element Momentum and profile look-up tables … that in turn "delivers" the boundary conditions for the quasi-steady wake deficit simulation
  - WT generator model included
  - WT control algorithms included
  - Output is power and forces/moments in arbitrary selected cross sections

The TOPFARM platform in brief – module 4 (1)

- Basic simplifying approach:
  - Only costs that depend on wind farm topology and control – variable costs - are of relevance in a topology optimization context
  - Fixed costs may be included in the objective function (Module 5). However, as seeking the stationary points for this functional involves gradient behaviour only, the fixed costs will not influence the global optimum of the objective function

The TOPFARM platform in brief – module 4 (2)

- Examples of required cost models … to transform the physical quantity in question into an economical value:
  - Financial costs
    - Foundation costs
    - Grid infrastructure costs
    - Civil engineering costs
  - Operational costs
    - Turbine degradation (fatigue loading/lifetime)
    - Operation and maintenance costs (O&M)
  - Electricity production/wind resources

The TOPFARM platform in brief – module 5

- Objective function (OF):
  - The value of the wind farm power production over the wind farm lifetime, *WP*, refers to year Zero
  - All operating costs (in this example *CD* and *CM*) refer to year Zero … with the implicit assumption that the development of these expenses over time follows the inflation rate … and that the inflation rate is the natural choice for the discounting factor transforming these running costs to *net present value*

$$FB = WP_n - C\left(1+\left(\frac{r_{c1}-r_i}{N_L}\right)\right)^{XN_L}, \quad WP_n = WP - CD - CM ,$$

  - *C* denotes the financial expenses (e.g. including grid costs (*CG*) and foundation costs (*CF*))

Demonstration example 1 (1)

- Generic offshore wind farm:
  - 6 × 5MW offshore wind turbines
  - Water depths between 4m and 20m

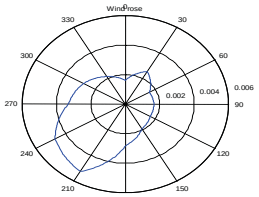

Wind direction probability density distribution

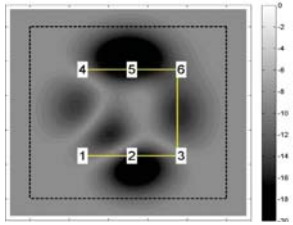

Gray color: Water depth [m]
Yellow line: Electrical grid

Demonstration example 1 (2)

- Result of a gradient based optimization (SLP):

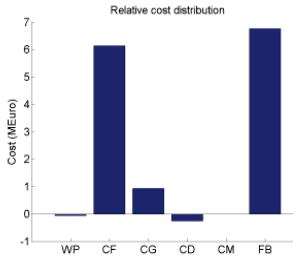

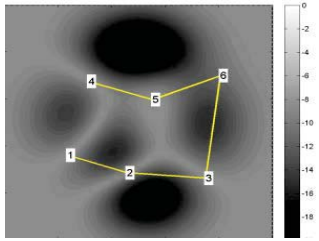

Demonstration example 1 (3)

- Result of a genetic algorithm + gradient based optimization (Simplex)

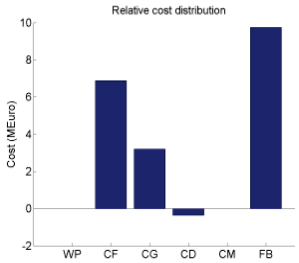

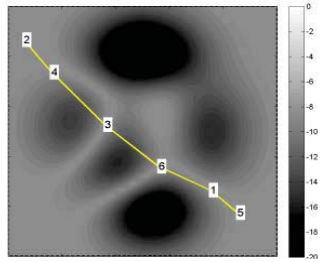

Demonstration example 2 (1)

- Middelgrunden

Demonstration example 2 (2)

- Middelgrunden

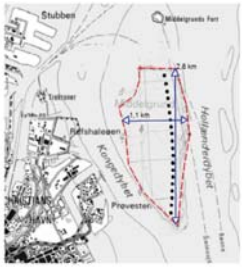

Allowed wind turbine region

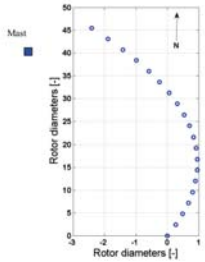

Middelgrunden layout

Demonstration example 2 (3)

- Middelgrunden - ambient wind climate

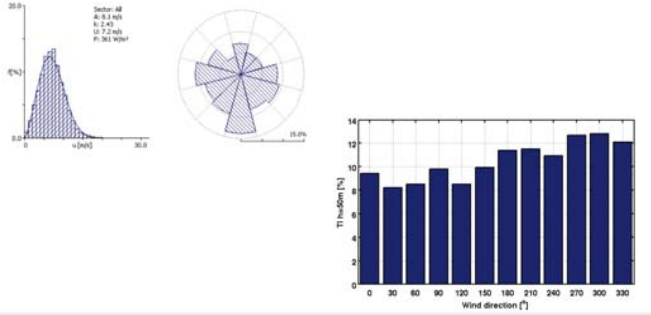

Demonstration example 2 (4)

- Middelgrunden iterations: 1000 SGA + 20 SLP

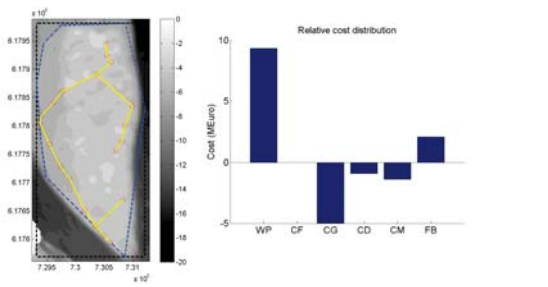

Optimum wind farm layout (left) and financial balance cost distribution relative to baseline design (right).

Demonstration example 2 (5)

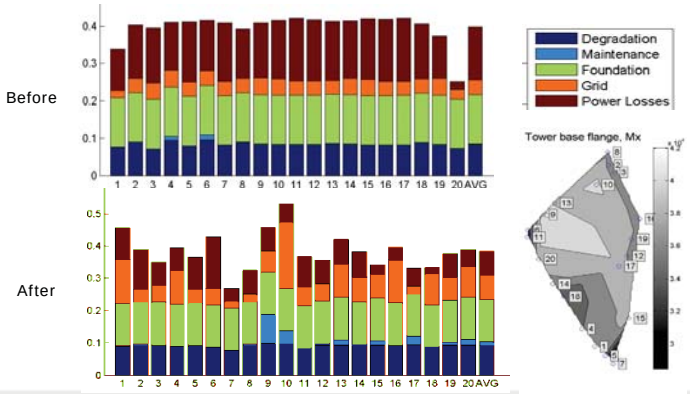

Demonstration example 2 (6)

- Evaluation:
  - The baseline layout was largely based on visual considerations
  - The optimized solution is fundamentally different from the baseline layout … the resulting layout makes use of the entire feasible domain, and the turbines are not placed in a regular pattern
  - The foundation costs have not been increased, because the turbines have been placed at shallow water
  - The major changes involve energy production and electrical grid costs … both were increased
  - A total improvement of the financial balance of 2.1 M€ was achieved compared to the baseline layout … over the WF lifetime

Conclusion (1)

- A new approach has been developed that allow for wind farm topology optimization in the sense that the *optimal economical performance,* as seen over the lifetime of the wind farm, is achieved
- This is done by:
  - Taking into account both loading (i.e. WT degradation, O&M) and production of the individual turbines in the wind farm in a realistic and coherent framework …. and by
  - Including financial costs (foundation, grid infrastructure, etc.) in the optimization problem
- The model has been implemented in a wind farm optimization platform called TOPFARM

Conclusion (2)

- Proof of concept has, among others, included various sanity checks … and optimization of a generic offshore WF, an existing offshore WF and an existing onshore WF
- The results are over all satisfying and give interesting insights on the pros and cons of the design choices. They show in particular, that inclusion of the fatigue load degradation costs gives some additional details in comparison with pure power based optimization
- The multi-fidelity approach is found necessary and attractive to limit the computational costs of the optimization

Future activities

- More detailed and realistic cost functions
- Improvement of the code (e.g. parallelization)
- Inclusion of WF control in the optimization problem
- Inclusion of atmospheric stability effects in the WF field simulation … basically by developing a spectral tensor including buoyancy effects
- Cheapest rather than shortest cabling between turbines
- Inclusion of extreme load aspects
- Simplified aeroelastic computations in the frequency domain … to improved computational speed
- Development of a dedicated “self-generated” wake turbulence spectral tensor
- Development of a more DWM-consistent eddy viscosity

References (1)

- Larsen et al. (2011). **TOPFARM -** NEXT GENERATION DESIGN TOOL FOR OPTIMISATION OF WIND FARM TOPOLOGY AND OPERATION. Publishable final activity report. Risø-R-1805 (EN)
- Rethore, P.-E.; Fuglsang, P.; Larsen, G.C.; Buhl, T.; Larsen, T.J. and Madsen, H.Aa. (2011). TOPFARM: Multi-fidelity Optimization of Offshore Wind Farm. The 21st International Offshore (Ocean) and Polar Engineering Conference, ISOPE-2011, Maui, Hawaii, June 19-24
- Larsen, G.C.; Madsen, H.Aa.; Larsen, T.J.; Rethore, P.-E. and Fuglsang, P. (2011). TOPFARM – a platform for wind farm topology optimization. Wake Conference, Visby, Sweden, June 8-9

References (2)

- Buhl T. and Larsen G.C. (2010). Wind farm topology optimization including costs associated with structural loading. *The Science of Making Torque from the Wind, 3rd Conference, Iraklion, Greece*
- Larsen, G.C. (2009). A simple generic wind farm cost model tailored for wind farm optimization. Risø-R-1710(EN)
- Larsen, G.C. (2009). A simple stationary semi-analytical wake model. Risø-R-1713(EN)
- Larsen, G.C. et al. (2008). Wake meandering: A pragmatic approach. *Wind Energy*, **11**, 377-395

Wind and Wake Modelling – Blind Test 2

Professor Lars Sætran, NTNU

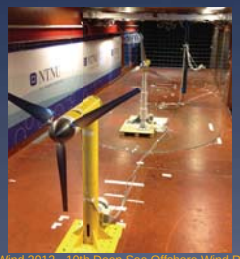

DeepWind 2013 - 10th Deep Sea Offshore Wind R&D Seminar
24-25 January 2013, Royal Garden Hotel, Kjøpmannsgata 73, Trondheim, NORWAY

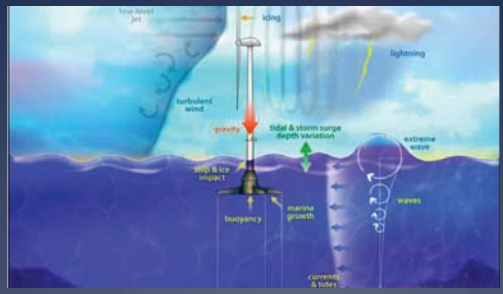

BT2 is a follow-up of **BT1**:
P-Å Krogstad and PE Eriksen; "Blind test" calculation of the performance and wake development for a model wind turbine. Renewable Energy 50 (2013) 325-333

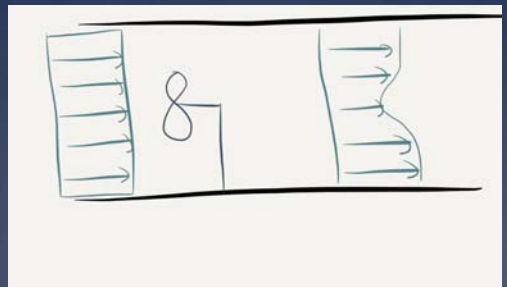

LR Saetran, F Pierella and P-A Krogstad; "Blind test" calculations of the performance and wake development for two model wind turbines in tandem. To be submitted for publication

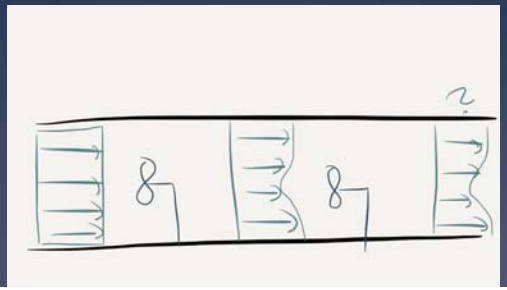

Contributors:

- Meventus (Agder Energy); V Bhutoria and JA Lund (OpenFOAM, ALM / LES (CFD))
- Alcona Flow Technology; E Manger (ANSYS FLUENT Version 14.0, CFD – Full Rotor)
- CMR Instrumentation; A Hallager and IØ Sand (Music, BEM + CFD)
- DTU Mech. Eng. And Linne Flow Center/KTH Mechanics; R Mikkelsen and S Sarmast (EllipSys3D/FLEX5, CFD, Actuator line)
- GexCon; L Sælen and M Kahlil (CMR-Wind, CFD (BEM))
- NTNU, Dept Marine Techn; J de Vaal L. (Fluent ASAD, Axi-sym Actuator Disc)
- METU Center for Wind Energy; O Uzol and NS Uzol (Aerosim, Free-wake)
- Puerto Rico, Leonardi

Global performance
(Power and thrust coefficients)

Compulsory results: Turbine #1 Power coefficient Cp at best condition TSR= 6

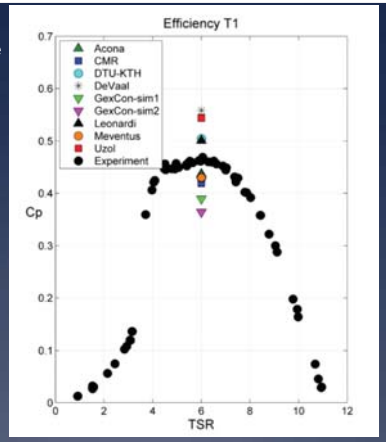

Compulsory results: Turbne #1 Thrust coeff Ct at best condition TSR= 6

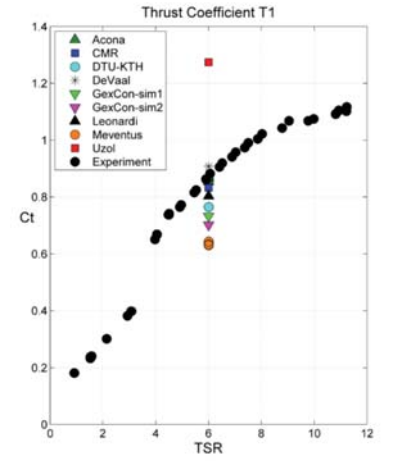

Turbine #2: Power coeff Cp for TSR= 2.5, 4 and 7

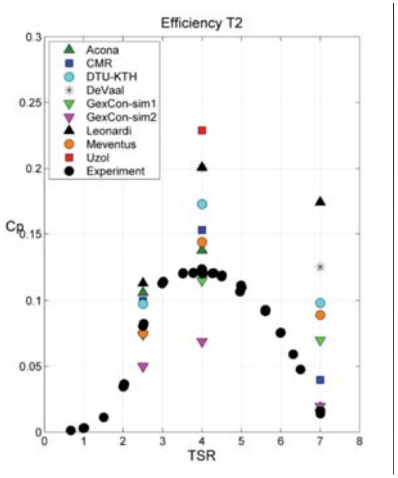

Turbine #2: Thrust coeff Ct at TSR= 2.5, 4 and 7

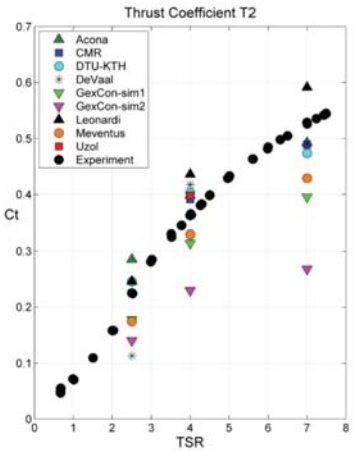

Now a close look at some wake data!

Wake data comparison: Simplest case; Design condition

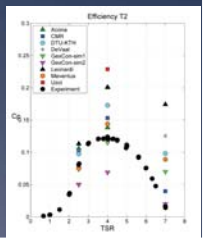

Wake 2nd turbine, TSR= 4, X/D= 1. Mean velocity U on a horizontal diagonal and on a vertical diagonal

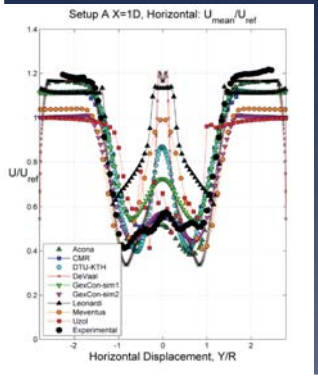

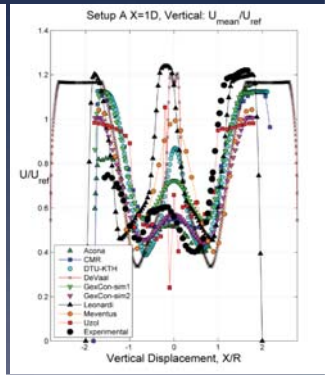

Wake 2nd turbine, TSR= 4, X/D= 1
Reynolds normal stress on a horizontal diagonal and on a vertical diagonal

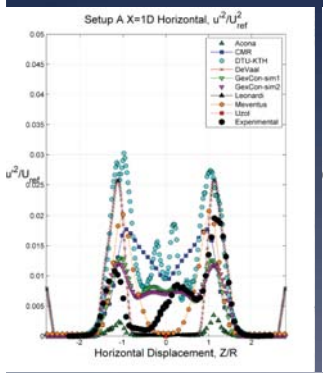

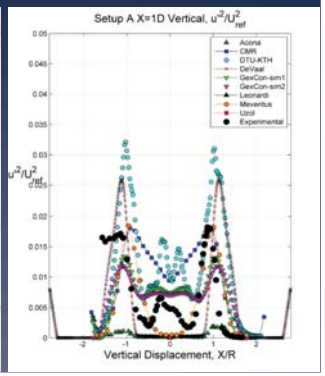

Wake 2nd turbine, TSR= 4. Mean velocity U on a horizontal diagonal

Wake profiles at X/D= 1, 2.5 and 4

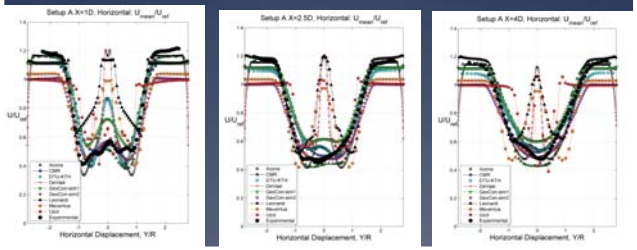

Wake 2nd turbine, TSR= 4, Reynolds normal stress on a vertical diagonal

Wake profiles at X/D= 1, 2.5 and 4

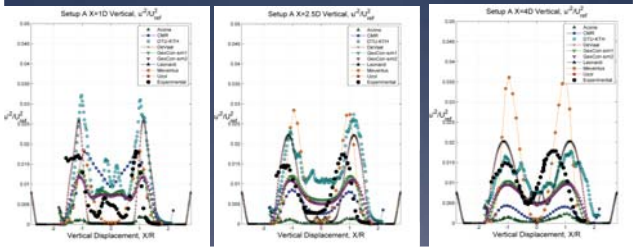

And what happens at low wind speeds?

TSR = 7

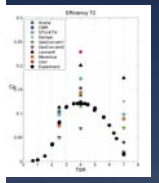

Wake 2nd turbine, **TSR= 7**. Mean velocity U on a horizontal diagonal

Wake profiles at X/D= 1, 2.5 and 4

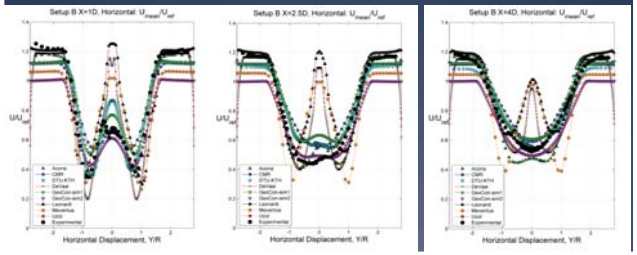

Wake 2nd turbine, **TSR= 7**, Reynolds normal stress on a vertical diagonal

Wake profiles at X/D= 1, 2.5 and 4

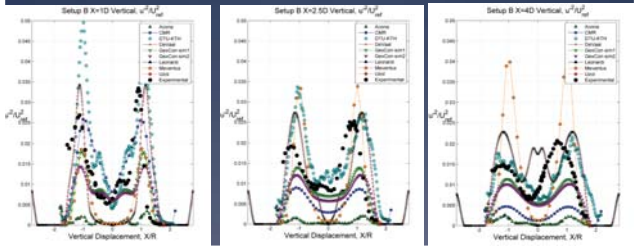

And now on to a tougher case: Low tip speed ratio; TSR = 2.5

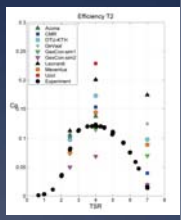

Wake 2nd turbine, **TSR= 2.5**. Mean velocity U on a horizontal diagonal

Wake profiles at X/D= 1, 2.5 and 4

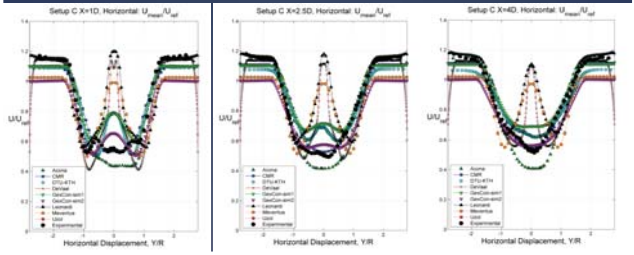

Wake 2nd turbine, **TSR= 2.5**, Reynolds normal stress on a vertical diagonal

Wake profiles at X/D= 1, 2.5 and 4

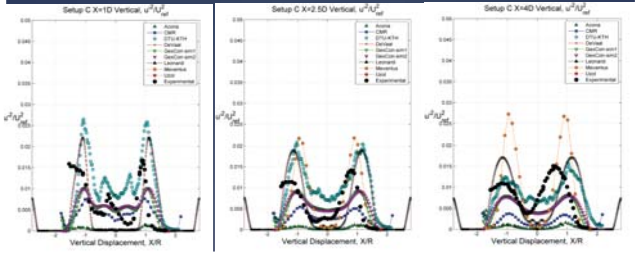

The wake is a complicated 3D periodic and turbulent flow

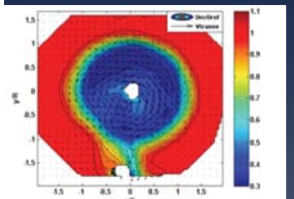

Fig. 7: Normalized velocity U_m/U_∞ as a color chart, arrows show the transversal velocity intensity and direction, measured at x/D=0.6 downstream of the tandem setup

Vorticity, Mikkelsen & Sarmast

Schumann, Pierella & Sætran (2013)

Transverse velocity after a "drag disk", Pierella

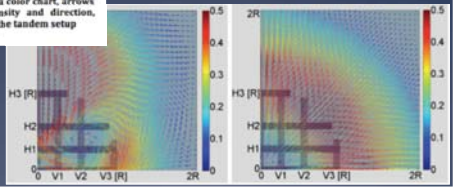

What is TURBULENCE in this case: “Are we comparing apples and bananas…?”

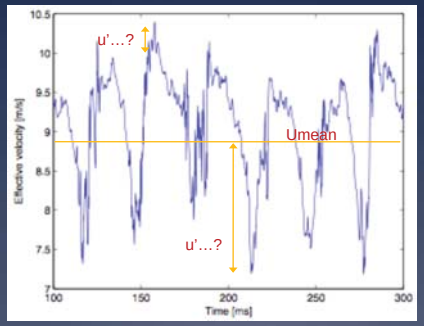

Tentative conclusions….

- Predictions for Cp and Ct at design condition for 1st turbine show more scatter than expected
- Large scatter for Cp and Ct for 2nd turbine, both on and off “best” condition
- Wake mean velocity field qualitatively OK?
- Wake turbulence intensity field: not necessary with logarithmic ordinate axis… (ref BT1)
- The following conclusions were for BT1 – are they still valid?
- Uncertainty even higher for C_t at high TSR and there does not appear to be a systematic trend with respect to methods or models used
- BEM as good as CFD for C_p and C_T
- Only one simulation (Manger using Fluent) performed as the experiment, i.e. with tower, nacelle and rotating blades in a stationary test section. Produced mostly correct profile shapes but not levels.
- Wake computed with *Spalart-Allmaras, k-e, k-w SST* turbulence models, as well as with *LES*. *LES* most accurate. No obvious winner among other models
- Many used *openFoam*, but results appear to be dependent on setup, boundary conditions and turbulence model rather than CFD code.
- Scaling of kinetic energy should be revisited. Too large differences to be due to turbulence models. Do the methods predict turbulence in the wakes behind solid bodies correctly?
- Turbulent diffusion appears to be underestimated in most models. Much longer fetch is needed to see when far wake profiles are predicted.

- The experimental date for BT2 will be published by Fabio Pierella (2013)
- A package with detailed description of the experiment and the experimental data is available. Email: lars.satran@ntnu.no

DeepWind'2013
10th Deep Sea Offshore Wind R&D Conference

Trondheim, 24-25 January 2013

A practical approach in the CFD simulation of off-shore wind farms through the actuator disc technique

F. Castellani, A. Gravdahl, G. Crasto, E. Piccioni, A. Vignaroli

Presenter: Dr. Giorgio Crasto, WindSim AS
Contact author: Prof. Francesco Castellani, University of Perugia

windsim

THE WindSim MODEL

Key features

- WindSim (WS) is commercial software package for wind flow simulations based on Computational Fluid Dynamics (CFD)
- WS provides a user-friendly interface for the CFD core PHOENICS (by CHAM)
- The code solves automatically the Reynolds Average Navier Stokes (RANS) equations (steady solution) on different direction sectors

✓ Very easy to setup a simulation on a real terrain case
✓ Easy grid control
✓ Quite fast solution

✓ Strictly Cartesian orthogonal grid
✓ Solution with RANS and quite standard turbulence models

The Grid

Using an orthogonal Cartesian grid WS is designed to operate on rectangular domains. This introduce different boundary layers conditions between orthogonal and skewed direction sectors.

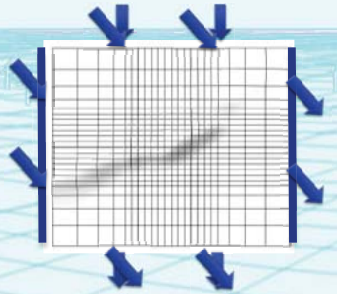

Skewed flows:
- 12 inlet
- 12 outlet
- 2 frictionless walls

Vertical distribution

TURBULENCE MODELS

The RANS equations are closed with different versions of the k-ε model or the k-ω model:
✓ k-ε Standard
✓ k-ε Modified
✓ RNG k-ε
✓ k-ε with YAP correction
✓ k-ω

There is a fundamental lack of physics when using RANS and the k-ε/k-ω model with relevant adverse pressure gradients (Réthoré *et al.*, 2010).

Appling some small changes on a open part of the code (Q1 file) it's possible to test even more solutions for turbulence models.

Réthoré P.-E., Sørensen N. N., Bechmann A. "Modelling Issues with Wind Turbine Wake and Atmospheric Turbulence." - The Science of Making Torque from Wind 2010

WAKES MODELLING

WindSim provides two different ways to consider wakes in the numerical solution:

1. **Using analytical models in the post-processing of the CFD/RANS calculations**
   a. Jensen model (momentum deficit theory)
   b. Larsen model (turbulent boundary layer equations)
   c. Model with a turbulent depending rate of wake expansion
2. **Use the actuator disc (AD) model within the CFD/RANS calculations**

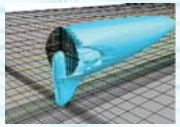

✓ Only axial forces are applied on the disc
✓ All rotational effects are disregarded
✓ The thrust is applied according to the thrust coefficient curve of the wind turbine using the actual speed calculated on the rotor (correction with axial induction).

USE OF THE TESTBATTERIES

- The test battery is a numerical tool designed to be used during the development of each new version of the code.
- With the test battery it is possible to run the model in a batch/silent mode, changing the calculation parameters automatically and check all monitored outputs.
- The test battery can be very useful also for research purpose.

A good part of the development of the test battery was carried-out at the WindSim headquarter in Norway by Emanuele Piccioni, a PhD student from the University of Perugia during his four-months stage within the Erasmus Placement project.

TESTING A NEW SOLVER WITH THE TESTBATTERIES

Adjusting the convergence criteria for the new GCV, a SIMPLE-C solver acting on a collocated, BFC grid.

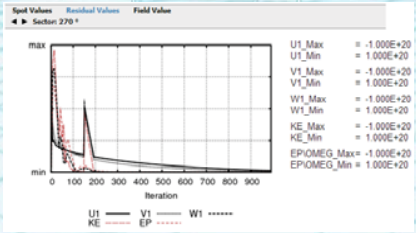

TESTING A NEW SOLVER WITH THE TESTBATTERIES

Assessing the performance on complex-terrain

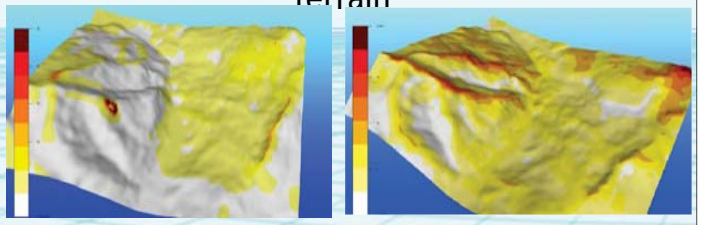

Coupled solver with staggered grid

GCV solver with collocated grid

RESULTS FROM THE SINGLE-WAKE CASE

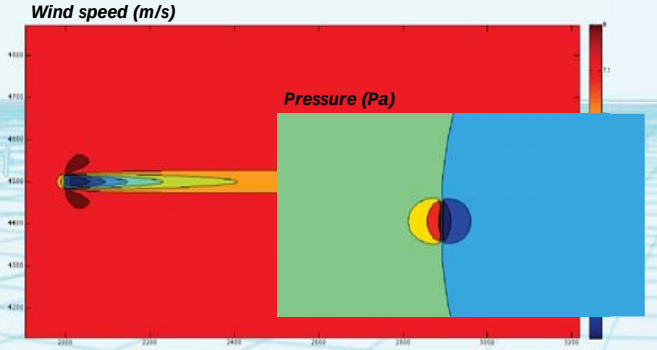

RESULTS FROM THE SINGLE-WAKE CASE

Using the testbattery to reach the upstream wind speed conditions:

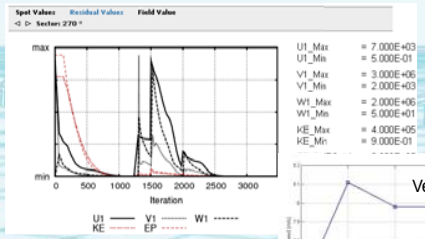

Iteration number	Power (kW)	Velocity upstream (m/s)
1500	79.58	7.54
2000	98.61	8.11
2500	93.87	7.98
3000	93.86	7.98
3500	93.86	7.98

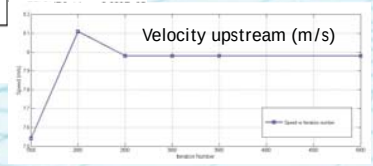

RESULTS FOR THE DOUBLE WAKE CASE

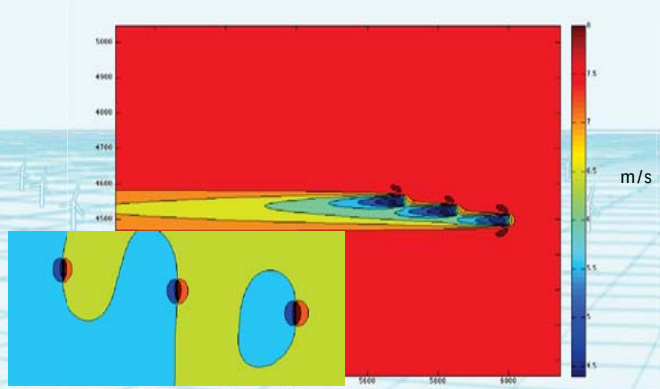

DEALING WITH SKEWED FLOWS

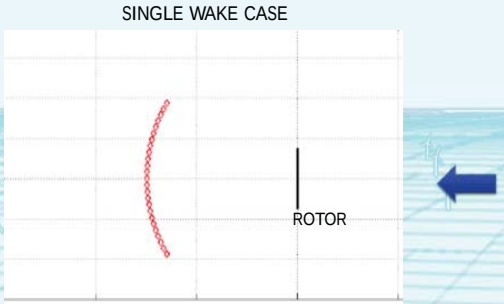

Due to the flow symmetry it is possible to move the sensor rather than changing the wind direction.

DEALING WITH SKEWED FLOWS

DOUBLE WAKE CASE

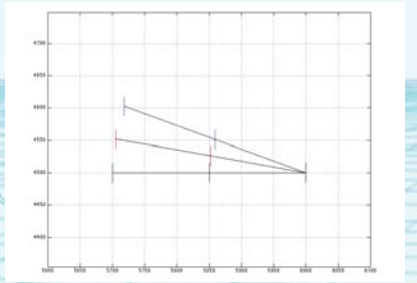

In this case it is necessary to rotate the layout (and the sensor positions). If the terrain is not flat also the rotation of the DTM is needed. This is the only possibility to have the rotors exactly facing the wind.

CALCULATING THE REYNOLDS STRESS TENSOR COMPONENTS

The eddy viscosity was estimated according to the chosen turbulence model (RNG k-ε) in order to solve the equations:

$$-\rho u_i' u_j' = \mu_T \left(\frac{\partial u_i}{\partial x_j} + \frac{\partial u_j}{\partial x_i} \right) \qquad \mu_T = \rho C_\mu \frac{k^2}{\varepsilon}$$

$$C_\mu = 0.0845 \qquad k = \frac{1}{2}(u'^2 + v'^2 + w'^2)$$

The turbulence is modeled as isotropic; the partial derivate of the wind speed components were evaluated using a discrete approach.

ESTIMATION THE POWER OUTPUT

wind speed field

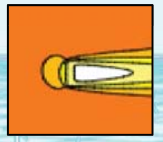

pressure field

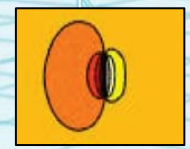

$$power = \int_{As} \overline{u} \cdot \Delta p \cdot dA$$

A_s is the swept area

$\overline{u}$ is the bulk velocity over the swept area

Δp is the max pressure drop over the swept area

The Sexbierum test-case (1/4)

- The Sexbierum case is a well-investigated wind farm with a very detailed database of measurements; such case represents a reference case for benchmarking wakes numerical models.
- Sexbierum is located in the Northern part of the Netherlands (Cleijne 1992,1993), around **4 km from the seashore**.

Cleijne J.W., "Results of Sexbierum Wind Farm", *Report MT-TNO 92-388, 1992*

Cleijne, J.W., "Results of the Sexbierum Wind Farm; Single Wake Measurements", *TNO Report No.93-082 for JOUR-0087* project, 1993.

The Sexbierum test-case (2/4)

18 turbines HOLEC three-bladed machines, hub height 35 m, power of 310 kW, for a total power of 5.4 MW.

The wind farm layout is a semi-rectangular grid of 3×6 turbines.

Seven fixed met-masts M1-M7 and a mobile met-mast used to measure the wake along the main wind direction T18-T27.

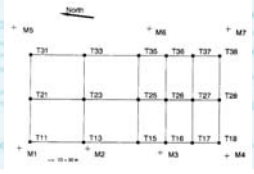

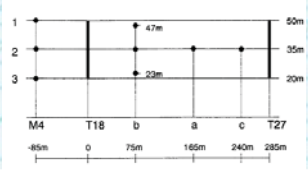

The Sexbierum test-case (3/4)

(a) Speed ratio U/Uref

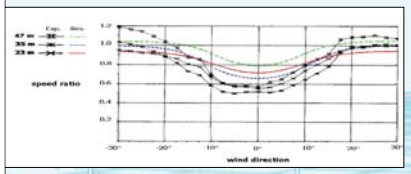

(b) Turbulent kinetic energy ratio TKE/TKEref

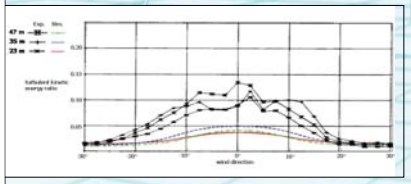

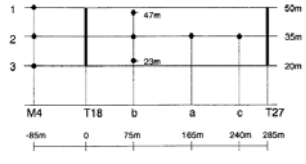

Figure 5: speed (a) and turbulent kinetic energy (b) ratio profiles at different level observed 2.5 diameters downstream – position b, 75 m downstream of T18.

The Sexbierum test-case (4/4)

(a) Speed ratio U/Uref

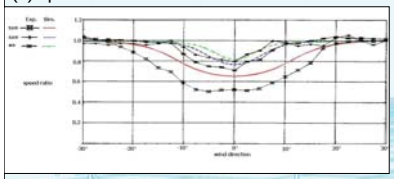

(b) Turbulent kinetic energy ratio TKE/TKEref

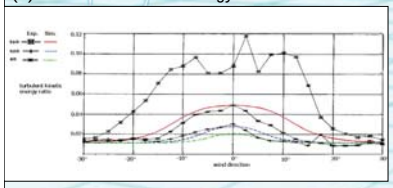

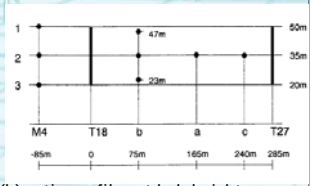

Figure 6: speed (a) and turbulent kinetic energy (b) ratio profiles at hub height observed 2.5, 5.5 and 8 diameters downstream.

Validation, Horns Rev (first 3 rows)

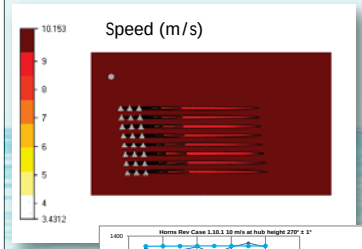

Computational characteristics:

Resolution	D/10 (8 meter)
# cells	5.0 M

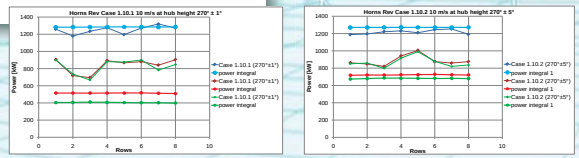

Production for all eight turbines in each three first columns for case with income wind from 270° and wind speed of 10 m/s at hub height. Variability due to sector division.

Validation, Lillgrund

Lillgrund is an offshore wind farm located in Øresund consisting of 48 wind turbines (Siemens SWT-2.3-93)

The presence of shallow waters caused the layout of the wind farm to have regular array with missing turbines (recovery holes).

- Very close inter-row spacing
- Onshore effects
- Interesting wind farm for wake simulations

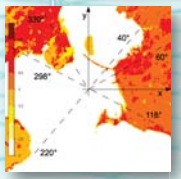

Roughness (m)

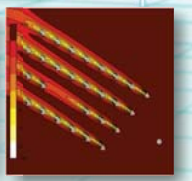

Speed (m/s)

Raphaël Désilets-Aubé. *Developing boundary conditions using the nesting technique on simple terrain.* Thesis, Gotland University, Visby, Sweden, 2011

Validation, onshore wind farm

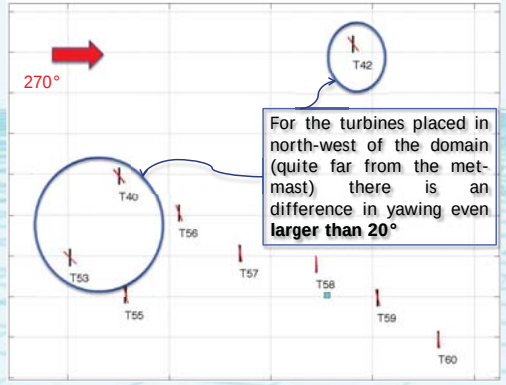

This misalignment is not fully captured by the actuator disc implemented. Orographic but also metereological effects.

Conclusions

1. WindSim with the Actuator disc model can be a useful tool for simulation of wakes on real cases (offshore and onshore);
2. Using RANS and the k-ε turbulence model can introduce some critical issue for the model not realizable (near wake);
3. Another critical part of the model can be connected with the lack of swirl in the wake (near wake);
4. Comparison with SCADA data is possible but a large uncertainty can be introduced by rotors yaw misalignments (this issue is more critical in onshore wind farms).

FUTURE WORK

1. ***ON THE MODEL SIDE***
   a. Complete the simulations with different wind speed conditions using the testbattery
   b. Improving turbulence modeling (realizable models?)
   c. Define the best force distribution on the rotor
   d. Introduce thermal stratification
   e. Introduce swirl of wake
2. ***ON THE EXPERIMENTAL SIDE***
   a. Understand misalignments (for onshore application)
   b. Introduce much more information on the actual wind direction
   c. Analyze seasonal behaviors

THANK YOU FOR YOUR ATTENTION

If you want to know more about this tool …

***Dr. Giorgio Crasto*, WindSim AS (NO)**
giorgio@windsim.com

***Prof. Francesco Castellani*, University of Perugia (IT)**
castellani@unipg.it

3D hot-wire measurements of a wind turbine wake

Pål Egil Eriksen
PhD candidate, NTNU/NOWITECH

Per-Åge Krogstad
NTNU

Outline of the presentation

- Experimental setup
- Measurement technique
- Time averaged results
- Phase-locked-averaged(PLA) results
- Possibilities for further analysis of the data
- Conclusions

Experimental setup (1/2)

- Exact same setup which was used in Blind Test 1[1]
- Turbine positioned 4D from the entrance of the test section
- Test section
  - 11.2m x 1.8 m x 2.7 m
- Allows for measurements 5D downstream of the turbine
- Data collected at 1D,3D & 5D for $\lambda_R = 6$ along a horisontal line.
- Equipped with a balance and a traverse system
- Turbulence level
  - 0.3 %

Figure 1: Upstream view of the windtunnel

[1] "Blind test" calculations of the performance and wake development for a model wind turbine. Krogstad and Eriksen, Renewable Energy, 2013

Experimental setup (2/2)

- Wind turbine model
  - Diameter: 0.9 m
  - Hub height: 0.8 m
  - Re tip: ~100000 at λ_R=6.
  - Peak efficiency ~45% at λ_R=6.
  - Operated at a constant rpm using a frequency converter.
  - Instrumentation: Torque sensor, rpm measurement using photo cell & slip rings.
  - Photo cell and constant rotational speed makes phase locked averaging possible.

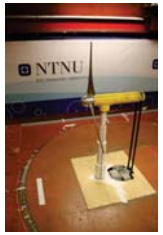

Figure 2: Model turbine

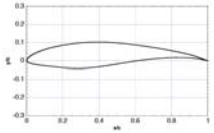

Figure 3: Blade profile (NREL S826)

Measurement technique (1/2)

- CTA hot wire anemometry
  - 2.5 µm wire -> capable of high frequency response
- Blind test 1
  - Used a single crosswire probe
    - Consists of two wires
  - Resolves two velocity components simultaneously
  - Neglects cooling velocities normal to the plane of interest
  - Can not resolve all shear stresses and third order moments

Figure 4: Sketch of crosswire

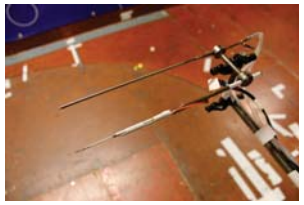

Figure 5: Crosswire mounted on traverse in wind tunnel

Measurement technique (2/2)

- Current experiment
  - Probe(hereafter called 2xw-probe) consisting of two cross wire probes measuring in orthogonal planes.
  - Resolves all three components of the velocity vector
  - Solved using an iterational procedure where binormal cooling is taken into account
  - Probe crossection ~ 2mm
  - Resolves all turbulent stresses

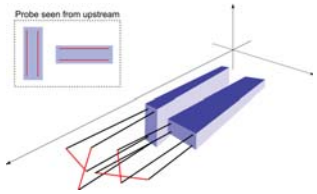

Figure 6: Sketch of 2xw-probe

Time averaged results (1/2)

- Velocity defect
  - Quite good match
  - Deviation in the freestream of the order of 2-3%
  - Probe rotation has a minor effect

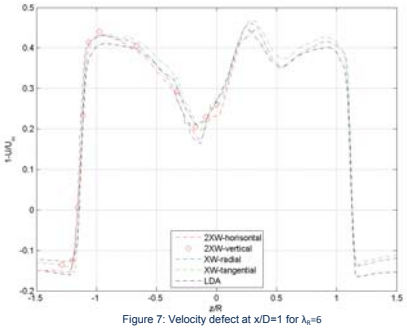

Figure 7: Velocity defect at x/D=1 for λ_R=6

Time averaged results (2/2)

- Turbulent kinetic energy
  - Quite good match
  - Some deviation near the peak. Could be due to:
    - Deviation in pitch angle
    - Difference in probe response to flowfield
  - Bump at z/R = -1.18. Why?
    - Phase-locked average of the data can give us the answer.

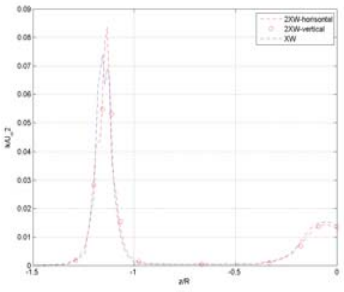

Figure 8: Turbulent kinetic energy at x/D=1 for λ_R=6

Phase locked average (1/4)

- Averaging with respect to rotor position
  - Position is determined using the rotational speed and the photo cell
- PLA of turbulent kinetic energy
  - Reveals position of tip vortices.
  - Shows that the tipvortex of one blade is located at a different radial coordinate.
    - May explains the bump in Figure 8.

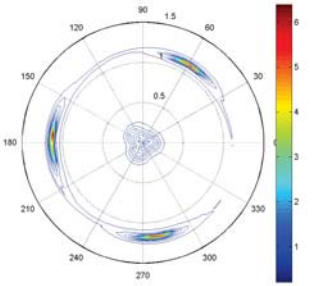

Figure 9: PLA of turbulent kinetic energy at x/D=1 for λ_R=6

Phase locked average (2/4)

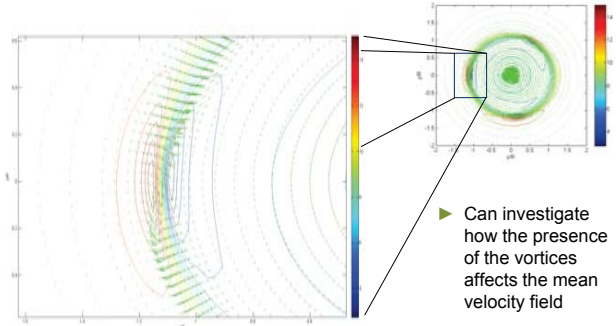

- Can investigate how the presence of the vortices affects the mean velocity field

Figure 10: Vector plot of [U_radial,U_tangential] at x/D=1 for λ_R=6. Overlapped with axial velocity contours.

Phase locked average (3/4)

- The turbulence level in the tip vortex region is dominating in the wake(as shown in figure 9)
- PLA can also be used to reveal more of the internal structure of the wake.
  - By plotting the axial normal stress on a logarithmic scale the turbulence produced by the boundary layer on the blade can also be visualized.
  - Can also see a peak in the centre with increased turbulence intensity.

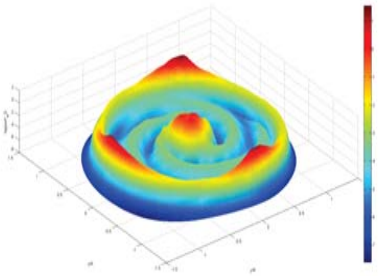

Figure 11: PLA of the streamwise normal stress at x/D=1 for λ_R=6. Logarithmic z-scale.

Phase locked average (4/4)

- A close up of the radial velocity reveals a 3p variation in the centre region
  - Could also be seen in Figure 9

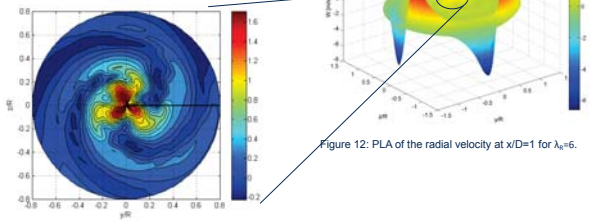

Figure 12: PLA of the radial velocity at x/D=1 for λ_R=6.

Figure 13: PLA of the radial velocity at x/D=1 for λ_R=6. Centre region

Other possibilities

- The dissipation rate ε can be estimated, eg. from the dissipation spectrum.
  - Relevant information for numerical modelers.
- Investigation of isotropy
- Triple correlations can yield information which can be useful for estimating terms in the transport equations for turbulent kinetic energy.

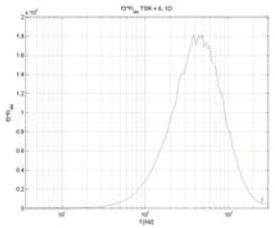

Figure 14: Example of dissipation spectrum obtained at x/D = 1. Not normalized.

Conclusions

- The new results match quite well with the old blind test results.
- Phase locked average can reveal a lot of information about the structure of the wake, which it is not possible to find from time averaged measurements.
- There are many possibilities for further analysis on the dataset.

Near and far wake validation study for two turbines in line

Marwan Khalil / Lene Sælen

GexCon AS

Trondheim, 25th of Jan. 2013

CMR-Wind

- FLACS
  - FLACS is a commercial CFD software used for explosion safety and mitigation studies
- CMR-Wind
  - *Research* version of FLACS developed within NORCOWE for the simulation of wind farms
- Solver
  - Reynolds-Averaged Navier-Stokes equations (RANS), transient and in 3D.
  - Incompressible, turbulence models, terrain, turbines
- Preprossesor
  - Scenario menu, terrain reader, visualization of turbines

Experimental setup

The CMR-Wind engine

- Staggered grid
- Cartesian grid
- Incompressible
- 2nd order accurate
- *k-ε* turbulence model with wall functions
- Terrain and sea roughness.
- Atmospheric stability.

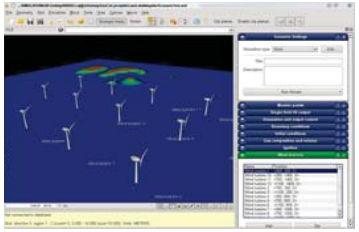

Energy capture

- Wind turbines are modelled by source terms in the momentum and turbulence equations in cells within the rotor area

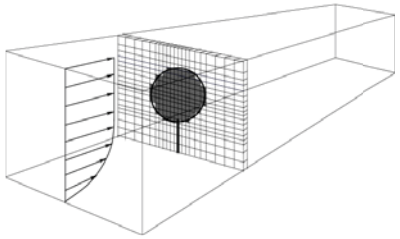

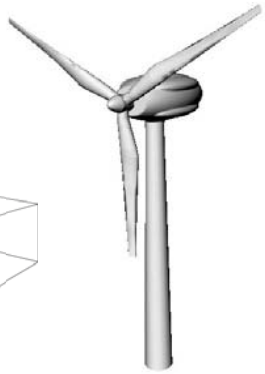

Wind turbine models

- Actuator Disc model
  - Model rotor area by a porous disk
  - Momentum sink uniformly distributed
  - Requires power and thrust curve as input
- Actuator disk + BEM
  - Model rotor area by a porous disk
  - Use BEM to calculate radial distribution of forces
  - Requires blade geometry (airfoil shape, cord length, twist angle) and drag and lift coefficients for the airfoil as inputs.

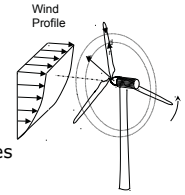

Simulation setup

- Tunnel walls included, constant cross section area
- Uniform inlet velocity: 10 m/s
- Turbulence intensity at inlet: 0.3%

Grid resolution	Δx	Δy	Δz
Coarse	0.1 m	0.06 m	0.06 m
Fine	0.05 m	0.03 m	0.03 m
Very fine	0.025 m	0.015 m	0.015 m

Power and thrust coefficient

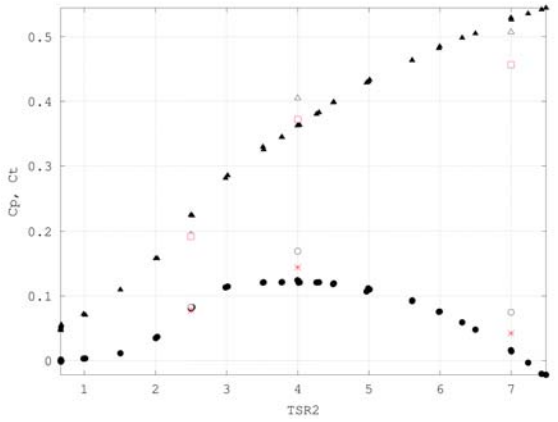

TSR=4, stream-wise mean velocity

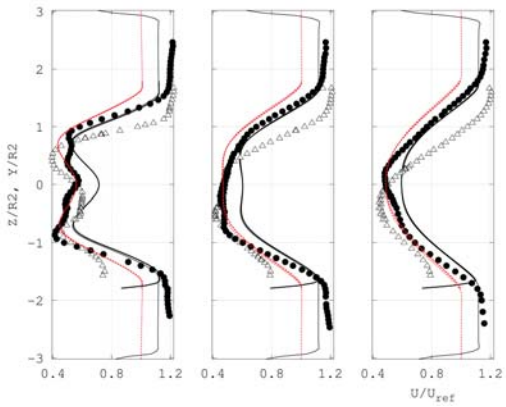

TSR=4, stream-wise turb. fluctuations

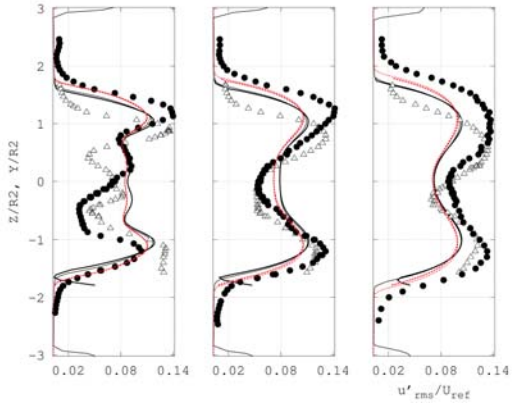

TSR=2.5, stream-wise mean velocity

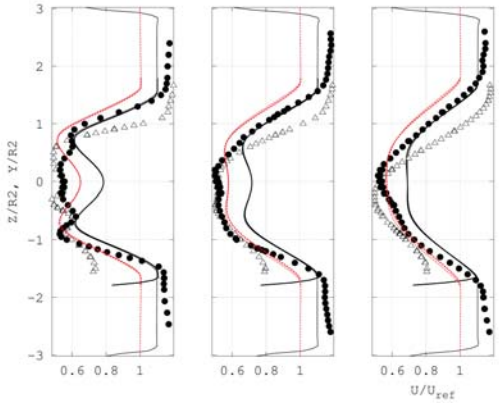

TSR=2.5, stream-wise turb fluctuations

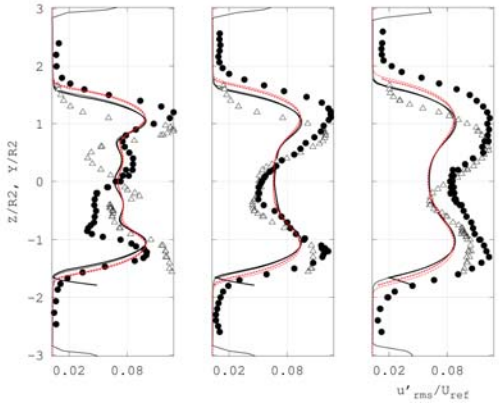

TSR=7, stream-wise mean velocity

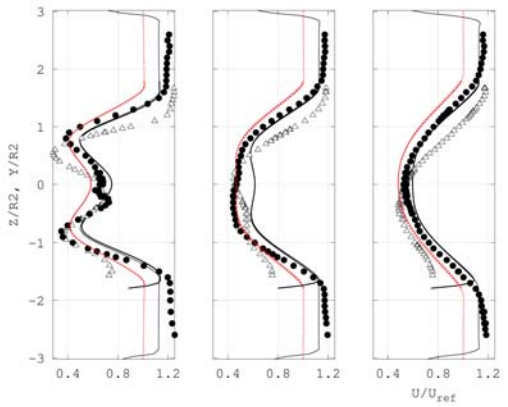

TSR=7, stream-wise turb fluctuations

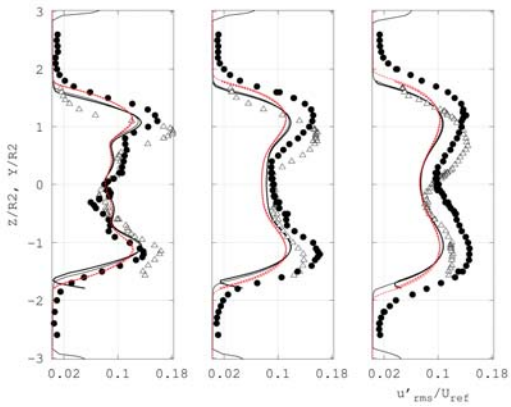

Summary

- Modeling of the wind tunnel wall is important.
- The model performs reasonably well but underestimates the wake effect.
- Measurements of the drag and lift coefficients of NREL S826 airfoil is needed.

Acknowledgements

- NORCOWE and NOWITECH funding.
- Krogstad PA, Stræn L, Pierella F, and Eriksen PE from (NTNU) for providing the experimental data and for fruitful discussions about the measurements.
- Lund JA from Meventus for providing the modeled drag and lift coefficients of NREL S826 airfoil.

Questions

Closing session

Deep offshore and new foundation concepts, Arapogianni Athanasia, European Wind Energy Association

Optimal offshore grid development in the North Sea towards 2030, Daniel Huertas Hernando, SINTEF Energi AS

New turbine technology, Svein Kjetil Haugset, Blaaster (no presentation available)

Deep offshore and new foundation concepts

Arapogianni Athanasia
Senior Research Officer
The European Wind Energy Association

Outline

1. Offshore wind industry – End of 2012
2. Market outlook – future trends
3. Deep offshore concepts
   a) State of the art
   b) Challenges
   c) Recommendations
4. Conclusions

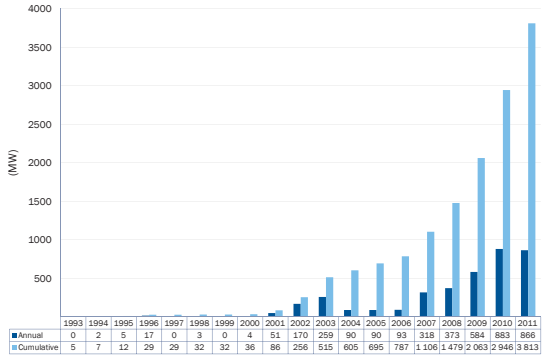

	1993	1994	1995	1996	1997	1998	1999	2000	2001	2002	2003	2004	2005	2006	2007	2008	2009	2010	2011
Annual	0	2	5	17	0	3	0	4	51	170	259	90	90	93	318	373	584	883	866
Cumulative	5	7	12	29	29	32	32	36	86	256	515	605	695	787	1 106	1 479	2 063	2 946	3 813

Offshore wind power

2012: Expected annual installations

ABOVE 1 GW

Total installed capacity close to 5GW in Europe

Share of installed capacity in Europe in 2012

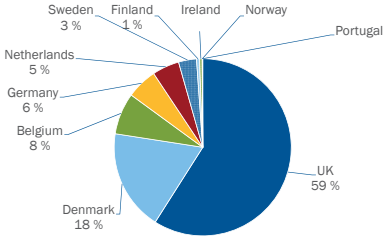

Sea Basins' share of cumulative installed capacity

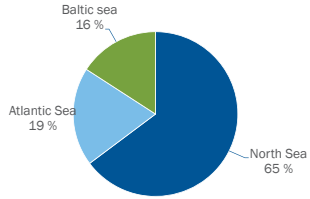

Substructure types

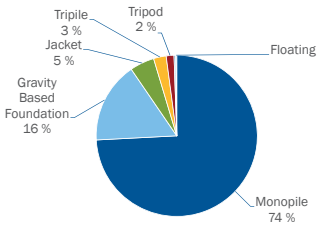

There are 4 foundations:
-Poseidon 33kW
-Sway150kW
-Hywind 2.3 MW
-Windfloat 2MW

Market outlook

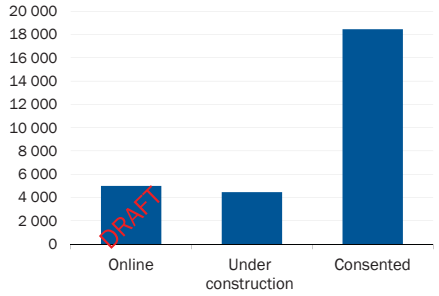

Site characteristics

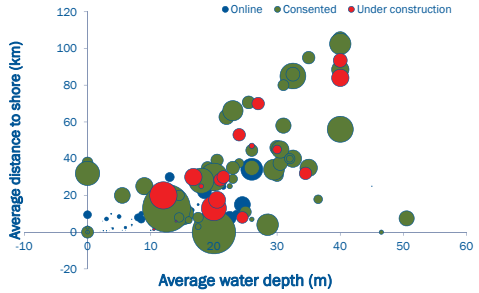

Deep offshore concepts – OWIG Task Force

The Task Force 'Deep Offshore & new foundation concepts' included representatives from:

- Acciona,
- Alstom,
- Blue H,
- Catalonian Institute for Energy Research,
- CENER,
- DNV,
- EDF,
- EDP,
- HEXICON,
- IDEOL,
- Nass & Wind,
- National Technical University of Athens,
- Principle Power,
- Risø DTU,
- Statoil,
- The Glosten Associates

Deep offshore task force

1. Definitions
2. State of the art
3. Identifying Challenges
4. Recommendations

Deep offshore - definitions

Deep offshore

Deep offshore environment starts at water depths **greater than 50 m**.

Concept maturity

- **R&D stage**: research and development on various designs using modelling tools.
- **Demonstration stage:** numerical demonstration of concept feasibility including dedicated experiments of the concept.
- **Pilot stage:** testing a down-scaled model in a controlled environment to provide realistic indicators for feasibility and cost effectiveness.
- **Prototype stage:** testing a full scale model to assess its concept maturity before commercialisation.
- **Pre-production:** deploying a limited number of full scale devices in one location to validate overall system principles, fabrication and installation methodologies.
- **Serial (commercial) production stage:** commercial deployment following pre-commercial deployment, within a wind farm layout.

Deep offshore wind concepts

Nr	Project name	Company	Type of floater
Grid connected systems			
1	Hywind	Statoil	Spar buoy
2	WindFloat	Principle Power	Semi - submersible
Concepts under development			
1	Advanced Floating Turbine	Nautica Windpower	Buoyant tower and downwind turbine
2	Aero-generator X	Wind Power Ltd, Arup	
3	Azimut	Consortium of Spanish Wind Energy Industry leaded by Gamesa	Generating the know-how required to develop a large-scale marine wind turbine
4	Blue H TLP	Blue H	Submerged deepwater platform
5	DeepCWind Floating wind	Consortium: University of Maine, AEWC, Seawall, Maine Maritime Academy, Technip, NREL,MARIN, etc.	Design of one or more scale floating wind turbine platforms
6	Deepwind	EU project	Floating and rotating foundation plus vertical wind turbine
7	DIWET Semisub	Pole Mer	Semi - submersible floater
8	EOLIA	Acciona Energy	SPAR, TLP and semisubmersible
9	IDEOL	IDEOL	Concrete floater
10	GICON TLP	GICON et.al.	Modular tension leg Platform
11	Hexicon platform	Hexicon	floater
12	HiPRwind	EU project	
13	Karmoy	Sway	Spar buoy
14	Ocean Breeze	Xanthus Energy	Taught tethered buoyant
15	Pelagic Power	W2power	Hybrid wind & wave energy conversion plant

Deep offshore wind concepts

Nr	Project name	Company	Type of floater
16	Pelastar	Glosten Associates	Tension leg turbine platform
17	Poseidon Floating power	Floating Power	Semi - submersible
18	Sea Twirl	Sea Twirl	Floating spar and vertical wind turbine
19	Trifloater Semisub	Gusto	Semi - submersible
20	Vertiwind	Technip/Nenuphar	Semi - submersible
21	WindSea floater	Force technology NLI	semi-submersible vessel with 3 corner columns
22	Winflo	Nass and Wind/DCNS	Semi - submersible
23	ZÉFIR Test Station	Catalonia institute for Energy Research	The development of a new, highly complex technology for deep-water offshore wind turbines
24	Haliade	Alstom	Floating substructure

Key challenges and recommendations

Technical
- Modelling and numerical tools
- Optimised wind turbines
- Control of the whole system
- Connection to the grid – cabling
- Installation
- Economics

Non technical
- Stable and clear legislative framework
- Spatial planning
- Risk perception
- Standardisation - cooperation

Conclusion

- Vast potential still to be tapped
- The deep offshore concepts provide a solution
- The deployment has already started
- The industry is getting ready to develop numerous concepts
- Attention to be paid on the challenges and their assessment for a successful deployment

Thank you

Optimal offshore grid developments in the North Sea towards 2030

Daniel Huertas Hernando
Daniel.Huertas.Hernando@sintef.no
www.sintef.no/energy

Deep Wind 2013 – Strategic Outlook Session
25th January 2013

SINTEF
NOWITECH
Norwegian Research Centre for Offshore Wind Technology
20 20 Twenties
OffshoreGrid

Motivation: Strategic Outlook – 2030

Hydro power
(Flexibility, Storage, Balancing)

Grid

Offshore wind
(Penetration, Variability)

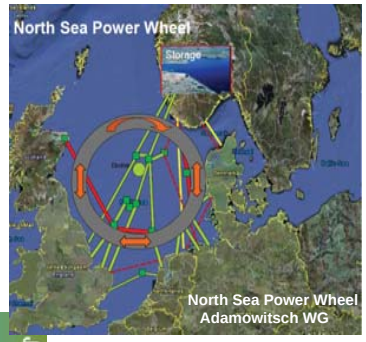

North Sea Power Wheel
Adamowitsch WG

SINTEF
NOWITECH
Norwegian Research Centre for Offshore Wind Technology

Motivation: Strategic Outlook – 2030

- What is the **Strategy** to reach this Vision?
- How to define a **robust development path** to deploy our **Strategy**?

SINTEF
NOWITECH
Norwegian Research Centre for Offshore Wind Technology

Motivation: Strategic Outlook – 2030

- **Strategy:**

"An interconnected offshore grid in the North Sea in 2030"

- Can be highly beneficial from an economic perspective
- Contributes to reaching the European 20-20-20 targets and beyond
- Will increase the security of supply
- Is a step towards an integrated electricity market
- Helps to smooth fluctuations and integrate RES
- Connects northern storage capacities to the power system

(Conclusions of IEE-EU project OffshoreGrid)

OffshoreGrid

IEE OffshoreGrid

OffshoreGrid

- Techno-economic study
- Cost-benefit analysis of different design options
- First in-depth analysis of how to build a cost-efficient grid in the North and Baltic Seas
- Coordinator 3E, 8 partners, consultancy & applied research
- **SINTEF** : Harald Svendsen, Leif Warland, Magnus Korpås, DHH

www.OffshoreGrid.eu

Intelligent Energy Europe

Offshore Grid grid topology

cost-efficient grid in the North and Baltic Seas

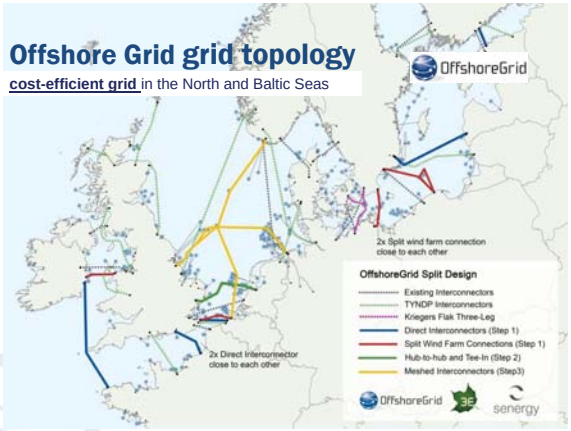

www.OffshoreGrid.eu

Intelligent Energy Europe

Sensitivity Analysis & Robustness

Main Aspects considered

- Potential for **large scale offshore wind deployment**.
- Potential for **flexible generation** – increased **hydro power potential** in Norway.
- Analysis of **onshore grid reinforcement strategies** for **offshore grid topologies**
- **SINTEF**: Hossein Farahmand, Stefan Jaehnert, DHH

SINTEF

NOWITECH Norwegian Research Centre for Offshore Wind Technology

European Interconnected Network (2030)

Tool: Power System Simulation Tool (PSST) – DC Power Flow

Detail model of Norway

Offshore Grid

Detail model of the UK

Detail model of ENTSO-E

SINTEF

NOWITECH Norwegian Research Centre for Offshore Wind Technology

Wind Power Scenarios in Northern EU

Country	2020				2030			
	Total installed Capacity (GW)		Offshore wind power (GW)		Total installed Capacity (GW)		Offshore wind power (GW)	
	Base	High	Base	High	Base	High	Base	High
Belgium	4.26	4.66	2.16	2.16	6.72	7.01	3.96	3.96
Germany	49.8	55	8.81	13	78.01	92.01	24.06	32.38
Denmark	6.51	7.21	2.81	3.21	9.48	11.19	4.61	5.81
Estonia	0	0	0	0	1.7	1.7	1.7	1.7
Finland	2.35	2.95	0.85	1.45	5.58	7.34	3.61	5.16
France	22.93	23.94	3.94	3.94	30.65	34.67	5.65	7.04
UK	30.06	37.68	16.31	22.78	54.29	71.77	36.2	51.77
Ireland	6.37	7.48	2.12	2.38	8.81	10.66	3.22	4.48
Lithuania	0	0	0	0	1	1	1	1
Latvia	0	0	0	0	1.10	1.10	1.10	1.10
Netherlands	8.8	10.3	5.3	6.80	17.40	22.38	12.79	17.29
Norway	3.6	5.14	0.42	1.02	9.49	12.27	5.31	7.64
Poland	10.5	12.5	0.5	0.5	18.46	19.84	5.30	5.30
Sweden	9.08	11.13	3.08	3.13	14.76	16.94	6.87	8.22
	154.26	177.99	46.3	60.37	257.45	309.88	115.38	152.85

Offshore wind farms in 2020 (red) and 2030 (red+black)

Technical University of Denmark DTU

www.twenties-project.eu

Scenario Analysis of Hydro Power Potential (D16.2 & CEDREN SINTEF Report http://www.cedren.no)

Plant	2020 (MW)	2030 (MW)
Pump Storage Plant Tonstad	1400	1400
Pump Storage Plant Holen	700	1000
Pump Storage Plant Kvilldal	1400	2400
Power Plant Jøsenfjord	1400	2400
Pump Storage Plant Tinnsjø	1000	2000
Pump Storage Plant Tinnsjø	1400	2400
Power Plant Lysebotn	400	1800
Power Plant Mauranger	-	400
Power Plant Oksla	700	700
Pump Storage Plant Tysso	700	1000
Power Plant Sy-Sima	700	1000
Power Plant Aurland	700	700
Power Plant Tyin	700	1000
Amount of new power capacity	11200	18200

E. Solvang, A. Harby, Å. Killingtveit, "Increasing balance power capacity in Norwegian hydroelectric power stations (A preliminary study of specific cases in Southern Norway)," SINTEF Energy Research, CEDREN Project, Project No. 12X757, 2012

www.twenties-project.eu

Grid Implications of Hydro Power Flexibility in Norway

- Grid reinforcement in Norway according to Statnett grid development plans
- Special attention is paid to the corridor where the hydro production capacity expansion is proposed (highlighted in yellow)

Offshore Grid Alternatives

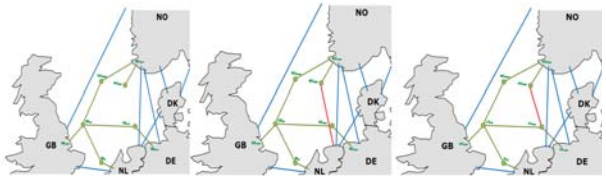

Case A Case B Case C

www.twenties-project.eu

Internal Constraints

Detail model of the UK

Reinforced Grid in Norway – allows use of Hydro flexibility potential

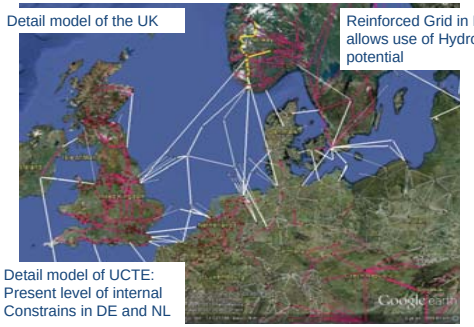

Detail model of UCTE: Present level of internal Constrains in DE and NL

Internal Constraints + Expansion

Detail model of the UK+ TYNDP 2012

Reinforced Grid in Norway – allows use of Hydro flexibility potential

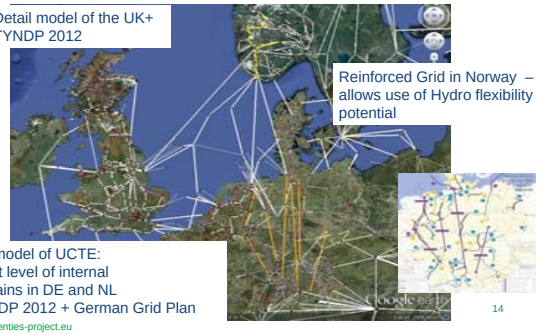

Detail model of UCTE: Present level of internal Constrains in DE and NL + TYNDP 2012 + German Grid Plan

No-Internal Constraints

Detail model of the UK

Reinforced Grid in Norway – allows use of Hydro flexibility potential

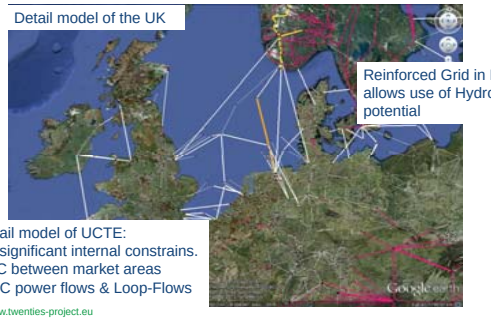

Detail model of UCTE: No significant internal constrains. NTC between market areas + DC power flows & Loop-Flows

Operating costs

Onshore Grid Constraints in the ENTSO-E and the UK	Offshore grid Cases	Cost (Milliard EUR/a)
1.No constraint	Case A	92.8462
	Case B	92.7498
	Case C	92.7665
2. Internal Constraint	Case A	95.5779
	Case B	95.5273
	Case C	95.517
3.Internal Constraint with Expansion	Case A	92.9928
	Case B	92.9288
	Case C	92.9274

The Impact of Internal Onshore Constraints (average annual exchange)

1-Case B, No internal Constrains

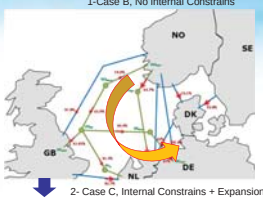

2- Case C, Internal Constrains + Expansion

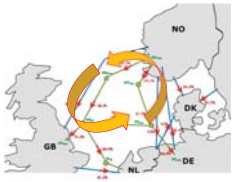

3- Case C, Internal Constrains

The Impact of Internal Onshore Constraint

Onshore grid constraints *inland* strongly influence the optimal use of wind and hydro resources; Limitations to transfer the power inland hence increase the operating cost significantly.

North Sea Power Wheel
Mr. G.W. Adamowitsch

This work has performed a detailed techno-economic study to quantified this effect.

Pumping Strategies

Specific Case (Tonstad & NorGer HVDC cable)

Tonstad Reservoir in Norway

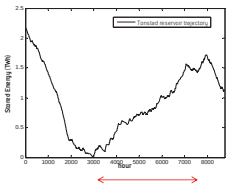

Pumping Strategies

Specific Case (Tonstad & NorGer HVDC cable)

- The reservoir is drained very fast during winter time until hour 3000
- From hour 3000 to 6000 there is a filling season with high natural inflow to reservoir
- During the above period, small fluctuations have been observed
- The small fluctuations are assumed to be the effect of wind production variability

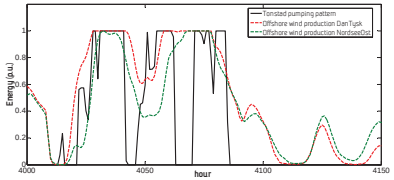

Summary

- Work done in IEE-EU OffshoreGrid, FP7- TWENTIES, FME NOWITECH have performed detailed **techno-economic** studies of:
  - In-depth analysis of how to build a **cost-efficient grid** in the North and Baltic Seas
  - Identification of **required transmission** capacity between the Nordic region and Northern Continental Europe for **optimal** use of hydro power and wind power generation.
  - Sensitivity analysis on effect of **onshore grid constrains**

Main conclusions

- **Onshore grid** constraints strongly influence the flows across a **meshed offshore grid**, therefore affecting the optimal use of wind and hydro
- **Long term strategies** for the development of **offshore grids** and **onshore grid expansion** must be done in a coordinated way to ensure **optimal developments**.
- The analysis demonstrates the **correlation** between the pumping strategies in the Norwegian system and the onshore and offshore wind variations around the North Sea

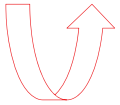

Thank You !!

BACK-UP SLIDES

Motivation: Strategic Outlook – 2030

- How to define a **robust development path** to reach this **Vision?**
- Research can contribute to this task by:
  - Considering different **Scenarios** including different configurations of offshore grids in the North Sea.
  - Perfoming sensitivity analysis of the considered configuration(s) on different important **key parameter & assumptions**
- The main focus of a such analysis is to gain knowledge about the key relationships and driving forces so better decisions can be made (today), about the best strategy to reach our **Vision.**

Grid Implication Studies: Northern Europe

- **Tool**
  - Power System Simulation Tool (PSST) – DC Power Flow
- **Generation portfolio and demand:**
  - The scenarios and data are consistent with Market Model
- **Grid Model**
  - ENTSO-E UCTE Study Model (winter 2008)
  - British (National Grid-Seven Year Statement)
  - Nordic and Eastern Europe data (SINTEF-NVE & TradeWind)
- **Modelling Development**
  - 5651 buses, 2410 generators, 9611 branches
  - 2020, 2030 Scenarios

www.twenties-project.eu

Hydro modelling

- Since there is a limited amount of water storage in hydro reservoirs, its long-term utilisation is essential to be optimised
- The water values reflect the expected future value of the other types of production that the hydro generators substitute
- The water values are imported from the market model (EMPS) and used as exogenous input to the next model (PSST)

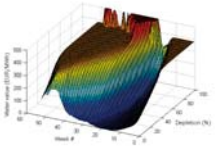

Calculated Water Values For a Reservoir in Southern Norway

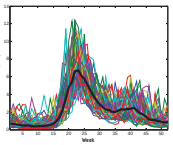

Inflow Scenarios in the Norwegian Power System

European Interconnected Network (2030)

PSST + Offshore Meshed Grid (IEE-EU OffshoreGrid Project)

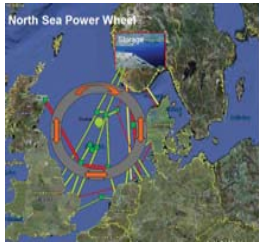

North Sea Power Wheel
Mr. G.W. Adamowitsch

www.twenties-project.eu

Main Results in a Nutshell – Total costs

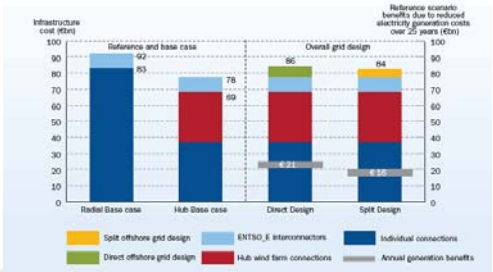

- Hub connection saves €14 bn .
- Additional interconnections costs €5-8bn and bring benefits €bn 16-21
- The financial numbers speak clearly for an offshore grid.

www.OffshoreGrid.eu

Reservoir Trajectory in Norway in 2030

The simulated reservoir (black curve) follows the seasonal variation

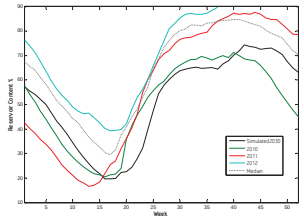

Average Normal Hydrological Year

Comparing Tonstad Simulated Reservoir Trajectory

- IC: Present Internal constraint
- ICE: Expanded transmission according to TYNDP2012+ German Grid Plan
- NC: No internal constrains – NTC limited

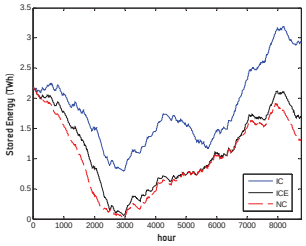

High Wind Scenarios

Increase of WPP up to 63 GW

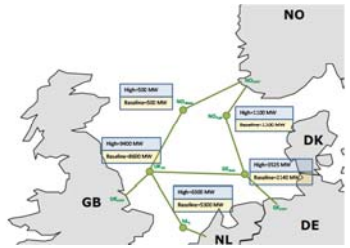

Reservoir Trajectory in Norway

The wind energy surplus is stored in the Norwegian hydro reservoir by pumping the water from low to high altitude reservoirs

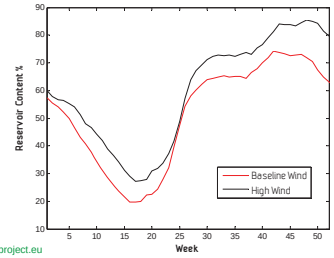

Dry Year and High Wind Scenario

Wind energy is stored in the Norwegian reservoir helping the Norwegian power system to cover the load in depletion season and fill up the reservoir in the filling season

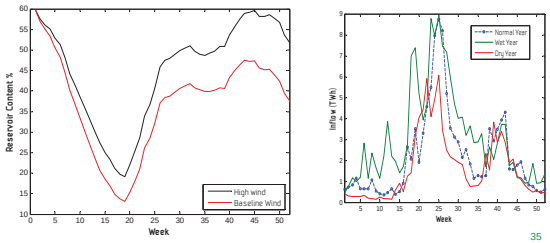

Exchange Variation (high and baseline wind-dry year)

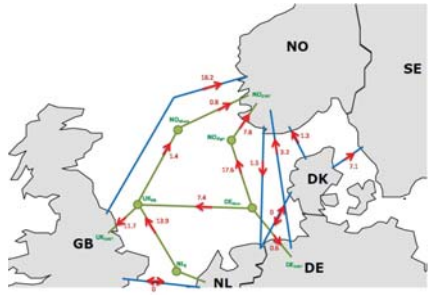

Material shown IEE-EU OffshoreGrid project (Leif and Harald)
TWENTIES (Hossein Farahmand, Stefan Jaehnert)

Cross-border capacities

- Significant expansion of cross-border transmission capacities

NorNed	Nordlink	Cobra	BritNed	Skagerrak	Storbælt	Konti-Skan	Kontek	Baltic
700	-	-	-	900	500	720	550	525
1400	700	700	1000	1600	500	720	600	600

SwePol	Fenno-Skan	Nemo	NorBrit		DK-DE	DE-NL	DE-BE	NL-BE
450	550	-	-		1400	4000	-	1400
450	1100	1000	1400		2400	6300	1600	2400

Marginal profit

High marginal transmission profit on corridors crossing the North and Baltic Sea in 2030 (due to price differences) => arbitrage / investment potential

2010

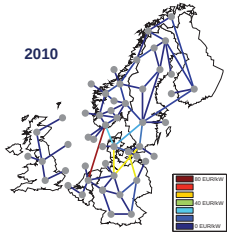

2030

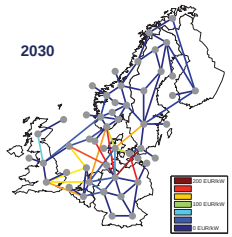

Transmission Expansion - Investment algorithm

- **Two-step methodology:**
  1. **Detailed power market simulation**
  2. **Investment decision based on outcome of power market simulation**
- **Impact of investments on electricity price is taken into account**
- **Investment based on marginal profit**

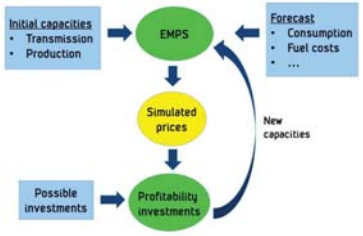

Transmission expansion

- Although marginal profits Main expansion only occurs around the North Sea
- Increasing the capability of transmitting energy from renewable energy sources (Sweden, Scotland) to load centres (Southern Germany, Southern UK)
- No expansion within the North Sea due to high investment

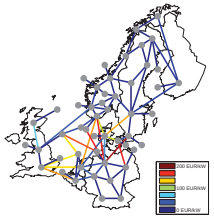

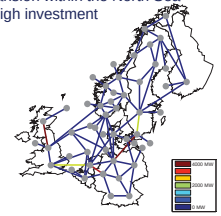

Electricity prices – before and after transmission expansion

Alignment of prices in the Nordic region, Great Britain and continental Europe

Before:

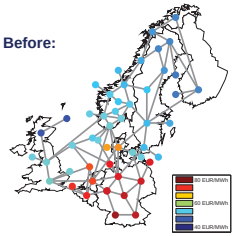

After:

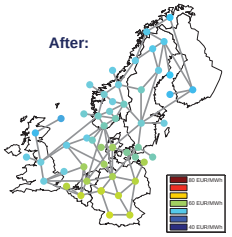

Generation portfolio / Mix

- Increase of WPP up to 191 GW
- Decommissioning of nuclear / lignite power plants

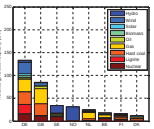

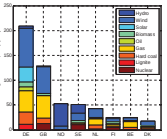

ENTSO-e (2010) 2010 2030

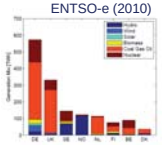

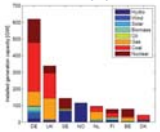

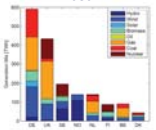

2010 scenario calibrated to generation mix reported by ENTSO-e
Significant shift of generation sources up to 2030

Hydro power production (Norway)

- **Increased production variability due to balancing of WPP**
- **2010**

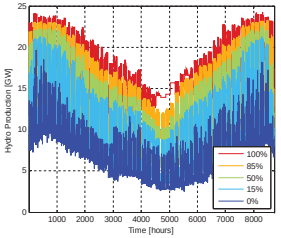

2030

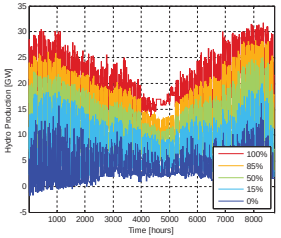

The Grid Expansion in the German Power System

DE and NL + TYNDP 2012 + German Grid Plan

The Grid Expansion in the British Power System

The UK+ TYNDP 2012

Some "*hints*" of the North Sea Power Wheel

Without Expansion

With Expansion

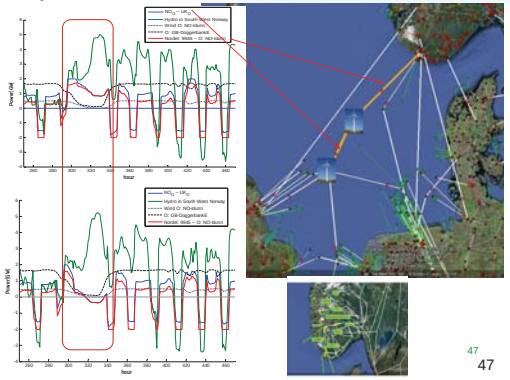

Technology for a better society

www.sintef.no